eman ta zabal zazu
Universidad del País Vasco
Euskal Herriko Unibertsitatea

Ingeniaritza Goi Eskola Teknikoa
Escuela Técnica Superior de Ingeniería
Bilbao

Departamento de Ingeniería de Comunicaciones
Komunikazioen Ingenieritza Saila

Ph.D. Thesis

Solutions for New Terrestrial Broadcasting Systems Offering Simultaneously Stationary and Mobile Services

Author Jon Montalban Sanchez
Advisor Dr. Manuel Vélez Elordi

December 2014

- ISBN: 978-84-9082-231-9

Author's e-mail: jon.montalban@ehu.es

ABSTRACT

Since the first broadcasted TV signal was transmitted in the early decades of the past century, the television broadcasting industry has experienced a series of dramatic changes. Most recently, following the evolution from analogue to digital systems, the digital dividend has become one of the main concerns of the broadcasting industry. In fact, there are many international spectrum authorities reclaiming part of the broadcasting spectrum to satisfy the growing demand of other services, such as broadband wireless services, arguing that the TV services are not very spectrum-efficient.

Apart from that, it must be taken into account that, even if up to now the mobile broadcasting has not been considered a major requirement, this will probably change in the near future. In fact, it is expected that the global mobile data traffic will increase 11-fold between 2014 and 2018, and what is more, over two thirds of the data traffic will be video stream by the end of that period. Therefore, the capability to receive HD services anywhere with a mobile device is going to be a mandatory requirement for any new generation broadcasting system.

The main objective of this work is to present several technical solutions that answer to these challenges. In particular, the main questions to be solved are the spectrum efficiency issue and the increasing user expectations of receiving high quality mobile services. In other words, the main objective is to provide technical solutions for an efficient and flexible usage of the terrestrial broadcasting spectrum for both stationary and mobile services.

The first contributions of this scientific work are closely related to the study of the mobile broadcast reception. Firstly, a comprehensive mathematical analysis of the OFDM signal behaviour over time-varying channels is presented. In order to maximize the channel capacity in mobile environments, channel estimation and equalization are studied in depth. First, the most implemented equalization solutions in time-varying scenarios are analyzed, and then, based on these existing techniques, a new equalization algorithm is proposed for enhancing the receivers' performance.

An alternative solution for improving the efficiency under mobile channel conditions is treating the Inter Carrier Interference as another noise source. Specifically, after analyzing the ICI impact and the existing solutions for reducing the ICI penalty, a new approach based on the robustness of FEC codes is

presented. This new approach employs one dimensional algorithms at the receiver and entrusts the ICI removing task to the robust forward error correction codes.

Finally, another major contribution of this work is the presentation of the Layer Division Multiplexing (LDM) as a spectrum-efficient and flexible solution for offering stationary and mobile services simultaneously. The comprehensive theoretical study developed here verifies the improved spectrum efficiency, whereas the included practical validation confirms the feasibility of the system and presents it as a very promising multiplexing technique, which will surely be a strong candidate for the next generation broadcasting services.

LABURPENA

Pasa den mendearen hasieran lehenengo telebista seinaleak transmititzen hasi zirenetik, irrati-difusio zerbitzuek berebiziko aldaketak izan dituzte. Berriki, sistema analogikoak digitalizatzearen ondorioz eratorritako zatikizun digitala, irrati-difusio enpresen afera bilakatu da. Izan ere, nazioarteko espektro erakunde frankok irrati-difusioaren espektroan zenbait atal beste zerbitzuetarako askatu nahi izan dute, haririk gabeko banda zabaleko zerbitzuetarako kasu, irrati-difusio zerbitzuen eraginkortasun espektral eskasa argudiatuz.

Bestalde, orain arte irrati-difusiorako zerbitzu mugikorrak ezinbestekotzat jo ez badira ere, etorkizun hurbilean egoera hau aldatu egingo da. Azkenengo ikerketen arabera, datu mugikorren trafikoa hamaika aldiz handituko da 2014 eta 2018 urteen bitartean; areago, epe honen bukaera aldera, trafiko osoaren bi heren bideo streaming-a izango da. Honenbestez, bereizmen handiko telebista hargailu mugikorren bidez edonon ikusi ahal izatea, ezinbesteko baldintza izango da datozen belaunaldiko edozein irrati-difusio sistementzat.

Lan honen helburu nagusia aurretiaz aipatu diren arazoen konponbiderako irtenbide teknikoak aurkeztea da. Zehazki, bi dira konpondu beharreko erronkak: espektroaren erabileraren eraginkortasuna eta zerbitzu mugikorren hobetzea. Finean, helburu garrantzitsuena zerbitzu finko eta mugikorrak aldi berean modu eraginkor eta malguago batean igortzeko proposamen berriak aurkitzea da.

Lan zientifiko honen lehen ekarpen inportantea irrati-difusio mugikorrarekin hertsiki loturik dago. Hasteko, hartzaile mugikor baten ikuspegitik OFDM seinaleen azterketa matematiko sakona egin da. Kanalaren igortze ahalmena maximizatu nahian, kanala berreskuratzeko teknika berriak eta ekualizazio algoritmoak aztertu dira, ondoren haien errendimendua hobetuko duen algoritmoa aurkezteko.

Horrez gain, hargailu mugikorren eraginkortasuna hobetzeko, tesi honek ikuspegi berria proposatzen du: mugikortasunaren ondorioz sortutako ICIa distortsio legez tratatzea. Horretarako, ICIaren eragina eta berau konpontzeko existitzen diren aukerak aztertu eta gero, distortsio honen zuzenketa FEC algoritmoen esku uztea proposatzen da.

Bukatzeko, lan honen azken ekarpen garrantzitsua LDM teknikaren aurkezpena izan da. Izan ere, proposamen honen bidez zerbitzu finko eta mugikorrak aldi berean igor daitezke, espektroaren erabilera eraginkorragoa bultzatuz, eta horrez gain, zerbitzu mugikorrak hobetuz. Aurrera eramandako

analisi teorikoek eraginkortasun espektralaren hobekuntza egiaztatzeaz aparte, hemen aurkezten diren ikerketa praktikoek sistemaren erabilgarritasuna balioztatzen dute hurrengo belaunaldiko irrati-difusio sistemetarako.

RESUMEN

Desde el comienzo de la transmisión de las primeras señales de televisión a principios del siglo pasado, la radiodifusión digital ha evolucionado gracias a una serie de cambios relevantes. Recientemente, como consecuencia directa de la digitalización del servicio, el dividendo digital se ha convertido en uno de los caballos de batalla de la industria de la radiodifusión. De hecho, no son pocos los consorcios internacionales que abogan por asignar parte del espectro de radiodifusión a otros servicios como, por ejemplo, la telefonía móvil, argumentado la poca eficiencia espectral de la tecnología de radiodifusión actual.

Asimismo, se debe tener en cuenta que a pesar de que los servicios móviles no se han considerado fundamentales en el pasado, esta tendencia probablemente variará en el futuro cercano. De hecho, se espera que el tráfico derivado de servicios móviles se multiplique por once entre los años 2014 y 2018; y lo que es más importante, se pronostica que dos tercios del tráfico móvil sea video streaming para finales de ese periodo. Por lo tanto, la posibilidad de ofrecer servicios de alta definición en dispositivos móviles es un requisito fundamental para los sistemas de radiodifusión de nueva generación.

El principal objetivo de este trabajo es presentar soluciones técnicas que den respuesta a los retos planteados anteriormente. En particular, las principales cuestiones a resolver son la ineficiencia espectral y el incremento de usuarios que demandan mayor calidad en los contenidos para dispositivos móviles. En pocas palabras, el principal objetivo de este trabajo se basa en ofrecer una solución más eficiente y flexible para la transmisión simultánea de servicios fijos y móviles.

La primera contribución relevante de este trabajo está relacionada con la recepción de la señal de televisión en movimiento. En primer lugar, se presenta un completo análisis matemático del comportamiento de la señal OFDM en canales variantes con el tiempo. A continuación, con la intención de maximizar la capacidad del canal, se estudian en profundidad los algoritmos de estimación y ecualización. Posteriormente, se analizan los algoritmos de ecualización más implementados, y por último, basándose en estas técnicas, se propone un nuevo algoritmo de ecualización para aumentar el rendimiento de los receptores en tales condiciones.

Del mismo modo, se plantea un nuevo enfoque para mejorar la eficiencia de los servicios móviles basado en tratar la interferencia entre portadoras como una fuente de ruido. Concretamente, tras analizar el impacto del ICI en los receptores

actuales, se sugiere delegar el trabajo de corrección de dichas distorsiones en códigos FEC muy robustos.

Finalmente, la última contribución importante de este trabajo es la presentación de la tecnología LDM como una manera más eficiente y flexible para la transmisión simultánea de servicios fijos y móviles. El análisis teórico presentado confirma el incremento en la eficiencia espectral, mientras que el estudio práctico valida la posible implementación del sistema y presenta la tecnología LDM como una candidata ideal para ser parte de los estándares de nueva generación.

Index

Figure Index

Table Index

"Exactly!" said Deep Thought. "So once you know what the question actually is, you'll know what the answer means."

"The Hitchhiker's Guide to the Galaxy"-

Douglas Adams

CHAPTER 1: **INTRODUCTION AND THESIS OBJECTIVES**

The dawn of the new century has brought a substantial revolution to the broadcasting world, changing the traditional way in which this technology has been understood during the last decades. In this chapter, a brief description of the recent digital television history is included. In this summary, the most important technological milestones have been highlighted, such as the first digital generation, the first introduction of mobile services, the digital switch over and the digital dividend. It is important to bear in mind that the terrestrial broadcasting technologies are not a static structure of physical rules, but a dynamic framework that has been continuously evolving from the very beginning. According to the presented context, the motivation and objectives of this thesis are defined.

1. TERRESTRIAL BROADCASTING SYSTEMS: DRAWBACKS AND CHALLENGES

It is widely agreed that television broadcasting, as a one-to-many service, can be considered as one of the most cost-effective technologies for informing, educating and offering entertainment all over the world. For instance, according to the International Telecommunications Union (ITU) in 2010 there were more than 1.4 billion households with a TV set. Moreover, in 72.4% of the households of developing countries there is at least one TV set, while this number increases up to 98% in the case of developed countries [1]. Therefore, there is no doubt that the television still plays a pivotal role in the current society, and what is more, from a business point of view, the broadcasting must play a key role in the near future media consumption. As matter of fact, television broadcasting has been in a relatively privileged position since the beginning, being the primary medium for video transmission. Recently, it has had also an important contribution as an Emergency Alert System (EAS), providing interactive emergency information. As a matter of fact, these kinds of services have already been successfully implemented in USA, Japan or Korea.

When the customers first met these one-to-many services in the beginning of the last century, broadcasting was entirely based on analog technology. Afterwards, the 21st century brought a substantial change, digitalizing not only the delivered contents but also the transmitting and receiving communication equipment. This first generation of digital terrestrial television was designed to overcome the main shortcomings associated to analog systems, for instance, the spectrum efficiency could be improved up to four times. Admittedly, this movement towards the digitalization brought also the very first steps for the mobile TV delivery; however, the first attempts were not too satisfactory. Among others, one of the main reasons for this failure were the very challenging receiving conditions for handheld/mobile terminals on urban and indoor environments. A planning solution based on changing the network topology, increasing the number of transmitters, was not feasible. What is more, from a business point of view, it was not be very easy to penetrate a market which has already been proved more profitable with other technologies. It requires strong backing from handset manufacturers, mobile operators and administrations. Nevertheless, a more practical solution could be to design more protected mobile services that can be understood as an additional capability of an already existing legacy system. In other words, a simultaneous delivery capability that might provide the broadcasters the advantage to sustain or even increase the profits with new offerings without the need to change the network is a more desirable approach.

Another major problem of the broadcast industry is the scarcity and the cost of available spectrum. Regarding the regulatory issues, probably the main side effect of the digital switch over was the digital dividend, which refers to the spectrum released in the process of digitalization of the television transmission [2]. As the broadcasting technology spectrum efficiency was increased, part of the electromagnetic spectrum was freed up. The problem of the digital terrestrial television is that, although it needs less RF spectrum than analog television, it is still much more inefficient than other technologies. In fact, this is why many spectrum authorities have been reclaiming part of the spectrum to satisfy the growing demand of other services, such as broadband wireless services [3][4].

Nevertheless, as it has always been done, the broadcasting industry structure did not lie dormant, and thus, there have been launched attempts all over the world to present a new generation broadcasting systems able to cope with the modern requirements. In particular, there are several international consortiums, stakeholders and important companies all around the globe that have taken some important steps to evolve the actual digital television systems to the new era of the telecommunications. For instance, the European DVB's NGH bluebook [5] or the North American ATSC 3.0 [6], which plans to have a worldwide candidate by the end of 2015. These new times have also given rise to a growing willing for the definition of an international worldwide standard, allowing the user to buy one single terminal that will be able to receive any broadcasted service all over the world. An example of this trend is the Future of Broadcasting Television Initiative (FOBTV) [7], which aims to develop technologies for next-generation terrestrial broadcasting systems and make recommendations to standardization organizations around the world.

1.1 The Birth of Digital Terrestrial Television (DTT)

Historically, Michael Faraday's law of electromagnetic induction, presented in 1831, is considered the birth of broadcasting. However, it was not until 1930s when the first electromechanical devices were manufactured. Shortly after, in 1936, regular television broadcasting services began in England by the British Broadcasting Corporation (BBC) using the 405-line Marconi-EMI system, and followed in 1939 in the United States. Three years later, in 1942, the Federal Communications Commission (FCC) adopted the recommendation of the National Television System Committee (NTSC), being its main characteristic a set of 525 scanning lines with 60 fields (30 frames) per second [8]. Just a decade after the monochromic standard was approved, in 1953, the first commercial color

television system was submitted by the NTSC, delaying the first color broadcast service to the January of 1954 [9]. Meanwhile in Europe the adoption for color television system was not establised until the period ranging from 1953 to 1967. During those years, Sequential Couleur A Memoire (SECAM), the Phase Alternating Line (PAL) or any of their several variants were adopted across the continent [10]. The first one was mainly used in France and URSS, while the second one was implemented in the vast majority of Europe and other countries around the world [11].

The exponential growth of the multimedia consumption user continued during the following decades, and meanwhile, the viewers were demanding not only more services but also higher quality. Indeed, prior to the development of the fully digital TV systems, there were various attempts to improve the existing analog systems, such as Japan Broadcasting Corporation (NHK) HDTV project in Japan [12][13], the Eureka EU 95 Project [14] or PALplus [15] in Europe, and Advanced Compatible Television in the United States [16]. Nevertheless, the spectrum is a very scarce resource, and even after the potential analog television throughput increase, it was extremely inefficient: it required a complete RF channel to transmit just one television service. This has been the main drawback of the system in vogue for over 50 years and it had never been completely solved: the jump to the digital world was inevitable. As their analog predecessors, the first generation of digital television standards were also rolled-out in parallel in different parts of the world due to a mixture of technical and geopolitical reasons. Within the existing consortiums the main standardization groups were: European Digital Video Broadcasting (DVB) Project, the North American Advanced Television Systems Committee (ATSC) and in Japan, the Association of Radio Industries and Business (ARIB).

The first digital television broadcasting standard, DVB-T [17], was published by the DVB consortium in 1997 and several international organizations, such as the European Telecommunication Institute (ETSI), the European Committee for Electrotechnical Standardization (CENELEC) and the European Broadcasting Union (EBU) were actively involved in its development. In theory, the system was designed not only to offer high capacity services for fixed roof-top reception, but also to allow the reception of the TV signal under mobile conditions. The system was Coded Orthogonal Frequency Division Multiplexing (COFDM) based; it split the digital data stream into a large number of slower digital streams, each of which digitally modulated a set of closely spaced adjacent sub-carrier frequencies. It was firstly broadcasted in the United Kingdom (UK) in 1997 and in the following years

its implementation has been quite successful covering regions in Europe, Asia and the Middle East.

The physical layer of the North American standard differs completely from the European one. The main reasons behind that dissimilarity can be placed in the regulatory and market differences between the two continents. The standardization committee named as Advanced Television System Committee (ATSC) was created in 1982 by the former member organizations of the Joint Committee on Intersociety Coordination (JCIC), and the standard was approved by the Federal Communications Commission (FCC) in 1996 [18]. The main characteristic that made ATSC unique among other first generation standards was that it was not a COFDM system. As a matter of fact, instead of a multi-carrier system, it employed a single carrier system: an AM modulation of the digital content that has been previously mapped following an 8-VSB scheme. It was chosen because it was supposed to have some advantages in terms of power consumption both on the transmitter and the receiver sides. In addition, thanks to the continuous advance of equalizing techniques, the attainable performance of 8-VSB in multipath channels was supposed to be close to OFDM, although a more complicated scheme must be implemented. However, the single carrier system had also its own particular drawbacks. For instance, the single carrier mode did not allow the deployment of Single Frequency Networks (SFN).

Although the Japanese public broadcaster's (NHK) willing for transmitting HDTV employing digital technology can be traced back to the 80s, the specification for the digital terrestrial system, ISDB-T, was not approved by ARIB until 1998 [19]. During the physical waveform definition, there were two main constraints for the system to be satisfied. First, due to the scarce resource of frequency spectrum, a more efficient system was required; and second, the conveyance of HDTV was a challenge with which the Japanese broadcasters had been struggling for too long. Like DVB-T, ISDB-T is also a COFDM system, but it has some substantial differences. For instance, ISDB-T can only be employed in a 6 MHz channel and it was designed as a Band-Segmented Transmission OFDM (BST-OFDM). Therefore, the entire bandwidth is divided into 13 basic frequency blocks called segments, having each one the capability to use different modulations and coding configurations. Thus, it can be used to integrate different services in just one RF channel, for instance, 1 HD service (12 segments) plus 1 mobile TV program (1 segment) or 4 SDTV programs (4 segments). Therefore, it can be considered as one of the first attempts to deliver simultaneously mobile and stationary services.

In China, the development of the digital television system started on 1996, but it was not until 2006 when the Government published the first digital terrestrial television standard known as Digital Terrestrial Broadcast (DTMB)[23][24]. It was an important milestone for the international telecommunication market as China is one of the largest consumer groups with even a 30% of the total TV households over the world. During the standardization process the final candidate was selected among other competitors such as Advanced Digital Television Broadcasting or Terrestrial Interactive Multiservice Infrastructure (TiMi). It was designed to offer both stationary and mobile services, with a variable throughput which can vary from 4.8 Mbps up to 32.5 Mbps. The system is OFDM based, and therefore, it supports both multiple and single frequency networks.

To sum up, TABLE 1.1 gathers the main characteristics of the physical layers of the first generation standards, including the source coding algorithms and the main parameters of the physical waveforms.

TABLE 1.1. Main characteristics for the four first generation DTT systems [21].

	ATSC 1.0	**DVB-T**	**ISDB-T**	**DTMB**
		SOURCE CODING		
Video	MPEG-2	MPEG-2	MPEG-2	MPEG-2
Audio	Dolby AC-3	MPEG-2 Dolby ATC3	MPEG-2 AAC Audio	
		TX SYSTEM		
Outer Coding	R-S	R-S	R-S	R-S
Inner Coding	Trellis code (Rate 2/3)	Punctured Convolutional Code	Punctured Convolutional Code	LPDC
Code Rate	$\frac{2}{3}$	$\frac{1}{2};\frac{2}{3};\frac{3}{4};\frac{5}{6};\frac{7}{8}$	$\frac{1}{2};\frac{2}{3};\frac{3}{4};\frac{5}{6};\frac{7}{8}$	$\frac{1}{2};\frac{3}{4}$
Modulation	8-VSB 16-VSB	QPSK 16-QAM 64-QAM	DQPSK QPSK 16-QAM 64-QAM	QPSK 16-QAM 32-QAM 64-QAM
GI	-	$\frac{1}{32};\frac{1}{16};\frac{1}{8};\frac{1}{4}$	$\frac{1}{32};\frac{1}{16};\frac{1}{8};\frac{1}{4}$	$\frac{1}{9};\frac{1}{7};\frac{1}{4}$
FFT sizes	-	2k,8k	2k,8k,32k	4k
Bit Rate (Mbps)	19.63	5-30	3.65 - 23.23	4.8-32.5

1.2 **The World towards Mobile Generation**

By the early nineties, it was observed that the consumer habits were evolving very fast toward handheld and mobile devices. As a matter of fact, the popularity of mobile phones clearly pointed the way forward for the broadcasting industry.

For instance, by 2014 the number of mobile subscriptions is expected to almost reach the global population figure. In other words, during the following years, there will be nearly as many mobile-cellular subscriptions as people in the world, or even more [20]. For instance, according to the market results in 2011, for the first time in their history, the number of sold smartphones overtook personal computers. In addition, as it can be seen in Figure 1.1 the usage of video content on mobile phones is entering a new phase, with customers increasingly asking for video access on their mobile devices. As regards the future, it is expected that the global mobile data traffic will increase 11-fold between 2014 and 2018, and thus, the users' expectations are continuously increasing looking for higher quality services. For example, the China Multimedia Mobile Broadcasting (CMMB) standard has been an overnight success, estimating that for 2014 more than 20% of the users will be using this mobile TV platform.

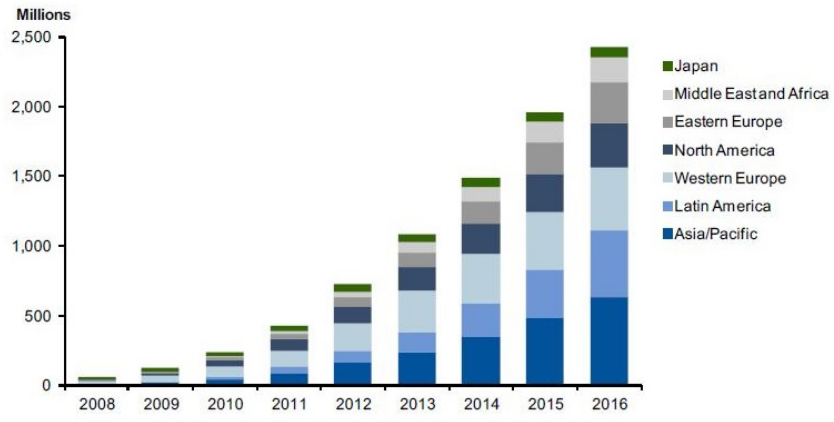

Figure 1.1. Expected mobile video exponential growth for the following years [22].

In general, there are three major technology groups that might satisfy the growing demand for mobile video services. The first option comprises the mobile operators (LTE), the second one broadcasting industry, and the third one the wireless broadband technologies (mobile WIMAX). According to this, and in order to not get driven out of the market by direct competitors, the broadcasting industry should come with a competitive solution. What is more, tt must be ready to target the new market requirements and to expand the traditional service offer.

One of the first attempts at mobile broadcasting was the European DVB-H [25]. It is considered an upgraded version of DVB-T, designed to overcome the main drawbacks of its predecessor in the task of delivering portable services to handheld terminals. It was fully oriented to portable devices, such as mobile

phones, pocket PCs or digital assistants. Therefore, one of the preliminary conditions of the system design was the ability to reduce the power consumption, and consequently, the size of the batteries of these mobile devices. In addition, the indoor reception, where the multipath can be critical, performance was improved. Finally, in order to maintain the device's handiness the small built-in antenna size was taken into account. In order to cope with the previous impairments, the two main novelties presented on the standard were the Multi-Protocol Encapsulated data (MPE-FEC) and the time slicing [26]. The first was an attempt to increase the signal robustness, and the objective of the second technique was twofold: first, to reduce the power consumption of the device, and second, to enable a smooth frequency handover.

With the purpose of delivering high quality mobile services, in North America a set of solutions to solve the problems related to the mobile receptions were proposed. They proposed techniques were similar to the approaches taken before by their European colleagues. First of all, the ATSC M/H was designed to implement an independent mobile stream, which was protected with a more robust forward error correction that was able to provide a gain up to 13 dB compared to the stationary ATSC. Second, the standard also proposed a time slicing scheme that allowed the receiver to be dormant for a major part of the cycle, providing a great battery save. Additionally, it included H.264 (MPEG-4/AVC) for video coding, which permitted carrying up to 16 low capacity TV services (300-600 kbps) in one RF channel. The final version of the standard was approved in May 2009 and in many places it is also known as "ATSC mobile DTV" [27]. As in the DVB case, this mobile oriented standard is fully backward compatible with the existing first generation terrestrial digital television system.

Regarding the Japanese standard, as previously commented, ISDB-T divides the RF channel into 13 segments, being 12 of them used for various SDTV services or just one HDTV service, and the remaining segment is allocated for mobile TV. This is the origin of the 1seg service name. The total net data rate is around 416 kbps employing the most effective MPEG-4/H.264 AVC video coding algorithms.

Within the group of Mobile TV family there is also a video standard extension of the Digital Audio Broadcasting (DAB). The first broadcast mobile TV services of this kind were launched in Japan in October 2004 under the services of S-DMB using satellite services, and just one year later, T-DMB was launched in Korea. By the end of 2009, the T-DBM service had become the world's largest terrestrial broadcast mobile service with more than 20 million customers. The physical layer

structure was very similar to DAB, and as a matter of fact, T-DBM has been considered as an enhancement of DAB, which allows the employment of MPEG-4 as source video coding algorithm.

Last but not least, amongst the Asian standards there is also another OFDM based system: the China Multimedia Mobile Broadcasting (CMMB). It was formerly known as STiMi (Sattellite Terrestrial Interactive Multiservice Infrastructure) and it was created by the Chinese broadcasting authority SARFT (State Administration of Radio Film and Television). It can be considered a hybrid standard, as both the *S* band and the terrestrial transmission are specified in the standard. In addition, the OFDM frame structure permits the broadcaster to implement both SFN and MFN networks. During 2008 Summer Olympic Games there was a nationwide program that boosted the use of this technology, and as a consequence, since then it has become a popular standard.

In short, TABLE 1.2 gathers the main characteristics of the previously presented standards, including the main source video coding algorithms and physical waveform characteristics.

TABLE 1.2. Main characteristics for the first generation mobile standards.

	ATSC M/H	**DVB-H**	**T-DMB**	**1seg**	**CMMB**
		SOURCE CODING			
Video	H.264	H.264	H.264	H.264	MPEG-2
Audio	HE-AAC	HE-AAC	HE-AAC	HE-AAC	
		TX SYSTEM			
Outer Coding	R-S	R-S	-	R-S	R-S
Inner Coding	Trellis code	Punctured Conv. Code	Turbo Codes	Punctured Conv. Code	LDPC
Code Rate	2/3	$\frac{1}{2};\frac{2}{3};\frac{3}{4};\frac{5}{6};\frac{7}{8}$	$\frac{1}{2};\frac{2}{5};\frac{1}{3};\frac{1}{4}$	$\frac{2}{3}$	$\frac{1}{2};\frac{3}{4}$
Modulation	8-VSB	QPSK 16-QAM 64-QAM	DQPSK	DQPSK QPSK	BPSK QPSK 16QAM
GI	-	$\frac{1}{32};\frac{1}{16};\frac{1}{8};\frac{1}{4}$	-	$\frac{1}{32};\frac{1}{16};\frac{1}{8};\frac{1}{4}$	
FFT sizes	-	2k,4k,8k	-	2k,8k,32k	1k,4k

1.3 **Digital Switch Over and Digital Dividend**

The spectrum regulation is based on allocating parts of it to particular services, such as broadcasting, mobile services, fixed services, aeronautical navigation, radars and so on[28][29]. Occasionally, it may also be the case where a given piece of the spectrum is shared by more than one service. As the distribution of the spectrum among international partners and services can be quite troublesome, the subject is normally managed by international bodies and organizations: International Telecommunications Union (ITU), European Commission (EC), the Federal Communications Commission (FCC), etc. Their main responsibility is to specify the conditions under which the spectrum can be shared based on the main characteristics of the provided service. In few words, they are in charge of the spectrum regulation all over the word.

The first step for this regulation, and one of the most relevant international frequency plans in the recent history of telecommunications, was discussed in Stockholm in May of 1961[30], when more than a 90% of the country members of the European Broadcasting Area met to discuss a European level frequency plan for FM and television in the VHF (30-300 MHz) and UHF (300-3000 MHz) bands. After nearly thirty years, in 1989, the next milestone for the international frequency plans was held in Geneva, where a more ambitious plan which included Europe, the whole Africa and some countries in Asia was presented, gathering a total of 71 participating states. Even if the resultant plan contained more than fifty thousand assignments, more than 1483 cases were left unsolved [31].

The plan that suppressed ST61 in Europe and GE89 in Africa was the GE06, which was established according to the terms agreed in two conferences held in 2004 and 2006 in Geneva. The first petitions to the ITU to consider replacing the outdated frequency planning were sent in 2000, jointly with the definition of the first digital television European standard DVB-T. Companies and broadcasters were seeking a rapid introduction for a fast digitalization of the market. After some discussions, the decision was taken to convene a Regional Radiocommunication Conference (RRC) for the revision of the Stockholm Agreement including the services in Region 1 (parts of the Region 1 to the west of meridian 170° E and to the north of parallel 40° S) and the Islamic Republic of Iran, for bands 174-230 MHz and 470-862 MHz. Furthermore, they also decided that the analogue transmission would be granted until the digitalization transition was finished. Additionally, Bands III, IV, and IV will not be exclusively used for broadcasting, and therefore, the overall plan should take into account the protection of other services: fixed, mobile, aeronautical, etc. Finally, another major decision at RCC-06

was to fix a deadline for the transition from analog to digital television: they agreed that the transition should be met by June 2015, even though some non-European countries could delay it until 2020 [2].

As it has been stated before, the most important consequence of the digital switch-over agreement was the digital dividend. A straightforward definition can be given making reference to the increase of transmission capacity; in short, the capacity of a single analog TV service in a 8 MHz channel was risen to 3-4 digital TV programs over the same space [32]. Therefore, only about the 25% of the previous spectrum was needed to accommodate all the existing services, and therefore, 66-75% of the previously occupied channels were assigned to different services.

This issue and the continuous growth of the mobile market drove many spectrum authorities to reclaim part of the terrestrial broadcasting spectrum for auction to satisfy the growth demand of broadband wireless services [33]. The ITU has kept conducting every three to four years a World Radiocommunication Conference (WRC) to revise the ITU-R Radio Regulations (RR) for the entire electromagnetic spectrum relevant for telecommunication services ranging from 9 KHz to 1000 GHz.

The first WRC after the GE06 agreement was carried out in 2007 in Geneva. In principle, it was stated that the investigations of the assignations of the upper part of the UHF spectrum (470-862 MHz) after the digital switch-over were still ongoing, and therefore, it was premature to request the allocation for mobile services in that band. Furthermore, although the main idea was to delay the decision until the next WRC, it was finally agreed to co-allocate mobile services at the 790–862 MHz band in Region 1 [3]. In Region 3, the entire UHF band was allocated for mobile services, while in Region 2 mobile services could be accommodated down to 614 MHz. Five years later, in 2012, the ITU took a step forward and in the WRC-12 it was proposed to allocate the frequency band 694-790 MHz on a co-primary basis to mobile services [4].

In short, it seems that this trend will be maintained during the following years, and consequently, the available spectrum for broadcasting services will be decreasing more and more.

1.4 New Generation Broadcasting Systems

It is widely agreed that this is the golden age for mobile devices, whether tablets or smartphones. Being a very active market, it is expected that the broadcasting industry should evolve substantially at least to match the pace of this new era, not only switching from analog to digital, but also offering high quality contents with full connectivity. The main difference with the previous requirements is that due to the new mass media, the users want now to experience HDTV or even UHDTV services on the move or even in the personal devices when they are at home. These demands lead to a twofold impact. First, the content providers are being forced to generate high quality contents for handheld devices, and second, the broadcasters are being pushed to include new broadcasting standards in their deployed networks in order to cope with those throughputs.

As commented before, even if some mobile television services have been considered successful (CMMB, T-DMB), the truth is that the vast majority of them have experienced minimal or null implementation (DVB-H, MEDIA-FLO…). According to the experts, the actual design of mobile services, which have a physical structure completely different from that of the stationary terrestrial services, can be pointed out as one of the main reasons behind this unsuccessful deployment. Probably, that is why the recently developed efforts are focusing on the generation of composed data frames that will be able to carry simultaneously the protected mobile services and high-capacity stationary programs over the same RF channel. This approach has the huge advantage of introducing a new capability, the mobile service, over an already deployed network.

1.4.1 DVB-T2

The main goal of the DVB community when they issued the second generation standards was not only to give answer to the challenge of delivering higher throughputs, but also to include in the physical layer some of the most advanced techniques that were out of the first generation. Nevertheless, the backward compatibility should be maintained, and thus, the existing domestic antennas and transmitter structure should be reused. In addition, the capability to deliver mobile services for handheld devices should be enhanced.

DVB-T2, as the rest of the standards gathered in the DVB family, chose OFDM for the physical modulation. As for the Forward Error Correction (FEC), it set aside the convolutional codes and implemented a concatenated version of Low Density Parity Check (LDPC) and BCH codes [34]. In order to increase the

throughput, the new standard also looked for an overhead reduction, and therefore, new signalling procedures and pilot patterns were presented. Another important feature of this system was that it included some techniques to reduce the Peak to Average Ratio (PAPR), one of the main drawbacks of OFDM systems. Thanks to these updates, and many more, the maximum system throughput for DVB-T2 was increased up to 50 Mbps. Another important novelty introduced in DVB-T2 was the concept of the Physical Layer Pipes (PLP), which allow service-specific robustness with different coding and modulation schemes within the same frame. This feature can be understood as a very first attempt to deliver simultaneously mobile and stationary services based on the Time Division Multiplexing (TDM).

Moreover, the last update to the standard has been to incorporate a new profile known as LITE, which is basically designed to deliver mobile services to the final user. The silicon footprint required for this profile demodulation is about the half of that of DVB-T2, due to the reduction of the required configuration parameters to a minimum. For instance, the LDPC codeword is always fixed to 16K, the 256-QAM option is removed and some pilot patterns are not included. In addition, the compulsory power consumption saving is easily achieved thanks to the time slicing capability provided by the multiple PLPs. In this profile, among other minor improvements, a lower code rates and smaller maximum interleaving size is also included.

1.4.2 NGH

The LITE profile can be considered as a patch to a system that was primarily considered for stationary reception (DVB-T2). Actually, since the first generation attempt (DVB-H), it was not until the NGH CfP when the DVB consortium bet heavily again on the design of a mobile broadcasting system. The DVB-NGH Call for Technologies was issued in 2009 [35], and 6 months later, the Commercial Requirements were launched [36], being one of the main targets the capability to be merged with DVB-T2 in one RF channel. This approach could be easily achieved through the use of the DVB-T2's Future Extension Frames (FEF), and that is the reason why, DVB-NGH is strongly inspired by the second generation standard.

According to the call, "*to facilitate this Rich media content consumption, an efficient, flexible and robust Next Generation Handheld (NGH) system is needed to accompany digital switch over and convergence of fixed and mobile services as well as telecommunication services*." In other words, NGH had to provide an extent to DVB-T2 capabilities, enhancing

the user mobile experience. In order to do that, it incorporated some of the new most promising technical novelties, such as Scalable Video Coding (SVC), Time Frequency Slicing (TFS), MIMO, etc.

Furthermore, in the resulting bluebook that gathered several years of work, the previously existing block time interleaving is improved, a hybrid satellite profile is added and the signalling overhead is reduced, while increasing its robustness. Finally, it also presents some new techniques for reducing the PAPR and allows the use of local services for local contents. More technical details can be consulted in [37]. Although the system was defined to have commercial devices available on the market in 2013, the truth is that the standardization process has been delayed due to the definition of the DVB-T2 Lite profile and the not very successful attempt to have an active cooperation with 3GPP.

1.4.3 Enhanced Multimedia Broadcast Multicast Service (eMBMS)

This is a solution that can be considered as a point-to-multipoint interface specification for 3GPP cellular networks, which is designed to provide an efficient delivery of broadcast and multicast services. In fact, it was defined to overcome the potential limitation of the 3G networks for unicast streaming of high-usage TV traffic. It is designed to allocate part of the spectrum (or some carrier resources) to the multicast transport channels in each cell, and that way, deliver both the unicast and multicast channels. Currently, eMBMS is supported for all defined bandwidths of LTE, including Frequency Division Duplexing (FDD) and Time Division Duplexing (TDD). In addition, it is defined for one effective transmitter antenna and two receive antennas, as the obtained MIMO gain for broadcast services is not as big as expected.

Nevertheless, this solution as currently specified in Release 9 [38] has several limitations when compared with current broadcasting systems. For example, the coverage ratio for LTE unicast data is very small (about 5-10km), whereas in broadcasting transmission this value can be notably increased. Another major difference may be the nonspecific presence of a time interleaver for LTE broadcast mode [39][40].

1.4.4 ATSC 3.0

Although the new generation standards are a good attempt to improve the classical problems of the broadcasting services, the truth is that there are still several challenges that remain unsolved. For instance, even if the mobile reception

and spectrum efficiency have been improved, they are not good enough to compete with other solutions [41].

In 2013, the ATSC 3.0 call for proposals was issued with a roadmap designed to have a finalized standard in 2015, with tight requirements for an efficient use of the broadcasting bands and better worldwide compatibility. The proposed new system should be able to deliver Ultra High definition (UHD) services on mobile devices, improving the reception robustness and the spectral efficiency [6][42]. Additionally, there is also a mandatory request for providing both mobile and stationary services simultaneously.

Regarding the increase of the spectral efficiency, it must range from 0.5 bit/Hz/s to 10 bit/Hz/s allowing multiple levels of content. Moreover, the previous generation data rate payload should be increased in a 30% and the required minimum receiving threshold must be reduced. In relation to the network design, it should allow the implementation of SFNs and it should be very flexible. As a future standard, it should guarantee mobile reception, while preserving the device battery. In short, it should overcome all the drawbacks that the current broadcasting systems have, offering high quality mobile services, while pushing the spectrum efficiency to the limit.

1.4.5 FOBTV

The FOBTV consortium (Future of Broadcast Television), founded by most of the relevant broadcast stockholders in Asia, Europe and America, is the most remarkable initiative towards the worldwide harmonization of broadcast technologies [43]. It was originally founded by 31 leading television broadcast organizations in 2011. Nowadays, its members represent broadcasters, manufacturers, network operators, standardization organizations, research institutes and others in more than 20 countries all over the world. According to this initiative, the broadcasting technology is "the most spectrum-efficient wireless delivery means for popular real-time and file-based media content". Therefore, appropriate technologies for next-generation terrestrial broadcasting systems must be developed taking into account business, regulatory and technical environments.

2. MOTIVATION OF THIS THESIS

After explaining the current situation of the DTT, it is clear that this is the right time, the perfect breeding ground for research studies willing to provide technical solutions for the new generation broadcasting systems. As a matter of fact, the industry is confronting one of the toughest periods of its recent history. Above all, it is repeatedly being accused of inefficiency in the spectrum management; secondly, it is also argued that systems are not able to deliver high throughput mobile services; and finally, it is also blamed for using outdated technologies. The main motivation of this thesis is to offer new technical solutions to overcome these problems, helping the broadcasting industry succeed into the new generation field.

In particular, the starting motivation of this thesis was to provide an alternative for the main weakness associated with broadcasting: the incapability for offering high quality services under mobile or indoor scenarios. Indeed, the problem of delivering HDTV or UHDTV services for mobile devices has not been fully satisfied yet, even though some of the latest standards, such as NGH or CMMB have already made a qualitative leap forward in the development of mobile broadcasting.

The second driving force for carrying out this work was another pressing issue that many authorities are pointing as crucial: the spectral inefficiency attributed to the existing broadcasting systems. As matter of fact, this work intends to find a more efficient way for multiplexing mobile and stationary services simultaneously over the same RF channel. This will be a key point for the future development of the new generation standards. In fact, it is one of the key requests of the newly released ATSC 3.0 proposal [6]: "*A primary goal of the ATSC 3.0 PHY layer is to provide TV service to both fixed and mobile devices. Multiple types of TV receivers, including fixed devices (such as traditional living room and bed room TV sets), handheld devices, vehicular screens and portable receivers will be considered*".

Additionally, it must be taken into account that this is the perfect time to be part of the research work which will help to the modernization of broadcasting technologies. The communication world is entering into the new era of mobile data consumptions. The most important broadcasting consortiums have answered to this challenge with several calls for updating their physical layers. In fact, within the development of the ATSC 3.0 physical layer, and the FOBTV initiative, a great group of breaking ground techniques has been proposed to pave the way for this change. Therefore, is there a better motivation for carrying out a PhD study that

tries to be part of the most recent turning point in the history of the broadcasting systems?

The window of opportunity is fully open, and one of the most ambitious motivations of this thesis was to be able to contribute to the standardization of the next generation broadcasting systems. Usually, there are no many opportunities to take part in the development of an international standard with companies that are world leaders in the telecommunications field. What is more, this occasion is unique, as there are two different standards that are being defined at the same time.

3. OBJECTIVES

Once the state-of-the-art and the motivation of this work have been explained, the next step is to clarify the main scope and the secondary objectives that have helped to organize the work. The **main objective** is to **provide technical solutions for an efficient and flexible usage of the terrestrial broadcasting spectrum for both stationary and mobile services**. In particular, this PhD thesis is organized to attain the subsequent partial objectives:

- **Study mobile broadcasting reception.** Current systems are not capable of satisfying the customers' demands for higher quality service delivery on handheld devices. What is more, in terms of efficiency they are way behind other technologies, such as satellite or broadband services. Therefore, the first part of this thesis is focused on analysing the broadcasted signal behaviour over time-varying channels. In order to do that, the following secondary objectives have been defined:
  - Present a theoretical analysis of the mathematical basis of the OFDM physical waveform over time-varying channels.
  - Study and evaluate in depth one of the most used solutions for increasing the spectrum efficiency over mobile channels: the doubly dispersive equalization techniques.
  - Propose a new equalization algorithm, which should improve the previous analyzed performance minimizing the required SNR threshold.

- **Propose an alternative approach for improving the efficiency of mobile reception.** The inter-carrier interference (ICI) due to the Doppler Effect is one of the main constraints for mobile receivers. Therefore, the OFDM symbol length is defined as small as possible with the purpose of minimizing the orthogonality loss due to the Doppler noise. This may lead to a non-efficient use of spectrum as the required guard interval duration overhead is larger for small FFT sizes. Therefore, the second objective is to find an alternative approach that may overcome that drawback. The associated partial objectives are:
  - Study theoretically the ICI impact on the receiver performance over time-varying channels.
  - Analyze the existing solutions for improving the penalty due the orthogonality loss.

  - Demonstrate through practical simulations the feasibility of the proposed technical contribution to cope with the Doppler Effect in OFDM systems.

- **Propose a more spectrum-efficient and flexible solution for offering simultaneously stationary and fixed services.** One of the reasons behind the commercial weakness of the first generation mobile broadcasting services was the need of implementing an independent content network. Consequently, a good approach for introducing mobile services is to propose a new solution for multiplexing them with the already existing stationary terrestrial television ones. The partial objectives within this third main goal are:

  - Find a more spectrum-efficient multiplexing technique for multiplexing stationary and mobile services.
  - Analyze theoretically the gain offered by the proposed multiplexing technique in terms of spectrum efficiency and flexibility.
  - Present a complete test bench for evaluating the proposed alternative. It will range from the more theoretical simulation results to more practical field trials.
  - Test the feasibility and study the performance of the presented new multiplexing technique.

As previously mentioned, all the research efforts presented in this thesis aim to contribute to the most important international consortiums that are now working on the next generation standards. In particular, the definition of the new ATSC 3.0 standard, the DVB technical studies towards the definition of an evolved terrestrial broadcasting system, and finally, the activities carried out inside the FOBTV international forum.

4. ORGANIZATION OF THIS DOCUMENT

This thesis will provide technical solutions for an efficient and flexible usage of the terrestrial broadcasting spectrum for the simultaneous transmission of both stationary and mobile services.

Chapter I. The main problems that cast doubt upon the future and sustainability of the digital terrestrial broadcasting systems are addressed. In addition, the main motivations for this research work and the related objectives are presented.

Chapter II. This chapter includes the theoretical characterization of the physical basis of time varying channels. In addition, it outlines the state of art of the existing solutions for improving the reception over mobile scenarios, and moreover, it presents a comprehensive study of their performance. All the mathematical concepts described here are essential for the understanding of the following work.

Chapter III. In this part, two main proposals for improving the reception over rapid time-varying channels are presented. The first one is based on the solutions presented in the previous chapter, whereas the second one presents a more novel approach.

Chapter IV. This chapter introduces a new broadcasting solution for the current mobile needs: the Layered Division Multiplexing (LDM), which grew out of the concept behind the Cloud-Txn approach. Apart from the main theoretical descriptions of the technique, a capacity gain comparison with other multiplexing techniques is presented.

Chapter V. The most practical aspects of the LDM practical implementations are studied in this chapter, including the main algorithms and technologies required at the receiver site for multiplexing stationary and mobile services are described.

Chapter VI. A complete Evaluation & Validation Platform (EVP) for studying the LDM feasibility and its performance boundaries is described in this chapter. Specific validation methodologies are defined and different studies are carried out, ranging from the most theoretical analysis to the more practical field trials.

Chapter VII. This last chapter summarizes all the concepts that have been mentioned through the work, highlighting the main contributions of this thesis and outlining the most remarkable conclusions that have been obtained. Future research topics, related with the results obtained in this work, are also presented.

The beginning is the most important part of the work.

-Platon

CHAPTER 2: **CHARACTERIZATION OF TIME-VARYING CHANNELS AND COMPREHENSIVE ANALYSIS OF THE EQUALIZATION TECHNIQUES**

This chapter deals with the daunting challenge of answering the customers' demands for higher quality on the digital broadcasting mobile services. In order to do that, first of all, the time-varying channel behaviour is theoretically analyzed both from a physical and mathematical points of view in order to get the required mathematical knowledge. This approach will offer the basis for identifying every single distortion process involved in the mobile channel reception, and consequently, it makes the implementation of the "divide and conquer" strategy for finding a technical solution easier.

Additionally, this chapter includes a comprehensive literature review of one of the long-established solutions for overcoming the issue of time-varying channels: the removal of the Inter Carrier Interference (ICI) through the usage of channel estimation and equalization algorithms specially designed for doubly dispersive channels. The whole mathematical formulation presented in this part is not only useful to understand the differences between the presented methods, but also critical to understand the techniques proposed in the following chapters.

1. THEORETICAL DESCRIPTION OF TIME-VARYING CHANNELS

1.1 Physical Basis

The existing broadcasting networks are usually planned following a point to multipoint scheme, where a static tower conveys the digital TV signal information to all the receivers located in the surrounding areas. As it can be seen in Figure 2.1, if the transmitter and the receiver antennas are in view of each other, the scenario is considered as Line of Sight (LOS), whereas when the path is partially obstructed and the electromagnetic waves are not directed to the receiver, the propagation is classified as Non Light of Sight (NLOS). This is the typical scenario of urban environments, where a high density of buildings and other kind of obstacles between the transmitter and the receiver are very common.

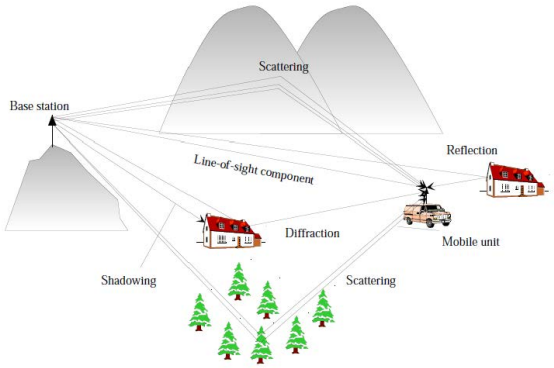

Figure 2.1. Graphical example of a point to multipoint broadcasting service [44].

Either way, the behavior of the transmitted radio waves is always determined by the Maxwell's equations according to the propagation environment [45]. Nevertheless, normally is unfeasible to solve those equations, due to the fact that the wave interacts with a large amount of dielectric or conducting objects, increasing the solution complexity exponentially, even if the scenario is already known. These interactions, commonly classified as reflections, diffractions and scattering, are the main sources of distortion for the electromagnetic wave. When the dimensions of the obstacles are much larger than the signal wavelength, the incident plane waves lead to the reflection phenomenon, whereas if the obstruction dimensions are on the order of a wavelength or less, the energy is redirected in many directions causing a scattered wave. Finally, according to Huygens-Fresnel's

principle [46], diffraction occurs when there is a blocking object in the receiver path and secondary waves are generated behind the obstruction [47].

1.1.1 Multipath

In general, there are always multiple obstacles in the transmission path, and therefore, the transmitted radio waves propagate along several different ways that terminate at the receiver. There the signal is presented as the sum of various copies of the transmitted signal, being each of them affected by different delay and phase values.

This physical phenomenon is known as multipath and a very clear example is depicted in Figure 2.1. Multipath is usually stronger in mobile communications, since the receiver antenna is usually located at low heights surrounded by obstacles; and what is more, omnidirectional antennas are typically used, which amplify a larger number of reflected echoes.

At the receiver, the different signal copies can be constructively or destructively added depending on their phases. Moreover, due to the different delays of the propagation paths, the receiver observes a spreaded-out version of the original signal, and that is why, these channels are also known as time-dispersive. According to the Fourier theorem, this time-dispersive behaviour has a multiplicative effect on the frequency domain; in other words, the time-dispersive channels can be also understood as selective channels in the frequency domain because each frequency is attenuated in its own way.

At the receiver site, the distortions caused by multipath are usually compensated by the equalizer, which has an estimate of the channel gains provided by the channel estimation process. It must be borne in mind that this process is much more critical for mobile environments, as shown in the following sections.

1.1.2 Doppler Effect

In a real communication scenario the multipath propagation is not the only source of distortion. There are other dispersion sources, for instance, the Doppler Effect, which is generally associated with the receiver mobility, but it can be also linked to the transmitter movement or non-static channel reflectors. Through this thesis the Doppler Effect should be understand as any distortion at the receiver related receiver mobility. Based on this definition, nowadays the overwhelming majority of the channels can be considered as time-varying, due to the fact that

there is always a non-static element involved in the communication chain. Nevertheless, there is another condition that must be satisfied prior to consider a channel as non-static: the time alterations must be faster than the system transmission rate. Thus, when the channel characteristics change, but the speed is inferior to the data rate, the system is considered to be time invariant or static.

From a physical viewpoint, the channel variability entails a frequency shift in each of the multipath components. The arrival angle α_n, which is defined as the angle of the n^{th} ray, compared to the receiver speed vector, determines the Doppler frequency shift f_n of the n^{th} incident ray and can be defined by (See Figure 2.2):

$$f_n = f_{\max} \cos(\alpha_n) \tag{2.1}$$

where the maximum frequency shift f_{max} depends on the mobile receiver speed (v_0), the speed of light (c_0) and the carrier frequency f_0:

$$f_{\max} = \frac{v_0}{c_0} f_0 \tag{2.2}$$

The sum of the different shifted rays that arrive to the receiver is known as the Doppler Power Density Spectrum, and it is one of the functions that characterize the frequency distortion due to the receiver mobility. Finally, it is important to note that the superposition principle applies to mobile channels, and therefore, they can be treated as linear channels.

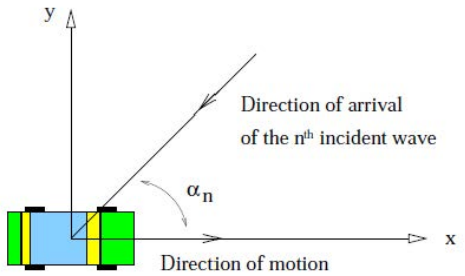

Figure 2.2. Graphic representation of the angle of arrival, which determines the Doppler frequency value [44].

1.1.3 Mathematical formulation

The vast majority of studies agree on considering the time-varying channels as Wide-Sense Uncorrelated Scattering (WSSUS), that is to say, the second-order moments of the channel are stationary and the different paths are uncorrelated. Nevertheless, the objective of this section is not to describe in detail the physics of the channel, but to describe its nature from a communication point of view [44][48][49].

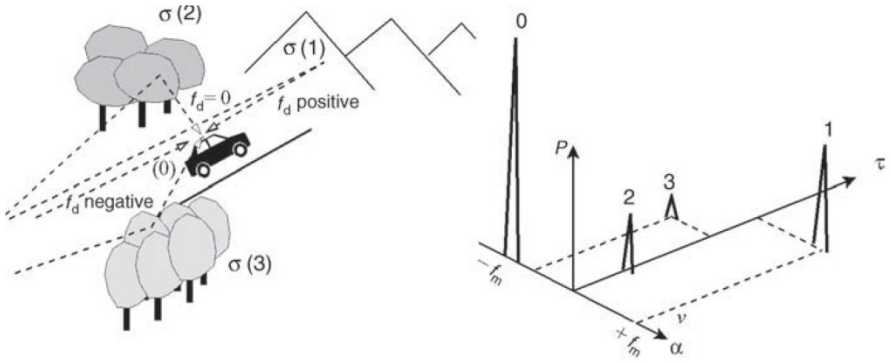

Figure 2.3. Graphical example of a mobile scenario and the correspondent scattering function [49].

In Figure 2.3 the left side proposes a visual example of a mobile receiver scenario, whereas the one on the right describes the scenario in mathematical terms based on the Doppler Shifts and delays of each path. For instance, the direct line of sight produces a high power peak with a null delay and a negative Doppler shift equivalent to $-f_m$ Hz, while the long distance echo from the hills is shifted f_m Hz. The third contributor is an echo from the woods, which is located perpendicularly to the receiver, without any frequency shift. Finally, there is an incident ray coming from the other trees in the left side with a smaller Doppler frequency.

The previous figure was a clarifying example; however, in order to produce a formula to express the physical behavior of the signal over a time-varying channel, the starting point is restricted to a simpler scenario with a transmitter under static multipath reception. According to signal processing basics [50], the relation between the transmitted signal, in its pass-band (x_{RF}) representation, and its associated complex envelope, (x_{CE}), is given by

$$x_{RF}(t) = \Re e\left[x_{CE} \exp\left(j2\pi f_0 t \right) \right] \tag{2.3}$$

where f_0 is the carrier frequency value. Using this complex baseband representation of bandpass signals greatly simplifies the notation for communication system analysis.

As it was stated, the channel is static, thus in a classical multipath scenario the receiver antenna collects a superposition of *N* attenuated and shifted copies of the transmitted signal; where d_i is the distance between the obstacle and the receiver, and τ_i, the time that the wave need to reach the receiver travelling at the speed of light (c).

$$y_{RF}(t) = \Re e\left\{\sum_{i=1}^{N} a_i x_{CE}(t-\tau_i)\exp\left[j2\pi f_0\left(t-\tau_i\right)\right]\right\} = \Re e\left\{y_{CE}(t)\exp\left(j2\pi f_0 t\right)\right\} \quad (2.4)$$

$$y_{CE}(t) = \sum_{i=1}^{N} a_i \exp\left(-j2\pi f_0 \tau_i\right) x_{CE}(t-d_i/c) \quad (2.5)$$

The amplitude and phase of the i^{th} path is represented in a_i, whereas the associated propagation delay is characterized by τ_i. Based on (2.4) and (2.5), the low-pass equivalent of the channel impulse response, h_{CE} , is given by

$$h_{CE}(\tau) = \sum_{i=1}^{N} a_i \exp\left[-j2\pi f_0 \tau_i\right]\delta\left(\tau-\tau_i\right) \quad (2.6)$$

Once the static multipath scenario is defined, the next step is to add another variable that will bring the mathematical formulation closer to the time-varying case: the Doppler Effect. Usually the received multipath components suffer from different Doppler shifts since the arrival angles and the velocities associated with the individual multipath components are typically different. Consequently, the time variability is represented by the receiver mobility (v_0) and by the angle of arrival α_i. Through the following equations, the existing frequency dispersion in the transmitted signal due to the presence of those shifts is shown. Providing that the time-variability is introduced in Eq.(2.7), the output signal expression is given by

$$y_{RF}(t) = \sum_{i=1}^{N} a_i \exp\left(-j2\pi f_0\left[\tau_i + \tau_i(t)\right]\right) x_{CE}\left(t-\left(\tau_i+\tau_i(t)\right)\right) \quad (2.7)$$

being the delays within the complex exponential attributed to the Doppler Effect:

$$\exp\left[-j2\pi f_0 \tau_i(t)\right] = \exp\left[-j2\pi f_0 \frac{V\cos(\alpha_i)t}{c}\right] = \exp\left[-j2\pi f_{d_i} t\right] \tag{2.8}$$

Hence, by using Eq. (2.3) and Eq. (2.8), the channel impulse response to the sum in Eq. (2.7) can be written as

$$h_{CE}(t,\tau) = \sum_{i=1}^{N} a_i \exp\left(-j2\pi f_0\left[t+\tau_i(t)\right]\right)\delta\left(t-\left(\tau_i+\tau_i(t)\right)\right) \tag{2.9}$$

In Eq. (2.9), the detailed theoretical definition of a time-varying channel is presented. The first variable, *t*, represents the observation time, and the second variable, τ, the delay. As explained before, these channels maintain the linearity condition, and therefore, they are also known as Linear Time-Varying (LTV). If Eq. (2.9) is compared with the static case in Eq. (2.6), the main difference is that the former is a two dimensional expression dispersive in both frequency and time domains, whereas the latter is just a one-dimensional frequency selective expression. From a signal processing point of view, Eq. (2.6) represents the channel response in a time, *t*, to an impulse transmitted τ seconds earlier. This expression does not depend on the observation time, and thus, it is just a function of the time difference between transmission and reception.

Nevertheless, when the channel is considered LTV (See Figure 2.4), the impulse response is also function of the observation time (t_i). Therefore, LTI channels can be understood as a special case of LTV channels, where the CIR maintains constant during all the observation time. Figure 2.4 represents the different amplitude values of the echo delays that compose the channel impulse response.

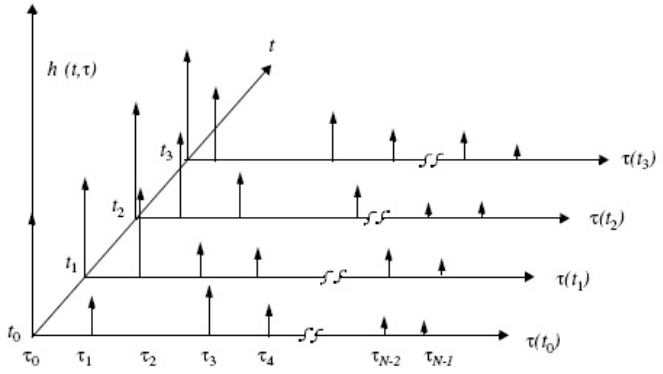

Figure 2.4. Example of a time-varying channel impulse response [48].

It can be seen how these values change as a function of the observation time, being this change the main characteristic of the time-varying channels.

1.2 **Channel System Functions**

Once the physical basis of the time-varying channel has been explained, the next step is to model its behaviour from a communication engineering point of view. The main idea is to define several functions that will contain as much as possible information related to the channel, both in time and frequency domains. This data will be very useful when it comes to the definition of new methods to cope with the time-varying channels degradation.

It must be borne in mind that, at the receiver site, after collecting the transmitted signal echoes, there is always an analog-to-digital converter. Therefore, from now on, the mathematical analysis will be carried out in the discrete domain. Let's suppose that defined channel impulse response defined in (2.9) has been sampled satisfying the Nyquist theorem [51]

$$h[n,l] = h_{CE}(t,\tau)\big|_{t=nT_s} \tag{2.10}$$

where T_s is the sampling time. As before, prior to shed light on the more complicated mobile scenarios, the easiest case will be explained: the LTI channel. The time domain description of a linear system is normally defined as the system time response in l to an impulse applied at n=0. In other words, l is the variable that represents the time offset between the application and observation time [52]:

$$y[n] = \sum_l h[l]x[n-l] = \sum_l x[l]h[n-l] \tag{2.11}$$

According to Eq. (2.11), the output signal, $y[n]$, can be represented in terms of a convolution between the input signal, $x[n]$, and the channel impulse response $h[l]$. As a matter of fact, the previous definition is the main difference with LTV channels, where the channel impulse response is characterized by $h[n,l]$, being defined as the system response to an impulse applied l samples before the observation time n. That is to say, within a frequency dispersive channel, the CIR changes its values depending on the observation time. In Eq. (2.12) the first

expression exemplifies the LTI case for two different observation times, whereas the expression below depicts the case for LTV channels where the CIR changes for each observation time.

$$\begin{aligned} h[n_1,l] &= h[n_2,l] = h[l] \\ h[n_1,l] &\neq h[n_2,l] \neq h[l] \end{aligned} \tag{2.12}$$

In Figure 2.5 the upper figure shows the case of a time invariant channel impulse response and it can be clearly seen that the shape of the function is the same, independently of the observation time. The lower figure shows the response for a time-varying case, and consequently, the CIR gains depends on the observation time.

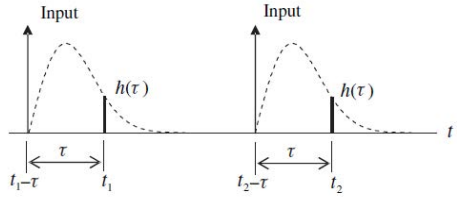

(a) Impulse response of time-invariant system.

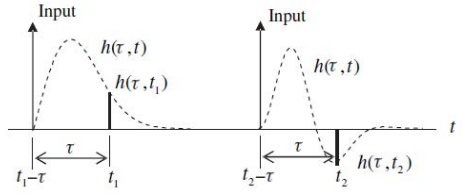

(b) Impulse response of time-varying system.

Figure 2.5. Graphical representation of the difference between LTI and LTV channels [44].

In Eq. (2.12) the variable *n* represents the observation time, in other words, the channel variability over each multipath component. Therefore, the input/output relation of a LTV channel in the time domain is given by

$$y[n] = \sum_l h[n,l]\,x[n-l] = \sum_l h[n,n-l]\,x[l] \tag{2.13}$$

$$h[n,l] = \begin{bmatrix} h[0,0] & h[0,1] & \dots & h[0,l] \\ h[1,0] & h[1,1] & \dots & h[1,l] \\ \vdots & \vdots & \ddots & \vdots \\ h[n,0] & h[n,1] & \dots & h[n,l] \end{bmatrix} \tag{2.14}$$

where $h[n,l]$ is the doubly dispersive channel impulse response. It depends on two different variables, and therefore, it must be represented as a matrix, instead of the usual vector notation (Eq.(2.14)). The horizontal axis of the matrix represents the different taps delay time, l, whereas the vertical axis is indicative of the observation time. In order to help to a better understanding of the bi-dimensional concept, the Figure 2.6 portrays the channel impulse response of a LTV channel.

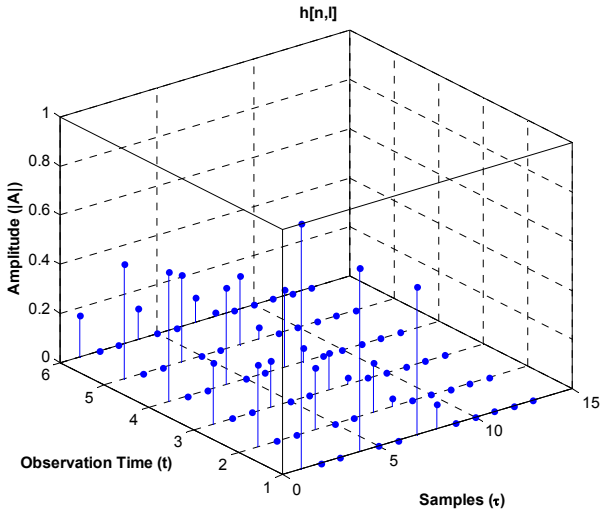

Figure 2.6. Graphical representation of a LTV channel impulse response.

In the case of LTI channels, it is already known that the input and output signals can be related not only in the time domain (CIR), but also in the frequency domain. Nevertheless, in the case of the mobile channels, as the channel definition depends on two variables, the input and output signals can be related to each other with another two variables. These new relations between variables were firstly described following the system functions introduced by Bello in 1963 [53], and since then, they have been crucial to understand the natural basis of the time-varying channels.

It must be noted that since every physical channel is causal, the following functions are not going to produce any impulse response until the channel is exited. Taking into account the previous consideration and if the N point Fourier Transform of the channel impulse response (2.14) for the variable n is calculated, the Scattering function $S[m,l]$ is obtained (see Eq. (2.15)).

$$S[m,l] = \sum_{n} h[n,l] e^{-j2\pi nm/N} \tag{2.15}$$

This function offers an insight into the distortion caused by the Doppler Effect that cannot be obtained with the other system functions. It is also called the Doppler-variant impulse response and determines the power of the Doppler spectra occurring along each path delay. That is to say, the value of the scattering function at a given point characterizes the overall complex attenuation and scatter reflectivity for each path. What is more, it describes the spreading of the conveyed signal in frequency domain. Figure 2.7 shows how representative it is, characterizing the different Doppler spectra amplitude (Z axis) and spread (Y axis) associated with each of the paths delay (X axis). In particular, the different path delays with the attached Doppler spectrums, which range from -50Hz to 50Hz are depicted.

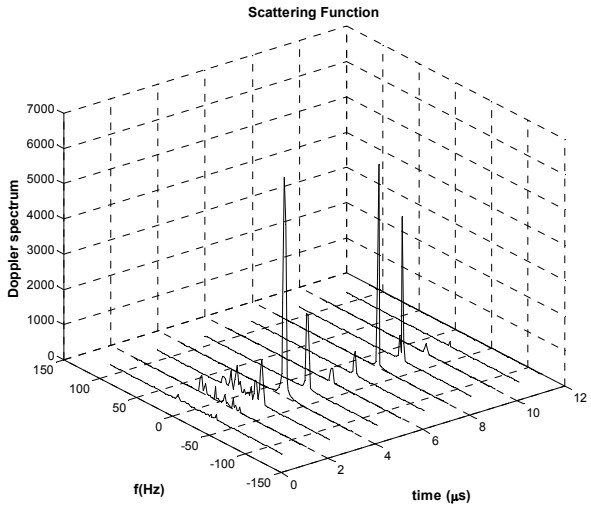

Figure 2.7. Example of a typical Scattering Function.

The LTV dispersion is twofold, on the one hand, the time selectivity causes frequency-dispersiveness, and on the other hand, the frequency selectivity causes time-dispersiveness. This dual selectivity is represented by the time-varying transfer function, $T[n,k]$, which is calculated applying the Fourier Transform over the delay variable of the channel impulse response:

$$T[n,k] = \sum_{l} h[n,l] e^{-j2\pi lk/N} \tag{2.16}$$

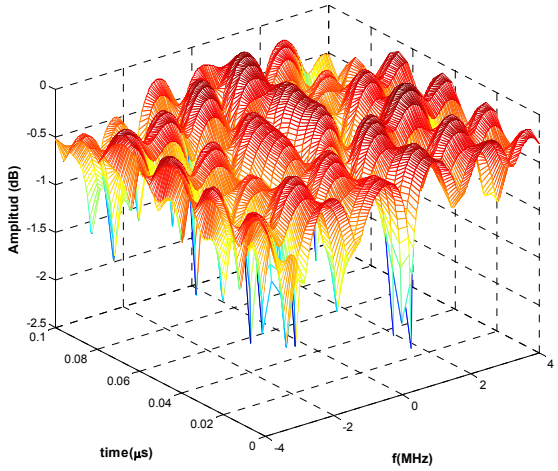

Figure 2.8. Time-varying transfer function of a mobile channel.

Figure 2.8 represents a real time-varying frequency response for an 8 MHz channel. Even although the amplitude changes depending on the observation time, it is does not provide any specific insight into the phenomena caused by the Doppler Effect. However, it offers a good hint about how difficult the channel estimation might be in those channels, as the frequency response changes from time to time, and thus, it may not be equal during adjacent symbols. For instance, in this type of channel it will not be possible to use a time-averaging window for reducing the noise floor.

Finally, $H[m,k]$ is the double Fourier Transform of $h[n,l]$, both in the observation and delay time. It is also called the Doppler-variant transfer function and is represented by

$$H[m,k] = \sum_{l}\sum_{n} h[n,l] e^{-j2\pi lk/N} e^{-j2\pi nm/N} \tag{2.17}$$

This is a key function for the time varying channel representation, as it will be shown in the next subsection. In short, it is the expression used to connect the input and output spectra of two signals over a time-varying communication channel. To sum up, Figure 2.9 represents the four deterministic functions that can represent a single time-varying LTV channel and their Fourier Transform relationship.

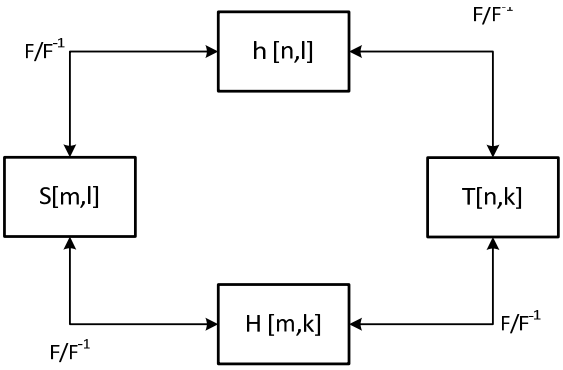

Figure 2.9. Fourier Transform between the four deterministic time-varying channel functions.

1.3 System Model

In this subsection, the physical basis and general properties of the time-varying channels will be transferred to a generic communication system model, which is based on OFDM for the physical layer waveform. Although its first uses date back to early sixties in the Bell laboratories [54][55], OFDM has been considered the waveform for encoding the last Digital Terrestrial Television (DTT) systems, such as the DVB family [56][57], the Japanese ISDB-T [58], LTE [59], WIMAX[60], or most recently, as the baseline waveform for the future ATSC 3.0.

The main objective of this generic implementation is to provide a communication environment able to test the channel time variability effects on an specific system: a generic terrestrial broadcasting system. The discrete baseband equivalent transmitter under consideration is depicted in Figure 2.10.

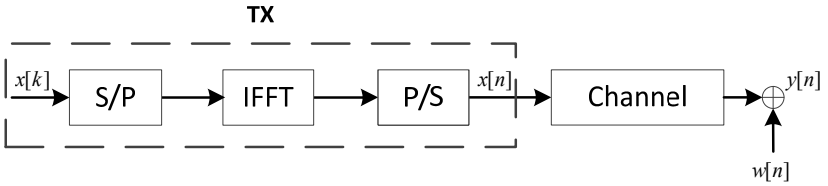

Figure 2.10. Equivalent baseband system transmitter and channel module.

Considering a data block of M-QAM-symbols $x[k]$ as the input data, the transmitted signal $x[n]$ is obtained after applying an N-point Inverse Fast Fourier

Transform (IFFT), where k represents the subchannel where the symbols have been modulated, as shown in Eq. (2.18).

$$x[n] = \frac{1}{N}\sum_{k=0}^{N-1} x[k] e^{j2\pi nk/N}, \quad 0 \le n \le N-1 \tag{2.18}$$

The second block accounts for the signal distortions due to the propagation channel, which acts as a time and spatial varying filter. The doubly selective fading channel is modelled as WSSUS, represented in the equivalent discrete-time domain [61]. The channel paths are generated as a set of independent, zero-mean, complex Gaussian white noise processes that are filtered by a Doppler filter according to the classical Jakes' spectrum [61]. Hence, assuming a causal discrete channel with maximum delay spread L shorter than the guard interval, the received signal $y[n]$ can be described as follows:

$$y[n] = \sum_{l=0}^{L-1} h[n,l]\, x[n-l] + w[n] \tag{2.19}$$

where $w[n]$ represents the additive white Gaussian noise (AWGN) with variance σ^2. At the receiver, perfect time synchronization is assumed.

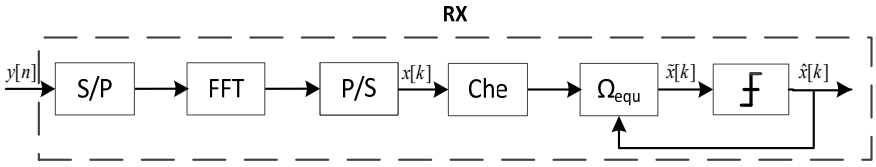

Figure 2.11. Equivalent baseband system receiver chain.

The receiver block diagram is depicted in Figure 2.11. After digitalizing the signal captured at the receiving antenna, an *N*-point FFT is applied to demodulate each OFDM symbol.

$$y[k] = FFT\{y[n]\} = \sum_{n=0}^{N-1}\left[\sum_{l=0}^{L-1} h[n,l]\, x[n-l]\right] e^{-j2\pi nk/N} \tag{2.20}$$

Afterwards, the frequency shift property, which connects a time delay [n-l] with a frequency shift equal to $e^{-j2\pi lk/N}$, is applied.

$$x[n-l]=\frac{1}{N}\sum_{m=0}^{N-1}\left(e^{-j2\pi lm/N}x[k]\right)e^{-j2\pi mn/N} \tag{2.21}$$

Then, Eq. (2.21) is introduced in Eq. (2.22)

$$y[k]=\sum_{n=0}^{N-1}\left[\sum_{l=0}^{L-1}h[n,l]\left[\frac{1}{N}\sum_{m=0}^{N-1}\left(e^{-j2\pi lm/N}x[k]\right)e^{-j2\pi mn/N}\right]\right]e^{-j2\pi nk/N} \tag{2.22}$$

Afterwards, the two main properties of the summations, the commutability and the scalability, are applied to rearrange the previous formulation.

$$\sum_{i=0}^{n}\sum_{j=0}^{m}a[i,j]=\sum_{i=0}^{m}\sum_{j=0}^{n}a[i,j] \tag{2.23}$$

$$\sum_{i=0}^{m}ca[i]=c\sum_{i=0}^{m}a[i] \tag{2.24}$$

Consequently, using Eq. (2.23)and Eq. (2.24) the output channel spectrum can be expressed as

$$x[k]=\frac{1}{N}\sum_{m=0}^{N-1}x[k]\left[\sum_{l=0}^{L-1}\left[\sum_{k=0}^{N-1}h[n,l]e^{-j2\pi nk/N}e^{j2\pi km/N}\right]e^{-j2\pi lm/N}\right] \tag{2.25}$$

After rearranging the exponential values in Eq. (2.25), it can be clearly identified the definition of the Scattering function, but in this case with a frequency shift over the Doppler frequency domain:

$$y[k]=\frac{1}{N}\sum_{m=0}^{N-1}x[k]\left[\sum_{l=0}^{L-1}\overbrace{\left[\sum_{k=0}^{N-1}h[n,l]e^{-j2\pi n(k-m)/N}\right]}^{S[k-m,m]}e^{-j2\pi lm/N}\right] \tag{2.26}$$

$$y[k]=\frac{1}{N}\sum_{m=0}^{N-1}x[k]\overbrace{\left[\sum_{l=0}^{L-1}S[k-m,m]e^{-j2\pi lm/N}\right]}^{H[k,m]} \tag{2.27}$$

Eventually, the received signal spectrum $y[k]$ is obtained as a function of $H[m,k]$, which is the double Fourier transform of the channel impulse response $h[n,l]$ defined by Bello, in terms of a circular-shifted convolution with the transmitted signal spectrum $x[k]$, plus the additive noise component:

$$y[k] = \frac{1}{N}\sum_{m=0}^{N-1} X[k]H[k-m,m] + w[k] \tag{2.28}$$

In short, when dealing with a time-varying channel, the output and the input signal spectrum are related in terms of a convolution over the Doppler frequency of $H[m,k]$. In other words, $y[k]$ represents the output spectrum as a superposition of a series of input signal spectrum, $[k]$, filtered and Doppler shifted. This is the main reason why the Doppler distortion is not just a simply frequency offset.

Next, in order to reduce the computation complexity in (2.28), and if the OFDM FFT basis is taken into account, a new variable **Z** can be defined, which represents the circular-shifted convolution of the expression in Eq.(2.28). That way, the received signal spectrum **y** can be represented as the matrix multiplication of **Z** and the transmitted symbol spectrum **x**, plus the additive noise given by **w**. Therefore, the channel matrix **Z** represents the different sources of distortion due to the mobile scenario, and as such, it might be expressed as a sum of two terms. On the one hand there is $\mathbf{Z}^{\mathbf{d}}$, a matrix containing the main diagonal of matrix **Z**, which is related to the channel attenuation due to the multipath fading; and, on the other hand, $\mathbf{Z}^{\mathbf{ICI}}$, which is composed of the rest of sub-diagonals and super-diagonals of matrix **Z**, and is connected to the ICI due to the Doppler Effect.

$$\mathbf{y} = \mathbf{Z}\mathbf{x} + \mathbf{w} = \left(\mathbf{Z}^{\mathbf{d}} + \mathbf{Z}^{\mathbf{ICI}}\right)\mathbf{x} + \mathbf{w} \tag{2.29}$$

This expression in Eq. (2.29) is the basis for the development of one of the most used proposals for dealing with time varying-channels: improving the classical one-tap frequency equalizers. Up to now, a widely accepted proposal for compensating the channel effects in the received signal is a special type of equalization algorithm, which is designed to be able to deal with these doubly dispersive channels. Commonly, this challenge can be summarized as a multipath problem, which may be solved using 2D channel estimation and equalization algorithms [62][63]. During the next section there will be presented several methods, which define their particular equalization matrix **Ω**, for dealing with those challenging scenarios. In addition, it will be also presented a two dimensional channel estimation algorithm (See Figure 2.11), which main objective is to feed the

equalization block with the best channel impulse response that the algorithm can provide.

2. THEORETICAL ANALYSIS OF EQUALIZATION TECHNIQUES OVER TIME-VARYING CHANNELS

After having analysed the channel behaviour from a mathematical point of view, it is observed that the rapidly-varying channel does not only destroy the orthogonally between carriers but also provides the reception with very useful time diversity for a posterior equalization ($\mathbf{Z}^{\mathbf{ICI}}$) [64]. Nevertheless, with regard to the receiver performance, the maximum capacity will not be achieved by any broadcasting system unless the received signal is perfectly equalized. Consequently, this section presents the main theoretical solution that solves the problem of the time variability: the doubly dispersive equalization [65][66]. Apart from that, dynamic channel estimation is also needed. Hence, a thorough analysis of the existing equalization techniques should also include a channel estimation algorithm for bringing the analysis closer to the real world [67].

2.1 Equalization Method Classification

In recent years different approaches have been presented in order to improve the equalization performance when the receivers are dealing with the further problem of time-varying channels. Through an exhaustive analysis, the best-known and widely used equalization techniques for time-varying channels have been identified and classified. A graphical representation of this classification is given in Figure 2.12 and a brief comprehensive list is provided in the following lines:

- **LINEAR EQUALIZERS:** the linear equalizers matched-filter (MF), zero forcing (ZF) and minimum mean square error (MMSE), are considered as valid solutions to cancel ICI without using any recursion algorithm [68][69].

- **ITERATIVE METHODS BASED ON LINEAR EQUALIZERS:** the iterative equalizers overcome the drawbacks of the linear equalizers thanks to the introduction of an iterative stage. Generally, these methodologies are based on the previous ones but demonstrate a notable outperformance. The iterative methods included in the comparison are the sequential iterative cancellation (SIC) [70][71] and the parallel iterative cancellation (PIC) [72].

- **KRYLOV ITERATIVE METHODS:** the recently proposed Krylov iterative equalizers, which are based on a totally different approach, are

supposed to be an alternative for equalization in the presence of large and sparse discrete channel models; in particular, an algorithm for sparse linear equations and sparse least squares to be called LSQR [73] and the generalized minimal residual method (GMRES) [74] are analysed.

- **REFERENCE EQUALIZERS**: the matched-filter bound (MFB) [75][76] is the reference equalizer, i.e., it is the gold theoretical standard against which the proposed practical methods will be compared.

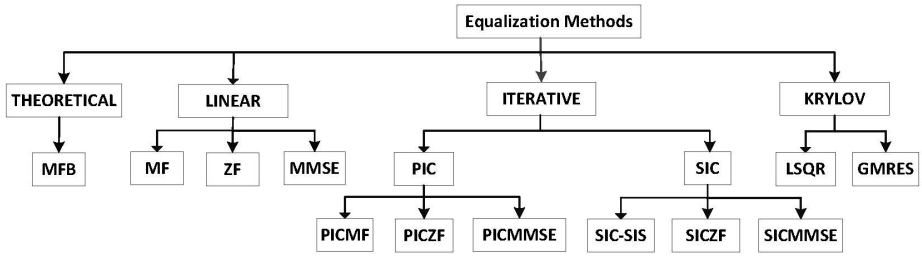

Figure 2.12. Equalization methods classification.

In addition, TABLE 2.1 summarizes in a few lines the most relevant characteristics of each method. There are described the main algorithms organized in three different groups. Each one presents the main equations involved in the process, the related complexity and the characteristics and the most relevant references. Afterwards, each of the algorithms will be described in deep to show its own advantages and drawbacks.

TABLE 2.1. Summary of equalization methods main characteristics.

	METHOD	CHARACTERITICS	Basic Algorithms	Previous Stage	References
LINEAR	*MF*	Able to cancel the distortion without using any recursion algorithm	$\mathbf{\Omega}_{MF} = \mathbf{Z}^H$	None	[67]
	ZF		$\mathbf{\Omega}_{ZF} = \left(\mathbf{Z}^H\mathbf{Z}\right)^{-1}\mathbf{Z}^H$	None	[67][81][82]
	MMSE		$\mathbf{\Omega}_{MMSE} = \mathbf{Z}^H\left(\mathbf{Z}\mathbf{Z}^H + N_0\mathbf{I}\right)^{-1}$	None	[82]
ITERATIVE	*PICMF*	Based on the linear ones, but demonstrate a notable outperformance thanks to the introduction of an iterative stage	$\mathbf{F} = \mathbf{Z}^H$ / /$\mathbf{B} = \mathbf{T} - \mathbf{T}^d$	MF output	[76][81]
	PICZF		$\mathbf{F} = \mathbf{Z}^H$ / /$\mathbf{B} = \mathbf{T} - \mathbf{T}^d$	ZF output	[76][81]
	PICMMSE		$\mathbf{F} = \mathbf{Z}^H$ / /$\mathbf{B} = \mathbf{T} - \mathbf{T}^d$	MMSE output	[76][81]
	SICSIS		None	None	[87]
	SICZF		$\mathbf{F} = \mathbf{D}^{-1}\mathbf{L}^{-1}\mathbf{Z}^H$ / /$\mathbf{B} = \mathbf{L} - \mathbf{I}$	$\mathbf{Z}_0 = \mathbf{Z}^H\mathbf{Z}$ *fact.*	[83]
	SICMMSE		$\mathbf{F} = \mathbf{D}^{-1}\mathbf{L}^{-1}\mathbf{Z}^H$ / /$\mathbf{B} = \mathbf{L} - \mathbf{I}$	$\mathbf{Z}_0 = \mathbf{Z}^H\mathbf{Z} + N_0\mathbf{I}$ *fact.*	[67][83]
KRYLOV	*LSQR*	An alternative for equalization in the presence of large and sparse discrete channel models	$\min\|\mathbf{Zx} - \mathbf{y}\|$	Pivoting (optional)	[88][89]
	GMRES		$\min\|\mathbf{y} - \mathbf{\Omega x}\|_2$	Pivoting (optional)	[74]
THEOR.	*MFB*	Reference equalizer. Supposed to be the gold standard against which the proposed practical methods can be compared	$\mathbf{F} = \mathbf{Z}^H$ / /$\mathbf{B} = \mathbf{T} - \mathbf{T}^d$	Transmitted data	[75][76]

2.2 **Reference Equalizers**

In some references [77][78], the Joint ML detection has been considered as the bound limiter method, as it is an optimal scheme that maximizes the diversity gain provided by a doubly selective fading channel without enhancing any of the distortion sources. However, its main drawback is the extreme complexity and the heavy computational requirement [76].

In consequence, the theoretical bound against which the equalizers are normally tested, is set by the MFB. That is, the lower bound on the achievable error rate for an uncoded received signal, obtained by a theoretical receiver where interference would be perfectly cancelled and data perfectly estimated. Its limit has been widely studied for frequency-selective fading channels [79][80] and

particularly for OFDM communication systems [75][76]. Its main advantage is that MFB does not make any assumption about the channel model, in other words, it may be used under any scenario. Indeed, it considers a hypothetical equalizer that somehow knows the value of the interfering symbols and cancels the ICI based on that knowledge. It works as follows, first the MF should be considered the first equalization block, in such a way that the filter output, **r**, is given by:

$$\mathbf{r} = \mathbf{Z}^{\mathbf{H}}\mathbf{y} = \mathbf{Z}^{\mathbf{H}}(\mathbf{Z}\mathbf{x} + \mathbf{w}) = \mathbf{T}\mathbf{x} + \mathbf{n} \tag{2.30}$$

Then, using the received signal's internal interference and the sub-diagonals and super-diagonals of the above defined matrix $\mathbf{T} = \mathbf{Z}^{\mathbf{H}}\mathbf{Z}$, the ICI is removed in a deterministic way as follows:

$$\tilde{\mathbf{y}} = \mathbf{r} - \left(\mathbf{T} - diag\{\mathbf{T}\}\right)\mathbf{x} \tag{2.31}$$

Afterwards, the received symbol interference is reduced to its multiplicative distortion and the modified received symbol, $\tilde{\mathbf{y}}$, is prepared to be equalized in the absence of other internal interferers.

2.3 Linear Equalizers

A linear equalizer can be conceived as a linear filter that is designed to reduce the noise and interference according to a predefined criterion. It is considered the simplest detector, and although it does not always perform as well as the more complex equalizers, it demonstrates considerably robustness against non-linearities. Subsequently, we are going to focus on the more general cases of linear equalizers for dealing with time-varying channels: MF, ZF and MMSE.

2.3.1 Matched Filter (MF)

It is the simplest linear equalizer and its performance is strongly dependent on the channel column vectors. Particularly, performance is nearly optimum in the absence of other interfering columns or when the existing channel columns are mutually orthogonal, that is, when the off-diagonal elements of the matrix **T** are negligible compared to the main diagonal elements. The former is not possible by the mathematical definition of the time varying channel impulse response, and the latter is unthinkable when the transmission is carried out over a realistic channel. In

brief, under a mobile scenario, this type of equalization suffers dramatically from ICI [67]. Its equalization matrix is given by:

$$\mathbf{\Omega}_{MF} = \mathbf{Z}^{H} \tag{2.32}$$

2.3.2 Zero Forcing (ZF)

The zero forcing linear equalization matrix is built so as to eliminate both interferences that affect the signals over doubly-selective channels: the distortions due to the Doppler effect and multipath fading. Nonetheless, this complete interference cancellation is responsible for its main drawback: the noise amplification at the slicer entrance [35][72][81]. Its equalization matrix is given by:

$$\mathbf{\Omega}_{ZF} = \left(\mathbf{Z}^{H}\mathbf{Z}\right)^{-1}\mathbf{Z}^{H} \tag{2.33}$$

In addition to that, when dealing with OFDM signals, the channel is represented by a square matrix **Z**, and therefore, is itself invertible. In other words, the equalization matrix is simplified to $\mathbf{Z}^{-1}$, which in the literature is also known as Gram matrix. Other authors named this method the least square (LS) solution [82], as its goal is to minimize the weighted squared errors between the estimations and the transmitted data.

2.3.3 Minimum-Mean Square Error (MMSE)

The MMSE equalization matrix is defined in order to minimize the mean-squared error between the data vector and the linear $E\{\boldsymbol{x} - \boldsymbol{\Omega_{MMSE}y}\}$ estimator [71][82]. Through this statistical viewpoint, the main drawback of the previous method is the insistence on completing the interference cancellation regardless of the interference strength and its influence on the noise enhancement. The matrix equalizer is defined by:

$$\mathbf{\Omega}_{MMSE} = \mathbf{Z}^{H}\left(\mathbf{Z}\mathbf{Z}^{H} + N_0\mathbf{I}\right)^{-1} \tag{2.34}$$

where N_0 is the noise power. As a result, the MMSE is designed as a much more balanced method, unlike the ZF detector, which minimizes interference but neglects noise, and unlike the MF detector, which minimizes noise but neglects non orthogonal interference. However, it is also true that this method ought to accept some residual interference.

2.4 Iterative Methods based on Linear Equalizers

When the time-varying channels are treated in order to deal with the double dispersiveness, the truth is that the time-variability is not a noise distortion any more. As a matter of fact, it can be used for increasing the equalizer performance. In general, the iterative methods are the ones which exploit better this characteristic. In this section, in order to take full advantage of the time diversity provided by the double selective fading channels while suppressing the residual interference and the noise enhancement, the following iterative methods are presented: SIC and PIC.

2.4.1 Serial Interference Cancellation (SIC)

It is a nonlinear method for channel equalization proposed by Duel-Hallen [83], where the principal idea is to reuse the previously detected symbols to estimate the following ones [67][84]. Although its performance is extremely good, it is computationally very complex when the symbol length is large. Even though, the method complexity can be significantly reduced if the original algorithm is modified, so that the matrix algebra can be used [85][86].

The SIC scheme divides the equalization process into two independent stages. In this manner, the first cancellation stage is performed out of the recursion part, in the initialization step, by the forward filter **F**, in contrast to the original method where the cancellation step is done iteratively, carrier by carrier.

In a second phase, the subtracting vector is the output of the feedback filter, **B**, multiplied by the decision vector $\hat{\boldsymbol{x}}$. The aim of this filter is to completely suppress the inter-carrier interference, and to achieve that it uses the hard-decision slicer output, $\tilde{\boldsymbol{x}}$, to feed in. The feedback filter $\mathbf{B} = \mathbf{L} - \mathbf{I}$ and the forward filter, $\boldsymbol{F} = \boldsymbol{D^{-1}L^{-H}D^{-H}}$, are designed based on the $L^H DL$ factorization of a matrix $\mathbf{Z_0}$, which depends on the used linear equalizer. This way, the factorizing matrix for MMSE equalization is $\boldsymbol{Z_0^{MMSE}} = \boldsymbol{Z^H Z} + N_0 \boldsymbol{I}$ and for ZF equalization is $\boldsymbol{Z_0^{ZF}} = \boldsymbol{Z^H Z}$.

The causality is not a problem because instead of trying to calculate the entire decision vector all at once, the components are calculated one by one beginning with the first one. That is to say, each component of the slicer output depends only on the previous decisions. In terms of the forward filter, the feedback filter can be equivalently defined as strictly lower triangular part of the cascade. Eventually, the equalization algorithm work as shown in TABLE 2.2, where Q {·}represents the slicer: It should be noted that the SIS (successive interference suppression)

method used in [87][88] is a special case of SIC when the main diagonal is used as cancellation matrix.

TABLE 2.2. SIC algorithm iterative process summary.

initialization:	**recursion:**
$i \leftarrow 1$	$i \leftarrow i+1$
$\hat{x} = \vec{0}$	$v[i] = g[i] - B[k,m]\hat{x}[k]$
$g[k] = F[k,m]y[k]$	$\hat{x}[i] = Q\{v[i]\}$
$\hat{x}[i] = Q\{g[i]\}$	

2.4.2 Parallel Interference Canceller (PIC)

The previous SIC algorithm cancels the interference from the carriers one by one, in sequential order, and hence, the performance has tough dependence on the detection order. As an alternative, in this section the parallel-interference canceller is described, an alternative equalizer, where interference from all symbols is cancelled simultaneously [81].

In fact, the PIC uses the same cancellation technique used by the basic methods, but then the full vector of hard decisions of $\hat{\boldsymbol{x}}$ is proposed to suppress the intercarrier interference. The filters are defined by $\boldsymbol{F} = \boldsymbol{Z}^H$ and $\boldsymbol{B} = \boldsymbol{T} - diag\{\boldsymbol{T}\}$ (see Eq. (2.30). The algorithm works as follows, where Q $\{\cdot\}$ represents the slicer and the number of iterations is previously defined:

TABLE 2.3. PIC algorithm iterative process.

initialization:	**recursion:**
$i \leftarrow 1$	$i \leftarrow i+1$
$r[k] = F[k,m]y[k]$	$g[k]_i = r[k] - B[k,m]\hat{x}[k]_{i-1}$
$g[k]_i = \Omega[k,m]y[k]$	$\hat{x}[k]_i = Q\left\{diag\left\{T[k,m]g[k]_i\right\}\right\}$
$\hat{x}[i] = Q\{g[k]_i\}$	

The input of the feedback is a vector of hard decisions, but not final decisions. The tentative decision may be the output from any of the linear equalizers described in the previous sections. The PIC iterative procedure works using the whole pre-detected symbol data, and hence, its performance is proportional to the

initialization stage result. Hence, a perfect decision vector should lead to the MFB bound.

2.5 Krylov Iterative Methods

The main drawback of the previous iterative methods (SIC, PIC) is that they involve the factorization and inversion calculus of equalization matrices (see TABLE 2.1). In this section another kind of generic-purpose equalizers for solving linear equations is explained, which provides especially good results for sparse, large and ill-conditioned matrices [74]. The basic approach of these methods is that it generates a sequence of approximate solutions for each iteration and then the equalization matrix is only employed in the context of matrix-vector multiplications. It is also important to note that the overall system performance in complexity terms could be improved through the use of matrix pivoting.

2.5.1 LSQR

LSQR is a numerical method similar to the well-known method of conjugate gradients (CG) as applied to the least-squares problem [73]. The name conjugate gradient is derived from the fact that this method generates a sequence of orthogonal vectors, residuals of each iteration process. Its main restriction is that the equalization matrix must be symmetric and positive definite, and in that case, the following expression is defined:

$$\varphi = \frac{1}{2}\mathbf{x}^H \mathbf{Z}\mathbf{x} - \mathbf{x}^H \mathbf{y} \tag{2.35}$$

Then, $\nabla\boldsymbol{\varphi} = \boldsymbol{Zx} - \boldsymbol{y}$ since, it follows that $\boldsymbol{x} = \boldsymbol{Z^{-1}y}$ is the unique minimizer of $\boldsymbol{\varphi}$. Subsequently, minimizing (2.35) and solving the linear system are equivalent problems. In the literature different methods for converging to that solution can be found: steepest decent, search general directions or A-conjugate search directions [89]. Based on this conjugate gradient method, Paige and Sunder proposed the particular case of LSQR algorithm [89]. It is equivalent to the conjugate gradient method for normal $\boldsymbol{Z^H Zx} = \boldsymbol{Z^H y}$ equations, but has better numerical properties. It works as follows, for each iteration an approximate solution is obtained by minimizing $\|\boldsymbol{Zx} - \boldsymbol{y}\|$, subject to the constraint that xi lies in the Krylov $K(\boldsymbol{Z^H Z}, \boldsymbol{Z^H} x, i)$ subspace.

2.5.2 Generalized Minimum Residual (GMRES)

This method is founded on the Lanczos based MINRES method for symmetric, possibly indefinite, $\boldsymbol{\Omega x = y}$ methods, which try to minimize $\|\mathbf{y} - \boldsymbol{\Omega x}\|_2$ through several iterations [90], where $\|\cdot\|_2$ represents the Euclidean norm. In practice, to converge to a solution, the same approach is taken aside from that Arnoldi vectors are used instead of Lanczos to handle unsymmetrical matrices. Thus, the main difference with respect to LSQR is that in this iterative algorithm the solution approximation is constructed within the subspace $K(\boldsymbol{Z}^H \boldsymbol{y}, i)$ and it can be implemented with non-symmetrical matrices [73].

3. PRACTICAL EVALUATION OF THE EQUALIZATION TECHNIQUES

As shown in the previous section, the use of two-dimensional equalization techniques is one of the most popular approaches for dealing with time-varying channels. In fact, in the literature, there are several published papers that present the performance of some of the previously presented methods for mobile environments as a valid solution [67][91][92]. However, they have the disadvantage of having been tested either for different channels or for different signal configurations. Thus, the objective of this section is to provide a comprehensive and wider analysis of the existing algorithms, while they are all analysed under the same conditions.

3.1 Evaluation Parameters

The purpose of this subsection is to present and describe the parameters under which the equalization techniques are going to be exhaustively analysed. Specifically, three main characteristics have been considered: BER performance, complexity and sensitivity.

3.1.1 Bit Error Rate (BER)

As generally agreed, it is the most used parameter for evaluating the equalizers performance. In digital telecommunication services, the bit error rate is the percentage of erroneous data bits relative to the total number of bits received in a transmission, usually expressed as ten to a negative power. It should be noted that through this section the system is dealing with uncoded symbol reception. Undoubtedly, the performance of a coded system will differ from that of an uncoded one. However, the aim of this chapter is to provide a comparative analysis of the existing equalization methods, and to do so, the obtained results do not depend on the coding performance.

3.1.2 Complexity

In the literature there are several studies that analyse in detail the complexity of the equalization methodologies [71][93]. Nevertheless, as the new generation systems tend to have bigger symbol lengths in order to maximize the data throughput in SFN networks, such a complex calculus is not necessary and a more generic analysis method can be implemented. For instance, in this work the direct

calculation of the complexity, based on the algebraic operation involved in the equalization process, is proposed. Apart from that, the computational saving obtained by the banding process presented in [85] for the MMSE and SICMMSE schemes is extended to the rest of the existing methods. The computational complexity reduction in equalization algorithms is another key point for a successful implementation into commercial receivers. In short, there are two ways of reducing computational complexity: banding processes and matrix factorizations.

3.1.2.1 Banding process

An equalization algorithm can be simplified applying a banding process to the channel matrix **Z** [85], that is, reducing the amount of sub-diagonals and super-diagonals of the matrix **Z** that are taken into account. A graphic representation of a banding process is shown Figure 2.13. In a banding process, the main diagonal and a ρ_{sub} number of diagonals on each side of the main diagonal are considered, so that the banded matrix bandwidth, ρ, is given by $\rho = \rho_{sub} + 1$. The normalized matrix bandwidth ρ_{norm} is expressed as a function of the channel matrix size N, according to (2.36):

$$\rho_{norm} = \frac{\rho_{sub}}{N-1} \cdot 100, \qquad \rho_{sub} \leq N-1 \tag{2.36}$$

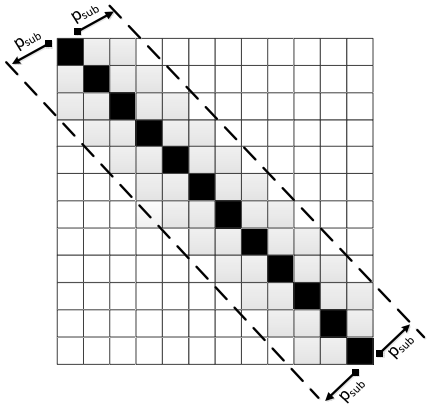

Figure 2.13. Graphic representation of a matrix banding process. In this case $\rho_{sub} = 2$ and $\rho = 3$.

As previously proved in the existing literature, the relative power of the sub-diagonals and super-diagonals with respect to the whole matrix power decreases as

the distance with the main diagonal increases [68][71]. Furthermore, this distance is closely related to the existing Doppler spread. That is why the banding process should be carefully applied: if a small banded matrix bandwidth is considered, complexity will be reduced but relevant channel information may be lost, leading to performance degradation.

3.1.2.2 Matrix factorization

Matrix factorization processes can also be applied in order to reduce the complexity of equalization methods. The main matrix factorizations are **LU**, **QR** and $\mathbf{L}^{\boldsymbol{H}}\mathbf{DL}$ [89]. LU decomposition factorizes a matrix as the product of a lower triangular matrix **L** and an upper triangular matrix **U**. QR decomposition is a factorization of a matrix into a product of an orthogonal matrix **Q** and an upper triangular matrix **R**, obtained by the application of the Gram–Schmidt process. Finally, in $L^{H}DL$ factorization, a Hermitian, positive-definite matrix is decomposed into the product of the diagonal matrix **D**, a lower triangular matrix **L** and its conjugate transpose **LH** [89]. TABLE 2.4 shows the computational complexity of the main algebraic operations and factorizations, which are the essential parts of the subsequently analysed equalization methods. In the table, complexity metric is given by the amount of floating point operations in terms of the matrix size, N, and banded matrix bandwidth, ρ.

TABLE 2.4. Computational complexity of different matrix operations.

	Multiplication	**Inverse**	**Back Subs.**	**LU**	**QR**	**LDL**
Normal	$O(N^3)$	$O(N^3)$	$O(N^2)$	$O(2N^3/3)$	$O(2N^3/3)$	$O(N^3/3)$
Banded	$O(N^2p)$	$O(N^2p)$	$O(2Np)$	$O(2Np^2)$	$O(2Np^2)$	$O(N(p^2+3p))$
Imp.	$O(N/p)$	$O(N/p)$	$O(N/2p)$	$O(N^2/3p^2)$	$O(N^2/3p^2)$	$O(N^2/3(p^2+3p))$

The first three columns show the complexity of the basic matrix operations and the last three indicate the computational cost of the main matrix factorizations. The first two rows represent the computational complexity order [89], while on the third the reduction achieved due to the banding process is calculated. Therefore, it is shown that the factorization is also a key point to simplify the computational complexity, but above all, after converting the original matrix into a banded one. Hence, the combination of both banding processes and factorizations can be used to simplify any equalizer [70][93][94][95]. Finally, it is also important to remark that the mentioned factorizations may also be used to improve the sensitivity of the

equalization matrix, and thus, the performance of the proposed methods, as proved later.

3.1.3 Sensitivity

In the literature there are two main approaches to the sensitivity analysis: on the one hand, some authors have employed the sensitivity to measure the capacity gains obtained from spatial multiplexing operation in MIMO wireless systems [95]; and other hand, the sensitivity has been studied to quantify the channel robustness against noise [96]. This work tilts for the second option, but instead of analysing the channel characteristics, it analyses the sensitivity of every matrix whose inverse is involved in the equalization process. The aim of this section is to demonstrate how a small perturbation due to noise in the received signal **y** could affect the solution vector $\hat{\mathbf{x}}$**.** The first approximation for measuring the sensitivity is made in terms of Singular Value Decomposition (SVD) of the equalizer matrix, $\mathbf{\Omega}$, where σ^i are the singular values and the vectors u_i and v_i are the ith left singular vector and the ith right singular vector respectively. Considering that the simplest equalizer may be seen as a linear system solver where the solution is obtained after taking the inverse of the coefficient matrix [82], the signal at the slicer input $\tilde{\mathbf{x}}$ can be obtained according to (2.37):

$$\tilde{\mathbf{x}} = \mathbf{\Omega}^{-1}\mathbf{y} = \sum_{i=1}^{N} \frac{u_i y_i}{\sigma_i} u_i^T \tag{2.37}$$

The previous expression shows that a small perturbation in the received symbol **y** can cause critical changes in the solution vector if the minimum singular value, σ^i, is extremely small. Even though the previous expression is a good example for understanding the importance of the sensitivity, it is not the best one for measuring its impact. Indeed, a more precise measure of a linear system sensitivity was developed in [89], considering a parameterized system where the coefficient matrix **S** is non-singular and is assumed to be perfectly known (i.e., there is not any perturbation associated to the matrix **S**. Based on this analysis, for our special case where the matrix **S** is always square, the matrix sensitivity is represented by the $K(\mathbf{S})$ parameter, which is also known as the condition number:

$$K(\mathbf{S}) = \frac{1}{\|\mathbf{S}\|\|\mathbf{S}^{-1}\|} \tag{2.38}$$

where $\|\cdot\|$ represents the classical Frobenius norm [89], and **S** is the matrix to be inverted during the equalization process. In other words, the condition number gives us an idea of the singularity of the coefficient matrix, i.e., its strength against noise. If $K(\mathbf{S})$ is large, then **S** is classified as an ill-conditioned matrix, and when the inverse is directly applied, the equalization performance under noisy channels will be substantially degraded.

3.2 Two Dimensional Channel Estimation

One of the aims of this study is to analyse the performance of the algorithms at the receiver, and moreover, to place the evaluation as close as possible to a realistic situation. So far, the vast majority of the existing references have considered perfect channel knowledge for this purpose, without further concern about time-varying channel estimation [67][85][91]. This is not a fair comparison, as the channel estimation is also a key module, which provides the channel gain to the equalization process. In this approach, the analysis tries to get closer to real applications by proposing and including a practical channel estimation algorithm. Moreover, that way, the robustness to channel estimation errors can also be taken into account in the study. Although the presented algorithm is based on the approach presented in [77][97], some modifications have been proposed in order to improve its performance, as following discussed. The presented algorithm consists of two steps: initialization and iterative stage.

3.2.1 Initialization

First of all, the conventional frequency response is calculated, by means of least squares estimation, from the pilot-tones sequence inserted into each OFDM symbol at the transmitter. Afterwards, an interpolation is applied in order to estimate the overall frequency response for all the data sub-carriers by using the channel information at pilot carriers. The estimated channel response $\tilde{h}[l]$ given by

$$\tilde{h}[l] = h_{ave}[l] + w_{ICI}[l] + w_{AWGN}[l] \tag{2.39}$$

As observed in Eq. (2.39), when dealing with doubly selective fading channels, the previously estimated impulse response does not represent the overall channel state information, but the mean value of the time-varying channel response, h_{ave}, plus Gaussian noise, w_{AWGN}, and a noisy term due to the ICI, w_{ICI}, as demonstrated in [77][97]. Moreover, in the literature it has been widely reported that, within a

symbol, the amplitude variation of the channel paths may be approximated as a linear function when the normalized Doppler factor is $f_d T_u < 0.1$ [77][97], where f_d represents the maximum Doppler shift and T_u is the symbol duration. As a result, the bi-dimensional channel impulse response can be obtained grouping M different symbols and performing a linear interpolation of the impulse response paths along the observation time [97] (see Figure 2.14).

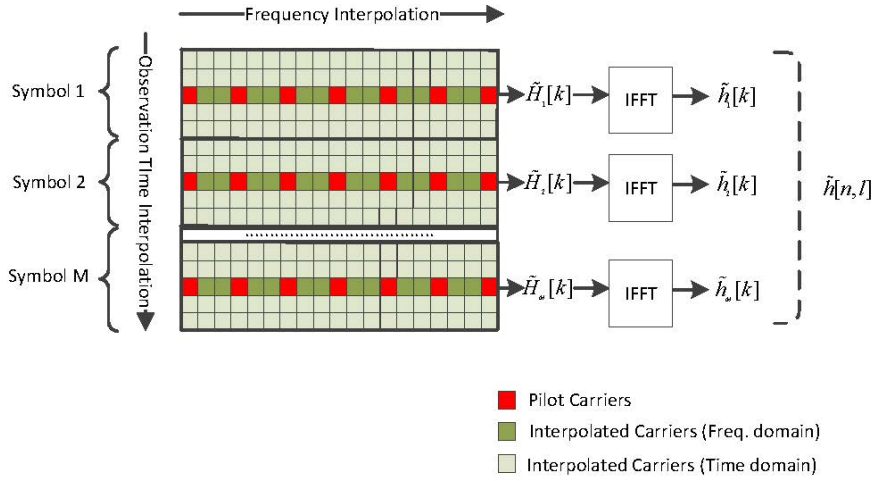

Figure 2.14. Initialization stage of the proposed channel estimation algorithm.

Therefore, at this point, the first challenge is to accurately estimate the delays of the channel paths, so as to avoid the noisy samples that might degrade the estimation performance. To that end, a low complexity technique is presented. It consists in the calculation of the average of the channel impulse responses located in each block of M symbols, assuming that the delays are invariant within it. Afterwards, the channel main path is located, and finally, those values that are below a previously defined threshold with respect to the main path are considered as noise, and therefore, they are not interpolated.

3.2.2 Iterative stage

The first channel estimation described above is affected by the presence of ICI noise in the channel mean value calculation, as shown in Eq. (2.39)[77]. In order to solve this problem, an iterative stage based in [97] is implemented, but instead of just considering the pilot carrier values, the whole previously detected symbol information is used, as defined in the decision directed channel estimation. The iterative stage is divided into three tasks: first, the transmitted data is detected using

the equalizer, and afterwards, the correspondent ICI noise is calculated; second, the ICI is removed from the received symbols; and finally, the channel is again estimated as in the initialization stage but using the whole symbol information. Therefore, in this iterative stage the first interpolation to obtain the frequency response is not necessary anymore, as the whole symbol data carriers are used. Although the iterative stage is quite complex computationally, its performance has proved to be close to the ideal condition of perfect channel knowledge, as shown in the next section.

3.3 **Results**

In this section, further insight into the previously explained equalization techniques is gained by simulating their practical performance under a time varying channel. One of the contributions of this section is that, whereas in previous studies the channel impulse response is assumed to be perfectly known [67][91], in this an algorithm is included. In addition to this, it should be noted that all the equalizers' performances have been tested under the same signal and channel conditions and for different mobility scenarios.

The simulations are carried out in the general platform described theoretically in Section 1.3, and the channel model is the TU-6 as recommended by COST 207 [98], where mobility is characterized by a maximum Doppler shift f_d. Even if originally the TU-6 channel was derived for narrowband transmission, it has been widely used in the most recent standardization processes [56]. The transmitted signal is configured so as to be close to one of the DVB-T2 modes [56]. More precisely, a QPSK-OFDM system with N = 1024 subcarriers and 8 MHz bandwidth is considered, and therefore, the symbol duration is set as $T_u = N/f_s$, where f_s is the sampling frequency. Jointly, the OFDM symbol has $\Delta GI = 1/8$ guard interval and there are $N_p = 1/8$ equally spaced pilot carriers.

The results of the simulations are divided into four subsections which represent the main characteristics of an equalizer algorithm: the goodness of channel estimation and the equalizer robustness against estimation errors are set up in subsection 3.3.1, BER performance is evaluated in subsection 3.3.2, complexity analysis in subsection 3.3.3 and sensitivity in subsection 3.3.4. These parameters are analysed for two different Doppler environments. The first one represents a low mobility environment with a normalized Doppler factor f_dT_u=0.01, and the second one represents a fast time-varying scenario where the mobility is increased to f_dT_u=0.1.

3.3.1 Channel Estimation

Figure 2.15 (a) shows the comparison of the normalized mean squared error NMSE as function of the signal to noise ratio SNR between the ideal channel impulse response, the estimated response after the initialization stage, and the response after the iterative stage when one of the different equalizers outputs has been used to re-estimate the time-varying path amplitudes. The error is calculated for the most demanding high mobility scenario where $f_d T_u$ is set to 0.1. It is clearly shown that, at the expense of increasing the complexity, the error is notably reduced after the iterative stage.

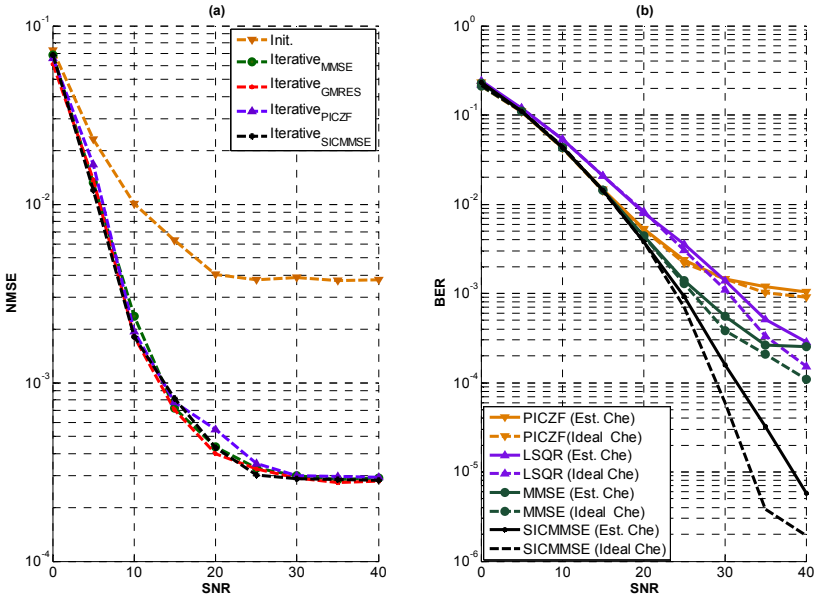

Figure 2.15. (a) Normalized mean squared error of the channel estimation algorithm when the normalized Doppler factor is f_dT_u=0.1. (b) BER comparison between perfect channel knowledge and implemented channel estimator for a TU-6 channel when the normalized Doppler factor is f_dT_u=0.1.

The goodness of the proposed channel estimator is also observed in the BER performance for the different equalization methods, which are quite similar to the cases where the channel is assumed to be perfectly known, as observed in Figure 2.15 (b). It is also proved that the performance of the iterative stage of the proposed channel estimator depends strongly on the previous stage reliability. The curves for the other equalization schemes have not been included in order to provide a clearer representation of the channel estimation behaviour, but the

conclusion is straightforward: the quality of the channel estimation relays on the ability of the equalization scheme to handle the time varying channels.

3.3.2 BER performance

Figure 2.16(a) shows the BER performance of the linear equalization methods for different mobility scenarios. It can be deduced from this plot that for low-mobility environments (f_dT_u=0.01, solid lines), the presented methods have practically the same behaviour, except for the MF method, whose performance is worse for the highest SNR conditions. Nevertheless, when the distortion due to the Doppler Effect starts to increase (f_dT_u=0.1, dashed lines), the well-balanced method, MMSE, has the very best performance. The main reason is that it has the best sensitivity against noise influence. It is also important to note that the MF behaviour is poorly conditioned for both mobility scenarios due to the lack of orthogonality in the columns of matrix **Z**, although this effect is more critical for the high mobility channel. However, the ZF sensitivity leads to even worse results than MF for high time varying scenarios, as later explained.

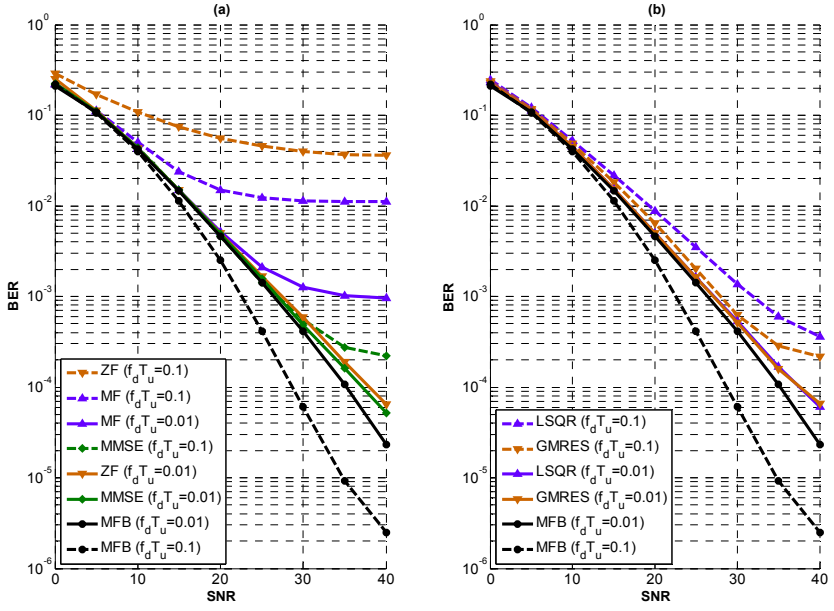

Figure 2.16.(a) BER for a TU-6 channel with linear equalizers when the normalized Doppler factor f_dT_u=00.1 (solid lines) and f_dT_u=0.1 (dashed lines). (b) BER for a TU-6 channel with Krylov equalizers when the normalized Doppler factor is f_dT_u=0.01 (solid lines) and f_dT_u=0.1 (dashed lines).

Figure 2.16 (b) shows the Krylov methods performance for respectively low and high mobility environments. It is clearly shown that for high Doppler scenarios their performance is close to the MMSE equalizer, the best of the linear equalizers. However, it should be also pointed out that this behaviour is strongly related to the number of iterations (in this case, the number of iterations is set to 150).

The next plot, Figure 2.17, shows the results for the PIC (a) and SIC (b) iterative methods. The PIC iterative stage has been simulated for the presented three linear equalization methods: MF, ZF and MMSE. However, the SIC method has not been simulated for the MF case as its equalization matrix does not fulfil the condition of being Hermitian-positive definite. In its place, as a third equalizer, the SIC-SIS method has been analysed.

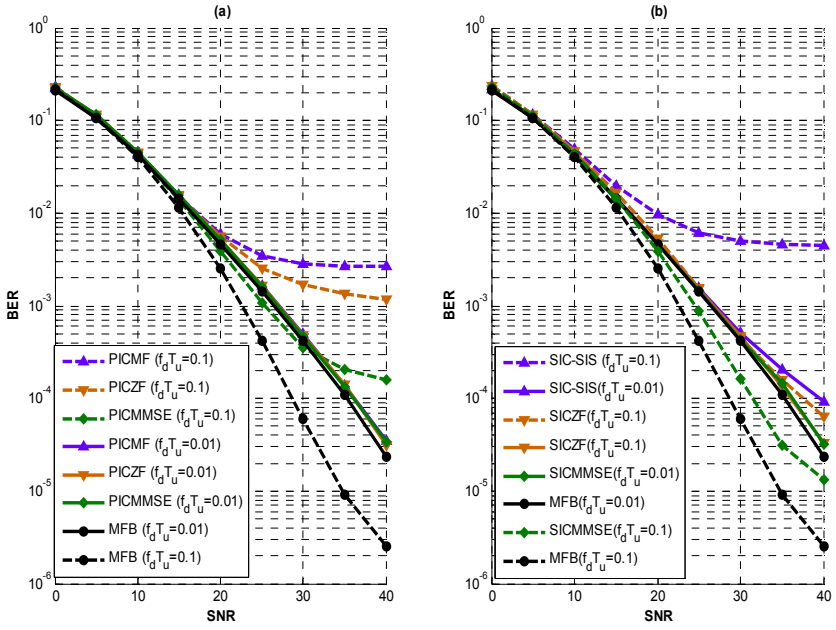

Figure 2.17. (a) BER for a TU-6 channel with PIC iterative equalizers when the normalized Doppler factor is f_dT_u=0.01 (solid lines) and f_dT_u=0.1 (dashed lines). (b) BER for a TU-6 channel with SIC iterative equalizers when the normalized Doppler factor is f_dT_u=0.01 (solid lines) and f_dT_u=0.1 (dashed lines).

Based on the figures, it is straightforward to conclude that for nearly stationary scenarios (f_dT_u=0.01, solid lines) the analyzed iterative schemes have practically the same behaviour independently of the chosen linear equalizer. What is more, they even achieve the bound depicted by the MFB. Nonetheless, for very high

normalized Doppler spreads (f_dT_u=0.1, dashed lines), the performance of PIC methods tends to decrease due to the error detection in the first stage, that is to say, the recursive stage is not able to correct all the misdetections. Furthermore, the best linear equalizer, the MMSE, does not improve as much as the other two algorithms when the iterative procedure is involved, as observed when comparing Figure 2.17 (dashed lines). By contrast, for high normalized Doppler spreads, the SIC methods improve their results taking full advantage of the time varying-selectivity of the channel, being the SICMMSE the best of them (see Figure 2.17). Regarding the last simulated SIC equalizer, the SIC-SIS, it can be observed that its performance is dramatically limited for high mobility environments because of the error floor due to diagonalization. It is also important to note that, in any case, there is not performance gain for SNR values smaller than 10dB.

3.3.3 Complexity

It is well known that the spectrum efficiency is a key point for the new generation standards, and the data throughput increase is the easiest way to overcome this drawback. This leads to larger data symbols, and therefore, it is enough to estimate the complexity of the basic algebraic operations involved in each equalizer to calculate their overall complexity. According to this approach, the different algorithms complexity based on the matrix computation are summarized in TABLE 2.5.

TABLE 2.5. Approximated computational complexity.

	METHOD	Before Banding	After Banding
LINEAR	MF	$O(N^2)$	$O(Np)$
	ZF	$O(N^3)$	$O(N^2p)$
	MMSE	$3{\cdot}O(N^3)$	$3{\cdot}O(N^2p)$
ITERATIVE	PICMF	$O(N^3)$	$O(N^2p)+k_{ite}O(Np)$
	PICZF	$2{\cdot}O(N^3)+k_{ite}O(N^2)$	$O(N^2p)+k_{ite}O(Np)$
	PICMMSE	$4{\cdot}O(N^3)+k_{ite}O(N^2)$	$3{\cdot}O(N^2p)+k_{ite}O(Np)$
	SICSIS	$O(N^2)$	$O(Np)$
	SICZF	$O(N^3)+O(N^3/3)+O(N^2)$	$O(N^2p)+O(N(2p+3p))+O(Np)$
	SICMMSE	$3{\cdot}O(N^3)+O(N^3/3)+O(N^2)$	$3{\cdot}O(N^2p)+O(N(2p+3p))+O(Np)$
KRYL	LSQR	$O(kN)$	$O(kN)$
	GMRES	$O(kN)$	$O(kN)$

To illustrate the performance penalty due to the banding process, the example for a banded MMSE linear equalizer is given, as it is the algorithm which better

shows the problematic. To do so Figure 2.18 represents several BER simulations for increasing values of the normalized banded matrix bandwidth ρ_{norm} for both mobility environments. First, the low mobility scenario is represented by solid lines, where it is easily noticed that the banding penalty is negligible because in these scenarios there is little relevant information in the matrix sub-diagonals and super-diagonals. Second, in the high mobility scenario (dashed lines), the banding performance degradation increases as the energy spread into the sub-diagonals and super-diagonals increases due to the Doppler Effect. This performance degradation is directly related to the matrix bandwidth, as expected. However, this performance penalty is not observed for low SNR conditions where the distortion due to time-variability is insignificant if compared to the multipath distortion and the Gaussian noise.

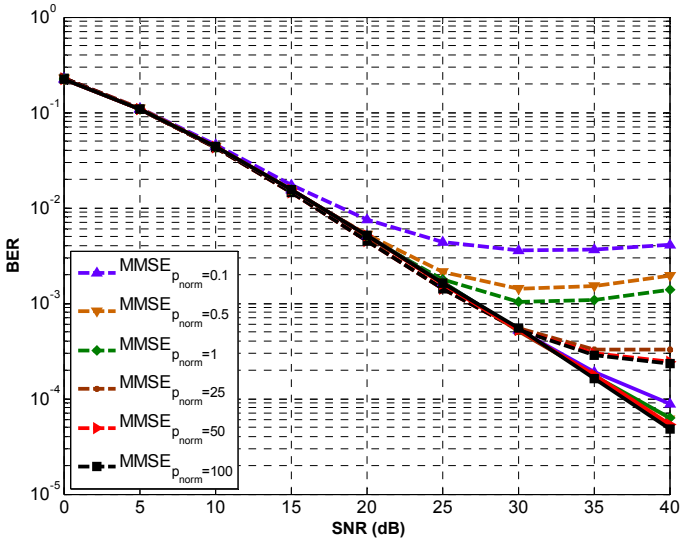

Figure 2.18. BER for a TU-6 channel when the normalized Doppler factor is (solid lines) f_dT_u=0.1 (dashed lines). In this case the f_dT_u=0.01 legend is omitted for the sake of clarity (the colour code is the same).

After that, in Figure 2.19 (a) and Figure 2.19 (b) further insight into this performance penalty is gained analysing the performance degradation for every proposed scheme. More precisely, for the sake of a better understanding, the performance results for SNR = 25 dB (Figure 2.19a) and SNR = 40 dB (Figure 2.19b) have been simulated. The first one is chosen because it is the limit where the interference due to the Doppler Effect becomes predominant regarding the weight of the other distortions, and for the same reason, the 40 dB case is when the

performance is more affected by the banding process. Both graphics show the presented methods BER performance variation in terms of the ρ_{norm} parameter.

The first noticeable outcome is that if the impulse response is considered quasi stationary, the banding process does not affect the equalizers performance (see Figure 2.19 (a) and (b), solid lines). As previously commented, under these conditions, the channel power is completely settled into the main diagonal and the information contained in the matrix sub-diagonals and super-diagonals is so negligible that it can be removed through a banding process without degradation. By contrast, the banding process affects the equalizers performance when dealing with high mobility environments (see Figure 2.19 (a) and (b), dashed lines). In this case, the channel varies within the symbol duration and the energy is spread into the adjacent sub-diagonals and super-diagonals of the channel matrix. For this reason, the banding process cannot be applied in these scenarios without previously assuming a performance worsening.

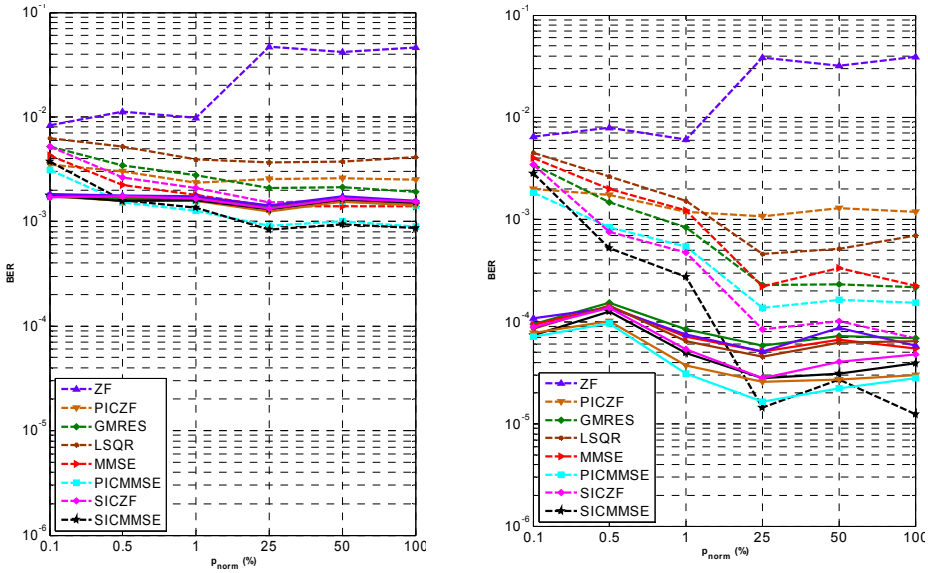

Figure 2.19. (a) Banded equalization matrices BER performance for a TU-6 channel when the normalized Doppler factor is f_dT_u=0.01 (solid lines) and f_dT_u=0.1 (dashed lines) (b) Banded equalization matrices BER performance for a TU-6 channel when the normalized Doppler factor is f_dT_u =0.01 (solid lines) and f_dT_u =0.1 (dashed lines).

In general, for high mobility scenarios, the BER performance degradation of the corresponding equalizing scheme is inversely proportional to the applied

banding bandwidth except for the ZF equalization. On the contrary, the ZF related equalizers improve their performance when a severe banding process is applied due to the sensitivity reduction after the banding process, as shown later (see Figure 2.19 (b), dashed lines).

To summarize, without a banding process the Krylov iterative methods are the less complex ones by definition, although the required number of iterations should be considered. As expected, next there are the linear equalizer methods and finally the iterative ones. Furthermore, the complexity of the corresponding equalization scheme can be drastically reduced after applying a banding process. Nonetheless, the banding bandwidth should be carefully chosen, as through the simulations it has been proved that, after the banding process, the BER degradation directly depends on the presence of Doppler interference: the more the impulse response varies within a symbol, the more the performance degrades after the banding process. Therefore, in order to select the banded matrix bandwidth, a trade-off solution between the complexity reduction and the performance degradation should be taken into account. For example, if a small banded matrix bandwidth is selected for the iterative methods, the resulting complexity is not much higher than the complexity of the linear methods, whereas the performance improvement is significant.

3.3.4 Sensitivity

Finally, the noise sensitivity hypothesis made in Section 3.1.3 is confirmed by several simulations. It should be remarked that, in this work, the sensitivity is used to test the robustness against noise, not the channel capacity. Therefore, the sensitivity has been tested for all the equalizer matrices involved in an inversion operation.

Firstly, instead of simulating the sensitivity of each equalization method, it is more attractive to run the simulations for the more representative expressions where the inverse calculus is involved and which are shared for several of them. The selected equations are: $\{\mathbf{Z}\}$ (used for the ZF and PICZF), $\{\boldsymbol{ZZ^H} + N_0\boldsymbol{I}\}$ (used for MMSE and PICMMSE), $\{\mathbf{L_{ZF}}\}$ and $\{\mathbf{D_{ZF}}\}$ (used for SICZF), and $\{\mathbf{L_{MMSE}}\}$ and $\{\mathbf{D_{MMSE}}\}$ (used for SICMMSE). Figure 2.20 shows the sensitivity, represented by the $K(\mathbf{S})$ parameter, as a function of the normalized Doppler frequency.

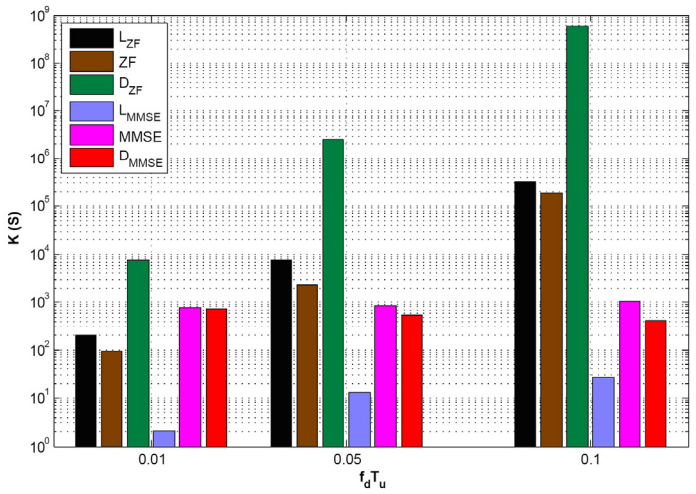

Figure 2.20. Sensitivity of the equalizer matrices when SNR=25 dB.

On the one hand, for the most sensitive methods (ZF, PICZF, SICZF), the sensitivity increases exponentially with the normalized Doppler frequency values. The ZF method is the only one which improves after applying a banding process, as shown in Figure 2.19(b). This is due to the sensitivity improvement achieved after the banding process application. On the other hand, the methods where the sensitivity is not dependent on the normalized Doppler frequency, i.e. the MMSE related ones, present nearly the same performance independently of the channel variability. In this case, when the banding process is applied, its performance decreases due to the loss of information as its sensitivity is not a critical parameter.

To sum up sensitivity, the obtained results have proved that, as mentioned previously, the noise enhancement due to the equalization process depends directly on the sensitivity of the channel equalization matrix (see Figure 2.19 (a) and (b)). It has also been shown how this sensitivity increases exponentially with the channel time-variability due to receiver mobility (see Figure 2.20), except for the MMSE related methods. Actually, those methods that are strongly affected by high sensitivity have worse performance in high Doppler environments. Finally, the equalization matrix sensitivity can be reduced using factorizations and/or converting the channel matrix into a banded matrix, which also leads to computational complexity reduction (see Figure 2.19 (a) and Figure 2.19 (b)).

3.3.5 Joint Comparison of the Evaluation Parameters

In this section there have been gathered, in a single plot, all the results that have been presented previously. In particular, Figure 2.21 depicts for low (a) and high (b) time-varying channels the main obtained conclusions. Both figures show the trade-off between complexity and BER performance for each- scenario (SNR = 40dB), while the area of each bubble indicates its sensitivity: the bigger the bubble is, the more affected by the sensitivity.

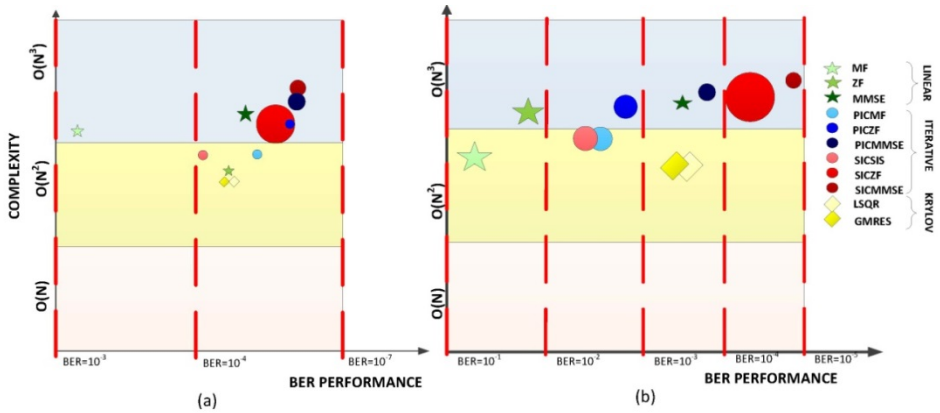

Figure 2.21.Analysis of the BER performance (y-axis), complexity (x-axis) and sensitivity (bubble size) for the equalization techniques (a) low time-varying channels and (b) high time-varying channels.

The first important outcome is that for low time-varying channels the vast majority of the methods show nearly the same BER performance. Nevertheless, once the Doppler increases the advantage of using iterative receivers is undoubtable. It is also important to note that the MMSE based methods have the same sensibility (same bubble size) for both cases, while the ZF methods shows the most pronounced increase. Finally, it is demonstrated that within the most complex algorithms the SICMMSE algorithm shows the best performance, whereas LSQR and GMRES tend to show the best trade-off between complexity and BER performance for rapid time-varying channels.

4. SUMMARY

The first part of this chapter has presented a comprehensive physical and mathematical analysis of the time-varying channels behavior. It has been demonstrated that the received signal spectrum, after going through a mobile channel, is composed by the superposition of a series of input signal spectrum replies, filtered and Doppler shifted. Therefore, the Doppler distortion cannot be considered just as frequency offset.

In addition, regarding the theoretical mobile reception, it has been proved that the time-varying behavior of a channel for an OFDM signal can be represented in terms of a two-dimensional matrix. This account for the doubly dispersiveness of the channel: the time and frequency selectivity. At the receiver site, the origins and essentials of the Doppler Effect and the related inter-carrier interference have also been explained.

In the second part of the chapter it has been demonstrated that the implementation of two dimensional channel estimators and equalizers is a very effective way of solving the mobility issue. Theoretically, they can achieve the maximum capacity as they take advantage of the time variability offered by the channel. As a matter of fact, one major contribution of this chapter relies on the fact that all the proposed algorithms have been tested under the same signal configuration and through the same channel model, and therefore, all of them have been compared under the same conditions

Consequently, a depth analysis of the most relevant doubly dispersive equalizers has been included in the second half, with the purpose of finding new alternatives for improving the current mobile reception capabilities. The study has started with a deep analysis of the existing bibliography, and afterwards, a mathematical analysis of the methodologies has been carried out. Finally, a practical evaluation of the previously described equalization algorithms has been presented in terms of the error correction capability, complexity and sensitivity. This last parameter offers a novel approach to analysis the robustness of the equalization methods against noise presence.

Eventually, whereas in previous comparison studies the channel is considered to be perfectly known, in this chapter a time-varying channel estimation algorithm is proposed and applied for the simulation of equalization methods' performance. The results have shown that the usage of two dimensional equalization matrices can remove or minimize the Doppler Effect impact on the OFDM receiver performance, especially in the case of iterative algorithms. Nevertheless, it has also

been shown that the main gains appear at relatively high SNRs (>15dB), and therefore, for low SNR, there should not be any gain. This is a critical issue as the urban mobile scenarios tend to have really challenging receiving conditions.

Eppur si muove.

-Galileo Galieli

CHAPTER 3: **ALGORITHMS FOR IMPROVING THE MOBILE RECEPTION**

The main objective of this chapter is to present technical solutions for improving the receiver performance over time-varying channels. In the first part, a novel equalization algorithm is proposed, which is a combination of some of the basic methods presented in the previous chapter and intends to outperform the existing methodologies. This solution follows the previous line of thought: treats the Doppler Effect as a second order multipath phenomenon. The main shortcoming of these algorithms is that the actual gain is noteworthy only for relatively high SNR values (SNR >15 dB). Consequently, in order to complete the possibilities, the second part of this chapter is focused on analyzing the Doppler Effect over more noisy environments. Through this part, the relation between the AWGN, the ICI and the FEC codes will be analysed. As a conclusion, a novel approach for dealing with the time-varying channel is presented.

1. DOPPLER EFFECT AS A TIME-VARYING MULTIPATH DISTORTION

The first proposed alternative for improving the mobile receivers' performance is based on the theoretical facts explained in Chapter 2. As a matter of fact, the implementation of two-dimensional equalization techniques is one of the most popular approaches for dealing with time-varying channels. In short, they can take full advantage of the time diversity provided by the double selective fading channels while suppressing the residual interference and the noise enhancement, and thus, they can maximize the channel capacity. In other words, they do not only reduce the inter-carrier interference, but also employ the time variability as a source of time diversity. The proposed hybrid equalizer is based on the previously explained concepts, and makes the most of the strengths of the analysed algorithms with the purpose of presenting a better solution for dealing with the time-variability as a source of diversity.

1.1 A Newly proposed Banded Hybrid Equalizer

The proposed equalizer is named as hybrid because it implements a concatenation of two different iterative stages: SIC and PIC. The basic structure of the proposed hybrid equalizer is shown in Figure 3.1.

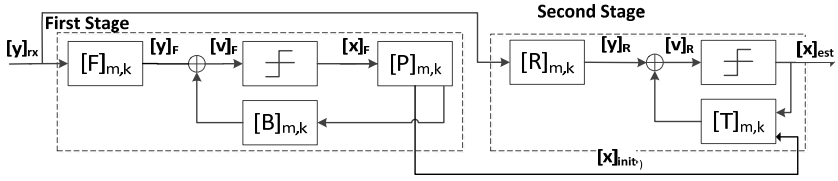

Figure 3.1. Proposed Hybrid SIC-PIC equalizer block diagram.

The first stage structure implements the sequential nulling and cancellation steps proposed in [67] through the usage of two filters: the first is **F**, the forward filter, whose purpose is to suppress interference due to undetected symbols and the second, the feed-forward filter, **B**, whose purpose is to suppress the already detected symbols. These filters are constructed based on the L^HDL decomposition of the matrix $\mathbf{B} = \mathbf{Z}^{\boldsymbol{H}}\mathbf{Z} + N_0$, where N_0 is the noise power. Equations (3.1) and (3.2) show the decomposition algorithm:

$$D[j,j] = B[j,j] - \sum_{k=1}^{j-1} L^2[j,k] D[k,k] \tag{3.1}$$

$$L[i,j] = \frac{1}{D[j,j]} \left(B[i,j] - \sum_{k=1}^{j-1} L[i,k] L[j,k] D[k,k] \right) \tag{3.2}$$

where **B** is the input matrix, **D** is the diagonal matrix and **L** the low triangular matrix.

In this successive cancellation algorithm, the signal to interference plus noise ratio (SINR) for each carrier is directly proportional to the values obtained in the diagonal matrix **D** of the **B** matrix factorization. Based on that, its performance can be improved if an best-ordering algorithm is applied: first, the matrix columns are rearranged in all the possible combinations, and afterwards, the different diagonal values for every permutation are calculated; finally, the detection order is defined by the permutation with the highest diagonal values. The main shortcoming is that, in the presented scenario, the number of carriers is quite large, and therefore, the method is very complex (*N*! permutations).

Furthermore, although in time-varying channels some channel energy is spread into the matrix sub-diagonals and super-diagonals, the main part remains located in the main diagonal. What is more, if the previous decomposition factorization formula is analyzed, it is clearly shown that the diagonal matrix values are mostly dependent on the input matrix diagonal values. Therefore, it is reasonable to consider that the high valued diagonal values will correspond to the highest singular values, and thus, define the best signal to noise ratios. That is why the proposed ordering method is based on the matrix **B** diagonal values, according to Eq. (3.3):

$$p_{ord}[m] = \arg \max \quad diag\left\{ \mathbf{Z}^{\mathbf{H}} \mathbf{Z} \right\}, \quad 1 < m < N \tag{3.3}$$

Nevertheless, the proposed ordering is not the optimal solution, and therefore, some residual error may be present. To make up for that performance degradation, a second equalization stage is proposed: the parallel-interference canceller (PIC) or multi-stage detector, whose aim is to cancel simultaneously the interference from all the symbols. The PIC stage is initialized with the first stage output, and then in the iterative step, the resultant hard decisions vector is used to suppress the inter-carrier interference.

1.1.1 Complexity Reduction

In principle, the proposed receiver requires $O(N^3)$ floating point operations as it involves inversion and multiplication of square matrices, whereas the second stage, employs $O(N^2)$, due to matrix to vector multiplication. Thus, the overall hybrid algorithm complexity might be approximated to $O(N^3)$ when N is large enough.

The algorithm raw implementation is too costly and a further step should be taken to reduce the complexity. As the proposed ordering method is completely based on matrix algebra, a matrix banding process can be applied in order to achieve a notably less complex scheme. The banding process consists in reducing the amount of sub-diagonals and super-diagonals that are taken into account, which besides reducing the complexity, it will allow us to handle equalization filters as sparse matrices. That way the previous mentioned complexity is reduced to $O(N^2\rho)$ where ρ is the matrix bandwidth, that is, the number of super-diagonals and sub-diagonals taken into account.

In addition, a method to calculate the maximum bandwidth reduction allowed, while the system performance is maintained is also proposed. First of all, the overall energy of the matrix sub-diagonals and super-diagonals is calculated excluding the main diagonal, according to Eq. (3.4):

$$E_t = \sum_{m=1}^{N-1} \left\| H(m,:) \right\|^2 \tag{3.4}$$

It should be noted that **Z** is a circular shifted version of **H**, the double Fourier transform of the channel impulse response. Afterwards, the matrix is banded just considering the number of sub-diagonals that contain a predefined percentage of the overall energy. That way, the equalizer complexity is automatically reduced without any significant performance loss. For instance, for a TU-6 channel with $f_d T_u$=0.1 (where f_d represents the maximum Doppler shift and T_u is the symbol duration) more than the 90% of the total energy is located within the 10% of the total sub diagonals.

1.1.2 Performance Evaluation

In order to prove the performance improvement of the proposed receiver scheme, the equalization capability is tested in the general simulation platform defined in Chapter 2. The method performance is evaluated for a TU-6 channel,

being the time variability of the channel defined by f_dT_u=0.1. The performance results based on the BER versus SNR plots are commented in the following paragraphs.

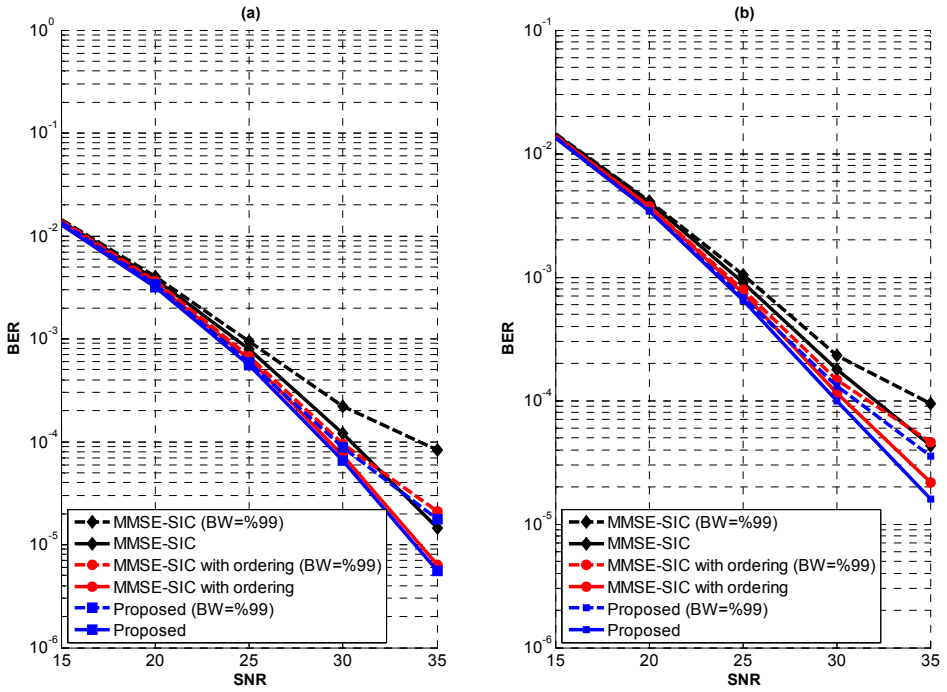

Figure 3.2. (a) BER for a TU-6 channel with the proposed equalizers for f_dT_u=0.1 and ideal channel estimation. (b) BER for a TU-6 channel with the proposed equalizers previously presented iterative channel estimation.

Figure 3.2 (a) gives the BER performance of the proposed method (blue line), compared to the regular MMSE-SIC (black line) and an MMSE-SIC with the proposed ordering (red line) when the CIR is perfectly known. On the one hand, the dashed line represents the methods where the banded process is applied, and on the other hand, the solid line indicates that the whole matrix is used. In the banding process a 99% of the energy is taken into account, which corresponds to the first sixty sub-diagonals, and therefore, a computational saving of 99% is achieved. Apart from that, the curve performance shows that the proposed ordering methods (red line) improve the basic MMSE-SIC method (black line), while the PIC stage provides a slight increase in the gain, as observed when blue and red lines are compared.

Figure 3.2 (b) shows the same methods performance, but when the iterative two dimensional channel estimation method presented in Chapter 2 Section 3.2 is used. It is clearly shown that the same relation is maintained, while the overall performance does not degrade too much. These results support the proposal of both the new ordering method and the iterative channel estimation algorithm, and it can be stated that the presented hybrid algorithm can outperform the equalization techniques presented in the previous chapter. Therefore, the main advantage of this proposal is that it achieves a great complexity reduction thanks to a banded process, while the proposed low complexity ordering and PIC stage offer an extra gain in terms of performance.

However, there is also a last consideration that must be taken into account. The results presented up to now confirm that the best performing algorithms offer some kind of gain when compared to the simpler ones. Nevertheless, it is also true that in order to provide significant improvement based on the time diversity, they require very high values of signal-to-noise ratio, even higher than 15 dB. Normally, this is a condition that the mobile channels are not going to fulfill and the receivers must be designed for working under very low SNR conditions. Therefore, the following questions rose: Does this approach have any kind of advantage when low threshold signals are used? How will the Doppler Effect be handled under very noisy environments?

2. DOPPLER EFFECT AS A NOISE SOURCE

The main benefit of using doubly dispersive equalization algorithms is that they are capable of turning the channel impulse response time-variability issue into a diversity gain (in the time domain). Nevertheless, the main shortcoming is that they performance gain is only meaningful for low noise environments (high SNR), and therefore, it is expected that there should not be much gain when strong error correction algorithms are included, even if they are compared with the one dimensional tap frequency equalizers.

Conseuqntly, in Figure 3.3 a one dimensional equalizer (red and purple lines) and one of the best performing two dimension algorithms (blue and green lines) presented in Chapter 2 (ordered SICPIC-MMSE) are compared, when the channel gain is totally known at the receiver site. The OFDM physical waveform is a 1K QPSK signal with an LDPC as FEC and the channel is a TU-6 where $f_d T_u$=0.1. The simulations include two different code rates, 1/3 and 5/6, the first one is targeting low SNR, whereas the second one is maximizing the signal throughput. The left subplot (a) shows the un-coded BER performance for both cases, whereas the right subplot depicts the performance at the decoder output.

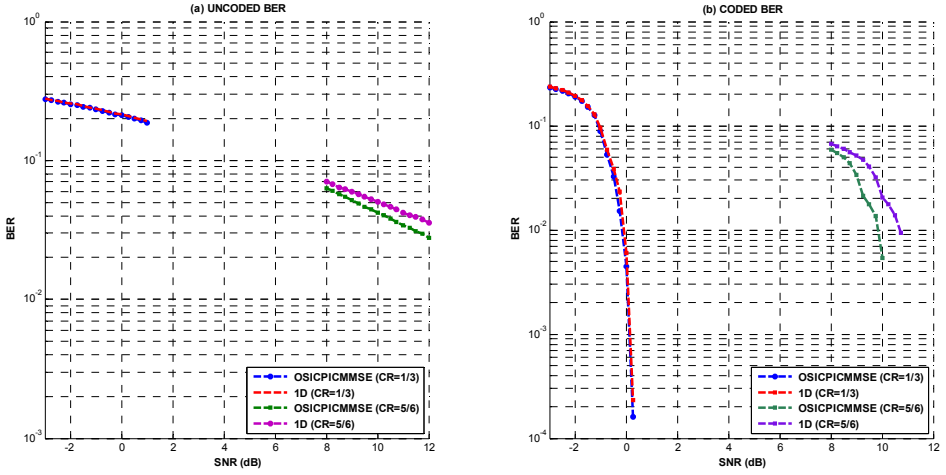

Figure 3.3. BER performance for two dimensional and one dimensional equalization algorithm with ideal channel estimation under mobile channels.

As expected, when the CR is robust (1/3) the receiving SNR is very low, about 0 dB (right side plot), and both algorithms show the same performance. In fact, if the uncoded BER is analysed (left side plot), it can be seen that the Gaussian noise

is so powerful that it is masking the time-varying diversity of the channel. Thus, there is no gain in including two dimensional equalization algorithms.

What is more, even for a very weak code rate (5/6), which converges for higher SNR values, the gain is not very high. It can be seen that the SIC-MMSE presents a slight gain for the un-coded signal (from 8 to 12 dB), and consequently, the two dimensional algorithm threshold after the FEC is just slightly better (0.75 dB) at the decoder output.

In few words, when the SNR is low, for example below 15 dB, the Gaussian noise masks the chance of using the channel time-varying behaviour as a diversity source, and the receiving thresholds does not depend on the equalizer, but on the FEC algorithm correction capability. Nevertheless, it must be noted that using one dimensional algorithms lead to a loss of the orthogonally of the OFDM carriers, and therefore, the addition of a new source of receiver noise: the inter-carrier interference. The next subsection will be focused on analysing the impact of this ICI and the chance of using one dimensional algorithm for dealing with time-varying channels.

2.1 ICI Impact on One Dimension Algorithms

The first step of this new approach is to understand the mathematical consequences of working with the doubly-dispersiveness of the time-varying scenarios with one dimension algorithms. In particular, it is important to connect the origin of the inter-carrier interference with this approach, and afterwards, analyse comprehensively the impact of this new source of noise in the channel estimation and equalization algorithms.

2.1.1 Origins of the Inter-Carrier Interference (ICI)

Taking into account the mathematical expression developed in Chapter 2 Section 1.2, the spectrum of a signal at the output of a time-varying channel can be expressed as a function of its Scattering function and the input signal spectrum (See Eq. (3.5)).

$$y[k] = \frac{1}{N}\sum_{m=0}^{N-1}\sum_{l=0}^{L-1} x[k]S[k-m,l]e^{-2j\pi lm/N} + w_{awgn}[k] \tag{3.5}$$

Next, the summation is split in two terms, the first one representing the multipath distortion, and the second one, the Doppler Noise due to ICI.

$$y[k] = \frac{1}{N}\overbrace{\left(\sum_{l=0}^{L-1} S[0,l]e^{-2j\pi lk/N}\right)}^{Mul.Distortion} x[k] + \overbrace{\sum_{m\neq k}^{N-1}\sum_{l=0}^{L-1} x[k]S[k-m,m]e^{-2j\pi lm/N}}^{ICI\ noise} + w_{awgn}[k] \quad (3.6)$$

Taking the definition of the Scattering function, it can be seen that the null component of the Scattering function is equivalent to estimating the average value of the time variation of each of the multipath components.

$$\frac{1}{N}S[0,l] = \frac{1}{N}\sum_{n=0}^{N-1} H[n,l] = h_{ave}[l] \quad (3.7)$$

Finally, inserting Eq. (3.7) into Eq. (3.5), the output signal spectrum can be simplified as the summation of the mean channel impulse response and two noise terms: the Gaussian noise and the Doppler noise.

$$y[k] = h_{ave}[k]x[k] + w_{ICI}[k] + w_{awgn}[k] \quad (3.8)$$

Therefore, when in order to perform the one dimensional frequency-domain channel estimation, the receiver first estimates the channel gain at pilot carriers, the following expression is obtained

$$\tilde{H}_P[k] = \frac{y_P[k]}{x_P[k]} + w_{ICI}[k] + w_{awgn}[k] \quad (3.9)$$

This means that independently of the existing Gaussian noise, there will always be an associated Doppler Noise.

2.1.2 Channel Estimation

In the vast majority of OFDM based broadcasting system, the pilot-aided channel estimation is performed using the in-band pilots. At the transmitter site the pilot carriers are spread in both time and frequency-domain to cope with both time and frequency-selectivity of the wireless mobile channels. The density of the pilots in the frequency domain will determine the maximum channel delay that the proposed configuration can achieve. This distance is known as the Nyquist limit (τ_{max}) and is given by:

$$\tau_{\max} = \frac{T_u}{D_x} \tag{3.10}$$

being $\mathbf{T_u}$ the symbol length and $\mathbf{D_x}$ the bearing carrier space between adjacent pilots. Depending on the selected pilot patter this value may be longer or shorter than the actual guard interval size. For reference, the scattered pilot pattern shown in Figure 3.4 is used. In this case, the pilot spacing is 1/12 and shifted by 6 sub-carriers over two OFDM symbols($\mathbf{D_x = 6, D_y = 2}$). This is also a very appropriate configuration for channel estimation in mobile conditions.

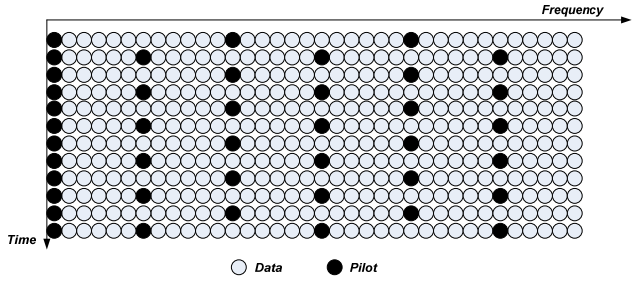

Figure 3.4. Scattered pilot pattern example.

Channel estimation for the pilot structure shown in Figure 3.4 can be efficiently performed with a concatenation of frequency-domain channel estimation and time-domain noise filtering. In order to perform frequency-domain channel estimation, the receiver first obtains the Least Square (LS) estimates on the pilots,

$$\tilde{H}_P[n,k] = \frac{Y_P[n,k]}{X_P[n,k]} \tag{3.11}$$

where $x_p[n,k]$ and $y_p[n,k]$ are the transmitted and received pilot symbols in the k^{th} sub-carrier of the n^{th} OFDM symbol. In the worst case scenario, where the maximum delay spread of the channel is larger than the Nyquist limit defined by the adjacent pilot carrier distance ($D_x \cdot D_y$), the actual pilot density can be increased taking into account the time domain density of the pilot pattern. In this case, prior to frequency domain interpolation a time domain interpolation is done (See Figure 3.5).

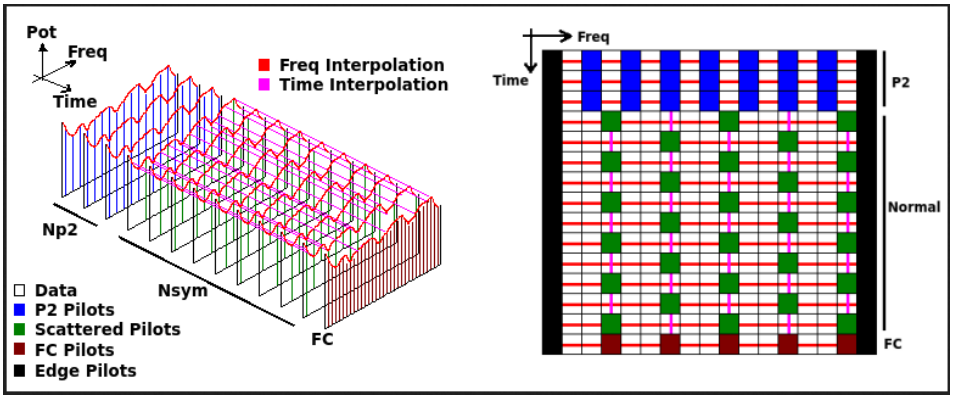

Figure 3.5. Graphical representation of time and frequency domain interpolation.

Either the pilot time-domain interpolation is done or not, the frequency-domain interpolation is performed to obtain the channel estimations on the data sub-carriers. This can be performed using many different interpolation techniques proposed in the literature [99]. Some popular interpolation techniques are: linear, cubic-spline and DFT-Interpolation [100].

Linear interpolation has the lowest complexity, but it provides the poorest performance for channels with high frequency-selectivity, i.e., channels with large delay spread. For such channels, cubic-spline interpolation is more accurate and the most commonly used piecewise-polynomial interpolation method, with reasonable complexity. The good performance of cubic-spline interpolation in frequency-selective channels is achieved by approximating the channel frequency response as a third-order polynomial. However, for very challenging channels with very large delay spread, such as 0 dB single-echo channels or SFN channels, this approximation is no longer accurate and therefore it might generate large estimation errors. Nevertheless, noise-filtering can be used to reduce the estimation noise generated from the cubic-spline interpolator, assuming that the channel delay spread is shorter than the OFDM guard interval. Finally, DFT-Interpolation performs an accurate interpolation using the *sinc()* function without making any assumptions on the frequency-domain channel response. To perform DFT-Interpolation, the time-domain channel response is first obtained by an IDFT operation as,

$$\tilde{h}_P = IDFT\left\{\tilde{H}_P\right\} \tag{3.12}$$

where $\tilde{h}_P$ is a vector of length M_P, being M_P the number of pilots in one OFDM symbol.

The interpolation is performed as:

$$\begin{aligned} &\tilde{h} = [\tilde{h}_P \; 0 \; 0 \cdots 0] \\ &\quad and \\ &\tilde{H} = DFT\{\tilde{h}\} \end{aligned} \tag{3.13}$$

where $\tilde{h}_P$ is expanded to an N-length vector, $\tilde{h}$, by appending zeros and performing an N-point FFT. When the channel delay spread is smaller than the number of pilots, the DFT-Interpolation provides accurate interpolation.

Up to now, the explained channel estimation methods have used the LS channel estimation on the pilot sub-carriers. More accurate estimates on the pilot sub-carriers can be obtained using the MMSE estimator described in [101]. However, this requires much higher complexity and the LS channel estimation on the pilots given by Eq. (3.11) already provides very close to limit performance, even for very challenging channel conditions. This suggests that using the highly complex MMSE estimator on pilots is not necessary at least for the considered system parameters.

2.1.2.1 Time-Domain Wiener Filtering

With the channel estimates obtained by frequency-domain channel estimation, time-domain Wiener filtering can be used to further improve the channel estimation accuracy. For the k^{th} sub-carrier in the n^{th} OFDM symbol, a $2A$-tap time-domain Wiener interpolator is performed as,

$$\hat{H}[n,k] = \sum_{m=-A, m\neq 0}^{A} u_m \cdot \tilde{H}[n-m,k] \tag{3.14}$$

where u_m are the Wiener filter coefficients. Coefficients of the Wiener filter in (3.14) are calculated as,

$$u = [u_{-A}, u_{-A+1}, \cdots, u_{-1}, u_1, \cdots, u_A] = R^{-1} \cdot p \tag{3.15}$$

and *R* is the time-domain correlation matrix for the fading process (of this sub-carrier) whose entries are given by,

$$R[m,n] = E\left\{H[m,k]H^*[n,k]\right\} + \sigma^2\delta_{m,n} = R_H[0,m-n] + \sigma^2 \cdot \delta[m-n] \quad (3.16)$$

where *n* is the time-index (OFDM symbol index) and *k* is the frequency index (sub-carrier index).

In Eq.(3.17), $R_H[\Delta n,\Delta k]$ is the space-time space-frequency correlation function of the mobile channel, σ^2 is the noise variance, and $-A \le m, n \le A$. The 2D correlation matrix function, $R_H[\Delta n,\Delta k]$, is defined as,

$$R_H[\Delta n,\Delta k] = E\left\{H[n+\Delta n,k+\Delta k]H^*[n,k]\right\} \quad (3.17)$$

The vector *p* in (3.15) is calculated as,

$$p = \left[R_H[A,0], \cdots, R_H[1,0], R_H[-1,0], \cdots, R_H[-A,0]\right] \quad (3.18)$$

For mobile channels with a classic U-shaped Doppler spectrum, the 2D correlation function is calculated as,

$$R[\Delta n,\Delta k] = \frac{J_0\left[2\pi f_d \Delta_n T_s / N\right]}{1 + j2\pi\Delta_k f_u \sigma_d} \quad (3.19)$$

where σ_d is the delay spread , f_d is the maximum Doppler shift, T_s is the OFDM symbol duration, f_u is the OFDM sub-carrier spacing and J_0 the zero order Bessel function.

2.1.3 Performance of channel estimation

In this section, the performance of the new technical proposal is evaluated. In particular, the previously presented channel estimation algorithms in combination with the one-dimensional tap equalizer have been tested for time-varying channels. Furthermore, as commented before, a very robust LDPC code (CR=1/4) has been added to test the capability of the proposed methodology to cope with time-varying channels. The results are once again obtained using the implemented general purpose platform defined in Chapter 2. The selected physical waveform is a

4K OFDM QPSK signal with a 1/8 guard interval modulated over a carrier frequency of 690 MHz.

For the proposed system with OFDM modulation, since the frequency-domain signal in the sub-carriers is regular modulus signal, a zero-forcing single-tap equalizer should provide a good enough performance for the LDPC decoding.

Regarding the channel models, the most possible challenging channels scenarios have been selected: TU-6 and 0 dB Echo. Both channels has been extensively used in the DVB-T and DVB-T2 standardization processes [34]. The last one presents a very challenging channel condition for broadcast signal detection, especially when the echo delay is long. Simulations were performed assuming a worst-case echo channel condition with a single echo as strong as the main signal, and an echo delay close to 90% of the guard interval. Finally, these are the considered channel estimation algorithms for the test:

- FD-Cubic: frequency domain cubic-spline interpolation with noise filtering.
- 2D-Cubic: frequency domain cubic-spline interpolation with noise filtering plus time domain Wiener filtering.
- FD-DFT: frequency domain DFT-interpolation
- 2D-DFT: frequency domain DFT-interpolation plus time domain Wiener filtering.

It must be noted that in these cases the 2D applies for the additional time-domain Wiener filtering and not for the two dimensional CIR used in the previous section. In the simulations, a time-domain Wiener filter with 10 taps is used, i.e. A=5 in Eq-(3.14). The first sets of results provide information about the performance of the LDPC coding applied to the tested signal, as well as the system performance when different channel estimation approaches are taken. In all the figures in this subsection, the dashed lines represent the LDPC output BER, whereas the solid lines account for the error at the LDPC decoder input, i.e., uncoded BER. In addition to the performance curves for the four channel estimators, the performance of an ideal receiver with perfect channel knowledge is also obtained and plotted in the following figures for comparison purposes. This curve provides a reference on how the channel estimators perform when compared to an ideal receiver. Figure 3.6 depicts the performance for static and slow varying conditions (50 km/h) in a 0 dB echo single channel, while in Figure 3.7 the

performance curves for a receiver moving at 50 and 100 km/h in a TU-6 channel are plotted.

In Figure 3.6 it can be shown that 2D-DFT shows the best performance for the different channel estimation techniques for stationary receivers. Using frequency-domain DFT-Interpolation with time-domain Wiener filtering (2D-DFT), the maximum gap with respect to the ideal case is just about 0.9 dB for the stationary case (left subplot).

Similar observations are made for a mobile receiver moving at 50 km/h. A slightly larger gap of 1.3 dB is observed between the performance obtained with 2D-DFT and that of the ideal receiver probably due to the ICI. It is important to keep in mind that the test channel is a worst-case scenario with both extremely strong echo and large delay. Therefore, the simulation results show that with a properly designed low-complexity channel estimator and a low code-rate, the mobile layer will have a very robust performance in extremely challenging mobile fading channels even if one dimension algorithms is employed.

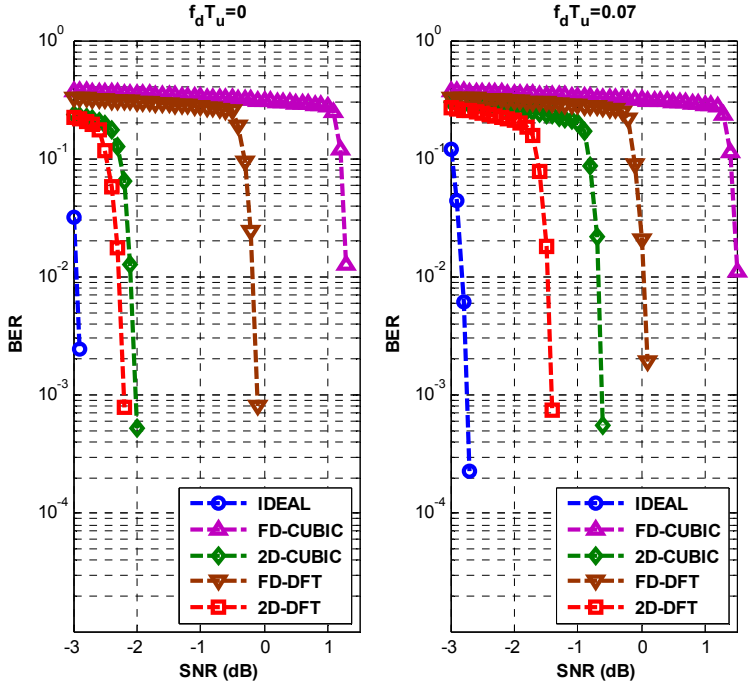

Figure 3.6. Mobile Layer BER performance in 0dB Single Echo Channel for stationary and mobile reception.

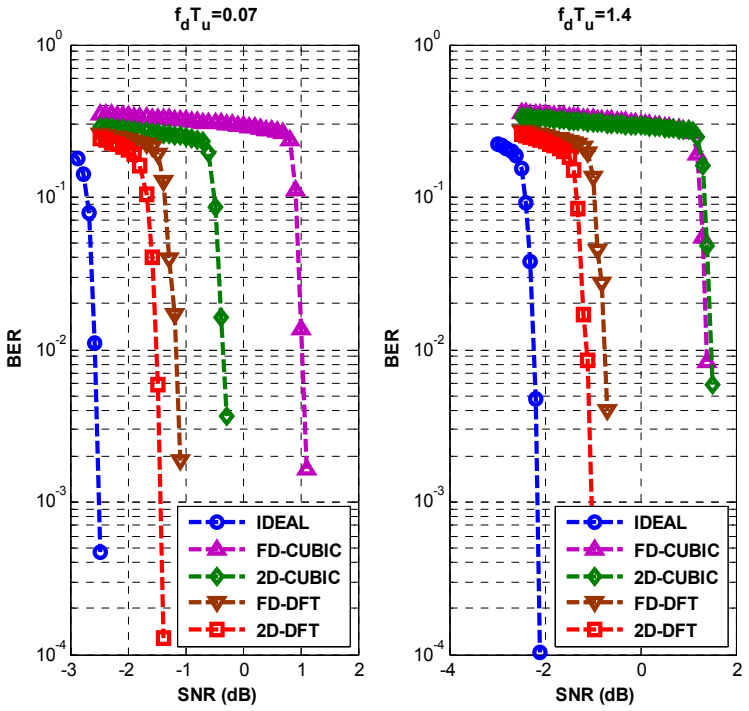

Figure 3.7. Mobile Layer BER performance in TU-6 channel for low and high speed reception.

In Figure 3.7 the same channel estimation methodologies are analyzed, but in this case, for mobile conditions, namely TU-6 channel. The left plot shows the results when the receiver is moving at 50 km/h, whereas in the right part the speed is increased up to 100 km/h. It can be seen that for this case the 2D-CUBIC algorithm shows the very worst performance, and therefore, the 2D-DFT is the best performing algorithm with just about 1 dB loss. It is also important to note that the channel performance has worsened just 0.4 dB when after doubling the speed.

All the performance results are summarized in TABLE 3.1. The first two rows show the simulation performance over TU-6 channel condition and the last two rows represent the 0dB echo wireless channel. In short, using frequency-domain DFT-Interpolation with time-domain Wiener filtering (2D-DFT), the maximum gap with respect to the ideal case is just about 0.8 dB for the stationary case and 1.2 dB for the mobile case.

TABLE 3.1. Minimum SNR thresholds for different channel estimation algorithms.

		Channel Estimation				
	$f_d T_u$	**Ideal**	**FD-Cubic**	**2D-Cubic**	**FD-DFT**	**2D-DFT**
TU-6	0.07	-2.4	1.2	-0.2	-0.1	-1.3
0 dB Echo	1.40	-2.0	1.5	1.6	-0.6	-0.9
	0.00	-2.8	1.4	-1.9	0.0	-2.1
	0.07	-2.6	1.5	-0.5	0.2	-1.3

2. LARGE SIZE FFTS OVER TIME-VARYING CHANNELS

In OFDM signals, the usage of large size FFTs reduces the guard interval percentage, and therefore, increases the data throughput reducing the data overhead. In addition, for the same pilot pattern, the distance between adjacent pilots is smaller, which improves the channel estimation. Nevertheless, up to now, they have not been considered for delivering mobile services as the Inter Carrier Interference due to the Doppler Effect is very critical.

In this chapter it has been shown that if the FEC correction code is strong enough, the ICI can be treated as another noise source. Therefore, a side-effect of this approach is that it should is feasible to use large sized FFTs for time-varying channels and to probe that is one of the main objectives of this section.. Apart from that, it offers two more contributions: first, it theoretically estimates the impact of the ICI degradations on the receiving thresholds, and second, the performance loss that may occur due to a mismatch in the noise power estimation is shown. Finally, several simulation results that reinforce the idea that large OFDM symbols are suitable for mobile channels are included[102].

2.2 Theoretical Modelling of Doppler Effect

Based on the mathematical model presented in previous sections, the distortion introduced by the Doppler Effect is twofold; it does not only introduce an additional noise, but also reduces the signal power, which is converted into ICI. In other words, due to the loss of orthogonality, at the receiver some part of the conveyed signal power is turned into ICI. Thus, it is clear that the higher the ICI is, the more the performance degrades. Providing that the Doppler noise can be treated as another type of noise, the theoretical performance loss can be obtained from (3.20) and (3.21)

$$K_{ICI}(dB) = 10\log_{10}\left[1 - 10^{\frac{\left((SNR)^{\min\_theor} + \Delta_{ICI}\right)}{10}}\right] \tag{3.20}$$

$$(SNR)^{\min\_real} = (SNR)^{\min\_theor} - K_{ICI} + 10\log_{10}\left(1 + 10^{\left(\frac{\Delta_{ICI}}{10}\right)}\right) \tag{3.21}$$

The correction factor K_{ICI} calculates the impact of the inter-carrier interference in the received signal, and in (3.20), the power division is added to this degradation. Both expressions use Δ_{ICI}, which is the power relation between the multipath component and the Doppler noise, i.e., the relative power of the ICI. Once the theoretical boundaries have been set up, the next step is to estimate the approximated values of the Δ_{ICI} component in order to see how deep its impact could be. As an example, the TU-6 channel model is selected.

Figure 3.8 demonstrates the Δ_{ICI} of OFDM modulation for different Doppler rates. A carrier frequency of 700 MHz is assumed, which is the worst case scenario for mobile broadcasting channels.

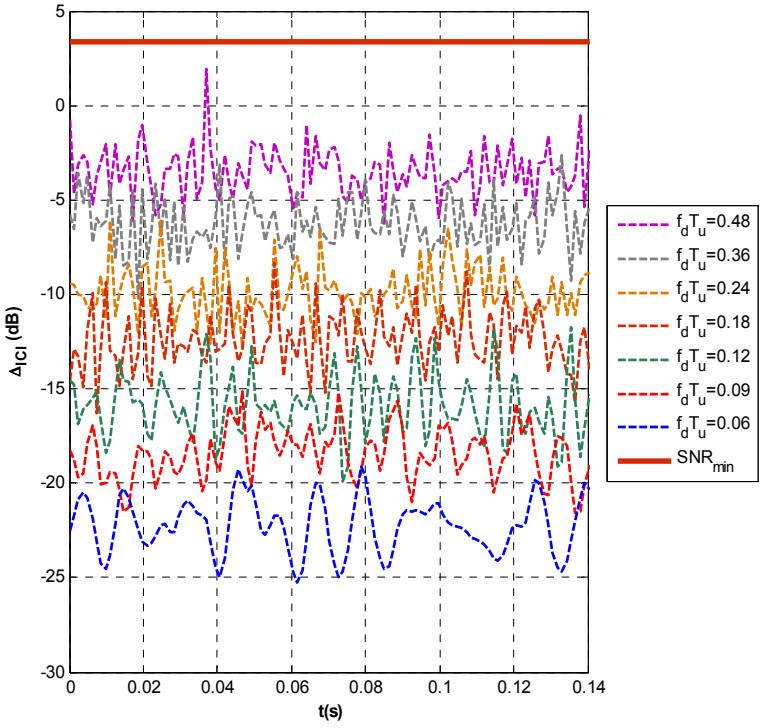

Figure 3.8. OFDM inter-carrier interference for different Doppler frequencies.

The ICI relation is given for different $f_d \cdot T_u$ values, which represent the relation between the maximum Doppler frequency f_d and the symbol duration T_u. The upper thick line, SNRmin, represents the overall noise power that an OFDM signal with an LDPC R=1/5 code can withstand. It can be seen that the blue line, corresponding to an 8K signal at 75 km/h, is more than 20 dB below the signal

power. Therefore, the ICI power is negligible if compared to the AWGN. This is the main reason why the 8K size is perfectly suitable for mobile scenarios. Furthermore, comparing the different ICI powers, it can be seen that there is about 6 dB increase when doubling the Doppler frequency. If the worst case is taken, that is, the purple line representing a 32K signal at 150 km/h, it can be stated that it is about 8 dB below the receiving threshold. This figure proves that if a strong error correction code is used, it is feasible to use large FFT sized signals for mobile scenarios. The main advantages of using larger sized FFTs are, first, that the data throughput is increased; and second, that for the same pilot and data carrier ratio, the distance between adjacent pilots is smaller. This will improve the channel estimation accuracy, leading to better signal cancellation and system performance. Although Figure 3.8 proves that large FFT sizes can be used, it is important to figure out what the actual performance loss will be. In order to do that, the theoretical expressions defined in (3.20) and (3.21) can be used. To do so, the ΔICI value is obtained as the mean value of multiple simulations similar to those shown in Figure 3.8.

The results are shown in Figure 3.8. It has been assumed that in the case of a nearly stationary TU-6, i.e., ICI free case, the minimum receiving threshold SNR^{min_theor} is about -3.1 dB for a code rate of 1/5. Based on those values and applying the mathematical formulation defined in (3.20) and (3.21), the approximated receiving thresholds after considering the ICI noise are calculated.

TABLE 3.2. Approximated calculation of the receiving SNR (dB) based on the possible estimation of the ICI power.

$f_d \cdot T_u$	0.06	0.09	0.12	0.18	0.24	0.36	0.48
Δ_{ICI}	-21.8	-18.0	-15.6	-12.2	-9.0	-6.0	-3.5
SNR_{est}	-3.1	-3.1	-3.0	-2.8	-2.5	-1.7	-0.6

According to the theoretical calculations, it seems reasonable to use large FFT sizes for mobile scenarios, although a performance loss must be expected. For instance, for the worst case considered, 32K and 150 km/h or $f_d \cdot T_u = 0.48$, this loss could be up to 2.5 dB. However, for the same FFT length but at 75 km/h or $f_d \cdot T_u = 0.36$, the performance loss is supposed to be about just 1.5 dB, when compared to the smallest Doppler contribution ($f_d \cdot T_u = 0.06$).

2.3 **Simulation Results**

In the previous section it has been theoretically proved that using very robust code rates, large size FFTs can be applied for mobile scenarios. The main objective of this section is to prove through simulations that the previous assumption is feasible. In order to test the real Doppler impact over existing broadcasting standards, an LDPC coding/decoding stage has been included in the system model presented before. The LDPC decoding should be performed using soft decision values or metrics, which are also known as Log Likelihood-Ratios (LLR). The LLR reliability depends on the channel estimation, ϱ, and overall noise power, $N_{0,}$ as shown in (3.22):

$$LLR_i\left(I_i, Q_i \middle/ x_i\right) = \frac{1}{2\pi N_o} e^{\frac{\left(I_i-\rho_I I_{x_i}\right)^2-\left(Q_i-\rho_Q Q_{x_i}\right)^2}{2N_o}} \tag{3.22}$$

where (I,Q) and (I_x,Q_x) represent the transmitted and received IQ pairs respectively. As shown before, if the channel time variability is high, the ICI power value should be taken into account, as its value is close to the existing Gaussian noise. If it is not considered, there might be an additional performance loss, not only due to the increase of Doppler related noise, but also due to a mismatch in the LLR calculation.

In TABLE 3.3, the results for different mobile use cases are shown. Three results are given for each scenario: in the first one, the Gaussian noise is the only noise power taken into account for the LDPC decoding (Case I), whereas for the second case, the LDPC input is fed with the sum of both distortion noises (Case II). The last column is based on the theoretical formula presented in Eq. (3.21) (SNR^{min_real}). It can be seen that the second option improves the performance of the LDPC decoding, showing a performance loss for the worst case of just 2 dB (when compared to the theoretical SNR^{min_theor} of -3.1 dB). What is more, for the 115 km/h case, a 32K signal just suffers 1 dB loss, which makes it feasible for real implementation. Furthermore, it must be taken into account that the TU-6 is a very challenging channel and that such high speeds are not expected in an urban environment. Finally, it is important to note that these practical values are close to the theoretical assumption of Eq. (3.21).

TABLE 3.3. Minimum receiving SNR threshold for different mobile scenarios.

	50 Hz (75 km/h)			**75 Hz (115 km/h)**			**100 Hz (155 km/h)**		
	I	II	SNR^{min_real}	I	II	SNR^{min_real}	I	II	SNR^{min_real}
8k	-3.1	-3.1	-3.1	-3.1	-3.1	-3.1	-3.0	-3.1	-3.0
16k	-3.0	-3.0	-3.0	-2.7	-2.9	-2.8	-2.6	-2.7	-2.5
32k	-2.6	-2.7	-2.5	-1.8	-2.1	-1.7	-0.2	-1.1	-0.6

As a conclusion, it is important to consider that large FFTs might be implemented for mobile channels, if the approach of using ICI power error corrections is considered. Apart from that, another major contribution has been to successfully present a theoretical formulation for modelling ICI incidence into the OFDM signal performance over time-varying channels.

3. SUMMARY

In this chapter there have been presented two new technical solutions for improving the receiver's performance under time-varying channels. In the first part of the chapter, a new hybrid equalization technique for dealing with doubly dispersive channels has been presented. The main advantage of the presented equalizer is that it can turn the shortcoming of the channel impulse response time-variability into a diversity gain. What is more, it has been shown that it outperforms the vast majority of the methods presented in the literature. In addition, a complexity reduction methodology based on banding matrices has been included. The only weakness of the presented method is that it requires high values of SNR for offering a noteworthy gain when compared to simpler one dimensional equalizers.

Based on this conclusion, the second part of the chapter has focused on demonstrating that if strong error correction codes are used (low SNR receiving thresholds), there is not a big gain in using very complex equalization algorithms. As a matter of fact, the resulting ICI due to the usage of one dimensional algorithms in both the channel estimation and equalization can be treated just as another source of noise. Furthermore, it has been proved that the more robust the signal is, the smaller the degradation due to the ICI.

Finally, following the line of thought of this second approach, it has also been demonstrated that the large size FFTs can be used for mobile channels. Up to now, the large size FFTs were not used due to the fact that the inter-carrier space is inversely proportional to the FFT size and therefore, the larger the symbol length, the bigger the ICI. Nevertheless, if the FEC is strong enough, the receiving threshold is so low that the Gaussian noise masks the ICI, and thus, there is no extra degradation. What is more, a theoretical formulation for estimating the performance loss due to the ICI has been presented. It must be borne in mind that the usage of large FFT sizes allows a more efficient usage of the spectrum, which is one of the main objectives of this work.

1. *Mathematics is the language of nature.*
2. *Everything around us can be represented and understood through numbers.*
3. *If you graph the numbers of any system, patterns emerge.*

-Pi: faith in chaos.

CHAPTER 4: **A NEW SOLUTION FOR CURRENT MOBILE NEEDS: LDM MULTIPLEXING**

In this chapter a new multiplexing technique is presented, known as Layered Division Multiplexing (LDM), which intends to fulfill two of the main objectives of this work. On the one hand, it improves the current mobile broadcasting reception, and on the other hand, it increases the spectrum efficiency.

LDM is a new technique, which grew out of the concept behind Cloud Txn approach, for enhancing the capacity of a transmission system, allowing the simultaneous transmission of stationary and mobile services. To begin with, basic block diagrams and operation of LDM transmitters and receivers are presented. After that, together with the basic technical explanations, the main theoretical considerations for its implementation are also included. Finally, a comparison with other existing multiplexing techniques (TDM, FDM) in terms of channel capacity is presented.

1. NEW APPROACHES FOR INCREASING THE SPECTRUM EFFICIENCY: LDM

As mentioned in Chapter 1, the efficient and flexible use of the spectrum is one of the engineering research areas that have driven more efforts during the last two decades. First with the analogue to digital transition and the adoption of the standards developed during the 90s, and later with the development of second generation broadcast standards during the first decade of the 21st century. After a brief analysis of the recent literature, it is clear that this topic has become more and more relevant to broadcasting research [34][37]. At the same time, other communication sectors have increased the pressure for further spectrum attributions to broadband wireless access [41], which is another catalyst that has fostered broadcasting technology developments for efficient use of spectrum. As a consequence of this problem, the new generation standards, such as ATSC 3.0, include in their call for proposals the imperative need for designing a spectral friendly system [6][42].

In addition to that, other mandatory requirement for Next Generation DTT is the capability of simultaneously delivering services with different capacities, in particular mobile and HDTV, or even mobile and UHDTV. The DVB technology family fulfills this issue through the implementation of different PLPs or the insertion of the mobile service within the FEFs of the fixed services [34]. Nonetheless, even though each solution has its own particularities, both are based on Time Division Multiplexing (TDM). Another example of combined mobile and fixed services is found in ISDB-m, where Frequency Division Multiplexing (FDM) is used for delivering different contents within the same frame.

The Layered Division Multiplexing (LDM) technique, which grew out of the concept behind Cloud-Txn [103][104][105], was included in the joint proposal by Communications Research Centre (CRC) and Electronics and Telecommunications Research Institute (ETRI), with the collaboration of the University of the Basque Country, to the ATSC 3.0 PHY Layer CfP [106]. Layered Division Multiplexing can be considered as a hierarchical spectrum reuse technique, where two synchronized signals (in frequency and power, but not necessarily in time) are broadcasted on the same RF television channel. This is possible due to the robustness provided by the FEC stage and cancellation and/or demodulation techniques at the receiver. With this approach, it is possible to inject a first signal targeting mobile services (Stream A), and on the same channel and certain dBs below Stream A, another signal (Stream B), where Stream B could be a DVB-T2 signal or another signal format for delivering high capacity services [56].

In principle, there is not any restriction for the second layer configuration; nevertheless, if the second layer is based on OFDM with the same FFT size, symbol period and pilot pattern as the upper layer, the receiver implementation will be significantly simplified.

Figure 4.1 shows a Layered Division Multiplexing graphical representation. At the transmitter, the signals of different streams are superimposed with specific injection levels, after being separately formatted and encoded. A third data Stream C can be further injected at e.g., 5 dB below Stream B. In this case, Stream C shares the same RF channel as that of Stream A and Stream B, and is frequency locked and clock synchronized with the other layers.

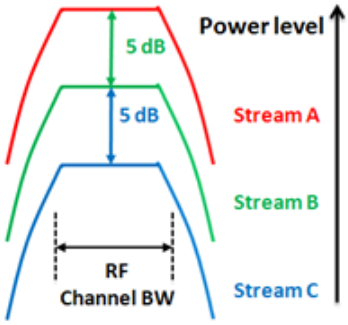

Figure 4.1. LDM system: Hierarchical spectrum re-use to improve spectrum efficiency.

The spectrum efficiency of Stream B ranges from 2 to 8 bit/s/Hz with a SNR threshold from 6 to 30 dB depending on the selected transmission mode (T2 limited to 256QAM) [57]. The combined multi-layer system spectrum efficiency ranges from 2.5 to 8.5 bit/s/Hz. For a 6 MHz TV band, the total expected data rates are in the range of 15 to 50 Mbps, with a very robust data rate of 2-3 Mbps for the mobile service and the rest for fixed multiple HDTV services or even UHDTV-4k service if HEVC coders are used [106]. It should be mentioned that injection levels between data streams are flexible, as well as the modulation and channel coding applied on each data stream for different reception robustness requirements.

Subsequent sections as well as Chapter 5 and Chapter 6 will be focused on Hierarchical Spectrum Reuse or Layered Division Multiplexing technique, as LDM has the potential to become an actual solution for the current broadcasting challenges: it offers the capability of delivering HD contents, and therefore, it addresses the objectives considered in the beginning of this work.

2. LDM TRANSMITTER AND RECEIVER

This section presents an overview of the basic structure and operation of transmitters and receivers implementing LDM.

2.1.1 LDM Transmitter

A generic block diagram of the LDM transmitter can be seen in Figure 4.2 The first important outcome is that each stream has its own BICM module, and therefore, data streams can be separately configured taking into account the different services that they may target. Once signals are modulated, the upper layer signal (stream A) is considered as the primary signal at the mapper output, and thus, it is superimposed to the lower layer signal (stream B) using the frequency hierarchical modulation (see Figure 4.2). In this architecture, the injection range (Δ) is the key parameter indicating how deep the lower layer signal is embedded, i.e, the superimposed signal is constrained by an injection level high enough so that lower layer signal does not severely interfere with the upper layer signal.

A third data stream C could be further injected at e.g. 5 dB, below the stream B. In this case, Stream C has also the same RF channel bandwidth as that of the other streams (A and B), and will be frequency locked and clock synchronized with the other layers. It is important to note that the decoding thresholds of all layers are affected by the corresponding injection levels, which is a critical feature in the LDM overall design.

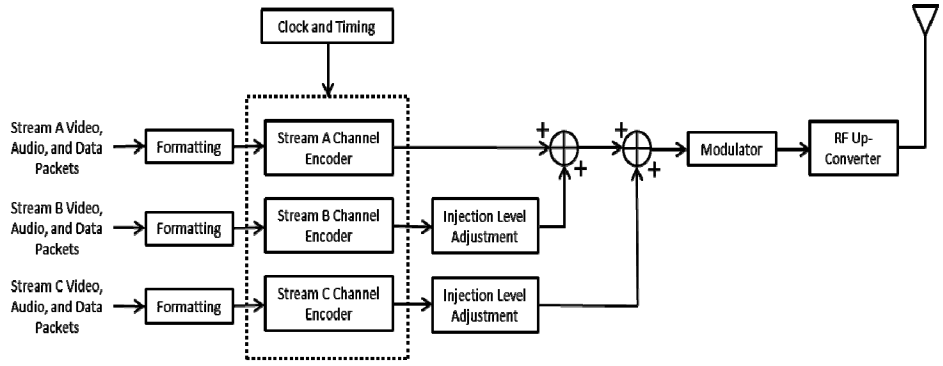

Figure 4.2. LDM system diagram with hierarchical spectrum-reuse.

Assuming that the different layers use the same OFDM-based physical-layer parameters, sharing the same FFT size, cyclic prefix, as well as the pilot pattern, the

frequency domain LDM signal at the transmitter output $x[k]$ can be represented as,

$$x[k] = x_{UL}[k] + 10^{(\Delta/20)} x_{LL}[k] \tag{4.1}$$

where $x_{UL}[k]$ is the modulated data stream of the upper layer, $x_{LL}[k]$ is the multiplexed high capacity stream, and k is the sub-channel index. The injection level, Δ, defines the relative power of the signal between the different transmission layers. Since the upper layer signal is defined to target mobile services, it requires higher power, and therefore, Δ has a value in $(-\infty, 0]$, where $-\infty$ can be understood as a single-layer mobile service transmission. For instance, a -5 dB injection level sets the LL signal 5 dB lower than the UL signal. In other words, the 80% of the power would be allocated to the mobile service.

2.1.2 LDM Receiver

At the receiver side the initial blocks after the antenna are the same as the standard OFDM receivers. These include: the RF front-end (tuner), IF system and AGC, carrier recovery, time synchronization, and equalization. For an OFDM modulation system, for simplicity, all layers should use the same size of FFT, same guard interval length and same in-band pilots. On the other hand, different modulation schemes can be applied on different layers or even on different data carriers in the same layer[107][108]. The physical layer pipe (PLP) concept used in the DVB-T2 system can also be applied on each layer. Actually, the multi-layer approach is equivalent to a layered PLP.

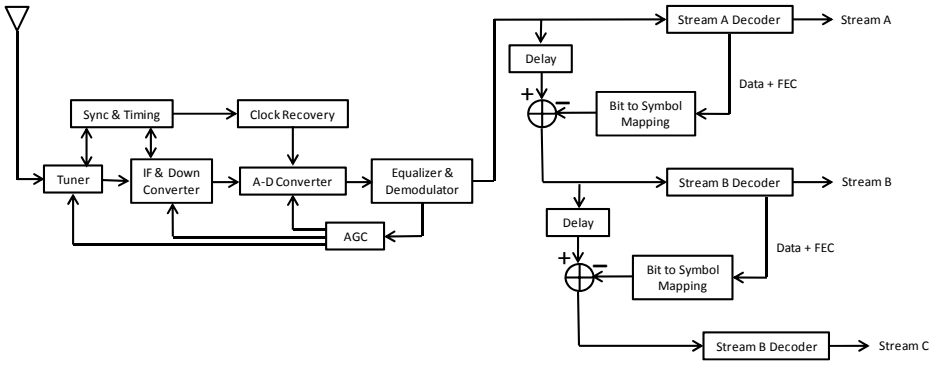

Figure 4.3. General block diagram of an LDM receiver.

For the decoding of the lower layer and the access to the high-data rate service, the LDM receiver has to carry out the following steps: first, correctly decode the upper layer, then, re-modulate the decoded data, and last, cancel the upper layer (UL) from the received signal. Once the upper layer has been removed, the decoding of the lower layer signal (LL) can proceed. As shown in the receiver block, to decode the upper layer signal, the LL service is treated as an additional noise source, being the impact of this interference controllable by assigning different injection levels to the LL signal. In order to decode the lower layer signal, the receiver first performs channel estimation and signal detection of the upper layer signal. It is important to note that, considering that the required SNR for lower layer decoding is much higher than what is required for error-free decoding of the upper layer, it is reasonable to assume that the upper layer signal can be perfectly reconstructed.

In the multiple layer system, for any OFDM symbol, the received signal in the k^{th} sub-carrier can be expressed as:

$$y[k] = h[k]\left(x_{UL}[k] + 10^{(\Delta/20)} x_{LL}[k] \right) + w[k] \tag{4.2}$$

To decode the lower layer signal, $x_{LL}[k]$, signal cancellation has to be applied as,

$$y_{LL}[k] = \frac{y[k]}{\tilde{h}[k]} - x_{UL}[k] = 10^{(\Delta/20)} x_{LL}[k] + i[k] + w[k] \tag{4.3}$$

where $\tilde{h}[k]$ is the estimation of the channel gain and $i[k]$ is the possible inter-layer interference,

$$i[k] = \left(h[k] x_{UL}[k] - \tilde{h}[k] \hat{x}_{UL}[k] \right) \tag{4.4}$$

In Eq. (4.4), it is demonstrated that the inter-layer propagation error depends mainly on the re-constructed upper layer and on the channel estimation accuracy. LDM inter-layer interference will be analyzed in detail in Chapter 5 – Section 4.

3. THEORETICAL CONSIDERATIONS FOR LDM IMPLEMENTATION

This section will present the main theoretical formulations behind the layered division multiplexing technique. First of all, the theoretical SNR are studied, and afterwards, a capacity comparison (based on Shannon-Hartley theorem) with the other main multiplexing techniques is presented. In particular, the main differences with the already existing TDM/FDM solutions are presented form a capacity analysis point of view. Finally, the main differences with the already existing hierarchical modulation technique are presented.

3.1 Theoretical SNR Thresholds for the Upper and Lower Layers

When the system is working on a multilayer hierarchical transmission, with two or more layers transmitted within the same RF channel, inter-layer interference appear. The lower layer signal acts as an interference source to the upper layer, reducing its noise tolerance capacity. Meanwhile, assuming a fixed total transmission power, adding the lower layer signal will also reduce the transmission power of the upper layer. Therefore, there is a twofold impact from the lower layer signal to the upper layer signal: acting as a noise interference source and reducing the transmission power.

3.1.1 Co-channel interference as a Gaussian noise

In the literature it has been already demonstrated that the OFDM co-channel interference can be considered as Gaussian noise [109]. Therefore, it seems reasonable to assume that the lower layer will be somehow acting as an additional AWGN for the upper layer. In the literature, AWGN is defined as a normal distribution with null mean and standard deviation $(0,\sigma)$. With this respect, if the co-channel interference can be treated as noise, the interference, a native OFDM signal, must satisfy the chi-square goodness-of-fit statistical test.

The idea is to evaluate the default null hypothesis that the data in the co-channel interference is white or not colored. The null hypothesis is tested against a predefined value of the significance level, in our case 5%. During the analysis, the mean and variance are estimated from the analyzed co-channel interference signal.

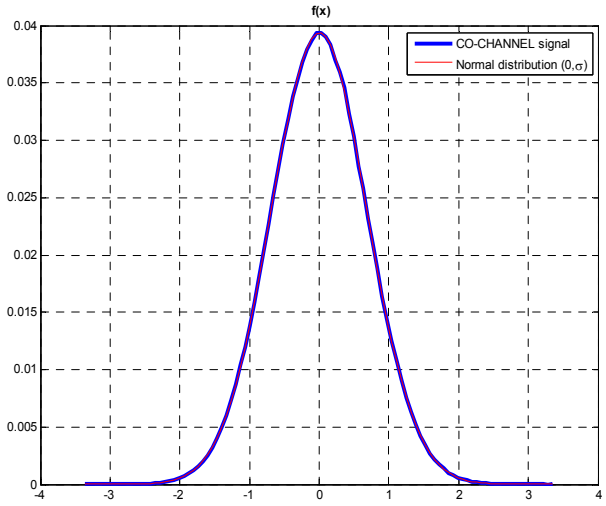

Figure 4.4. Probability density function comparison.

Figure 4.4 compares the probability density functions (pdf) of an OFDM co-channel interference samples and its corresponding normal distribution according to estimated mean and standard deviation. Basically, it confirms that both signals have nearly the same pdf. In general, almost 100% of the analyzed sample signals have confirmed that the co-channel interference corresponds to a normal distribution. What is more, the upper layer threshold is lower than the injection range. Consequently, when receiving the UL, the existing Gaussian noise power at the receiver is higher than the lower layer. This explains why the interference distribution deviates strongly to the Gaussian distribution.

3.1.2 Calculation of the SNR thresholds for the upper and lower layers

Usually, the SNR is calculated in reference to the total received signal power. Nevertheless, in the LDM case in the receiving threshold calculation the influence of the layered division must be taken into account. In particular, the correction factor *K,* that accounts for the noise injected by the lower layer, is given by (4.5), and the new signal to noise ratio for the upper layer signal $SNR_{UL\_overlay}$ is given by (4.6), where Δ is the injection level (dB):

$$K(dB) = 10\log_{10}\left[1 - 10^{\frac{(SNR_{UL\_th}+\Delta)}{10}}\right] \tag{4.5}$$

$$SNR_{UL\_overlay} = SNR_{UL\_th} - K \tag{4.6}$$

The overall power is now reduced as a function of the injection level (Δ). For instance, assuming that the upper layer SNR is -3 dB and the injection level is -5 dB, the total signal power can be calculated as 1.2 dB above the upper layer signal (see Figure 4.5). This is the total received signal power and should be the 0 dB power level reference in the receiver SNR calculation. The effective noise level for the upper layer system, will be the upper layer noise threshold minus the lower layer injection level. Therefore, the effective SNR for the upper layer system referenced to the total received signal power, will be the total signal power minus the effective noise power.

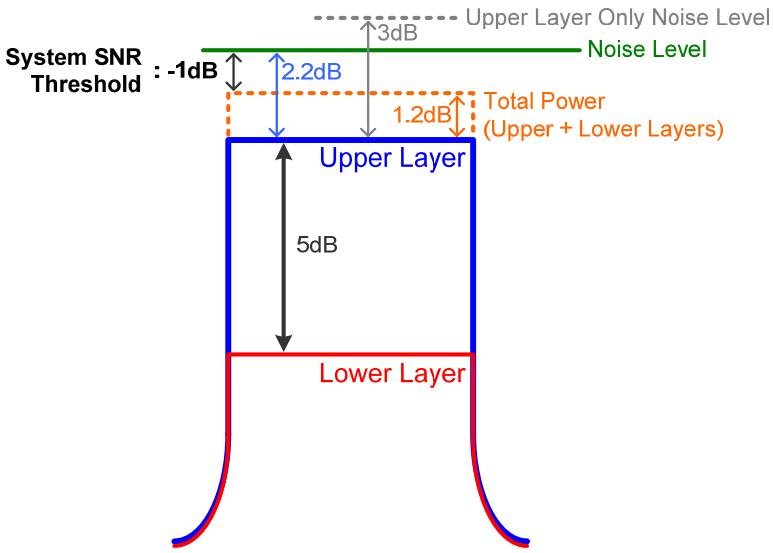

Figure 4.5. Calculation of the Inter-Layer interference of a 2-Layer system.

The required lower layer SNR in an overlay configuration ($SNR_{LL\_overlay}$) is calculated as

$$SNR_{LL\_overlay} = SNR_{LL} + \Delta + C \tag{4.7}$$

where SNR_{LL} is the original lower layer signal SNR (standalone SNR, the legacy system threshold), Δ is the injection level, and C is the power correction factor due to the fact that the transmitter distributes the nominal output power between the Upper and Lower Layers.

$$C = 10\log_{10}\left(1+10^{(\Delta/10)}\right) \tag{4.8}$$

3.2 **Differences with Hierarchical Modulation**

In the recent history of broadcasting, there are other systems that have merged two components on the transmitted signal in the form of hierarchical transmission. For instance, DVB-T or DVB-NGH have some working modes based on hierarchical modulation, which enable two layers with the same information message to be transmitted with different robustness [17].

Figure 4.6 shows an example of a DVB-T hierarchical 64-QAM constellation with an embedded QPSK stream. In a 64 QAM constellation 6 bits per 64QAM symbol can be coded. In hierarchical modulation, the 2 most significant bits (MSB) correspond to a QPSK service embedded in the 64QAM one [110].

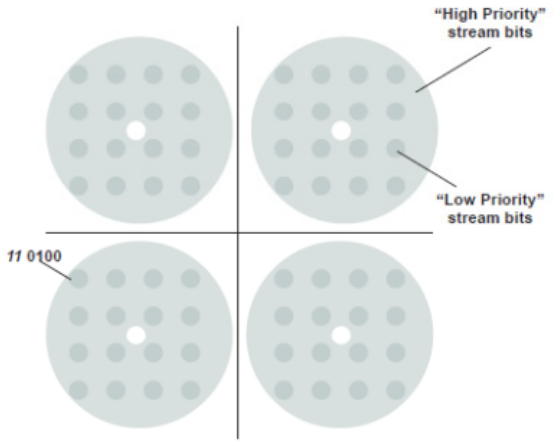

Figure 4.6. DVB-T Hierarchical 64QAM constellation with an embedded QPSK [110].

Likewise, Figure 4.7 shows an LDM multilayer constellation, which is the result of adding a 64 QAM signal for the lower layer and a QPSK for the upper layer, with injection levels of -3 or -6 dB respectively.

As observed when Figure 4.6 and Figure 4.7 are compared, LDM might be understood as a generalization of the hierarchical modulation concept. Nevertheless, the LDM scheme offers some substantial differences when compared to DVB hierarchical modulation. First, in LDM, the lower layer insertion is done at cell level, and therefore, it is possible to have different

transmission chains for each layer. That is to say, in the LDM system, the upper and lower layers may have different bit/cell and even time interleavers. This is a clear advantage as both layers are targeting different services, and thus, they have different requirements. In the classical approach, the modulation is done at bit level within the BICM, in such a way that both streams share the same transmission modules.

Second, in LDM, multilayer constellation points might not be in the same quadrant as the corresponding upper layer constellation point. That is to say, depending on the combination of upper and lower layer constellations and the injection range, multilayer constellation points corresponding to an upper layer constellation point of a certain quadrant may cross over to adjacent quadrants. As an example, Figure 4.7 shows an LDM multilayer constellation, which is the result of adding a 64QAM signal for the lower layer and a QPSK for the upper layer, with an injection level of {-3/-6} dB.

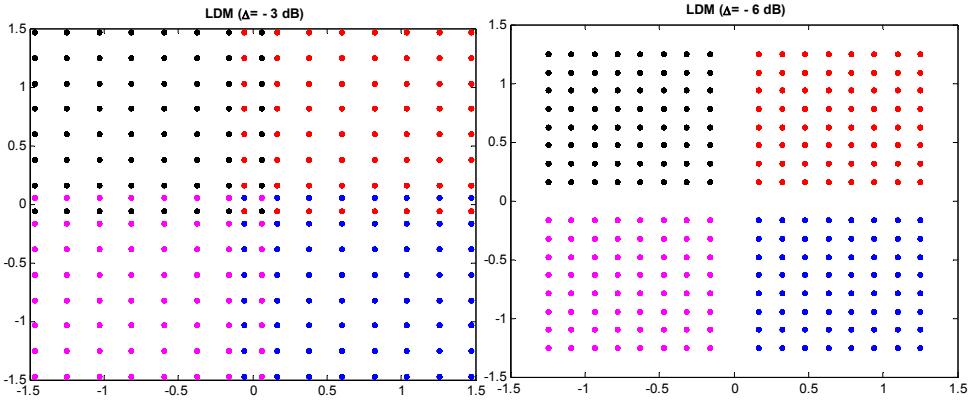

Figure 4.7. Example of LDM multilayer constellation, UL QPSK, LL 64QAM, (Injection Level -3/-6dB).

Figure 4.7 shows, on the left, the multi-layer constellation for a 64-QAM LL signal, where for each quadrant a coded color has been assigned. Thus, the black color is associated with the upper left quadrant whereas the red color marks the lower right points. The figure on the right shows the multi-layer constellation when a QPSK signal for the UL and a 64-QAM for the LL have been added with a -3dB injection level. It can be clearly seen how some points of the legacy layer constellation cross to other quadrants, and therefore, this is not the case of a classical hierarchical modulation.

Furthermore, in the classical concept of hierarchical modulation of DVB-T systems, only QPSK modulation can be used for the high priority bit stream, and only 16QAM/64QAM for the low priority bit stream [17]. In contrast, the idea of LDM allows any modulation on any layer, where modulation schemes among layers are independent, being the lower layer degradation independent from the upper layer constellation. Besides, in DVB-T, the injection levels between different layers are fixed values, whereas in the LDM system the injection levels are flexible.

The optimization of the injection levels (difference between upper and lower layers) and different constellation cancellation, demapping and decoding is still an open interesting topic for research.

3.3 **LDM Capacity Gain**

This theoretical analysis of the LDM capacity is another example of the international cooperation carried out during this work. As a matter of fact, this study was led by the CRC with the help of the UPV/EHU and ETRI.

The main objective of this section is to show that the proposed LDM technique is more spectrum efficient than other multiplexing schemes, and therefore, that it responds positively to one of the main challenges presented on the objectives of this thesis. Consequently, a theoretical capacity analysis comparison with the most used multiplexing techniques, TDM and FDM, will be provided. Considering the delivered capacity as the criterion for evaluating the techniques, it will be demonstrated that LDM is the best alternative when compared with TDM and FDM for offering simultaneously mobile and stationary services.

As a general concept, LDM allows a better exploitation of the spectrum, as it is uses the whole assigned RF channel 100% of the time. Even though, in order to test the efficiency from a theoretical point of view, the only alternative is to check the data capacity results. According to the channel capacity definition by Claude Shannon, the tightest upper bound on the information rate *(C)* can be calculated as the logarithmic relation between the signal power, P_S, and the additive White Gaussian noise *N*.

$$C = \log_2\left(1+\frac{P_S}{N}\right) \tag{4.9}$$

where the signal bandwidth has been normalized. It is important to note that the proposed technique allows the simultaneous transmissions of mobile and stationary services with different capacities: the upper layer is designed for delivering mobile services, whereas the lower layer is defined to offer high capacity services. Being the signal overall power P_s and the injection range Δ, the transmission power of each layer can be calculated as follows.

$$P_{UL} = \left(\frac{10^{\frac{-\Delta}{10}}}{1+10^{\frac{-\Delta}{10}}} \right) P_s \tag{4.10}$$

$$P_{LL} = \left(\frac{1}{1+10^{\frac{-\Delta}{10}}} \right) P_s \tag{4.11}$$

Based on the signal powers defined in (4.10) and (4.11), and applying the theoretical Shannon-Hartley theorem defined in Eq. (4.9), the capacity throughput of each layer over a Gaussian channel can be easily calculated as:

$$C_{UL} = \log_2 \left(1 + \frac{P_{UL}}{P_{LL} + N} \right) \tag{4.12}$$

$$C_{LL} = \log_2 \left(1 + \frac{P_{LL}}{N} \right) \tag{4.13}$$

For calculation of the lower layer signal capacity, the cancellation has been considered as perfect. Accordingly, there is non-significant error floor in the upper layer removal. Finally, in order to check the correctness of the estimation, using (4.12) and (4.13), it can be easily proved that the total capacity of the system is equal to the Shannon formula:

$$C_{UL} + C_{LL} = \log_2 \left(1 + \frac{P_s}{N} \right) = C \tag{4.14}$$

Furthermore, it is important to note that in LDM the channel capacity is distributed among different layers in a non-linear way and this capacity distribution is just dependent on the injection range. As mentioned before, the other two main options for multiplexing mobile and fixed services are TDM, used by the DVB family standards, and FDM, used in the ISDB-T standard. Although both of them

can be described by the same formulation, TDM has been chosen for the following analysis. When services are time multiplexed, there will be one time slot reserved for the mobile service (T_m) and another one for the fixed service (T_f), being the total duration equal to T_t. In that case, the power allocation for stationary and mobile services does not change, and therefore, the capacity is just dependent on the time slot percentage.

$$C_{mobile} = \left(\frac{T_{mobile}}{T_{total}}\right)\log_2\left(1+\frac{P_S}{N}\right) \tag{4.15}$$

$$C_{fixed} = \left(\frac{T_{fixed}}{T_{total}}\right)\log_2\left(1+\frac{P_S}{N}\right) \tag{4.16}$$

Eq. (4.15) and Eq. (4.16) demonstrate that in this case the channel capacity is linearly distributed for both mobile and stationary services. Previous equations show that both TDM and FDM are scaling the capacity while maintaining a constant value for the SNR, whereas LDM system varies SNR and uses the full bandwidth. Figure 4.8 depicts the RF channel usage for the TDM/FDM signal (left) and for the LDM case (right).

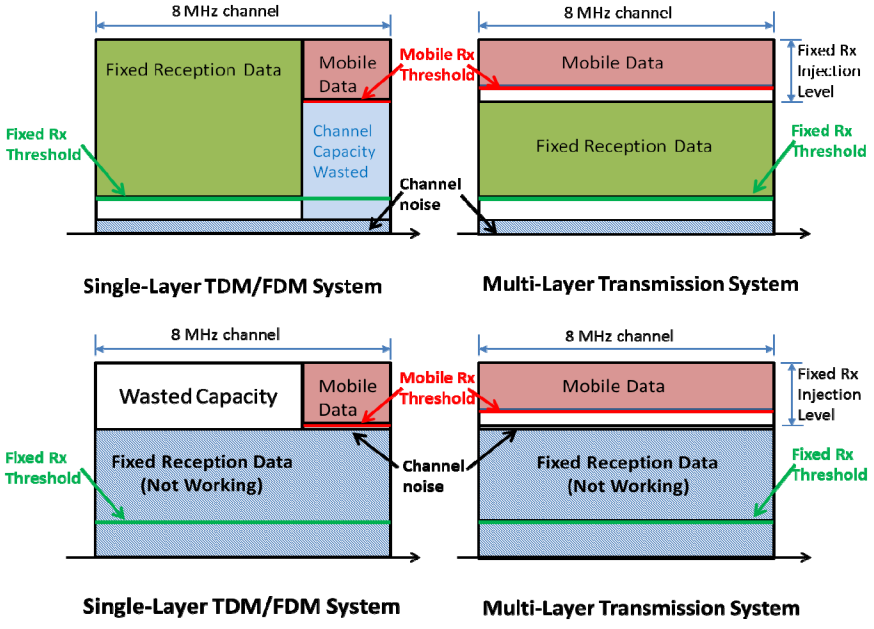

Figure 4.8. Capacity usage comparison between LDM (right figure) and FDM/TDM (left figure) for low/high SNR scenarios.

In the upper part of the figure it is shown how, in high SNR case, mobile and fixed services work well for both systems. However, TDM/FDM mobile system wastes some channel capacity. In the lower part of the figure, low SNR case depicted. In low SNR case, only mobile systems work, and it is clear that a single layer system wastes some channel capacity, because its mobile service only runs on a part of the RF channel. Therefore, it can be observed that while the hierarchical LDM allows a complete exploitation of the bandwidth, the other multiplexing techniques always leave a frequency band unused. The capacity gain offered by LDM depends strongly on the used injection range.

Figure 4.9 and Figure 4.10 show the channel capacity plots for some common use cases. The LDM signal is configured as a two layered system using an injection range of 5 dB, which allocates a 76% of the total power to the mobile layer and 24% for the high capacity layer. For fair comparison, TDM/FDM cases are also calculated for delivering simultaneous stationary and mobile services, with different time allocations (25%, 33%, 50%).

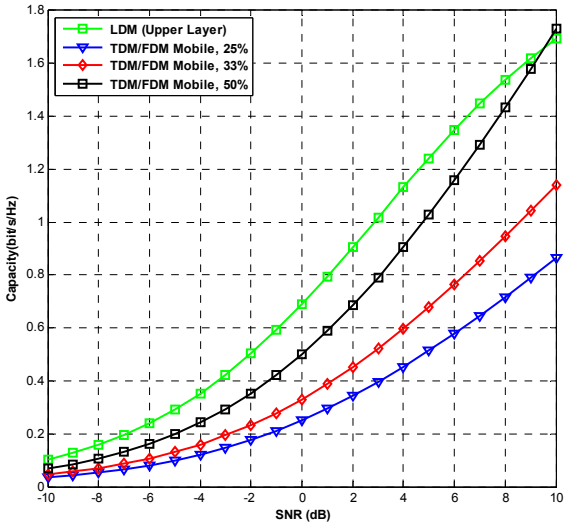

Figure 4.9. Mobile channel capacity of LDM and TDM/FDM.

Figure 4.9 shows the comparison for the mobile services. It can be noted that at low SNR (−10 dB to 10 dB), the LDM system presents a better usage of the potential channel capacity. Hence, for 0.4 b/s/Hz, the mobile service in LDM system is (1.8, 4.0, 6.0) dB better than the FDM/TDM system with (25%, 33%, 50%) mobile service allocation. What is more, at capacity of 0.8 b/s/Hz, the SNR advantages become (1.8, 4.5, 7.5) dB.

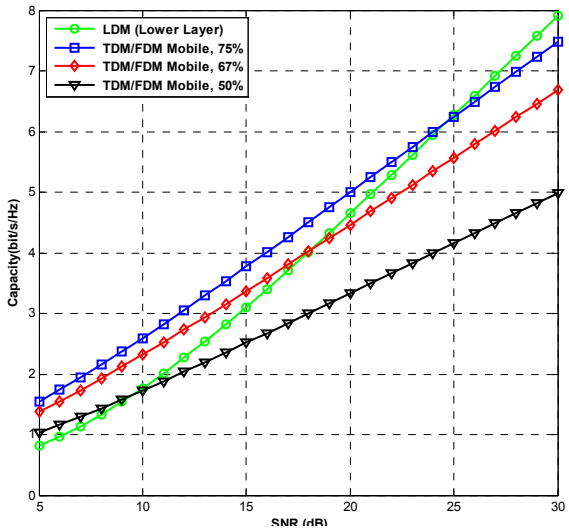

Figure 4.10. Stationary channel capacity of LDM and TDM/FDM.

The channel capacities of the stationary service channel in the LDM system and the single-layer TDM/FDM systems, are shown in Figure 4.10. It is proved that, at high SNRs, the LDM provides a higher channel capacity for the stationary service of the lower layer as compared to the three TDM/FDM systems. The LDM system provides higher channel capacity than the TDM/FDM system with (50%, 67%, 75%) stationary service allocation at SNR values higher than (10, 17, 25) dB respectively.

As it can be observed, the LDM system provides higher channel capacity for both mobile service at low SNR and fixed service at high SNR. Therefore, this multiplexing alternative provides the most efficient usage of the spectrum in the typical (and high priority) scenario of delivering a HDTV mobile service and a high data- rate UHDTV fixed service (or multiple HDTV services) in one RF channel. This advantage of the LDM system is mainly due to the nonlinear distribution of the channel capacity with respect to the power distribution. As shown in Eq. (4.12) , the capacity of different layers is calculated with the signal power distribution inside the logarithm operation; while for TDM/FDM systems, the capacities of different services are calculated in with the signal power distribution outside the logarithm operation.

Moreover, the injection level provides another control parameter for broadcasters in LDM system. In a TDM/FDM system, all OFDM carriers must be transmitted in the same level. So in a 8 MHz system, if an equivalent 2 MHz is

used for mobile in TDM/FDM approach, it means only 2/8 = 25% of power is allocated to mobile service. In a 2-layer LDM system, if the inject level is 6 dB apart between upper mobile layer and lower high-data rate layer, it means 80% of power is dedicated to mobile service and 20% of power is for fixed service. By varying injection level, the distribution of power to difference services can be controlled.

4. SUMMARY

In this chapter, a new application scenario, LDM multiplexing technology, has been presented for answering to one of the objectives of this work: increase the spectrum efficiency of current broadcasting systems.

In short, the presented spectrum overlay technology can be used to enhance the capacity of the transmission system, allowing the simultaneous transmission of multiple program streams with different robustness for different services in one RF channel. A multi-layer system makes a more efficient and flexible use of the spectrum, as each layer fully uses the entire RF channel bandwidth. That is to say, a two layer system is like implementing two independent mobile and stationary networks in one RF channel. The upper layer will normally be targeted for robust low SNR mobile services and robust stationary service with large coverage, whereas the lower layer would be best suited for high SNR, high data rate services.

Comparing with other advanced techniques such as MIMO or TFS, it has the advantage that there is no need for any substantial regulatory changes. Additionally, it allows a great flexibility without any need for changing the transmission power. In fact, other techniques such as TDM or FDM are more limited, in other words, they need to change the transmitted power to change the coverage footprint for any of the multiplexed services.

In this chapter, a theoretical calculus demonstrating that the LDM capacity can outperform TDM/FDM capacity has also been presented. In a TDM scenario, it seems reasonable that no more than the 50% of the resources (time) would be allocated to the mobile carrier, whereas in the LDM approach there is no restriction for the mobile/fixed power allocation ratio. The gain can be understood as a reduction of the required power for an error-free reception or as a capacity increase using the same transmission power.

Therefore, the main advantages of the Layered Division Multiplexing are the capability for offering simultaneously mobile and stationary services while maintaining the spectrum efficiency and flexibility. It has better time and spectrum diversity to achieve higher aggregated data rate and better flexibility on robustness and data throughput on different transmission layers.

To succeed, planning alone is insufficient. One must improvise as well.

-Isaac Asimov

CHAPTER 5: **IMPLEMENTATION ASPECTS OF THE LDM RECEIVER**

This chapter gains a deep insight into the specifics of the LDM receiver implementation, including some of the main algorithms required at the receiver site for the correct reception of the different layered services. Afterwards, a complexity analysis of the hardware requirements is included. In addition, a second thought is given to the classical channel estimation algorithms. As matter of fact, the proposed LDM receiver structure allows not only the implementation of the channel estimation algorithms presented in Chapter 3, but also the Decision Directed (DD), which is not based on the bare estimation of pilot carriers. Apart from that, a new frequency domain cancellation, which is required for accessing the legacy layer, is included. Several simulation results are also presented, which show the goodness and accuracy of the cancellation algorithm, demonstrating the feasibility of LDM for delivering simultaneously stationary and mobile services. Finally, to conclude this chapter, the possible inter-layer propagation error due to the cancellation stage is analyzed.

1. NEWLY DESIGNED LDPC CODES

One of the key technologies for the LDM technology implementation is the robustness of the upper layer. The receiver, at the upper layer, should be able to withstand very noisy environments, where the AWGN noise power may be higher than the actual noise power. In this case, the newly designed LDPC codes are very interesting, specifically, the rate compatible QC LDPC codes introduced in [111]. One of the main features of these raptor-like LDPC codes is that they can be easily shortened from their mother code to higher rate codes, while keeping relatively good performance. For instance, by truncating 50% and 83.3% of the quarter-rate mother Parity Check Matrix (PCM), rate R = 1/3 and 1/2 codes can be easily formed with decoding complexity reduced to 28% and 56%, respectively [111].

It should be noted that usually 80% of the broadcasting coverage areas have SNR values 5 dB above the required threshold. This means that 80% of locations do not need full error correction capabilities that are designed for the lowest SNR. In these locations, receivers can take advantage of the shortening capability of the LDPC code to achieve better power efficiency, i.e., longer battery life. Furthermore, the recently developed codes, which have been specially designed to work under very low SNR scenarios, can significantly outperform the DVB T2/S2 LDPC codes at low coding rate range. Even though, their design is fully compatible with the current DVB LDPC codes. In fact, both of them have the same parallel factor.

1.1 2D FEC with Rate-Compatible Codes

Taking advantage of their puncturing capability, these rate-compatible LDPC codes can be used to perform product code FEC blocks, which decoding complexity can be reduced when compared with concatenated codes. For instance, instead of the classical concatenated LDPC-BCH block, a two-dimensional LDPC-RS error correction code structure can be used, as shown in Figure 5.1 [112]. In this figure, both LDPC and RS code are linear systematic codes, where the LDPC encoding is performed vertically and the RS code implemented horizontally. The RS code rate should be in the range of 1% to 5%. The advantage of a 2 dimensional error correction structure is that, even if is error correction capability is equivalent to a concatenated error correction code, a less complex decoding process is allowed thanks to the puncturing capability.

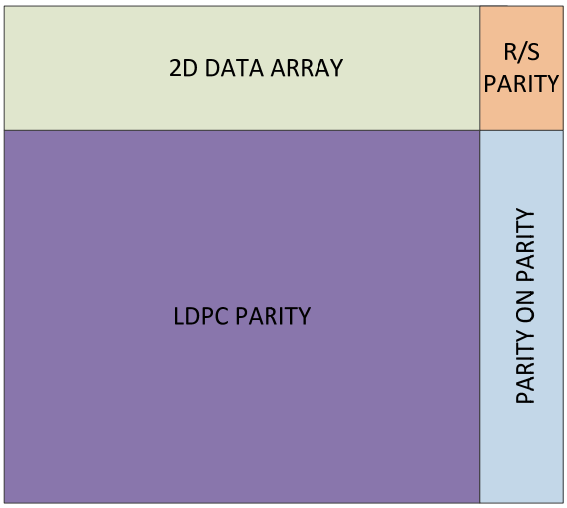

Figure 5.1. A 2-Dimensional LDPC-RS product code.

In addition, in the product code structure, within the codification process, a block time interleaving algorithm may be included. For an encoding process of the 2D code shown in Figure 5.1, the RS parity is first generated and horizontally added. After the horizontal RS encoding, the RS codeword is read row by row, top to bottom, and then LDPC parity is calculated and added vertically. At the receiver side, the RS decoding is conducted after the LDPC decoding. As depicted in Figure 5.2 this encoding method provides interleaving effects on both time and frequency domains.

For instance, considering a 1/2 LDPC code and that the whole matrix contains 1 sec of data and parity, the 2D matrix size should be less than 10.4 Mbits. If the designed LDPC code of 64800 bits is directly applied, the RS code will be less than 160 bits (≈10.4 Mbits / 64800). This will be a highly non-symmetric matrix, vertically very long and horizontally very narrow. In other words, the horizontal RS code-length will be very short, which will not be very efficient from the coding point of view. One way to mitigate this problem is folding the vertical LDPC code by 8 as shown in Figure 5.2. First, 160 LDPC codewords of 64800 bits are generated and disposed vertically. Then, data are read out row by row in 8-bit units, top to bottom, in such a way that RS codewords of 160 bytes are included horizontally.

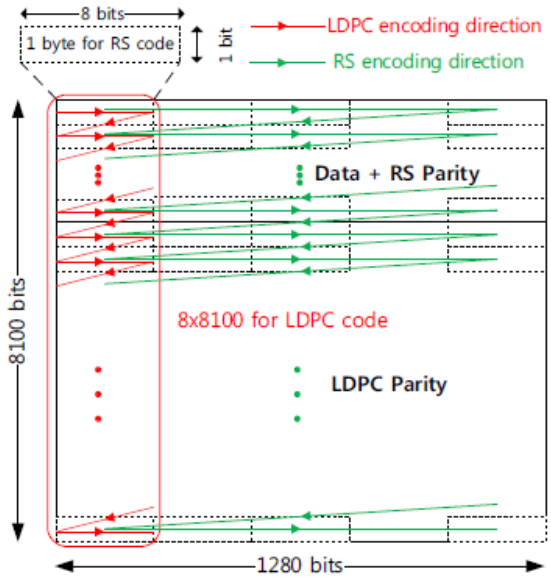

Figure 5.2. LDPC codeword folding (64800 code-length).

At the receiver, the bi-dimensional product code works as follows. The received data are written in row by row, top to bottom, in 8-bit units. Afterwards, the LDPC code is operated column by column, followed by RS (or BCH) code operated row-by-row.

The key point is that, as previously mentioned, the LDPC codes were designed as a rate compatible code that can be truncated for higher code rate. For example, when the SNR is high enough, the R = 1/4 code can be truncated to 50% of its length to form a 1/2 code. This way, the receiver does not have to fill up the whole time interleaving buffer as other block interleavers do. This will greatly reduce the coding latency by 50%, and also reduce the computation complexity. For these robust LDPC codes, when the SNR is 3 dB above the noise threshold of the LDPC code, the required iterations are reduced by 90%. If 5 dB more than the minimum receiving threshold are received, instead of 50 iterations, only 2 iterations are needed.

To put it another way, when the received SNR is well above the threshold, the 1/4 code can be truncated to 1/2 code, and therefore, the received decoding output can be obtained in "50% + x" of the 2D interleaver time, where "x" is the processing time to complete the truncated LDPC decoding. Thus, the 2D interleaver size is reduced by almost 50% and the corresponding memory

requirements for storage of the received data are also reduced by 50% (see Figure 5.3).

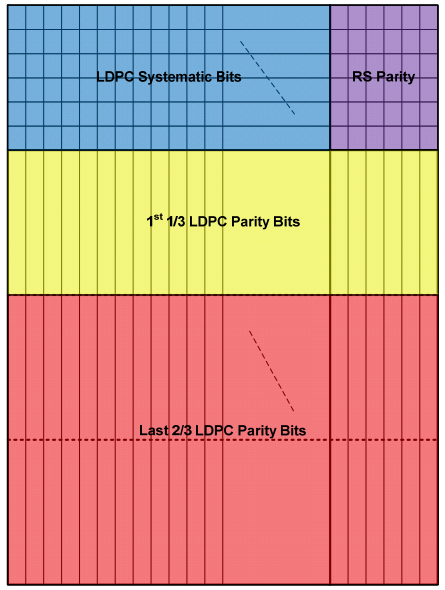

Figure 5.3. 2D FEC structure at the receiver site.

As the time interleaving is applied at bit level, the first 50% of the 2D FEC memory needs about 6 bits for soft LDPC decoding (LLR values). After the truncated LDPC decoding, only 1 bit is needed to store the LDPC decoded data. The last 2/3 of the parity bits can be encoded and hard quantized to 1 bit. Since there are 6 bits per unit in the top 50% of the 2D interleaver and only 1 bit used to save the LDPC output, some of the spare bits can be used to store the lower 50% of the LDPC parity bits.

2. LDM HW COMPLEXITY

This section includes an overall overview of the structure required for adapting the LDM solution to the new generation broadcasting market. Even if the chapter is focused on the receiver implementation point of view, a short description of the transmitter structure is necessary. What is more, it will be shown that the main infrastructure of the current broadcasting network could be maintained, while the receiver complexity is just slightly increased. As a matter of fact, the first HW prototype, build by ETRI, shows just a %12 computational complexity increase for LDPC computation and 1Mbyte memory increase for the two layered receiver.

2.1 Transmitter

First of all, it must be noted that when compared with a single layer transmitter, the LDM transmitter complexity is not substantially increased as the major part of the transmission modules are shared by both layers: frame builder, OFDM modulator, GI insertion and RF Up-Converter. Therefore, it is perfectly feasible to build a spectrum overlay transmitter that fulfils the cost-effectiveness criterion for a new generation standard. A more detailed block diagram of the transmitter can be seen in Figure 5.4. It is important to note that each stream has its own BICM module, and consequently, data streams can be separately configured taking into account the different services that they may target. As previously mentioned, in this architecture, the injection range (Δ) is the key parameter indicating how deep the LL is embedded.

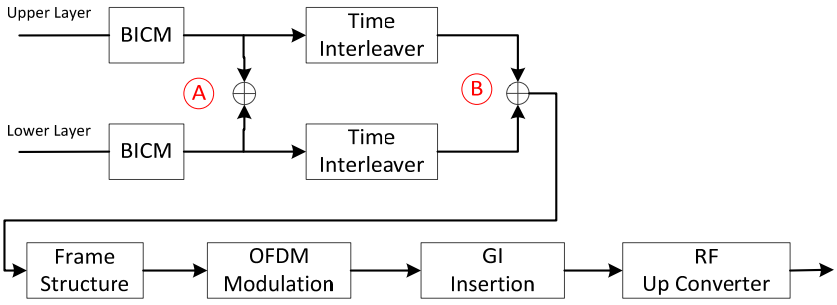

Figure 5.4. LDM system diagram with hierarchical spectrum re-use.

In Figure 5.4 it is also clearly depicted that there are two different points where data streams can be added. In fact, they can be either superimposed at the BICM

output (A) and share the time interleaver, or they can have independent time interleavers and be added at their respective output (B). It must be taken into account that even if there is not any computational complexity increase at the transmitter site depending on the injection point, it can have a dramatic impact on the receiver computational complexity.

2.2 Receiver

2.2.1 Upper layer-only reception

For a receiver that is designed to decode only the mobile (upper) layer signal, the system design can be really simple. The key is that just the mobile service decoder stream is required, without the need of additional stream decoders and re-modulations. Therefore, if the latest video and source coding techniques are included, the upper layer-only receiver is energy efficient and it can be easily integrated into new generation portable and handheld devices. What is more, as shown in Chapter 3 and 4, the implementation of robust LDPC codes can solve the inter-carrier interference problem, and therefore, low-complexity (one dimensional) channel estimation and equalization algorithms may be used.

2.2.2 Upper and lower layer reception

The general LDM receiver is depicted in Figure 5.5. It can be seen that for each additional layer decoding capability, a re-modulation/cancellation path and a decoding block is needed, whereas the same equalization and synchronization blocks will work for both layers. The accuracy of the signal cancellation process is closely related to the channel estimation.

It is clear that, to perform the signal cancellation, the receiver first needs to recover the UL transmission symbols. The best way to assure that there will be no errors in the upper layer stream is to rebuild the mobile service transmission signal. Although this cancellation processing involves additional complexity to perform channel decoding and re-encoding, it provides the most reliable UL signal estimate. However, it is important to note that, when there is sufficient SNR to decode the LL signal, UL signal is at very high S/(N+I) condition, and thus, the LDPC code only needs to run a few iterations to achieve error free decoding.

The buffer size memory and latency increase due the cancellation process is closely related with the injection point where the stationary service has been

injected. Depending on the transmission chain point where the overlaid signal is added, there are two different receiver implementations.

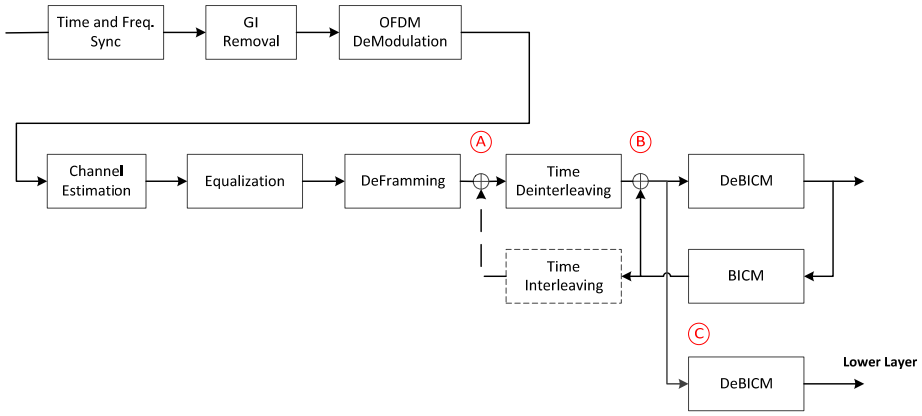

Figure 5.5. General block diagram of an LDM receiver.

2.2.2.1 Option A: LDM approach with independent Time-Interleaving

In this approach is taken, each layer has its own time interleaver, and thus, the first common module for both layers at the transmitter site is the frame builder. For each layer, the time interleaver algorithm could be either the 2D product code explained in Section 1.1 or any cell block interleaver (DVB-T2 or other). In general, the performance in terms of error correction capability is only a function of the interleaving depth. Therefore, even if the different algorithms can offer some other technical solutions, such the Variable Bit Rate (VBR) support or the zapping time reduction the performance depends only on the time depth. In principle, the mobile service is supposed to cope with slow-fading environments, and therefore, it is expected that its time interleaver should be longer.

Complexity

The main problem of this approach is that there is a high memory increase for the cancellation stage. In fact, in order to be able to re-modulate and cancel the Upper Layer, the multi-layer and channel impulse response buffers should have at least the same memory size as the UL time interleaver.

A possible solution to reduce the memory cells extension is the implementation of the bit based 2D product code explained before (See Chapter 5 Section 1). The main reason is that due to the use of rate compatible LDPC codes,

the buffer memory of the multi-layer receiver can be significantly reduced. As stated before, when the SNR is high (and for accessing the lower layer legacy system the SNR will always be high), the LDPC matrix, can be truncated, and therefore, usually there is no need for the last 2/3 of the parity bits and there can be hard quantized to 1 bit. Consequently, the upper layer buffer size requirements can be greatly reduced. In addition, in the cancellation stage the system is working well above the UL minimum threshold, and thus, the upper layer decoder LDPC iterations can be reduced almost a 90%.

Latency

Since the digital TV service is a constant video/audio streaming, there is no stringent requirement on the end-to-end delay. Once the receiver's data/video buffer is filled and the video starts to play, the end-to-end delay does not affect the program quality from the viewer's point of view. Nevertheless, for the viewers the initial delay is more perceptible, which is the time it takes for the receiver to start outputting the received service, after it is turned on or the channel is switched (the zapping time). One design target for any new generation DTT system should be a short initial starting time and short zapping time between program switching.

In a multilayer system although most of the delay is caused by video decoding, extra caution is needed to control the channel decoding delay. For the services carried in the Lower-Layer of an LDM system, there is an additional initial delay that is introduced by the Upper-Layer signal detection and cancellation. This delay is mainly introduced by the deinterleaving process and the channel decoding process of the Upper-Layer signal detection.

For example, a mobile broadcasting system typically has a data interleaver of about 0.25 s to be able to sustain the signal fading experienced in mobile reception environments. This means that the receiver has to wait for 0.25 s for the interleaver to buffer up to start the decoding; after that, re-modulation should not introduce a long delay. In this case, to decode the second layer signal, a receiver needs to wait for 0.25 s for the first layer signal decoding and additional time for the second layer interleaver to buffer up. However, it should be pointed out that the decoding SNR threshold for the second layer is likely to be, at least, 10 dB higher than the first layer. Under this condition, if there is sufficient SNR to support the second layer decoding, the first layer should have a 10 dB SNR margin and should not need a strong error correction code. For example, assuming the first layer FEC coding rate R = 1/4 (i.e., 25% are information bits and 75% are parity bits), when there is 5 dB additional SNR margin in the received signal, rate 1/2 code is sufficient to

decode the signal successfully. This means that only the 25% of the information bits and another 25% of parity bits are required to form a rate-1/2 code to decode the signal. The remaining 50% parity bits are not needed. Thus, with a specially designed interleaver structure and the Raptor-like rate compatible LDPC code [104][113] which can be easily truncated (cut the parity bits) into higher rate code, the decoding delay can be reduced by 50% in this example.

According to some studies the total zapping time should always be less than 2 seconds, and for an optimum experience it should be less than 0.5 sec [114][115]. For a multi-layer system, if there is sufficient SNR to decode the second layer signal, the first layer decoding delay can be, at least, cut by 50%. It should be considered that in DTV broadcast environments within the coverage area, at least 80% of the locations will receive the signal with a 5 dB SNR margin. Thus, in most of the receiving locations, the cancellation stage latency can be significantly reduced and turn negligible for the whole system delay when compared with the video decoding time.

2.2.2.2 Option B: LDM approach with cross Layer Time-Interleaving

The original LDM transmission was proposed with independent time-interleavers and a 2D-FEC structure for the upper layer to achieve exceptionally robust detection performance in harsh wireless channel environments. It has been shown that this 2D-FEC poses a notably memory requirement reduction as well as additional initial delay decrease for the second layer signal detection in an LDM system. Nevertheless, a straightforward solution to reduce the additional complexity increase is to use the same interleaving structure in the different layers of an LDM system. This is also called cross-layer interleaving (CL-Intlv). For example, assuming an LDM system with DVB-T2 signal as the lower-layer, the higher-layer should use the same interleaving structure of DVB-T2. In this section, it will be shown that the LDM system with CL-Intlv requires very little increase in the receiver complexity as compared to a single-layer transmission system. Furthermore, the early decoding property of the RC-LDPC can still be used to achieve shorter initial delay by starting the first layer signal detection earlier.

Complexity

In LDM with cross-layer interleaver (CL-Intlv), a single time interleaving structure is used simultaneously by several data transmitters. The block diagram of an LDM receiver with CL-Intlv is plotted in Figure 5.4 (option A).

The use of a shared interleaver allows the receiver to perform time deinterleaving simultaneously for the combined UL and LL signals. The upper layer signal detection and re-generation is performed after that, which greatly reduces the associated memory and delay required for UL signal cancellation. With the CL-Intlv, the only additional memory is that required for LDPC bit deinterleaving, which is insignificant (~64kB). If this increase is compared with the current receivers' total memory size, it can be seen that just about a 20% of increase is required. What is more, it can be reduced even more implementing smart memory storing algorithms.

Latency

As in the previous case, the SNR requirement is quite high for LL signal detection. This can lead to a very small LDPC decoding complexity for the UL signal detection because much less decoding iterations are required. It is known that only 3 to 5 iterations are enough in the LDPC decoding for high SNR. This also results in a smaller delay in the LDPC decoding process. What is more, in this approach the time interleaver is shared, and therefore, there is no need for an extra deinterleaving and re-interleaving processes. It offers the lowest computational burden with practically the same performance, and therefore, it is the most cost effective solution.

The only imposition of this solution is that both layers should share the same same interleaving length. However, it is known that signals targeting mobile services require a larger interleaver size to deal with possible deep fading due to the channel time variability. Therefore, the only constraint for this choice is that stationary services may have a slightly longer zapping time, as their time interleaver length is fixed by the mobile service requirements. Nevertheless, it is also true that this zapping time will be always lower than the maximum delay recommended for an optimum user experience.

2.2.3 Lower layer-only reception

In addition to the previous option, there is an extra low complexity profile for stationary receivers. The simplicity of this structure relies in the fact that there is no need for signal cancellation, as the lower layer directly decodes the lower layer (See Figure 5.5 (C)). Nevertheless, it may be valid for only some configurations of the multilayered signal (limited flexibility) and a degradation performance should be assumed. What is more, it may be a valid option for very low complexity receivers designed for fixed stationary reception that would not make use of the UL signal.

In order to access the lower layer without cancellation, the direct de-mapping should be applied, in other words, the sum of the two overlayed constellations is considered as a higher order constellation, whose modulated points are unequivocal. For instance, QPSK for the Upper Layer and a 64-QAM for the LL is used, the resultant multilayer constellation is a 256-QAM. Its final shape depends on the injection range.

At the receiver, providing that it knows both the UL/LL constellation and the injection range, the merged multilayer constellation can be easily calculated. Afterwards, the signal multilayer signal is decoded assuming the overlapped constellation, and finally, the constellation points are translated into the LL ones. This methodology performance, as always, will be closely related to the injection range, because this parameter is the one which dictates the shape of the multi-layered signal.

3. EVALUATION OF CHANNEL ESTIMATION FOR LDM SIGNAL CANCELLATION

As shown in the previous chapter, channel estimation is critical for signal detection at the LDM receiver, either to decode the upper layer under challenging conditions, or afterwards to perform an accurate signal cancellation. What is more, the inter-layer interference error due to the cancellation stage mostly depends on channel estimation. Therefore, in this section it will be carried out a comprehensive study of different channel estimation algorithms performance and their impact on the multilayer signal cancellation [116].

3.1 Decision-Directed Channel estimation

Up to now, it has been demonstrated that the key for a correct layered division reception is the implementation of a powerful frequency domain cancellation algorithm. For this purpose, the methods explained in Chapter 3 Section 4 for single layer mobile signals are perfectly suitable. Nevertheless, the LDM structure allows the consideration of a new channel estimation structure for the signal cancellation algorithm: Decision-Directed channel estimation.

In order to decode the upper layer signal, an estimate of the channel gain $\tilde{h}[k]$ is obtained with pilot-aided channel estimation. The accuracy of this channel estimate is enough for the upper layer signal detection due to the strong error correction coding. However, the knowledge of the transmitted upper layer signal at the cancellation stage allows implementing the decision-directed (DD) channel estimation techniques to pursue good signal cancellation performance.

For each OFDM symbol, the receiver can obtain a new frequency response applying the LS channel estimates on each sub-carrier as,

$$\tilde{h}[k] = \frac{y[k]}{x_{UL}[k]} \tag{5.1}$$

With the whole symbol LS channel estimation, more accurate estimates can be obtained by applying different frequency-domain smoothing filters, including but not limited to, the MMSE and SVD algorithms, the DFT-filtering, and the Wiener filtering [99]-[101]. Among these techniques, the decision-directed MMSE channel estimator is very complex to implement, since a matrix multiplication is required to decode each OFDM symbol. By contrast, DFT-filtering and Wiener filtering are

both practical techniques with relative low complexity. To further reduce the estimation noise, the output of the frequency-domain channel estimator can be processed by a time-domain Wiener filtering as in pilot-aided (PA) methods.

3.2 Practical Evaluation of the Channel Estimation Methods for LDM Signal Cancellation

Providing that the UL signal is re-coded, the channel estimation algorithm is the main source of inter-layer propagation error after signal cancellation (See Figure 5.6). Therefore, in this final part of the chapter, several simulations are presented to evaluate the performance of signal cancellation with both pilot-aided (PA) and decision-directed (DD) channel estimation algorithm.

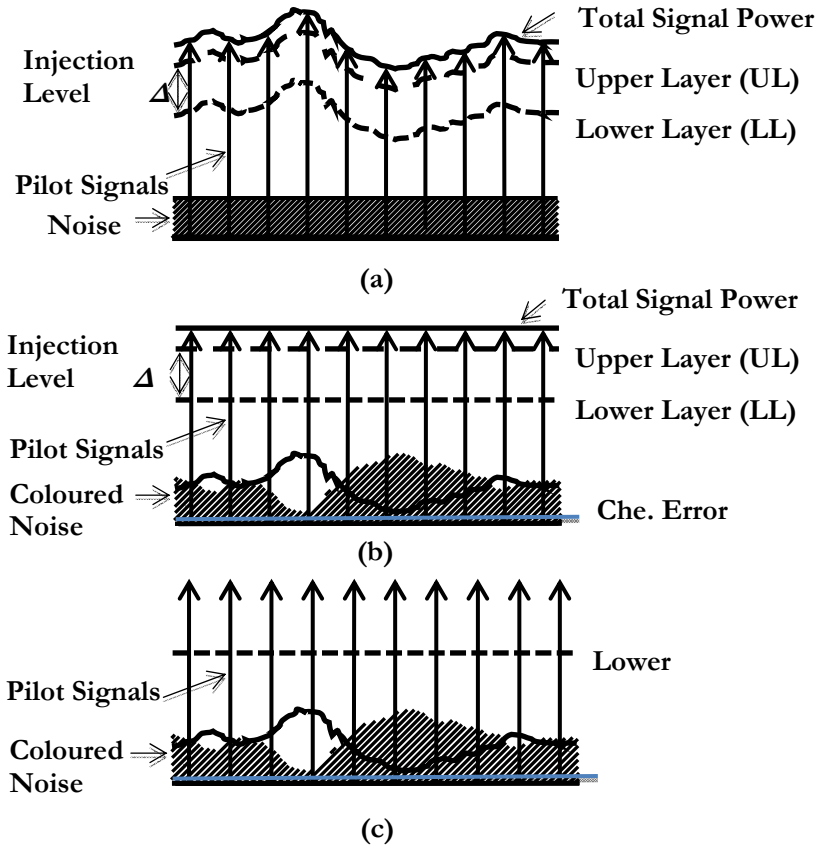

Figure 5.6. Cancellation algorithm stages. (a) LDM signal at the receiver input, (b) LDM signal after equalization output, (c) LL after signal cancellation.

In the simulations, a generic LDM system with two layers is assumed. The upper layer is a 4K FFT size mobile signal with a very robust LDPC code (CR=1/4) and QPSK modulation. For the lower layer, the most sensible scenario is presented, i.e., a lower layer signal with 256-QAM and LDPC code rate 2/3 is injected with a power level 5 dB lower than the upper layer signal. The possible residual error after cancellation is depicted in Figure 5.6 (c)

Channel estimation accuracy is analyzed using the mean square error (MSE) of the estimate (Che. Error in Figure 5.6 (b)), and the performance of the signal cancellation is characterized by the normalized mean square error (NMSE) referenced to the upper layer signal (Coloured Noise in Figure 5.6 (c)). The NMSE is essentially the power ratio of the cancellation residual errors referenced to the upper layer signal. Signal power is calculated as the total received signal power, i.e., the main received signal power plus all multipath signal powers. In the following figures, the performance of PA based and DD based channel estimation are compared assuming different SNR conditions for the LL signal.

In each figure, the upper subplot shows the NMSE versus OFDM symbol index. To simplify the simulation, a time-domain 40-tap Wiener filtering is performed over a block of 840 OFDM symbols. This causes the first and last few symbols having higher NMSE because there are not enough adjacent symbols to perform Wiener filtering. These symbols should be ignored, since in reality the time-domain Wiener filtering is performed continuously. The lower subplot shows the MSE versus sub-carrier (or sub-channel) index. It is observed that the sub-carriers close to the edges of the spectrum show higher MSE. This is due to the nature of the estimation algorithms, where the sub-carriers close to the edge have less correlation information to carry out the estimation.

Figure 5.7 and Figure 5.8 present the channel estimation MSE and NMSE of the residual of upper layer signal after the signal cancellation in 0 dB single echo channels with different echo delays. In this case, for the lower layer signal, stationary reception is assumed. In particular, Figure 5.7 shows the channel estimation methods for a short delay spread channel (D=1/4·GI). This is not a very challenging channel, and thus, the most common channel estimation techniques explained in Chapter 3 should be good enough. As matter of fact, it is observed that even the 2D-CUBIC performs better than 2D-DFT. Furthermore, DD-DFT provides 2 dB performance gain compared to 2D-CUBIC in terms of signal cancellation.

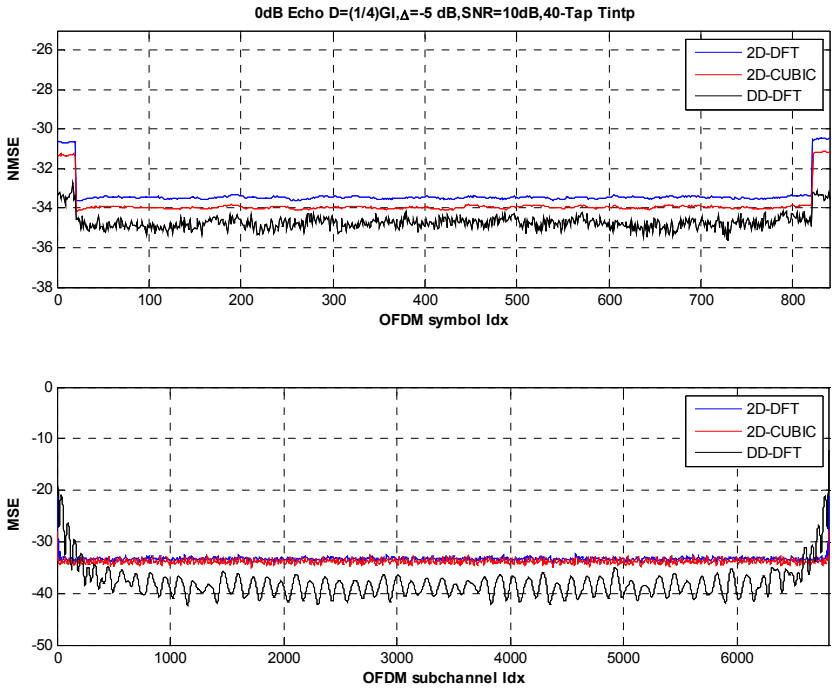

Figure 5.7. Signal cancellation performance, 0dBEcho (D=(1/4)·GI), 40-tap Wiener filter, SNR_{LL}=10 dB.

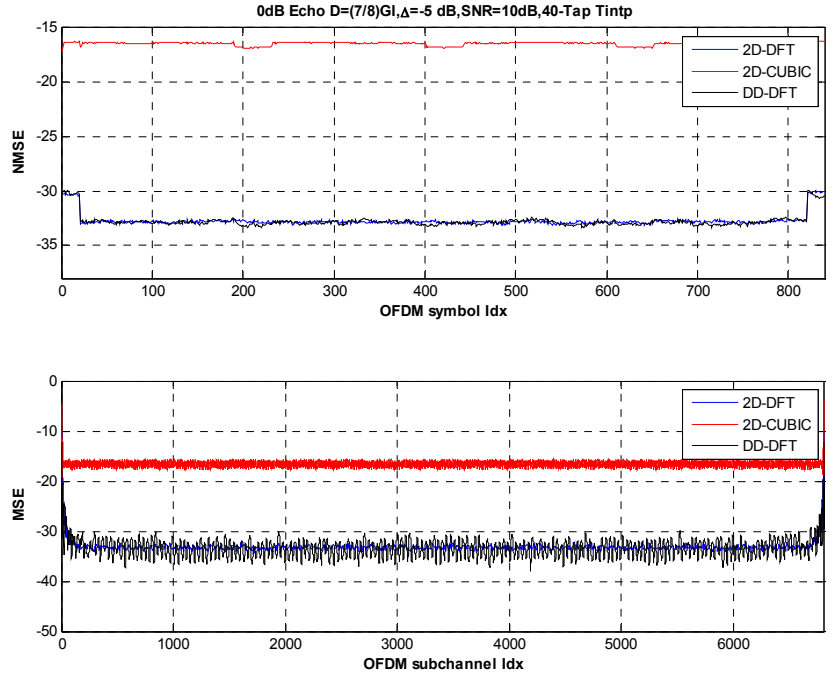

Figure 5.8. Signal cancellation performance, 0dBEcho (D=(7/8)·GI), 40-tap Wiener filter, SNR_{LL}=10 dB.

In Figure 5.8, the signal cancellation performance of an LDM receiver when the second transmitted signal arrives nearby the guard interval end (D=7/8·GI) is presented, which results in a channel with high frequency selectivity. In fact, this can be understood as the worst scenario that the LDM receiver may face. It is clearly observed that for this challenging channel, the 2D-CUBIC suffers significant performance loss, whereas 2D-DFT keeps very good cancellation performance. Indeed, its performance is very close to that offered by the DD-DFT. From now on, the 2D-CUBIC method will no longer be considered, as it is not good enough to deal with the worst 0 dB echo scenario.

As shown in Chapter 3, when the channel estimation algorithms are analysed in depth, the addition of a time-filtering module can substantially improve the channel estimation algorithm. Therefore, the evaluation of the impact of this time-domain interpolator length on the system performance has also been included. When looking closely at the NMSE vs OFDM symbol index curves, it can be observed that the center part is 3 dB better than the two ends. This is because the interpolator on the center OFDM symbols has twice as many taps as the end symbols. For static channels, the Wiener interpolator applied to the center OFDM symbols is essentially a moving average window. For comparison, the Wiener filter length has been doubled to 80-tap for the D=7/8·GI case and performance is shown in Figure 5.9. As expected, a 3 dB performance gain appears due to the use of a filter twice as long.

Finally, the impact of the AWGN at the receiver is analyzed. When the LL signal is designed for very high data-rate, a high SNR is required for reliable detection, and therefore, the PA-based channel estimation will have advantage because DD has a fixed SNR which is inversely-proportional to the LL signal injection level. Thus, in Figure 5.10, with an SNR of 20 dB for the LL signal, the performance of the PA-based and the DD-based signal cancellation are compared. As expected, due to the higher SNR on the pilots, 2D-DFT provides better performance than DD-DFT.

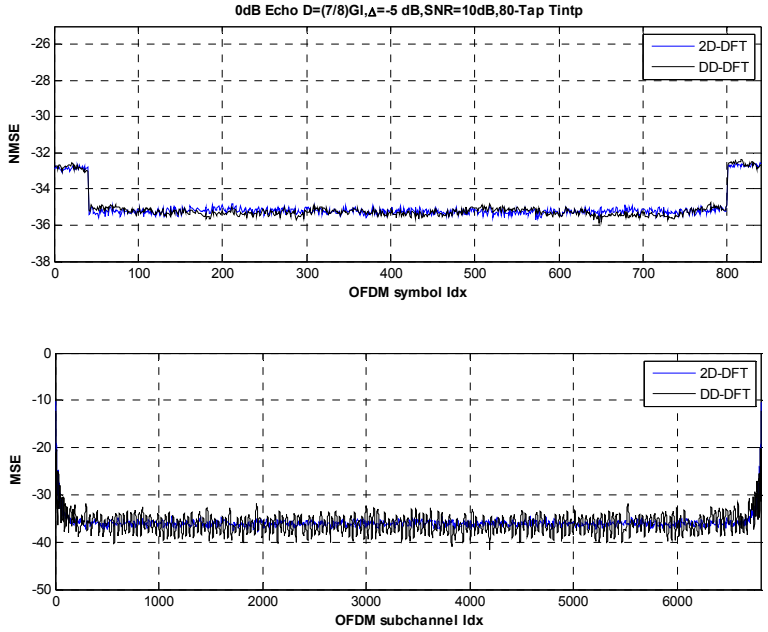

Figure 5.9. Signal cancellation performance, 0dBEcho (D=(7/8)·GI), 80-tap Wiener filter, SNR_{LL}=10 dB.

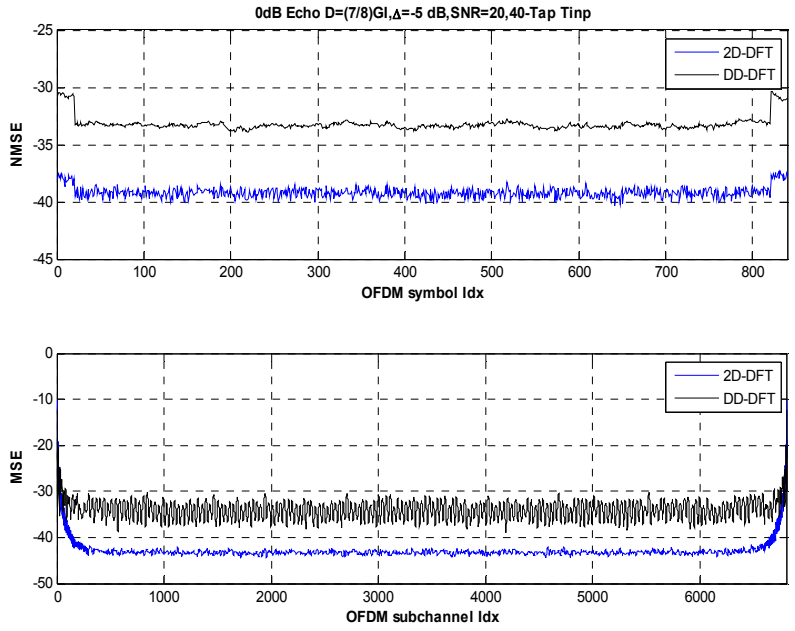

Figure 5.10. Signal cancellation performance, 0dBEcho (D=(7/8)·GI), 40-tap Wiener filter, SNR_{LL}=20 dB.

It can be concluded that a long time-domain moving average window is a good solution to obtain good signal cancellation. Furthermore, pilot-aided methods have advantage over decision directed methods when the SNR for the LL signal is high, for example, SNR=20 dB. Finally TABLE 5.1 sums up the frequency domain cancellation performance for different channel estimation algorithms.

TABLE 5.1. Normalized Mean Square Error for different channel estimation algorithms.

Channel Condition				**NMSE**		
				2D-CUBIC	**2D-DFT**	**DD-DFT**
	SNR_{LL}(dB)	Tap	f_dT_u			
0 dB Echo (D=1/4GI)	10	40	0	-34.0	-33.0	-35.0
0 dB Echo (D=7/8GI)	10	40	0	-18.0	-32.5	-32.5
0 dB Echo (D=7/8GI)	10	80	0	-	-35.5	-35.5
0 dB Echo (D=7/8GI)	20	40	0	-	-40.0	-32.5

Based on these results, it has been concluded that the 2D-DFT channel estimation is the best algorithm for performing an accurate channel estimation that will lead to a very clean signal cancellation. Thus, in the following chapter, where a practical analysis of the LDM proposal is carried out, the 2D-DFT algorithm will be used. Furthermore, it can be seen that the cancellation error floor is always very much lower than the Gaussian Noise of the receiving threshold.

4. LDM INTER LAYER INTERFERENCE

Once the frequency domain equalization algorithm has been theoretically presented, the next step is to analyze the potential weaknesses that the system may present. According to Eq. (4.4), there are two main sources of inaccuracy that might lead to an error floor after the signal cancellation, and therefore, degrade the lower layer signal performance: the upper layer signal regeneration error and channel estimation error. The aim of this section is to study the possible system degradation due to those interferences [117].

4.1 Upper Layer re-modulation Error

As previously mentioned, considering that the required SNR for lower layer decoding is much higher than what is required for error-free decoding of the upper layer, it is reasonable to assume that the upper layer signal will be always perfectly reconstructed. Therefore, this should be considered as a hypothetical problem that may occur if the upper signal is directly fed back to the cancellation module.Ideally, the UL signal should be decoded and reconstructed again prior to the subtraction in order to ensure that it is an error free signal. Nevertheless, if the equalizer output signal were directly re-mapped and used for the cancellation stage, it would be possible to decrease the delay due to the cancellation process and reduce the complexity. In that case, there would be no need to decode the mobile layer signal, and therefore, there would be some impurity in the upper layer signal which would cause error propagation for the legacy layer. As a matter of fact, at the receiver, every wrong re-coded sample can be considered a noise injection sample whose amplitude will be equivalent to the legacy layer injection range. Therefore, a significant number of mismatches in the upper layer detection can easily turn into important error propagation for the legacy layer. The errors can be mathematically represented as,

$$\Delta\Phi = \frac{\left(x_{UL}^{TX} - x_{UL}^{RECOD}\right)}{Num_{cells}} \tag{5.2}$$

where $\Delta\Phi$ is the difference between the actual transmitted signal and the canceller signal, divided by the total number of IQ samples per frame (Num_{cells}). This distortion could be understood as a very short duration error burst that may occur along the RF channel.

4.2 Channel estimation MSE

Apart from the errors in the upper layer feedback, the other critical parameter in the cancellation is the channel estimation accuracy. In general, the channel estimation performance depends strongly on the implemented algorithm, but other factors such as pilot boosting or pilot pattern scheme may also play important roles. The performance of the channel estimation algorithms are normally given by

$$\Delta\xi = h[k] - \tilde{h}[k] \tag{5.3}$$

This channel estimation inaccuracy might lead to an interlayer error $i[k]$ that can be approximated as a Gaussian random variable with zero mean and a variance that depends on the estimation error and the upper layer power. As mentioned before, the upper layer error $\Delta\Phi$ will be null when re-constructing the whole upper layer signal before cancellation. Nevertheless, the channel estimation error is not so easy to avoid, and therefore, the channel estimation is going to play a key role in the cancellation process.

4.3 Practical Evaluation

Within this section, the practical evaluation of the possible inter-layer propagation error is analysed. The results are obtained from a simulation platform, where the overall multilayer system, both the transmitter and the receiver, have been fully implemented. As the study is focused on the error propagation, other possible distortion sources have not been included, that is, ideal synchronization has been considered. Apart from the parameters defined in TABLE 5.2 (constellation and code rate), it is important to note that the signal FFT size is 32k and the GI is 1/32. All the obtained results are compared with the ideal receiving thresholds obtained after perfect cancellation as defined in TABLE 5.2. It should be noted that DVB-T2 is used as LL.

TABLE 5.2. Lower layer reception thresholds at BER=10^{-6} when Δ=-5 dB.

	AWGN	**RICE**
16-QAM,CR=2/3	15.0 dB	15.4 dB
64-QAM,CR=2/3	19.8 dB	20.2 dB
64-QAM,CR=5/6	22.9 dB	22.4 dB

The error power is measured as defined by the mean square error, and the error propagation impact is estimated analyzing the performance loss. In fact, the performance is evaluated by the signal bit error rate (BER), assuming a Quasi Error Free (QEF) situation when the BER value is lower than 10^{-6} at the outer decoder output.

4.3.1 Upper Layer re-modulation error

TABLE 5.3 shows the performance loss in dB due to error propagation when the upper layer signal is not perfectly detected over an AWGN channel. The first outcome is that the lower the modulation orders are, the more error is needed to see degradation start. In the same way, the stronger the code is, the more robust the system is to this kind of interference.

TABLE 5.3. Performance loss (dB) for different $\Delta\Phi$ vaues when Δ=-5 dB.

			$\Delta\Phi$						
			10^{-6}	$5{\cdot}10^{-6}$	10^{-5}	$5{\cdot}10^{-5}$	10^{-4}	$5{\cdot}10^{-4}$	10^{-3}
AWGN	16Q	2/3	0.1	0.1	0.1	0.1	0.1	1.8	3.1
	64Q	2/3	0.1	0.1	0.1	0.5	0.9	2.2	2.8
	64Q	5/6	0.1	0.1	0.4	0.7	1.2	2.1	2.9

Nonetheless, in order to minimize the performance loss, the error must be $\Delta\Phi < 10^{-5}$ and that is not feasible if the equalizer output is directly used for the cancellation process. Figure 5.11 shows the Symbol Error Rate (SER) of the UL equalizer output for the different multilayer configurations presented in TABLE 5.2. The red circle represents the points where the lower layer should be decoded so that no error propagation in the cancellation would be present. It can be seen that, in both cases, for the signal to noise ratios close to the non-degradation case, $\Delta\Phi$ is not even lower than 10^{-3}. Therefore, it is clear that for the real case, if the signal is directly fed back into the cancelation stage from the equalizer output, the loss will be higher than 3 dB, which is not reasonable. What is more, it occurs for the less demanding broadcasting channel with direct line of sight. For other, frequency-selective channels it may expect a greater performance loss. Nevertheless, this is not a major issue for LDM as the UL signal can be error corrected, and afterwards, rebuild again in order to eliminate this error, as proved before.

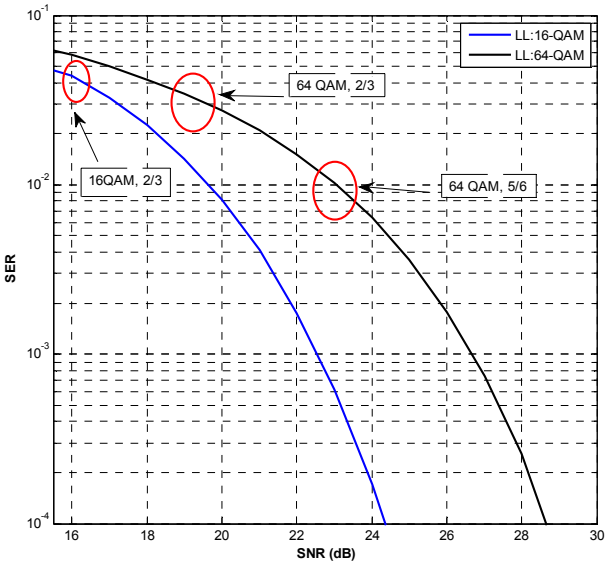

Figure 5.11. Upper layer BER performance for UL over AWGN channels.

4.3.2 Channel estimation error

TABLE 5.4 gathers the effect of interlayer degradation error due to non-ideal channel estimation in the cancellation algorithm for AWGN and Ricean channels. The implemented channel estimation algorithm has been the 2D-DFT, which is one of the best performing algorithms as shown in Chapter 3 Section 2.

TABLE 5.4. Performance loss (dB) for different $\Delta\xi$ Values when Δ=-5 dB.

			$\Delta\xi$						
			10^{-5}	$5\cdot10^{-5}$	10^{-4}	$5\cdot10^{-4}$	10^{-3}	$5\cdot10^{-3}$	10^{-2}
AWGN	16Q	2/3	0.0	0.0	0.0	0.1	0.1	0.7	1.7
	64Q	2/3	0.0	0.0	0.0	0.2	0.4	2.1	-
	64Q	5/6	0.0	0.0	0.1	0.4	1	-	-
RICE	16Q	2/3	0.0	0.1	0.1	0.1	0.1	0.9	2.1
	64Q	2/3	0.0	0.0	0.0	0.2	0.4	2.5	-
	64Q	5/6	0.0	0.1	0.1	0.6	1.2	-	-

The table shows the receiving threshold degradation with 0.1 dB accuracy. It must be borne in mind that 64-QAM modulation with CR=2/3 and CR=5/6 does

not include errors higher than $5 \cdot 10^{-3}$ and $1 \cdot 10^{-2}$ respectively. The main reason is that in those cases the cancellation error is higher than the minimum noise power that the system can withstand.

It can be seen that the error propagation penalty increases substantially when the noise floor is close to the maximum noise that the system can withstand. Nonetheless, the main conclusion is that, if the channel estimation is good enough ($\Delta\xi < 10^{-4}$), there is no additional performance loss. As matter of fact, the loss is very similar to the performance degradation due to non-ideal channel estimation of a single layer system. Finally, it is worth mentioning that, according to Eq. (5.3), the channel estimation error $\Delta\xi$ is always lower than 10^{-3}, even for the most challenging channels such as 0dB Echo, TU-6 or Rayleigh channels.

5. SUMMARY

In this chapter, the implementation aspects of the LDM multiplexing technology have been studied. The layered division multiplexing has been proposed as a candidate for future broadcasting system to achieve a robust mobile reception, large mobile TV coverage and more efficient use of the spectrum.

In the beginning of the chapter, the main applications of the newly designed Rate-Compatible LDPC codes have been explained. Afterwards, there have been analyzed the practical implementation HW complexity. It has been demonstrated the system flexibility, and thus, the final receiver complexity can be greatly reduced depending on the point where the legacy layer is inserted. In addition to that, at the transmitter site there is not any complexity increase as the major part of the modules are common shared: RF tuner, sampler, filter, etc. The complexity penalty of this technology is associated to the receiver side. It mainly concentrates on latency and memory requirements to perform cancellation. Nevertheless, as mentioned before the degree of complexity will strongly depend on the selected approach, and even in the worst case (independent time interleavers for upper and lower layers), the complexity can be greatly reduced using rate-compatible FEC structures.

In the second half of the chapter, the frequency domain cancellation algorithm performance has been evaluated. The results were obtained not only, from extensive simulations, but also from theoretical analyses. First of all, the channel estimation impact on the upper layer cancellation algorithm is studied. The results have shown that if a combination of a classical DFT frequency interpolation and a time-averaging Wiener is used, a cancellation accuracy up to 40 dB can be obtained. Thus, the cancellation error is negligible even for the most challenging channels. Afterwards, the possible interlayer propagation error is analysed. The main conclusion is that, implementing the proposed algorithms, there is no such an error. In other words, the legacy layer performance is not compromised by the cancellation error floor.

"I don't know anything, but I do know that everything is interesting if you go into it deeply enough"

-Richard Feynman

CHAPTER 6: **VALIDATION AND PERFORMANCE STUDY OF LDM TECHNOLOGY**

In this chapter, an Evaluation & Validation platform (EVP) is presented, which main objective is not only to test the implementation feasibility of the LDM proposal, but also to provide new technical solutions for improving its performance through a comprehensive analysis of the obtained results. In particular, the whole EVP can be divided into four different phases. The first one is based on the theoretical calculations that have been presented in the previous chapters. The second one, consisting in a computer based simulation platform, has the main objective of validating the theoretical calculations. In addition, it is also a valuable tool to discard some signal configurations that are not going to fulfill the service requirements placed for the new generation broadcasting systems. Afterwards, the third phase is to create a laboratory test bench, where the whole LDM proposal is tested in a more realistic environment. This is an important step, as for the first time, there is real HW implementation involved in the study, and therefore, it is possible to quantify the implementation losses and the additional performance degradation. Finally, there is one last stage, where all the outcomes previously obtained are applied to the most practical environment: field trials. In short, it is an iterative process where each stage feeds the following one, and in the same way, it is based on the previous one. It is also important to note that the validation methodology ranges from theoretical analysis to measurements under real world conditions.

1. INTRODUCTION TO THE EVALUATION & VALIDATION PLATFORM (EVP)

As explained in Chapter 1, two of the main objectives of this work are: first, the improvement of the performance of current mobile broadcasting services, and second, the increase of the current spectrum efficiency in broadcast transmissions. The proposed LDM multiplexing technique for enhancing the transmission capacity, delivering simultaneously stationary and mobile services is a technical solution for overcoming both issues. In the previous chapters, the theoretical analysis for proving the feasibility and goodness of the proposal has been presented. Eventually, in this chapter, an iterative Evaluation and Validation Platform (EVP) for validating and studying this technology performance is built.

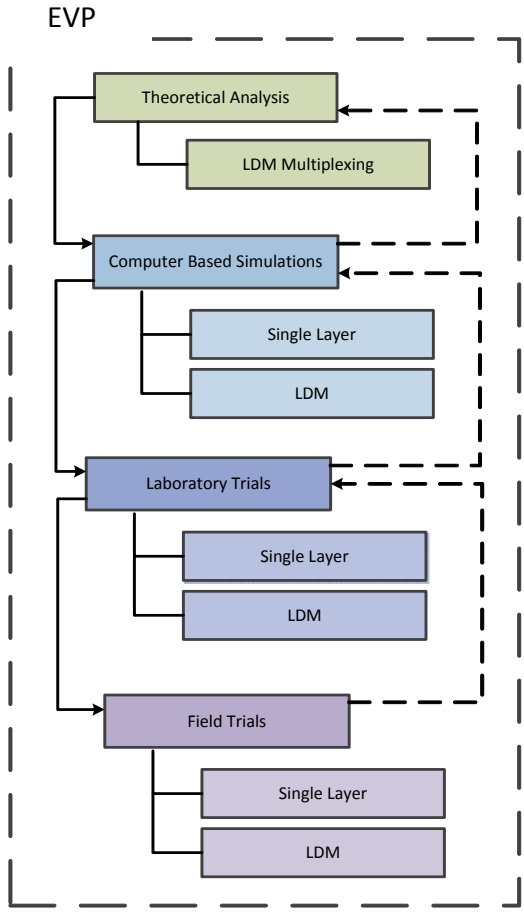

Figure 6.1. Graphical representation of the Evaluation and Validation platform.

Figure 6.1 depicts the block diagram of the proposed EVP. It is an iterative process, where each module can directly feedback its results to the previous stage. One of the main advantages of this platform is that, apart from the receiver chain, the transmitter scheme has also been defined. Therefore, if there are any conclusive results that show that the LDM signal performance may be improved by some changes in the transmission chain, they can be directly implemented. It is important to note that, in each phase, both single layer and LDM approaches will be analysed. This is fundamental to distinguish the regular performance losses (channel estimation, demapping…) from the LDM specifics (signal cancellation), if any. The main objective of this platform is to cover all the steps that are normally required to validate a new technology, ranging from the more theoretical computer simulations to the more practical field trials. In order to fulfill those requirements, multiple tools specifically designed for these tasks have been developed. Next, the different phases that are defined in the EVP are described.

Firstly, all the theoretical calculations presented in the previous chapters should be understood as the first phase of the evaluation proposal, where the theoretical bases for these new multiplexing techniques are presented.

Afterwards, the first step towards building a more practical model is taken: a complete Matlab based communication chain is developed (Phase 2). This platform is able to generate and decode the newly designed data streams, including the LDM multiplexing and cancellation schemes. It incorporates all the classical modules of a communication chain: BICM, time interleaver, equalizer. Nevertheless, it cannot be considered a real system as the platform lacks of some of the most important modules that are within a real receiver: the A/D & D/A converters, the multirate module or the carrier recovery part. In other words, it is a very controlled environment, which is very valuable for a development process but somehow limited for more practical demonstrations.

Therefore, the next step is based on bringing the overall EVP closer to the real world, including new modules into the transmitter/receiver chains. What is more, taking as a reference the computer simulation platform (Phase 2), a completely functional C/C++ based Software Defined Radio (SDR) receiver has been built. This SW is an upgraded version of a previous receiver, called Digital Broadcast Analyzer (DBA), which was able to decode either DVB-T2 or DVB-T2 Lite signals [118]. This software is able to process a great variety of formats, ranging from the general purpose IQ files to the proprietary DGZ or VWD files. Regarding the transmission part, in addition to the previous transmission chain, an extra-module has been included, which allows the generation of the vast majority of files

required by the HW transmission equipment. This third phase, also known as laboratory trials, is very close to a real scenario situation. What is more, it offers some advantage compared to it: smaller clock error, higher MER at the transmitter output… These characteristics are very useful to discard other types of errors in a validation process, and moreover, they help centering the analysis on the LDM specific impairments.

Eventually, as it can be seen in Figure 6.1, it remains one last step, which will bring the LDM feasibility test to its very end. The last phase will consist on a series of field trials, which will employ all the SW/HW tools that have been defined before in order to test the LDM feasibility and performance analysis under real world scenarios.

In short, it is important to note that this complex test environment will allow the user to test the different system specifications and performances under different reality degrees: it can be either very theoretical (computer simulations) or very realistic (field test). In addition, the process is iterative, and therefore, the analysis can always go back to square one to include a new feature to the transmission part: it can be said that this work has created a living test bench.

2. COMPUTER SIMULATIONS

After the theoretical analysis, the second phase of the EVP is focused on building a MATLAB based SW platform to simulate a complete communication chain. MATLAB has been chosen due to its processing capability, which offers a great number of predefined Digital Signal Processing (DSP) tools within the communications toolbox. In addition, its implementation is quite straightforward and it has one of the most complete debugging processes, which allows the user to analyse the code performance step by step. Finally, it is also important to note that it offers a very powerful tool for plotting the obtained results.

Figure 6.2 depicts a block diagram which gathers the main analytical processes involved in this phase. First of all, it can be seen that the whole analysis is divided into two main groups: the Single Layer (SL) and the LDM analysis. The main idea behind these structures lies in the fact that if the single layer performance is firstly studied, when the LDM multiplexing technique is analysed, the common error sources will be easily identified. In other words, this scheme makes it easier to identify the specific errors due to the hierarchical spectrum overlay.

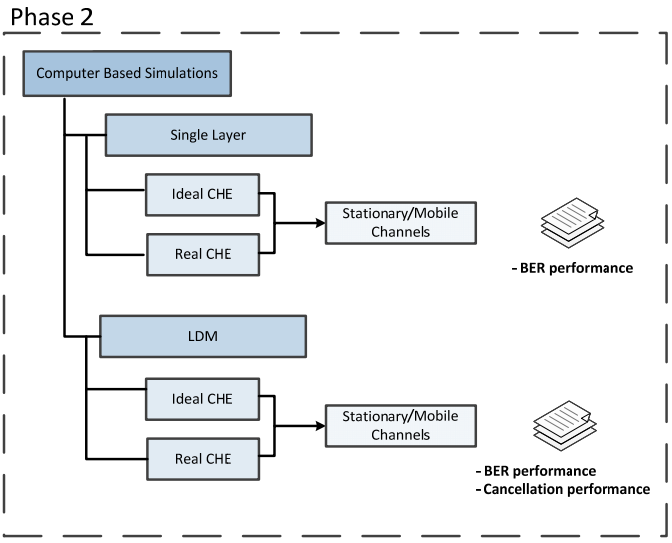

Figure 6.2. Scheme of the computer based simulation analysis.

In short, the SL analysis will be focused on studying the BER performance, whereas in the LDM analysis the proposed LDM cancellation will be also analysed. The obtained results will be compared with the firstly obtained theoretical calculations.

2.1 Set-Up Architecture and Simulation Configuration

The skeleton of the simulation chain was obtained from the DVB's Common Simulation Platform (CSP) [119], which was a software platform built by various members of the DVB consortium in order to evaluate the DVB-T2 standard. Based on that, a complete new simulation chain was built, which included several algorithms to get the simulation chain performance closer to a real receiver.

2.1.1 Signal Generation

The transmission part of the implemented computer based simulation platform is depicted in Figure 6.3. Within the BICM module the bit interleaving, FEC codification and modulation are included, whereas the frame structure includes the pilot insertion and the signalling parts.

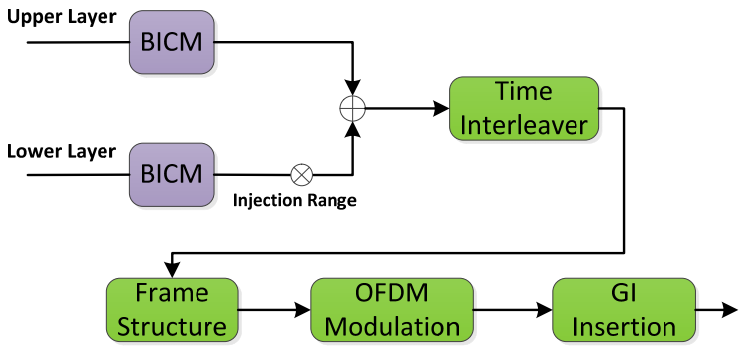

Figure 6.3. Block diagram of the computer based communication chain (transmitter part).

The transmitter can convey either a SL signal or an LDM signal depending on the selected configuration. Even though other injection points are available for LDM, in this study the legacy layer is inserted at the time-interleaver input, and thus, both layers implement the same interleaving depth. The generated signal is

always a random PRBS, whereas the rest of the configuration parameters are within a signalling structure included in the Frame Structure module. The signalling is also based in DVB-T2, but it includes some modifications to make it compatible with LDM.

2.1.1.1 Time Interleaver Consideration

As shown in the LDM proposal, there are two different places where the signal could be injected. This leads to two different receiver schemes, being the main difference between them the implemented time interleaver (TI) for the mobile layer. In fact, if the legacy system is superimposed prior to the time interleaving process, both layers will share the same time interleaver. This is the approach taken in this chapter as it is the less complex.

In addition, it is known that generally speaking the time interleaver performance just depends on the time depth. Therefore, in this approach the maximum allowable time interleaving within the frame duration has been chosen: 250 ms. As it has been mentioned in Chapter 4, any interleaver that spreads each FEC block evenly over the full TI duration basically has the same performance, if an appropriate bit or cell interleaver is used to disperse burst errors. Furthermore, the time varying frequency correlation time can be calculated as

$$Int_{depth} = \frac{1}{F_D} \tag{6.1}$$

where FD is the maximum Doppler frequency.

This means that the system TI will be able to deal even with a 4Hz Doppler Shift mobile layer, which corresponds to a speed of 2 km/h (on a 690 MHz RF channel) for the low speed environments. To sum up, through this Chapter the legacy system (DVB-T2) block time interleaver will be used for both, the LDM common interleaver approach and single layer case.

2.1.2 Signal Reception

Figure 6.4 shows the block diagram for the receiver part of the computer simulation platform for both the SL and LDM approaches.

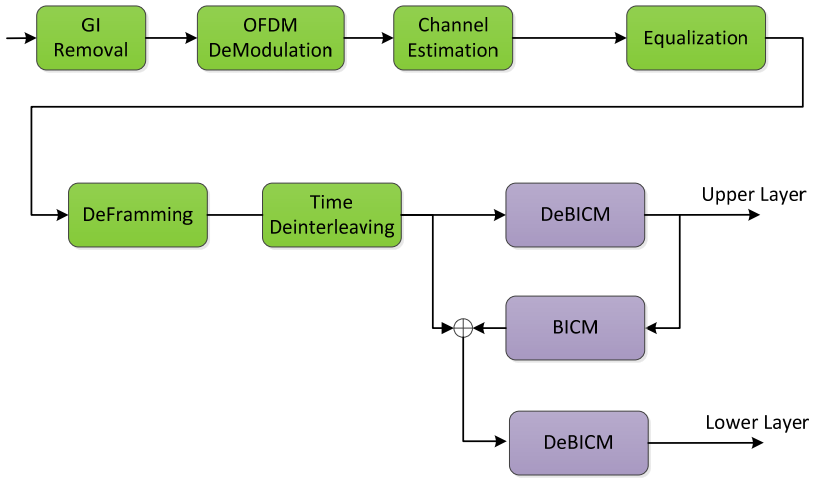

Figure 6.4. Block diagram of the computer based communication chain (receiver part).

Basically, it includes all the basic receiver modules associated with an OFDM receiver: GI removal, OFDM demodulation, de-framers, de-interleavers and decoders. In addition, it also includes the frequency domain cancellation algorithm presented in Chapter 4 for the LDM reception. It is also important to note that the channel estimation module includes not only ideal channel estimation, but also all the methods presented in Chapters 3 and 4.

2.1.3 Simulation Configuration

The simulation parameters described in this section are common for the computer based SL and LDM analysis. What is more, unless other indication is done, these are the values that should be considered through this chapter. As mentioned before LDM was a technology that grew out of the cloud transmission idea, and thus, both the upper layer in the LDM case or the SL case are also named as Cloud-Txn in reference to that origin.

2.1.3.1 OFDM Physical Waveform

In both cases, SL and LDM, the general parameters of the OFDM physical waveform are common shared. The FFT size has been set up to 16K and the guard interval has been defined as 1/8. This configuration allows the reception of echoes reflected from 90 km away without Inter Symbol Interference (ISI). What is more, it satisfies the current SFN maximum length requirements (84 km).

The generated signal will be tested against the most widely used channel models for testing broadcast systems (AWGN, Ricean, Rayleigh, 0dB Echo and TU-6) [56]. Therefore, the densest DVB-T2 based PP2/PP1 pilot patterns will be used [120]. The separation of pilot bearing carriers (D_x) is three, while the numbers of symbols forming one scattered pilot sequence (D_y) is either two (PP2) or four (PP1). According to the Nyquist limit, these pilot patterns will be enough to estimate channels with delay spreads up to 240 km. In addition, in order to reduce the channel estimation performance loss at the receiver, the scattered pilot carriers are boosted by 2.5 dB. In the SL case the boosting is applied against the normalized data carrier amplitude, whereas in the LDM the pilot linear amplitude is maintained to make it compatible with some DVB-T2 receivers..

The computer based simulations will present two different receiving thresholds for each scenario. The first one will be the most theoretical case, where the raw data is employed (no framing included) and the channel gain is known at the receiver site. This theoretical value will offer the lowest boundary against which the channel estimation algorithms will be tested. Therefore, the second receiving threshold will correspond to a complete signal (including pilot boosting), where a practical channel estimation methodology is implemented.

Nevertheless, for fair comparison, it must be taken into account that the raw values do not consider the SNR reduction resulting from boosted pilots. Net values of SNR can be derived from the raw SNR values plus a correction factor such as:

$$\Delta_{BP} = 10\log_{10}\frac{\left(N_{data} + N_{NBP} + N_{BP}\cdot B_{BP} + N_{CP}\cdot N_{CP}\right)}{N_{data} + N_{NBP} + N_{BP} + N_{CP}} \tag{6.2}$$

where N_{data} is the number of data cells per OFDM symbol, N_{NBP} the number of non-boosted pilots per OFDM symbol, N_{BP} the number of boosted pilots per OFDM symbol, N_{CP} the number of continual pilots and B_X the boosted values for those carriers[34]. TABLE 6.1 gathers the calculated pilot boosting losses depending on the selected FFT mode. The previous pilot boosting correction should be applied, not only in the single layer case, but also in the LDM case, as both share the same pilot scheme.

TABLE 6.1. Correction factors for pilot boosting (dB).

	SL		**LDM ($\Delta = -4dB$)**		**LDM($\Delta = -5dB$)**	
	PP1	**PP2**	**PP1**	**PP2**	**PP1**	**PP2**
8K	0.41	0.39	0.18	0.18	0.17	0.16
16K	0.41	0.38	0.18	0.17	0.17	0.15
32K	-	0.37	-	01.6	-	0.15

It is shown that the total pilot boosting penalty for the LDM case will be reduced with respect to the SL case. The main reason is that, if the actual pilot carrier amplitude is maintained, whereas the data carrier value is increased, the relative boosting is reduced. Finally, it should be taken into account that if the channel estimation algorithm is very accurate, the gain offered by the pilot boosting is reduced.

During this test phase, the channel estimation is done by a frequency domain DFT interpolation, plus an additional time-domain Wiener filtering. The time filtering window is 10 tap long and the negative symmetric algorithm has been used for padding the estimated LS pilots. Regarding the pilot pattern, the first three stationary channel estimations have been obtained using PP2. Nonetheless, in accordance to the Nyquist limit, the 0 dB echo channel requires the usage of the PP1 together with an additional lineal time-domain interpolation of pilot carriers.

It is important to note that the communication chain includes bit, cell and time interleavers for reducing the performance loss due to the different noise sources. These modules will be the same as the ones defined in the DVB-T2 standard. Regarding the TI functionality, it has been defined just one block TI within the frame, being the interleaving depth the maximum size of the frame (250 ms). Therefore, the number of symbols per frame is 93, which is very close to the maximum symbol number allowable by the frame length in a 6 MHz bandwidth.

2.1.3.2 Channel Models

The proposed signals will be tested against the most implemented (and most challenging) channel models employed within the last decade standardization processes [56]. On the one hand, for testing stationary scenarios: AWGN, RICE, RAYLEIGH and 0dB echo channels are considered, and on the other hand, for mobile channels, the TU-6 is selected.

TABLE 6.2 shows the equivalencies between the considered maximum Doppler frequency and the corresponding speed value, assuming that in the future the upper part of the broadcasting spectrum is going to be at about 600 MHz. The test will be carried out for receiver speeds ranging from 5 km/h (handheld devices) to 180 km/h (motorway or high speed trains).

TABLE 6.2. Doppler frequencies and the speed correspondence.

f_d (Hz)	V (km/h)
5	3.0
50	90
75	135
100	180

2.1.3.3 QoF (Quasi Error Free) Condition

Regarding the Quality of Service (QoS), the signal reception will be considered error free when the BER value at the outer coder output is lower than 10^{-7}. For stationary channels, the Gaussian noise is injected in the time domain, after estimating the overall signal power. It must be borne in mind that the implemented channel models, as well as the transmitter signals, are previously normalized. In order to obtain an accurate threshold value, the performance evaluation for signal to noise ratios close to the error free reception are averaged using random noise sources.

When dealing with mobile channels a new methodology has to be followed. First of all, as the channel is time-varying, for each receiving speed several channel realizations must be averaged; and secondly, the noise must be injected symbol by symbol in the frequency domain. Therefore, when dealing with time-varying channels, the noise is inserted in the frequency domain calculating the signal power at the channel output for each symbol. Finally, the simulation step is fixed at 0.1 dB, which offers a very accurate waterfall for each of the performance curves.

2.2 Single Layer

The first part of this section is focused on analyzing the single layer performance. This layer could be also called Cloud-Txn layer, which is a very robust layer which targets handheld and vehicular mobile services under very challenging conditions.

The minimum bit-rate to be delivered has been fixed at 1.8 Mbps, which is supposed to be enough to offer several SD (Standard Definition) services or at least one HD services when the latest HEVC video coding techniques are implemented. Based on that requirement, six different combinations have been defined, which range from the minimum bit rate (1.87 Mbps) to a higher mobile throughput (6.28 Mbps), which is even slightly higher than the current mobile services (DVB-T2 Lite, NGH…). TABLE 6.3includes the selected configurations, along with their corresponding spectral efficiencies and bit rates. It must be noted that all the included LDPC codes, {x/15}, are fully compatible with the actual DVB-T2 TX/RX architectures. In this section there will be first analysed the results regarding the stationary channels, and afterwards, there will be the chance for the mobile case.

TABLE 6.3. Single Layer configuration table and obtained bit rate in Mbps.

CONSTELATION	Code Rate	Spectral Efficiency (Mbps/Hz)	Bit Rate (Mbps)
QPSK	3/15	0.33	1.87
	4/15	0.44	2.51
	5/15	0.55	3.14
16-QAM	3/15	0.66	3.75
	4/15	0.88	5.02
	5/15	1.10	6.28

2.2.1 Stationary Channels

First of all, TABLE 6.4 gathers the obtained SNR thresholds for the raw data of the proposed configurations over the most common stationary channels. In other words, in these simulations the signals do not include any kind of pilot carriers or signalling, and the channel is known at the receiver site. These receiving thresholds are the lowest boundaries against which the channel estimation values will be tested. As expected, the receiving threshold difference between the most challenging channel (Rayleigh) and the less critical one (AWGN) is smaller for the most robust configurations. For instance, this difference is just 0.7 dB for the QPSK-3/15 case, whereas for the 16QAM-5/15 the value increases up to 1.5 dB.

TABLE 6.4. Single layer thresholds for stationary channels with ideal channel estimation (required SNR to achieve BER=$1x10^{-7}$).

		AWGN	RICE	Rayleigh	0 dB Echo
QPSK	3/15	-4.3	-4.2	-3.6	-3.9
	4/15	-2.9	-2.7	-2.0	-2.3
	5/15	-1.7	-1.5	-0.5	-0.9
16-QAM	3/15	-0.9	-0.7	0.4	0.0
	4/15	0.7	0.9	2.1	1.7
	5/15	2.3	2.6	3.8	3.5

For comparison purposes in TABLE 6.5 the required minimum receiving thresholds when real channel estimation is implemented are included, in other words, when the channel is not known at the receiver and the signal framing is included. For each configuration the difference between different layers are mostly maintained. It must be bore in mind that the pilot carriers are boosted, and consequently, there is an avoidable performance loss.

TABLE 6.5. Single layer thresholds for stationary channels with real channel estimation (required SNR to achieve BER=$1x10^{-7}$).

		AWGN	RICE	Rayleigh	0 dB Echo
QPSK	3/15	-3.9	-3.8	-3.1	-2.8
	4/15	-2.5	-2.3	-1.5	-1.3
	5/15	-1.3	-1.1	0.0	0.1
16-QAM	3/15	-0.5	-0.3	0.9	1.2
	4/15	1.1	1.3	2.7	2.7
	5/15	2.7	3.0	4.5	4.3

In addition, in order to have a general picture of the performance losses, Figure 6.5 collects the exact degradations when TABLE 6.4 and TABLE 6.5 are compared. It can be seen that all the signal configurations show almost the same performance degradation for each channel. As matter of fact, using the proposed two-dimensional channel estimators (2D-DFT), for the first three channels the performance is very close to that of an ideal receiver with perfect channel knowledge after the pilot boosting penalty is taken into account.

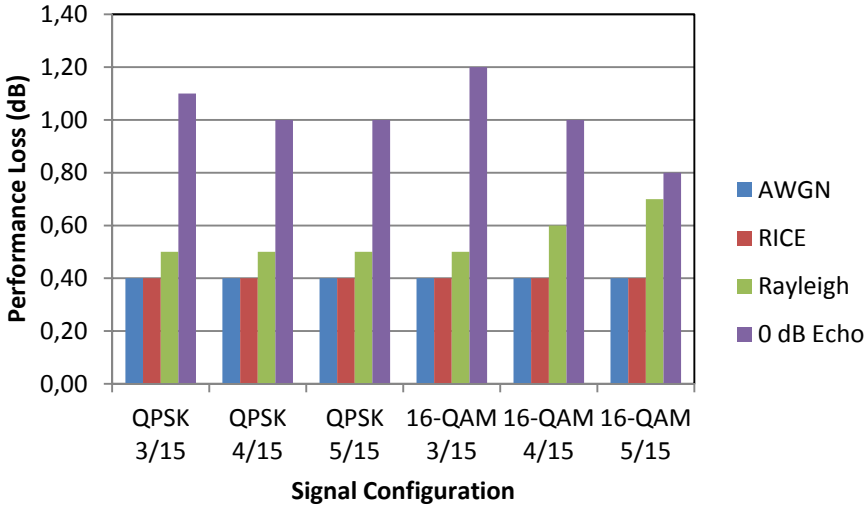

Figure 6.5. Performance loss due to real channel estimation on stationary channels.

For instance, the performance gap is just about 0.4dB for the first two channel models (AWGN and RICE), which represent the case where there is direct line of sight and a very weak multipath component. However, the last two rows represent more interesting channels for testing real services, as they represent the most challenging scenarios that the signal may suffer. Even so, it is proved that implementing the previously presented algorithm, it is perfectly feasible to deliver an accurate representation of the frequency response even under a very frequency selective channel. For example, for the portable indoor channel (Rayleigh), the loss is only about 0.5-0.7 dB, whereas for the most critical 0 dB Echo, the degradation increases up to about 1.0-1.2 dB.

It is important to note that for the first three cases, when QPSK is used, the final SNR threshold including channel estimation remains negative, and therefore, the system will be able to withstand a noise power which is actually higher than the transmitted signal power. In principle, these three combinations are the most suitable ones to be used as an upper layer for the LDM multiplexing, if the negative receiving threshold for the upper layer needs to be maintained.

The signal configurations implementing 16-QAM can be used for achieving notably higher bitrates, but unfortunately they do not offer receiving thresholds well beyond the 0 dB SNR margin, and thus, they will not be considered for the LDM upper layer case. However, the regular MFN can be implemented without

any problems for delivering more than one HD or even UHDTV services for the mobile channel.

2.2.2 Mobile Channels

The first objective of this section is to prove the suitability of the proposal for implementing large sized FFT signals (16k) for mobile scenarios. In addition, the secondary objective is to confirm the idea that the ICI problem can be overcome with strong FECs. Finally, the performance losses will be compared to the LDM case to verify that there is not an extra loss for the hierarchical spectrum reuse. In this case, in TABLE 6.6, all the receiving thresholds for both cases have been gathered, the raw data with ideal channel estimation and the frame structured data with real channel estimation.

TABLE 6.6. Single layer thresholds comparison for mobile channels (require SNR to achieve BER=$1x10^{-7}$).

		f_d=5 Hz		**f_d =50 Hz**		**f_d =75 Hz**		**f_d =100 Hz**	
		Ideal	*Real*	*Ideal*	*Real*	*Ideal*	*Real*	*Ideal*	*Real*
QPSK	**3/15**	-2.1	-1.6	-2.4	-1.5	-2.3	-1.7	-2.4	-1.5
	4/15	-0.9	-0.3	-1.2	-0.4	-1	-0.2	-0.6	0.4
	5/15	0.4	1.4	0.1	1.0	0.4	1.2	0.8	1.6
16-QAM	**3/15**	1.6	3.1	1.3	2.1	1.4	3.1	2.0	3.7
	4/15	2.8	4.2	3.2	4.2	3.5	4.7	3.9	5.4
	5/15	4.4	5.5	4.8	6.1	5.1	6.5	5.9	7.5

In addition to the summary in TABLE 6.6, Figure 6.6 gathers the different performance losses for an easier analysis. The first important outline is that, as expected, the more robust the configuration, the less significant the ICI noise is, and therefore, the lower the performance loss. For instance, it can be seen how the performance loss for the most rapid time-varying channel case (100 Hz) decreases from 1.6 dB (16-QAM, CR=5/15) to 0.9 dB (QPSK, CR=3/15). Overall, the implemented channel estimation offers small losses which range just from 0.5 dB to 2 dB, which is within the real implementation impairments. The results of this section should be understood as a behaviour trend, because they are not targeting to give an exact receiving threshold value, but a performance pattern to compare with the LDM proposal.

As a matter of fact, another important outcome of these results is the idea that large sized FFTs may be used for time-varying channels if the proposed FEC is

robust enough. For the most robust configurations (QPSK, CR={3-5}/15) the difference between low-speed cases (5 Hz) and high-speed (100 Hz) is always less than 1.5 dB. This is very important for LDM implementation. In this multiplexing scheme, both layers share the same FFT size, and therefore, the use of large sized FFTs will significantly reduce the overhead due to the guard interval.

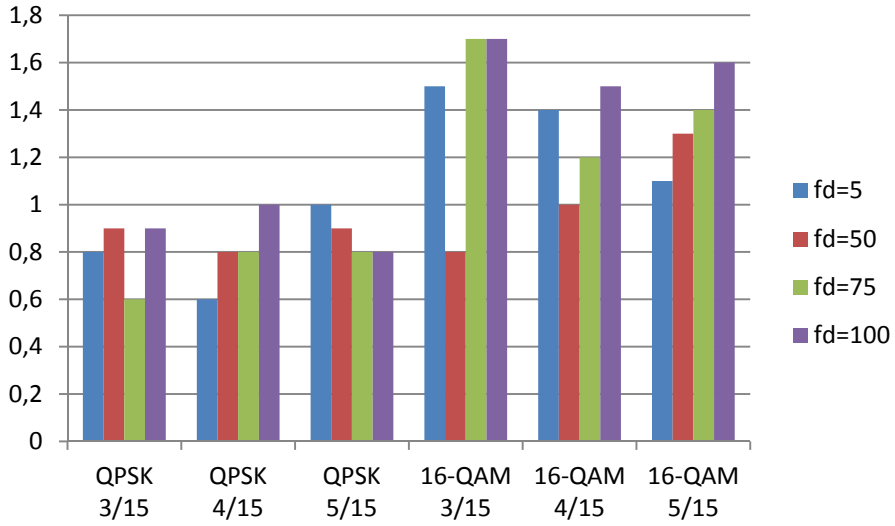

Figure 6.6. Performance loss due to real channel estimation over time-varying channels.

2.2.3 Granularity

Finally, the following graph shows the granularity of the previously presented modulation and error rate combination for the stationary AWGN case. It can be seen that the proposed configurations offer a good granularity with almost an equally spaced combination that ranges from 1.8 Mbps to 6.2 Mbps.

Nevertheless, it can be clearly seen that the 16-QAM modulation configurations are offering positive SNR values even for an AWGN case. In fact, if the mobile channel section is analysed, it can be seen that in the case of single layer, those values are pretty high. Thus, when considering the LDM case, only QPSK signals will be considered for the mobile layer, which will assure a very extensive coverage and signal robustness will allow the service stream to withstand high noise powers.

This is a very important conclusion to the presented EVP iterative process. As a matter of fact, it indicates that as a first approach, 16-QAM modulation will not be considered as upper layer for the LDM case.

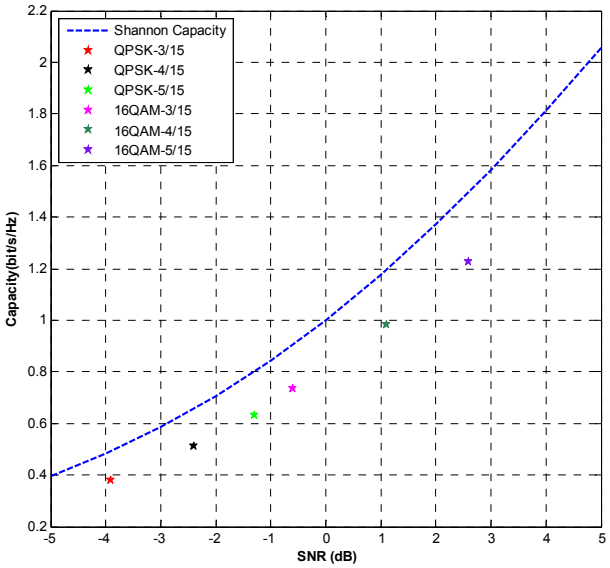

Figure 6.7. Single layer capacity vS SNR granularity representation.

2.3 **Layered Division Multiplexing (LDM)**

One of the main objectives of this thesis is to provide technical solutions for the new generation broadcasting systems, which aim at the simultaneous delivery of stationary and mobile services. In Chapters 4 and 5, it has already been theoretically demonstrated that, from the capacity point of view, the most efficient multiplexing technique is the power division or layered division multiplexing. The objective of this section is to gain deep insight into that assumption providing computer simulation results that confirm the expected performance for the proposal. In this case, within the configuration parameters, apart from the modulation and code rate, the injection range is also considered, which offers an additional degree of freedom for higher flexibility. In few words, it is a parameter which controls how much power is assigned to the mobile service and how much to the stationary service.

A LDM signal is a multiplexed data stream that is the addition of at least two signals (upper and lower layers), the first one targeting mobile devices, while the

second one aims at the high capacity stationary programs. The upper layer has been designed to offer a very robust service even under very challenging conditions, such as severe multiple channels, very noise environments, and high interference channels; while the high-capacity service has been configured to offer enough capacity to deliver various HD services or even UHTV. Therefore, the upper layer stream is configured with the most robust mod-cod (modulation & coding) configurations, whereas the lower layer tends to use much higher modulations and less robust code rates. The capacity values in TABLE 6.7 have been calculated for a 6 MHz channel taking into account the signal overhead due to the signalling data and frame structure.

TABLE 6.7. LDM configurations and associated bit rates.

	Const.	Code Rate	Spectral Efficiency (bps/Hz)	Bit Rate (Mbps)
Upper Layer	**QPSK**	3/15	0,33	1.87
	QPSK	4/15	0,44	2.51
Lower Layer	**16-QAM**	3/4	2.49	14.21
	64-QAM	2/3	3.32	18.94
	256-QAM	2/3	4.42	25.25

As in the previous use case (Single Layer), the minimum bit-rate to be delivered has been fixed at 1.8 Mbps. In addition, the possible configurations for the upper layer have been reduced following other constraints: the upper layer minimum threshold should be close to 0 dB, and the legacy system SNR cannot be higher than 30 dB. The first condition is applied in order to allow the upper layer to withstand noise powers higher than the actual signal power. The second one is fixed by the actual MER output of a real transmitter. More precisely, three different configurations for the lower layer have been considered: services up to 14.21 Mbps (16QAM, CR=3/4), up to 18.94 Mbps (64-QAM, CR=2/3) and up to 25.25 Mbps (256-QAM, CR=2/3), which may suffice for a UHDTV service. Regarding the injection range, two of the more balanced values have been selected, -4 and -5 dB, which will offer a great trade-off between the mobile service enhancement and the stationary service power assignation.

2.3.1 Stationary Channels

As in the SL case, this section provides simulation results for the LDM multiplexing technique for both the raw data with ideal channel estimation and the frame structured signal with a real channel estimation algorithm. Although in this

work, DVB-T2 has been chosen as a legacy layer, the layer division multiplexing technique can be used with any OFDM signal waveform. Nevertheless, prior to anything, TABLE 6.8 and TABLE 6.9 offer the comparison between theoretical receiving thresholds and ideal channel estimation simulations for the selected configurations, when the injection range values are -4 and -5 dB respectively, and when a code rate of 3/15 is selected for the UL. The theoretical values are based on the mathematical formulations presented in Chapter 4, which depend on the ideal single layer results and the selected injection range. The main purpose of this comparison is to validate the theoretical formulation employed up to now.

TABLE 6.8. Stationary channels: receiving thresholds for LDM services (injection range -4 dB, UL CR=3/15). Theoretically estimated and ideal channel estimation simulations.

			AWGN		**RICE**		**Rayleigh**		**0 dB Echo**	
			Theor.	*Ideal*	*Theor.*	*Ideal*	*Theor.*	*Ideal*	*Theor.*	*Ideal*
UL	**QPSK**	**3/15**	-2.1	-2.1	-2.0	-1.9	-1.3	-0.9	-1,7	-1.3
LL	**16QAM**	**3/4**	15.5	15.5	16.0	15.9	18.9	18.9	18.8	18.8
UL	**QPSK**	**3/15**	-2.1	-2.1	-2.0	-1.9	-1.3	-0.9	-1,7	-1.3
LL	**64QAM**	**2/3**	18.9	18.9	19.3	19.2	21.6	21.5	21.4	21.3
UL	**QPSK**	**3/15**	-2.1	-2.1	-2.0	-2.0	-1.3	-0.9	-1.7	-1.3
LL	**256QAM**	**2/3**	23.2	23.2	23.5	23.5	25.8	25.7	25.8	25.8

TABLE 6.9. Stationary channels: receiving thresholds for LDM services (Injection range -5dB, UL CR=3/15).

			AWGN		**RICE**		**Rayleigh**		**0 dB Echo**	
			Theor.	*Ideal*	*Theor.*	*Ideal*	*Theor.*	*Ideal*	*Theor.*	*Ideal*
UL	**QPSK**	**3/15**	-2.6	-2.6	-2.5	-2.4	-1.8	-1.5	-2.1	-1.8
LL	**16QAM**	**3/4**	16.2	16.2	16.7	16.6	19.6	19.5	19.4	19.4
UL	**QPSK**	**3/15**	-2.6	-2.5	-2.5	-2.3	-1.8	-1.4	-2.1	-1.9
LL	**64QAM**	**2/3**	19.6	19.5	20.0	20.0	22.3	22.2	22.0	22.0
UL	**QPSK**	**3/15**	-2.6	-2.6	-2.5	-2.4	-1.8	-1.4	-2.1	-1.9
LL	**256QAM**	**2/3**	23.9	23.9	24.3	24.3	26.5	26.5	26.5	26.5

In addition, for a more detailed comparison purposes TABLE 6.10 and TABLE 6.11 present the same comparison, but for a less robust UL case (CR=4/15), which will offer a bit rate increase for the mobile layer.

TABLE 6.10. Stationary channels: receiving thresholds for LDM services (injection range -4dB, UL CR=4/15). Theoretically estimated and ideal channel estimation simulations.

			AWGN		**RICE**		**Rayleigh**		**0 dB Echo**	
			Theor.	*Ideal*	*Theor.*	*Ideal*	*Theor.*	*Ideal*	*Theor.*	*Ideal*
UL	**QPSK**	**4/15**	-0.5	-0.4	-0.2	-0.1	0.7	1.3	0.3	0.8
LL	**16QAM**	**3/4**	15.5	15.5	16.0	15.9	18.9	18.9	18.8	18.8
UL	**QPSK**	**4/15**	-0.5	-0.4	-0.2	-0.1	0.7	1.2	0.3	0.8
LL	**64QAM**	**2/3**	18.9	18.9	19.3	19.2	21.6	21.5	21.4	21.3
UL	**QPSK**	**4/15**	-0.5	-0.4	-0.2	-0.1	0.7	1.3	0.3	0.8
LL	**256QAM**	**2/3**	23.2	23.2	23.6	23.5	25.8	25.7	25.8	25.8

TABLE 6.11. Stationary channels: receiving thresholds for LDM services (injection range -5 dB, UL CR=4/15). Theoretically estimated and ideal channel estimation simulations.

			AWGN		**RICE**		**Rayleigh**		**0 dB Echo**	
			Theor.	*Ideal*	*Theor.*	*Ideal*	*Theor.*	*Ideal*	*Theor.*	*Ideal*
UL	**QPSK**	**4/15**	-0.8	-0.8	-0.7	-0.6	0.2	0.5	-0.2	0.0
LL	**16QAM**	**3/4**	16.2	16.2	16.7	16.6	19.6	19.6	19.4	19.4
UL	**QPSK**	**4/15**	-0.8	-0.8	-0.7	-0.7	0.2	0.5	-0.2	0.0
LL	**64QAM**	**2/3**	19.6	19.6	20.0	20.0	22.3	22.2	22.0	22.0
UL	**QPSK**	**4/15**	-0.8	-0.8	-0.7	-0.6	0.2	0.6	-0.2	0.1
LL	**256QAM**	**2/3**	23.9	23.9	24.3	24.3	26.5	26.5	26.5	26.5

The first outcome is that the presented theoretical model is very accurate for the LL receiving threshold estimation. As a matter of fact, after a proper cancellation, the lower layer threshold degradation only depends on the injection range. In other words, there is no signal cancellation error. In addition to that is important to note that the theoretical calculation of the receiving threshold applies equally for any type of channel. Regarding the upper layer, there seems to be an issue with rich multi-scattered channels (Rayleigh & 0 dB Echo). In order to make it easier to analyse, the differences between simulated values and the theoretical models for the upper layer case have been summarized in TABLE 6.12. As mentioned before, it can be seen that for the vast majority of the cases in the LL, the error is 0 or within 0.1 dB, which is the simulation step. Basically, this means that the theoretical model is really accurate for the LL threshold calculation. Furthermore, it also proves that the LL performance degradation does not depend on the UL configuration.

TABLE 6.12. Performance loss due to the LDM multiplexing technique: injection range -4dB/-5dB.

			AWGN	RICE	Rayleigh	0 dB Echo
-4dB	**QPSK**	**3/15**	0.0	0.1	0.4	0.4
		4/15	0.0	0.1	0.6	0.5
-5dB	**QPSK**	**3/15**	0.0	0.1	0.3	0.2
		4/15	0.0	0.1	0.4	0.3

When the UL case is analysed, there seems to be a mismatch with the highly-scattered channels, where the difference is higher than 0.1 dB. In fact, it ranges from 0.2 dB (0 dB Echo, CR=3/15, $\Delta = -5dB$) to 0.6 dB (Rayleigh, CR=4/15, $\Delta = -4dB$). The difference increases for the less robust and lower injection ranges. Therefore, it is clear that there is a problem related with the UL decoding when there is a LL injected signal. Based on the results, it is concluded that this difference is probably due to a mismatch in the LLR calculation for the LDPC decoding.

$$\tilde{x}_{UL}[k] = \hat{x}_{UL}[k] + \hat{x}_{LL} + w[n] \cdot h^{-1}[k] \tag{6.3}$$

According to Eq. (6.3), after the equalization, the actual Gaussian noise is weighted by the channel impulse response inverse gains for the LLR estimation. However, the LL, which is also considered a noise source, it is not weighted and this difference may be the responsible for the additional degradation. It is a very interesting topic for further research.

Once the starting point has been clarified the next step is based on providing more realistic receiving thresholds, where a real channel estimation algorithm has been also implemented. The main idea is to show that there is not and additional lose for the LDM multiplexing technique implementation when compared with the SL case..

Accordingly, TABLE 6.13 and TABLE 6.14 compare the receiving thresholds for ideal and real channel estimation conditions for the low, medium and high capacity lower layers when the mobile layer code rate is fixed at 3/15 and for -4 dB and -5 dB injection ranges.

TABLE 6.13. Stationary channels: receiving thresholds for LDM services (injection range -4dB, UL CR=3/15). Ideal and real channel estimation.

			AWGN		**RICE**		**Rayleigh**		**0 dB Echo**	
			Ideal	*Real*	*Ideal*	*Real*	*Ideal*	*Real*	*Ideal*	*Real*
UL	**QPSK**	**3/15**	-2.1	-1.9	-2.0	-1.7	-0.9	-0.6	-1.3	-0.5
LL	**16QAM**	**3/4**	15.4	15.7	15.9	16.2	18.8	19.4	18.7	19.4
UL	**QPSK**	**3/15**	-2.1	-1.9	-1.9	-1.7	-0.9	-0.6	-1.3	-0.3
LL	**64QAM**	**2/3**	18.9	19.2	19.2	19.6	21.5	22.1	21.2	22.5
UL	**QPSK**	**3/15**	-2.1	-1.9	-2.0	-1.7	-0.9	-0.6	-1.3	-0.2
LL	**256QAM**	**2/3**	23.2	23.7	23.5	23.9	25.7	26.3	25.8	27.0

TABLE 6.14. Stationary channels: receiving tresholds for LDM services (Injection range -5dB, UL CR=3/15). Ideal and real channel estimation.

			AWGN		**RICE**		**Rayleigh**		**0 dB Echo**	
			Ideal	*Real*	*Ideal*	*Real*	*Ideal*	*Real*	*Ideal*	*Real*
UL	**QPSK**	**3/15**	-2.6	-2.3	-2.4	-2.1	-1.5	-1.1	-1.8	-0.7
LL	**16-QAM**	**3/4**	16.2	16.5	16.6	17.0	19.5	20.1	19.4	20.2
UL	**QPSK**	**3/15**	-2.6	-2.3	-2.3	-2.1	-1.4	-1.1	-1.9	-0.7
LL	**64-QAM**	**2/3**	19.5	20.0	20.0	20.4	22.2	22.8	22.0	23.2
UL	**QPSK**	**3/15**	-2.6	-2.3	-2.4	-2.1	-1.4	-1.1	-1.9	-0.7
LL	**256QAM**	**2/3**	23.9	24.2	24.3	24.6	26.5	27.0	26.5	27.7

Similarly, TABLE 6.15 and TABLE 6.16 summarize all the results, but for a case which delivers a higher capacity for the mobile services. It must bear in mind that the simulation step has been set up to 0.1 dB.

TABLE 6.15. Stationary channels: receiving thresholds for LDM services (injection range -4dB, UL CR=4/15). Ideal and real channel estimation.

			AWGN		**RICE**		**Rayleigh**		**0 dB Echo**	
			Ideal	*Real*	*Ideal*	*Real*	*Ideal*	*Real*	*Ideal*	*Real*
UL	**QPSK**	**4/15**	-0.4	-0.2	-0.1	0.1	1.3	1.6	0.8	1.7
LL	**16QAM**	**3/4**	15.4	15.7	15.9	16.2	18.8	19.3	18.7	19.5
UL	**QPSK**	**4/15**	-0.4	-0.2	-0.1	0.1	1.2	1.6	0.8	1.8
LL	**64QAM**	**2/3**	18.9	19.2	19.2	19.6	21.5	22.0	21.2	22.5
UL	**QPSK**	**4/15**	-0.3	-0.1	-0.1	0.1	1.3	1.6	0.8	1.7
LL	**256QAM**	**2/3**	23.2	23.5	23.5	23.9	25.7	26.3	25.8	27.0

TABLE 6.16. Stationary channels: receiving thresholds for LDM service (injection range -5dB, UL CR=4/15). Ideal and real channel estimation.

			AWGN		RICE		Rayleigh		0 dB Echo	
			Ideal	*Real*	*Ideal*	*Real*	*Ideal*	*Real*	*Ideal*	*Real*
UL	**QPSK**	**4/15**	-0.9	-0.7	-0.6	-0.4	0.5	0.9	0.0	1.1
LL	**16QAM**	**3/4**	16.2	16.5	16.6	17.0	19.6	20.1	19.4	20.2
UL	**QPSK**	**4/15**	-0.9	-0.7	-0.7	-0.4	0.5	0.9	0.0	1.2
LL	**64QAM**	**2/3**	19.6	20.1	20.0	20.5	22.2	22.8	22.0	23.3
UL	**QPSK**	**4/15**	-0.9	-0.7	-0.6	-0.4	0.6	0.9	0.1	1.1
LL	**256QAM**	**2/3**	23.9	24.4	24.3	24.8	26.5	27.0	26.5	27.8

In addition, Figure 6.8 shows the channel estimation performance degradation when compared with ideal simulations. As it has been mention before, a DVB-T2 signal has been used as legacy layer, and that is why, in the shared scheme the DVB-T2 pilot boosting has been maintained. The UL performance will be independent from the LL, and therefore, the different channel estimation penalties for different LL configurations have been averaged. In addition, the LL channel estimation performance is not affected by the LDM multiplexing technique, and thus, the penalty values have been averaged over the two different injection ranges.

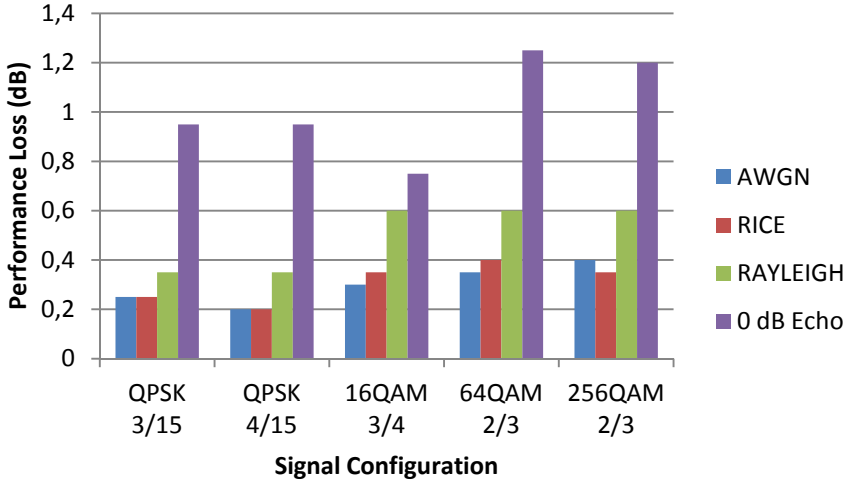

Figure 6.8. Stationary channel estimation loss for LDM.

As expected, degradation for the upper layer is pretty low (< 0.6 dB) for both case, on both injection ranges and for the vast majority of the channels excluding the 0dBEcho. For the lower layer the first three channels models show also a small degradation, but bigger than the UL case. In particular, it goes from about -0.3-0.4 dB in the AWGN and Rice cases to about 0.7-0.9 dB in the Rayleigh channel. This values match pretty well with SL case: the less robust the configuration the more it can be affected by the channel estimation error. As a matter of fact, the channel penalty is smaller due to the smaller boosting, which is compensated with very good performing channel estimation. Nevertheless, it must be borne in mind that for the most challenging channel, the 0 dB Echo, this value may increase up to 0.9-1.3 dB for both upper and lower layers. This degradation is once again very well aligned with the single layer results

As the main conclusion, it has been shown that is perfectly feasible the LDM reception over the stationary channels, even under the most challenging Rayleigh and 0 dB Echo conditions, without an additional performance loss for LDM multiplexation cancellation stage. What is more, it has been proved that the already known one dimensional channel estimation is accurate enough for the required frequency domain cancellation.

2.3.2 Mobile Channels

As shown in Chapter 5, one of the main advantages of LDM when compared with other multiplexing systems such as TDM and FDM is that it enhances the mobile layer performance. In fact, the major part of the transmission power can be assigned to the mobile service, while the lower layer service requirements are maintained in a reasonable working margin. The first aim of this subsection is to show that there is no extra degradation in the channel estimation performance due to the existence of a lower layer superimposed to the main signal as both share the same pilot carriers. In addition, the second objective is to prove that the error due to the usage of larger FFT symbols, and the related Doppler Effect, does not have big impact on the degradation for LDM when robust configuration are used.

In order to do that, in TABLE 6.17 and TABLE 6.18 the minimum receiving thresholds for the UL under TU-6 channels are presented for injection ranges of -4 and -5 dB respectively. What is more, the receiving thresholds for ideal and real channel estimation are compared. The LL performance is not shown, as it is designed just for a stationary service, and consequently, the receiver cannot access to the information in the lower layer in such receiving conditions. First of all, if the ideal cases are compared, it can be seen that the difference between the low speed

channel and the high-speed ones is always less than 1dB. This means that if a robust configuration is implemented, the degradation due to the receiver mobility is reduced as the ICI is masked by the Gaussian noise even for the 180 km/h case. For instance, in TABLE 6.17 can be seen that the ICI penalty is reduced to 0.5 dB for the most protected case (QPSK,CR=3/15).

TABLE 6.17. Simulated mobile channel performance for LDM mixed service when injection range is -4dB.

		f_d=5 Hz		**f_d =50 Hz**		**f_d =75 Hz**		**f_d =100 Hz**	
		Ideal	*Real*	*Ideal*	*Real*	*Ideal*	*Real*	*Ideal*	*Real*
QPSK	**3/15**	0.0	0.7	0.0	0.7	0.1	0.9	0.4	1.3
	4/15	2.0	2.7	2.3	3.3	2.4	3.4	2.9	3.7

TABLE 6.18. Simulated mobile channel performance for LDM mixed service when injection range is -5 dB.

		f_d=5 Hz		**f_d =50 Hz**		**f_d =75 Hz**		**f_d =100 Hz**	
		Ideal	*Real*	*Ideal*	*Real*	*Ideal*	*Real*	*Ideal*	*Real*
QPSK	**3/15**	0.3	0.6	0.0	0.5	0.0	0.5	0.3	0.8
	4/15	1.3	2.1	1.5	2.3	1.7	2.4	2.2	2.8

Eventually, the performance loss due to channel estimation has been summarized in Figure 6.9, where the first two groups of columns are calculated for an injection range of -4 dB and the other ones to -5 dB. It can be seen that the performance loss is practically the same in each configuration for different Doppler Frequencies. However, it can be also shown that the loss is increased when there is less power assigned to the mobile services and when the less robust configurations are selected. In these cases, the power difference between the Gaussian threshold and the actual ICI noise is reduced.

Another important outcome is that, after the channel estimation, the expected degradation due to the existence of ICI noise is always less than 1.5 dB even if a maximum Doppler frequency of 100 Hz is considered. This result reinforces the idea of using large sized FFT OFDM signals for time-varying channels even with LDM multiplexing. What is more, when these results are compared with the stationary channel results it is clear that there is no extra performance loss in the channel estimation part.

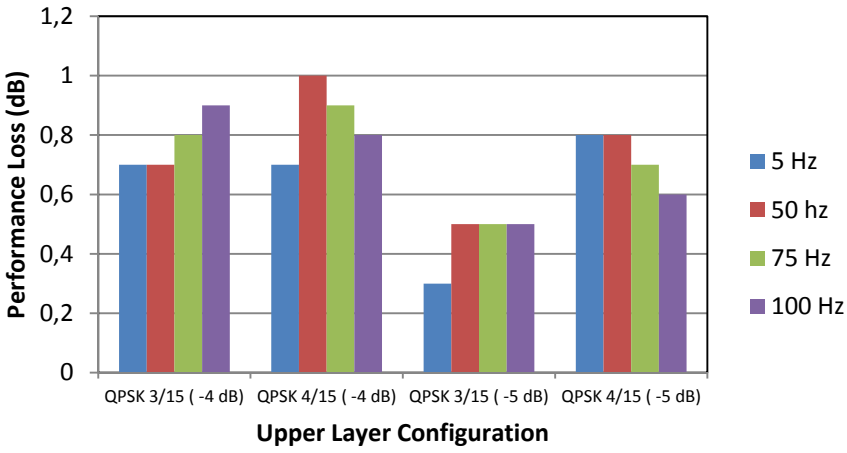

Figure 6.9. Upper layer channel estimation degradation over time-varying channels.

3. LABORATORY TESTS

The laboratory tests are the first necessary attempt to bring the proposed study closer to the real world casuistry. The importance of laboratory trials is that, for the first time, there is hardware equipment involved in the test. Therefore, there are some parameters that are not ideal anymore: the transmitted signal MER, the clock error, the bit quantification and the tx/rx sampling rates. That is why the laboratory measurements are an essential step prior to field test and subsequent to the computer based simulation results. What is more, laboratory performance results are usually very close to field test results, and thus, they will help to identify the weaknesses of the system, if any, before the whole infraestructure for the field trials is prepared.

As part of the EVP strategy, and based on the results from the previous phase, the number of configurations avalaible for analysis has been reduced. In particular, in the single layer case, only the more robust QPSK configurations are taken into account, whereas for the LDM case only the two more robust MOD-COD combinations are implemented. Finally, it must be noted that these laboratory tests are designed not only for evaluating the system performance, but also for identifying some weaknesses, whose modifications may lead to an improvement of the LDM overall performance.

3.1 Set-Up Architecture and Simulation Configurations

The overall system architecture of the laboratory trials carried out at the University of the Basque Country is depicted Figure 6.10, where a photo of the real test bench has been included.

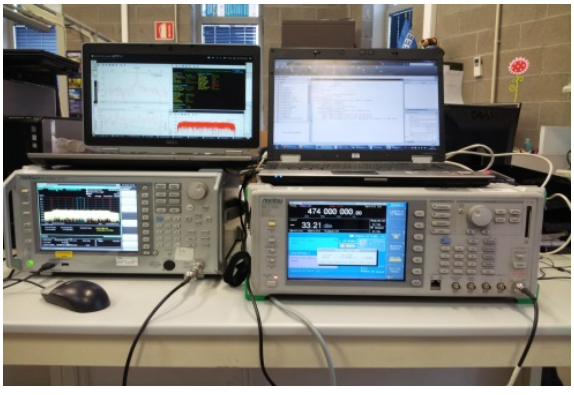

Figure 6.10. HW set up for laboratory measurements.

Even if in the following subsections, the different transmission and reception modules are explained in detail, the Figure 6.11 is a good example of the involvement equipment.

3.1.1 Signal Generation

Figure 6.11 depicts the block diagram of the transmitter site. The first half of the process is SW based, and consequently, the signals are generated in a PC running a modified version of the previously presented simulation platform. The main modifications are two: in the first place, the inclusion of a preamble for the posterior carrier recovery at the receiver site, and secondly, the addition of a module to convert the generated signal into an Anritsu IQ producer program TXT compatible file. It is also important to note that the channel model and the convolution with the transmitted signal are also generated in the SW platform. This is a great advantage as it allows easily controlling the simulated channel, and therefore, directly comparing the obtained results with the estimations of the previous phase. This SW is very flexible and allows generating either single layers or LDM multiplexed signals with different injection ranges. As in the previous case, the lower layer is DVB-T2 compatible, whereas the upper layer, Cloud-Txn, is based on some of the new tools provided through the ATSC 3.0 standardization process.

According to Figure 6.12 the HW part consists on a general purpose Vector Signal Generator (VSG), namely the Anritsu MG 3700A model.

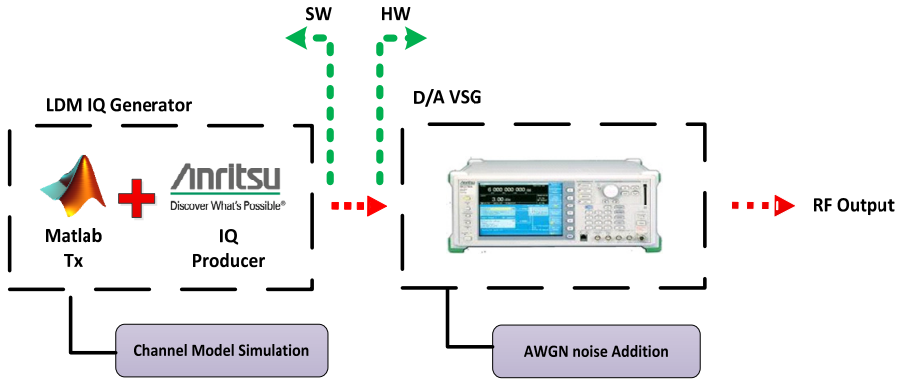

Figure 6.11. Laboratory trials transmitter block diagram.

As input files, only the proprietary file types .wvd and .wvi are allowed, which are obtained after processing the Matlab based TXT file with the Anritsu IQ producer software. Apart from the conversion, this program also carries out the multirate conversion to the signal sampling frequencty (f_s=48/7 MHz).

What is more, the MG3700A model has the capability for internally adding two different signals (already pre-loaded in the hard disk with the same sampling frequency) and modulating them into the required RF channel. For this test bench, one input is used for the desired signal (red box, see Figure 6.12), and the other one is employed as AWGN noise source (green box, see Figure 6.12).

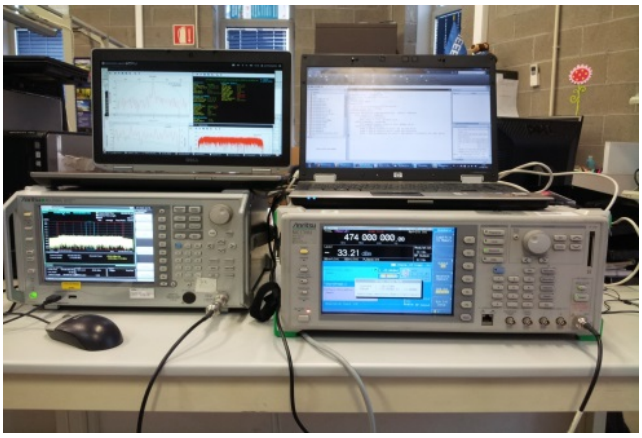

Figure 6.12. Screen capture of the Anritsu MG3700A vector signal generator.

In order to obtain the desired Signal to Noise ratio, signal powers are measured in the bandwidth of interest (5.71 MHz), and afterwards, the power is adjusted to obtain the wanted SNR. For instance, if the goal is to analyse an LDM signal with a SNR of 20 dB, the transmitted LDM signal power can be fixed at -40 dBm, meanwhile the additional noise source power is fixed to -60 dBm.

3.1.2 Signal Reception

The block diagram of the receiver part is depicted in Figure 6.13. At the receiver site, the generated signal is recorded by the Anritsu MS2690A Vector Signal Analyzer (VSA), which digitalizes the signal fed into the RF input. Afterwards, the signal is sampled according to the predefined sampling rate and stored into the internal HD. After that point, there is an offline SW processing, which basically consists on a SDR receiver.

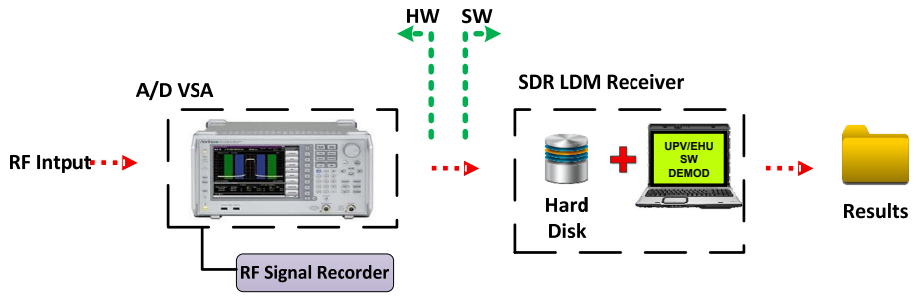

Figure 6.13. Laboratory trials receiver block diagram.

This SDR receiver can post-process all the signals that have been previously recorded. It offers a great range of practical values for analysing the signal performance, such as BER, channel impulse response and signal MER. This receiver is also known as Multilayer DBA and is an evolution of the already developed DVB-T2 receiver [118]. The obtained results can be used within the EVP process to identify the main weaknesses of the system and to propose some technical solutions or configurations to overcome them.

3.1.3 Processing Methodology

All the simulation configurations described in phase two (Section 2.1.3) apply also for this third step. Nevertheless, there are some specifics for the Lab HW trials that are going to be described in this section.

First of all, the data is generated using the SW/HW combination presented in the previous section, and afterwards, is feed to the receiver scheme presented in Section 2.1.2. At this point, the recorded signal duration is fixed to 5 s at a sampling rate of 20 Mbps with 16 bit resolution, and therefore, each recorded signal needs about 400 Mbyte of storage. The measured internal noise of the analyzer is -131 dBm in a 5.61 MHz channel. In Figure 6.14 a screen capture of the mentioned VSA can be found.

Figure 6.14. VSA screen capture.

The recorded data is properly labeled, and afterwards, it is stored in a series of hard disks for a posteriori offline analysis. The LDM SDR analyzer is the SW in charge of evaluating the performance of the recorded signals. Depending on the signalling it will work either for single layer signals or for the multiplexed ones. Although it can offer several relevant parameters, for testing the signal performance and in order to confirm the results obtained in the previous section, the Frame Error Rate (FER) will be the key value. This value gives the number of FEC blocks that have not been successfully decoded per frame, and therefore, it offers a clear picture of the system performance. In addition, there are other values that are analyzed in parallel, such as the channel impulse response, the Doppler spread and the MER. Although these parameters are not as important as FER, they can be used for understanding the specifics of the troublesome points. The test considers that there is a data loss when there is at least one error at the FEC output in a 5 second frame. This is the same requirement that has been place in the ATSC call for proposals.

The channel estimation included in this SDR is based in a DFT frequency domain interpolation and a prior time domain interpolation, similar to those explained in Chapter 3. In addition, it includes a time domain noise filtering. More information can be found in [118].

Finally, it is important to note that when mobile channels are considered, the previously presented methodology has a substantial disadvantage. In particular, the main problem with this type of channels is that frequency response can have great variations from symbol to symbol and so does the associated signal energy of the

received symbol. Thus, if a very long signal is used for estimating the signal power, and afterwards Gaussian noise power for a particular SNR is inserted, it may be the case where there are huge imbalances in the associated SNR for each symbol.

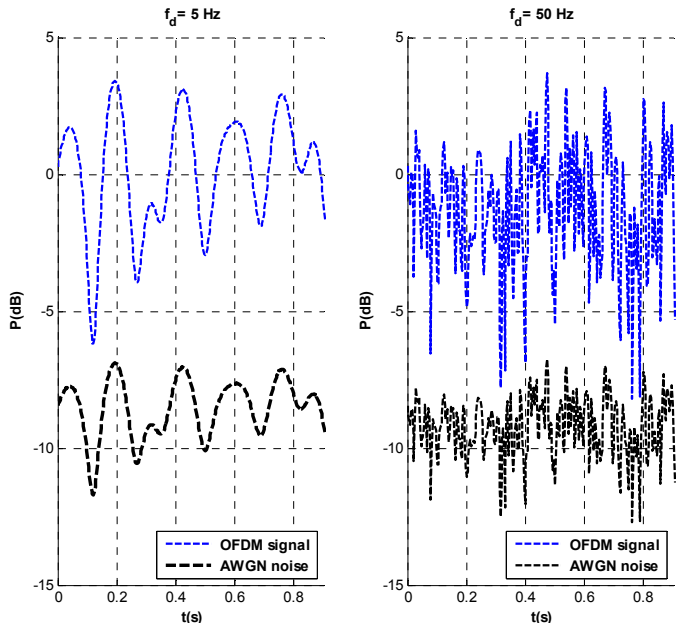

Figure 6.15. Noise power evolution over time-varying channels.

The proposed solution for these channels is to insert the corresponding noise symbol by symbol, in the transmission part. In this case, the signal at the channel output is totally controlled, and consequently, the Gaussian noise can be inserted in the frequency domain, symbol by symbol, guaranteeing a constant relation between the signal power and the noise (See Figure 6.15). Eventually, the signal can be received by the SDR LDM receiver. It is important to note that in this process there are also quantifications or clock error involved, but even though, the most problematic areas are the real channel estimation and the carrier recovery

3.2 **Single Layer**

The main objective of this chapter is to test the implementation feasibility of the LDM multiplexing technique in a more realistic scenario involving HW

equipment. Nevertheless, the single layer approach must also be analysed in order to have a fair comparison with LDM proposal. In this phase, for the single layer case, only the configurations that have shown suitability as upper layer in the computer based simulations will be considered. In order words, those ones that offer a negative threshold even for the most challenging channels. In particular, according to the previous results, the candidate will be the QPSK based configuration with {3,4,5}/15 LDPC codes.

3.2.1 Stationary Channels

First of all, the receiving thresholds for different stationary channels have been analyzed, targeting from the roof-top antenna reception (AWGN, RICE) to the most challenging chanels (RAYLEIGH, 0dBECHO). The 0dB echo channel has been slightly modified, changing the second path amplitude by 1 dB (This channel is depicted as "0dBECHO(*)" in the obtained results). The main problem with the regular one was that the two paths have practically the same amplitude, and therefore, the receiver does not know where it should be synchronized. This can lead to an extra loss that does not depend on the LDM multiplexing technique, and thus, it has been slightly modified.

TABLE 6.19 compares the results obtained in the laboratory, with the simulation results obtained when real channel estimation was considered.

TABLE 6.19. Stationary channel performance for SL.

		AWGN		**RICE**		**Rayleigh**		**0dBECHO(*)**	
		Sim.	*Lab.*	*Sim.*	*Lab.*	*Sim*	*Lab.*	*Sim*	*Lab.*
QPSK	**3/15**	-3.9	-3.4	-3.7	-3.2	-3.1	-2.8	-2.8	-0.4
	4/15	-2.5	-2.2	-2.3	-2.0	-1.5	-1.2	-1.3	0.4
	5/15	-1.3	-1.0	-1.1	-0.8	0.0	0.2	0.1	1.2

In addition, in Figure 6.16 the error degradation between the simulation results with real channel estimation and the LAB measurements is depicted. In this case, the x-axis is representing the channel models, whereas the vertical axis is representing the performance loss. It is important to note that the simulation step in this case has been increase to 0.2 dB. The main reason for this increase is the fact that the 0.1 dB precision has been considered too small as it is quite close to the VSG precision.

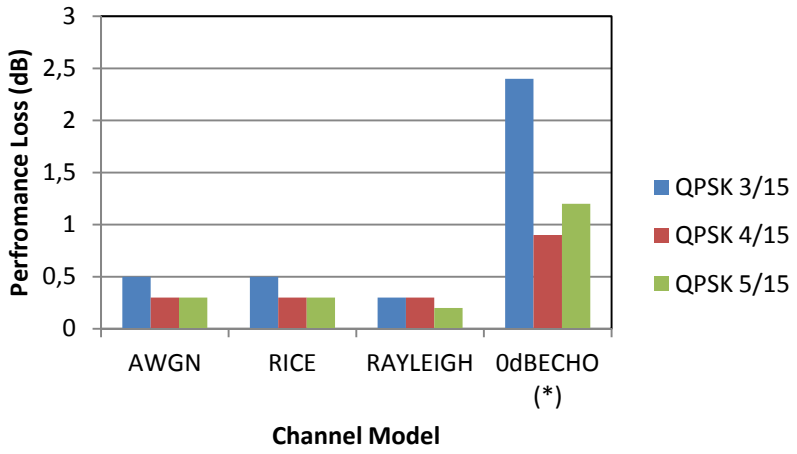

Figure 6.16. Performance loss in laboratory HW trials, when compared with computer simulations.

The first important outcome is that, for each configuration, it can be clearly seen how the performance penalty remains constant for all the different stationary channels. This means that the implemented channel estimation on the SDR is accurate enough to deal with rich multipath channels without additional degradation. Furthermore, it can also be seen how the penalty decreases when the code rate increases. This behavior is due to the challenge of estimating the actual noise power in the received constellation. This value will be one of the critical components of the LLR calculation for the LDPC decoding. The lower the code rate, the higher the theoretical SNR threshold and therefore, the easier is to give an accurate estimation of the AWGN power. Finally, as expected the most problematic case is the modified 0dBEcho. The QPSK,CR=3/15 offers by far the worst performance with a degradation of about 2.4. Behind this behaviour lies the fact that the SDR receiver is not able to perform the carrier recovery for such noisy channels.

3.2.2 Mobile Channels

Following the defined methodology, in TABLE 6.20 the obtained results for the presented configurations under mobile channels are summarized. The receiver mobility is represented by a TU-6 channel, whose maximum Doppler may range from 5 Hz (handheld devices) to 100 Hz (motorway).

TABLE 6.20. Single layer thresholds for mobile channels.

		f_d=5 Hz		f_d =50 Hz		f_d =75 Hz		f_d =100 Hz	
		Sim.	*Lab.*	*Sim.*	*Lab.*	*Sim.*	*Lab.*	*Sim.*	*Lab.*
QPSK	**3/15**	-1.6	-1.4	-1.5	-1.0	-1.7	-1.2	-1.5	0.0
	4/15	-0.3	-0.2	-0.4	0.0	-0.2	1.2	0.4	2.4
	5/15	0.9	1.2	1	1.4	1.2	3.0	1.6	6

It is important to note how when the FEC is robust enough (CR=3/15), the difference between computer simulations (Phase 2) and laboratory trials (Phase 3) is smaller. In particular, it is lower than 1.5 dB for the worst case. In addition, for those robust configuration the different between the maximum speed and minimum mobility case is also lower than 1.5 dB, meaning that the receiver can work with large FFT sizes over mobile channels. Nevertheless, it must also be noted that for the less robust case (CR=5/15) this value can increase up to 4.4 dB. This is an expected result, as it has been seen before: the more robust the system it is, the less it is affected by the ICI. Furthermore, the channel estimation penalty is very high with about 4.4 dB for the worst case.

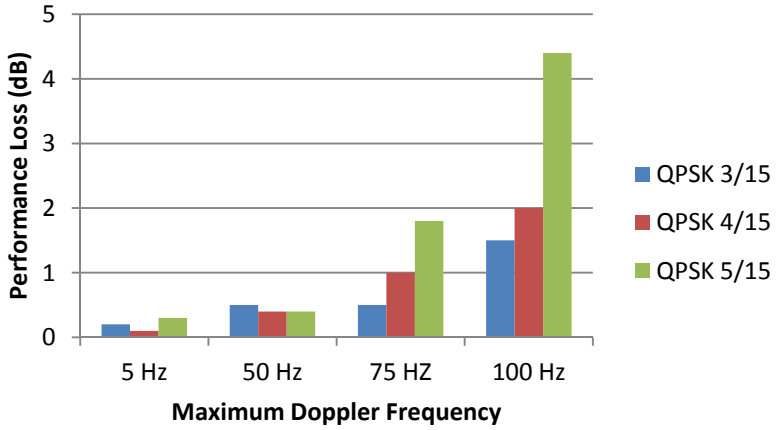

Figure 6.17. Performance loss in laboratory HW trials, when compared with computer simulations for time-varying channels.

Finally, a graphical comparison between computer simulation and laboratory trials is depicted in Figure 6.17. It is shown how while the degradation increases exponentially with the channel maximum Doppler frequency value. Among other

things, this is due to the problems to perform accurate channel estimation, plus the carrier recovery issues. One possible solution for reducing the channel estimation penalty could be to increase the OFDM pilot carriers boosting.

3.3 **Layered Division Multiplexing**

After the single layer analysis, the second step in this third phase of the EVP platform is to test the LDM proposal when there is hardware equipment involved. As an iterative process, and based on the previous results, the candidate configurations for the upper layer have been reduce to the QPSK modulation with the two more robust code rates of {3,4/15}, which will offer throughputs of 1.87 and 2.51 Mbps respectively. The reduction is based on the preliminary condition of having a negative SNR for the upper layer over most challenging channels.

As for the lower layer, the same configurations presented in phase two (computer based simulations) are considered. It is important to note that for the laboratory trials the 0dB Echo channel has been modified once again, in order to reduce the performance degradation related to the sync problem, which this is not an specific issue of the LDM proposal.

3.3.1 Stationary Channels

The first step is to compare the results obtained in the laboratory with the simulation tables presented before. The purpose is to identify the LDM HW degradation and compare it with the single layer case. In order to do that, TABLE 6.21 gathers the obtained receiving thresholds for the proposed HW set up for stationary channels and draws a compilation with computer simulations. As the lower layer performance is independent from the upper layer configuration, their receiving thresholds have been averaged for different upper layer configurations. With the purpose of completing the analysis, the rest of the values for the -5 dB case are calculated in TABLE 6.22.

TABLE 6.21. Stationary channels: receiving thresholds for LDM services (injection range -4 dB). Simulations with real channel estimation and laboratory trials.

			AWGN		RICE		Rayleigh		0dBECHO(*)	
			Sim.	*Lab*	*Sim.*	*Lab*	*Sim.*	*Lab*	*Sim.*	*Lab*
UL	**QPSK**	**3/15**	-1.9	-1.6	-1.7	-1.4	-0.6	-0.4	-0.5	2.0
	QPSK	**4/15**	-0.2	0.2	0.1	0.4	1.5	1.8	1.7	3.4
LL	**16QAM**	**3/4**	15.7	16.0	16.2	16.4	19.4	19.6	19.4	20.4
	64QAM	**2/3**	19.2	19.6	19.6	19.8	22.1	22.4	22.5	23.8
	256QAM	**2/3**	23.7	24.2	23.9	24.8	26.3	27.2	27.0	28.4

TABLE 6.22. Stationary channels: receiving thresholds for LDM services (injection range -5 dB). Simulations with real channel estimation and laboratory trials.

			AWGN		RICE		Rayleigh		0dBECHO(*)	
			Sim.	*Lab*	*Sim.*	*Lab*	*Sim.*	*Lab*	*Sim.*	*Lab*
UL	**QPSK**	**3/15**	-2.3	-1.8	-2.1	-1.8	-1.1	-1.0	-0.7	1.4
	QPSK	**4/15**	-0.7	-0.4	-0.4	0.0	0.9	1.2	1.1	2.4
LL	**16QAM**	**3/4**	16.5	16.6	17.0	17.2	20.1	20.4	20.2	21.0
	64QAM	**2/3**	20.0	20.4	20.4	20.8	22.8	23.0	23.2	24.0
	256QAM	**2/3**	24.2	25.0	24.6	25.6	27.0	28.0	27.7	29.2

In the phase 2 it has also been demonstrated that the channel estimation loss is not related with the injection range, and therefore, in the summary chart of Figure 6.18 the differences for each injection range and realization have been averaged. The picture is clear, broadly speaking, the performance loss due to HW implementation (LAB measurements) is always smaller than 0.5 for most the cases and just 0.8 dB for the worst Rayleigh channel, when compared with computer based simulations.

It can be seen that for the upper layer case (QPSK {3,4}/15) the performance loss is higher for the first combination, and in the legacy system case, the (256-QAM,CR=2/3) combination shows the highest degradation. The main reason is that, as in the single layer case, the implemented SDR receiver has some difficulties in estimating the actual noise power for the LLR calculation. Obviously, this task is tougher when the modulation is high and the code rate is low. Apart from that, as in the SL case, the modified 0dBECHO (*) is the most challenging channel. In this

case, the worst performance is for the QPSK,CR=3/15 case, where the degradation increases up to 2.3 dB. For the rest of the channels, the threshold increase is reduced to less than 0.5 dB. The most probable reason for that behaviour is the receiver difficulty to sync in a single echo channels with such a noisy environment.

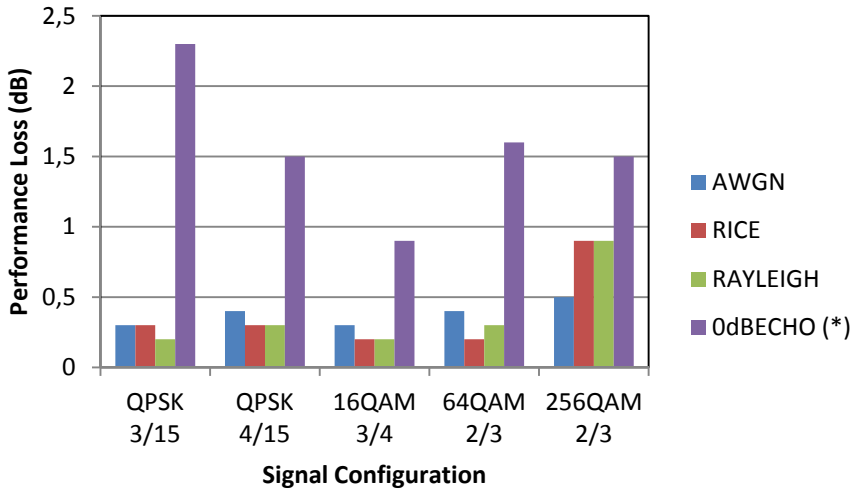

Figure 6.18. Performance loss average for LDM HW LAB trials on stationary channels.

Finally, it should also be taken into account that the SDR receiver does not include a time averaging window for reducing the channel estimation error floor. Furthermore, there may also be a small penalty for the carrier recovery and digitalization process. Overall, it can be stated that the developed SDR receiver shows quite impressive results.

3.3.2 Mobile Channels

Computer simulations have shown that the mobile layer reception when LDM multiplexing technique is employed is perfectly feasible. Furthermore, it has been proved that even if there is HW involved, the degradation of the different services over stationary channels is less than 2.5 dB for the single layer case. Eventually, the last step is to test the mobile layer performance for LDM signals when real HW equipment is involved.

TABLE 6.22 and TABLE 6.23 gather the obtained results for two of the most used configurations. The first one provides the implementation loss for the most robust combinations with a -4 dB injection range, whereas the second one tries to offer a capacity gain (including -5 dB injection range value).

TABLE 6.23. Mobile channels: receiving thresholds for LDM services (injection range -4dB). Simulations with real channel estimation and laboratory trials.

		f_d=5 Hz		**f_d =50 Hz**		**f_d =75 Hz**		**f_d =100 Hz**	
		Sim.	*Lab.*	*Sim.*	*Lab.*	*Sim.*	*Lab.*	*Sim.*	*Lab.*
QPSK	**3/15**	0.7	1.0	0.7	1.4	0.9	1.6	1.3	3.6
QPSK	**4/15**	2.7	3.0	3.4	3.8	3.4	5.2	3.7	7.0

TABLE 6.24. Mobile channels: receiving thresholds for LDM services (injection range -5dB). Simulations with real channel estimation and laboratory trials.

		f_d=5 Hz		**f_d =50 Hz**		**f_d =75 Hz**		**f_d =100 Hz**	
		Sim.	*Lab.*	*Sim.*	*Lab.*	*Sim.*	*Lab.*	*Sim.*	*Lab.*
QPSK	**3/15**	0.6	0.8	0.5	1.0	0.5	1.6	0.8	3.8
QPSK	**4/15**	2.1	2.2	2.3	3.6	2.4	4.0	2.8	6.2

It can be seen how the performance degradation increases even exponentially with the maximum Doppler Frequency due to the increase of the ICI noise. Furthermore, as always, it must be noted that the loss is lower for the {3/15} code rate, mainly because of the power difference between the existing AGWN and the Doppler noise.

Finally, Figure 6.19 depicts the averaged performance loss for each upper layer configuration over each maximum Doppler frequency and both injection ranges. As expected the loss increases with the receiver speed, and what is more, the less robust configurations show the highest dB loss. In the 100 Hz case the channel variations are very fast, and thus, the degradation increase may be reduced if the time interpolation is disabled within the channel estimation problem. These modifications of the actual SDR algorithms are very interesting research topics for the future research.

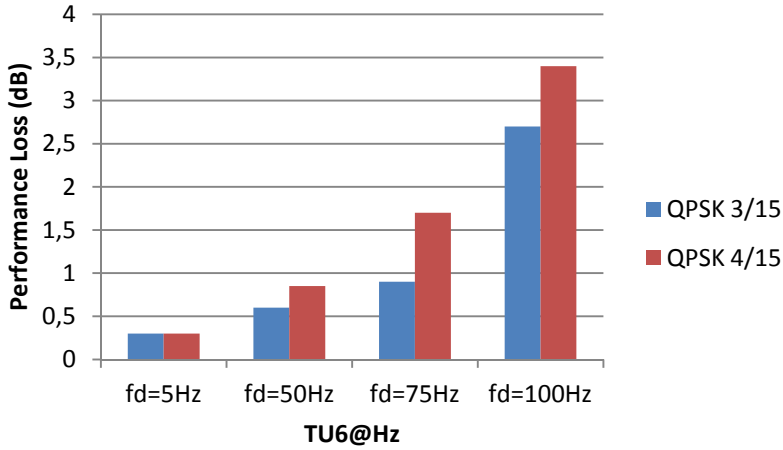

Figure 6.19. Performance loss after LDM multiplexing for mobile layer under TU-6 channel.

4. FIELD TESTS: ENBIDO PROJECT

Eventually, as the final phase of the presented validation process, a couple short field trials have been carried out. The main objective of these field trials has been to prove the feasibility of the layered division multiplexing technique under real world conditions. Therefore, these field tests were not intended to analyse all the existing configurations, but to validate this new technique over real scenarios. That is the reason why these LDM measurement campaigns were in reality field tests with short term predefined targets. The first campaign was carried out in 2013, whereas the last two took place in 2014.

ENBIDO project is a co-operative effort of the University of the Basque Country, the network operator ITELAZPI and several companies (MIER, BTESA and dualStream) to lead the possible introduction of new generation terrestrial broadcasting systems in the Basque Country. The main objectives of this collaboration are:

- Breaking ground research in broadcasting technologies.
- Future deployment of new broadcasting systems in the Basque Country
- Possible built of a test bench for equipment manufacturers.

The overall project was divided into three different work packages. The first one, WP1, was based on planning and setups, whereas the second one was focused on the field trials. Finally, there was a last WP, which consisted in preparing the possible result dissemination.

4.1 Transmission Infrastructure

Regarding the infrastructure, signals were broadcasted using the transmitter site of Banderas, which is located on a hill of about 216 meters high and 3 km far from the city centre of Bilbao (See Figure 6.19). The main characteristics of the transmission station are gathered in TABLE 6.25. The selected RF frequency was 690 MHz (channel 48), one of the free mobile channels available in the surrounding spectrum. The antenna is 48 meters high, which is sufficient to overcome the main obstacles of the environment, and the maximum ERP is 5 kW.

TABLE 6.25. Transmitter center main characteristics.

Name	Bilbao-BANDERAS
Coordinates	UTM 30T 503862 4791964
Altitude	216 meters
RF Channel	48 (690 MHz)
ERP max.	5000 W
Antenna Height	48 meters
Radiation Pattern	Directive (105º-175º)
Polarization	Vertical

Figure 6.20. Experimental network location.

Prior to anything, preliminary coverage area estimation has been done in order to delimit the boundaries for the mobile campaign. The antenna is radiating towards the center of Bilbao city, and therefore, it is expected that urban scenarios will prevail. Figure 6.21 depicts the obtained results, which show that really good coverage within the whole city is expected.

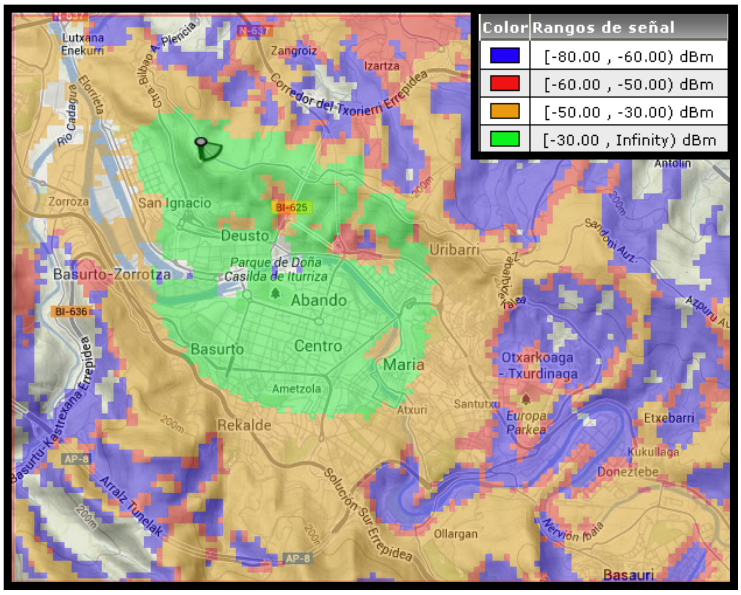

Figure 6.21. Preliminary study of the expected coverage area.

Figure 6.22 shows the transmission set-up used for the measurement campaign. The LDM or SL signals were generated with a SW tool that provided the IQ samples. These samples were generated at IF and up-converted to 690 MHz. The output of the amplified signal was broadcasted with the radiation system. The transmission parameters were remotely controlled from the mobile unit via 3G and a virtual private network (VPN).

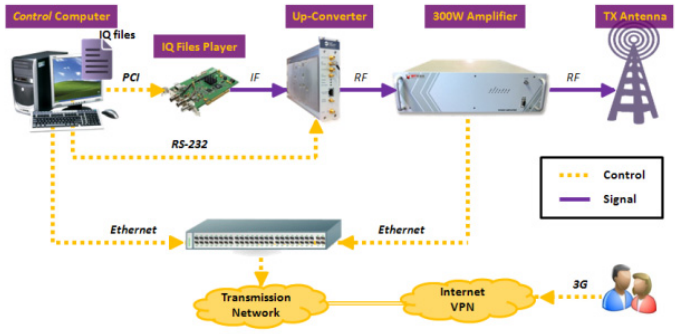

Figure 6.22. Scheme of the transmission process.

4.2 **Reception Infrastructure**

The measurement campaigns were carried out using a mobile unit (a van), property of TSR group, which is specially designed for stationary and mobile field trials (see Figure 6.23). The reception equipment consisted of an IQ signal recorder connected to a tuned antenna. Two types of antennas were used, being both of them connected to a filter for removing possible co-channel interferences. The first one was a directional log-periodic antenna (UHF Yagi, 15.5 dB gain) installed on the 8 meter mast of the measurement vehicle, which, along with an appropriate measurement location selection, led to results applicable to Rice channels (equivalent to roof top antenna reception). The second antenna is a non-active monopole used for mobile measurements, which provided results applicable to mobile and handheld reception.

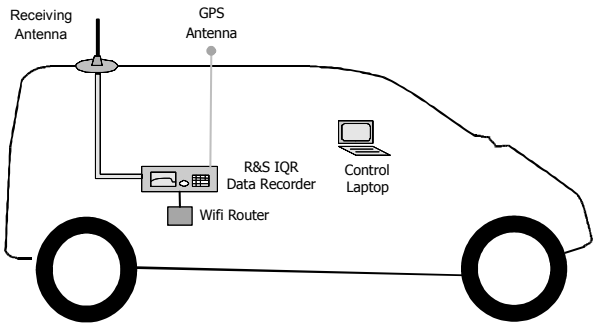

Figure 6.23. Mobile unit equipment graphical description.

In addition, the measurement system also included a GPS system connected to the receiver in order to record the van coordinates and speed. Finally, there is a VSA for recording the different signals. It must be noted that there is not any commercial receivers for LDM signal reception, and therefore, the obtained signals are recorded for posterior off-line laboratory signal demodulation and processing, which provides greater flexibility in order to obtain performance results.

4.3 **Banderas-Bilbao Field Test A**

The main objective of this first campaign was to test the feasibility of the LDM proposal. During this first step, there were some technical solutions that there were not fully deployed. For instance, the {x/15} DVB-T2 like codes were not finished

yet, and that is the main reason why this first configuration is not including them. Furthermore, the deadline for these results was the ATSC Call for Proposals, as they were presented as a physical demonstration of the LDM feasibility. As a matter of fact, these results were finally included as an annex in the CRC, ETRI and UPV/EHU joint proposal for the physical layer [106].

4.3.1 Signal Configuration and Measurement Planning

These first field tests were carried out in Bilbao during summer and autumn 2013. Some of the technical solutions described in this thesis, for instance {x/15} LDPC codes, were not yet available, and that is why different signal configurations were used. The test cases included in this first round of field trials are shown in TABLE 6.26:

TABLE 6.26. Banderas-Bilbao field test A. LDM configuration and associated bit rates.

	Const.	Code Rate	Bit Rate (Mbps)
Upper Layer	**QPSK**	1/4	2.35
Lower Layer	**64-QAM**	2/3	18.24
	256-QAM	2/3	25.25

The rest of the physical waveform parameters remain equal to the whole E&V process. The FFT size was set up to 16K, the guard interval was defined as 1/8, PP2 pilot pattern was used, and injection range was -5 dB. For this first attempt, the field measurements were carried out for stationary reception in urban environments with direct line of sight. At each location, both modes were measured sequentially at 690 MHz. The locations selected for analysing the SNR requirements are labeled in Figure 6.23.

Figure 6.24. Bilbao map with place marks at the measurement locations.

4.3.2 Methodology

As mentioned before, the whole EVP is based on an iterative process, and therefore, for laboratory signal post-processing, the receiver scheme is the same employed in phase 3, which had been already tested.

In order to analyse the system performance, the test methodology consisted on adding different amounts of white noise to the previously recorded signals in order to find BER vs. SNR curves and system thresholds associated to each one of the receiving locations. This process is equivalent to the one presented in phase 3. The only difference is that the UL cancellation and LL decoding is not done in the SDR. Instead, the signal at the equalizer output is fed to the MATLAB chain described in phase 1. It should be considered that, by that time, the whole LDM system was not yet implemented in the SDR receiver.

4.3.3 Results

TABLE 6.26 provides a visual summary of the results for the selected modes, which provide the highest bitrates on the lower layer. The results are obtained from averaging the thresholds obtained for several measurements in the two measurement locations shown in Figure 6.24. The difference with respect to the laboratory results are quite low, less than 2 dB. It should be noted that the carrier to noise ratios for the lower layer component refer to the overall received power.

These results were the first practical demonstration of the LDM technology. As a matter of fact, there were included in the Cloud-Txn proposal [106] presentation as a practical proof of its implementation feasibility. Afterwards,

based on these results and thanks to the EVP iterative structure, the LDM parameter design was changed. New modulation and coding algorithms were selected and tested again in phase 2. Additionally, some other small problems, such as the signalling issues and the carrier recovery difficulties were also detected, and therefore, there had been corrected in the next iteration of the EVP chain.

TABLE 6.27. Banderas-Bilbao field test A. System thresholds for LDM.

	Const.	Code Rate	SNR threshold (dB)
Upper Layer	**QPSK**	1/4	-0.5
Lower Layer	**64-QAM**	2/3	20.8
	256-QAM	2/3	25.3

4.4 Banderas-Bilbao Field Test B

This second field test was carried out in March 2014. By the spring, the new FEC codes for the mobile layer were already included in the SDR receiver, and therefore, it was used to test the mobile layer performance. The main objective of this field test was to evaluate the single layer performance, and show that large sized FFTs can be used for mobile services when the FEC is robust enough.

4.4.1 Signal Configuration and Measurement Planning

The single layer field trials are based on the comparison between different OFDM configuration parameters (FFT and code rates) in order to determine the best choices for a trade-off between capacity and coverage in mobile urban environments. Moreover, another important objective was to prove in the field that large sized FFTs can be used for mobile channels. The main configuration parameters for the selected broadcasting system are shown in TABLE 6.27.

TABLE 6.28. Main transmitted signal configuration parameters.

Configuration	Code Rate	FFT Size
1	3/15	8k
2	3/15	16k
3	3/15	32k

Figure 6.25 shows the main routes followed for these second short field trials. Each colour corresponds to one route.

Figure 6.25. Measured routes at Bilbao field trials.

4.4.2 Methodology

As previously mentioned, for these second field trials the receiver chain varies slightly. As a receiver, a nearly fully working C++ based SDR was used. In fact, by this time, the single layer SDR receiver included the 1 sec bit-based time-interleaver described in Chapter 4. However, even if this time interleaver is not used in the previous EVP phases, the obtained results are very helpful to test the capability of using large FFTs.

In this case, the study is not based on SNR thresholds, but on the actual coverage area. In particular, the main objective is to show that when low code rates are used, large sized FFTs can be used with low power transmissions. Therefore, the methodology consists in measuring the received power, and the correctly decoded signal frames are analyzed in order to find the percentage of correct demodulated frames in the route.

For instance, Figure 6.26 shows the histogram of the received power along the recorded route (route 2 (green) in Figure 6.25) for configuration. The coverage percentage of the route was calculated as the percentage of correctly decoded FEC frames of the received mobile frames.

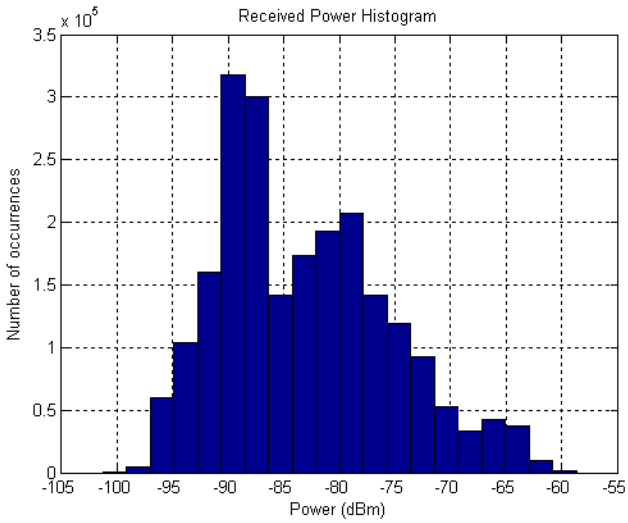

Figure 6.26. Received power histogram.

4.4.2.1 Results

After a brief analysis, it was concluded that the transmitted power is high enough to offer full coverage in all the selected routes. Therefore, after considering that the broadcasted power is too high for obtaining erroneous frames along the urban route measured, AWGN (Additive White Gaussian Noise) was added to the recorded signals in the laboratory in order to simulate lower transmitted power levels. Noise power levels of 20 dB, 30 dB, 33 dB and 36 dB over the system noise floor were added to the received signals in order to simulate 50 W, 5 W, 2.5 W and 1.25 W ERP transmitted powers. Figure 6.27 summarize the percentage of coverage obtained with these simulated transmitted power levels.

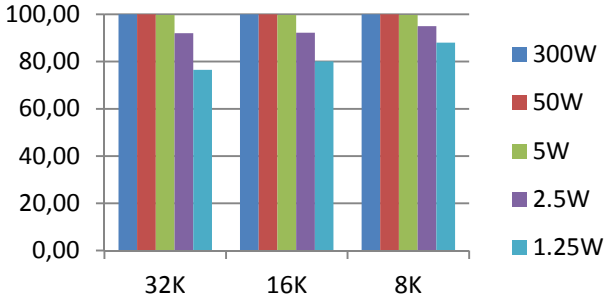

Figure 6.27. Correctly received FEC blocks percentage for CR=3/15 signals.

First of all, broadly speaking, it can be stated that the coverage percentage is clearly reduced with the transmitted power decrease. Nevertheless, this is a general truth, and the fact that the 32K size can be 100% received for 50 W is far more interesting. Furthermore, it seems that, as previously proved theoretically, the ICI noise challenge can be overcome with strong LDPC codes. Nevertheless, these are preliminary results for showing the feasibility of the system, which are based on the location coverage, but without SNR thresholds. In order to obtain them for the different modes, an in depth post processing is needed to evaluate the location coverage and link it to the receiver speed. This topic is considered for further work.

Even if the results are not definitive, they have given very useful information for the EVP iterative process. In particular, they have confirmed that if the Phase 2 selected configurations are strong enough there should not be any problem for the usage of large sized FFTs for mobile services. In addition, they have pointed out that the mobile impact on the carrier recovery is not as critical as expected.

5. LDM LIVE DEMO

Finally, based on all the information and conclusions obtained from the previously presented E&V platform, an LDM live DEMO has been built as a special case of phase 4. This set up must be understood as a small live example of a real time field measurement. The main aim of this DEMO is to show the LDM technology at work for different configuration and scenarios. In fact, this DEMO has been already successfully shown in the IEEE BMSB 2014 international conference and in several ATSC 3.0 meetings for the definition of the new generation broadcasting standard in June and September 2014, respectively.

Figure 6.28 shows the LDM live demo set-up, including a TV set in order to clearly visualize all the information provided by the SDR receiver.

Figure 6.28. Picture of the LDM demo general set-up.

5.1 Demo Structure

As in a real system, the signal is transmitted and received in RF, and moreover, communication is divided into two clear sub-structures: the transmitter and the receiver. The transmitter part is very close to the scheme presented in the lab trials, but with some changes that allow real time transmission of the signal (see Figure 6.29). For instance, instead of the Anritsu VSG, a generic purpose Dektec card is used. This card has a very powerful VHF/UHG modulator, whose output power ranges from -46 dBm to -18 dBm. Its MER is higher than 40dB and the phase less

than -95dBc @ 10Khz, therefore, it is suitable for signals that require high SNR at reception. In addition, the card has also the capability to add extra AWGN or simulate any kind of channel.

Regarding the SW part of the transmitter, it is very similar to the previous one. However, in this case, the computer generated PRBS signals are sampled into IQs using a specific script created for this purpose, instead of the propetary program needed for the Anritsu VSG.

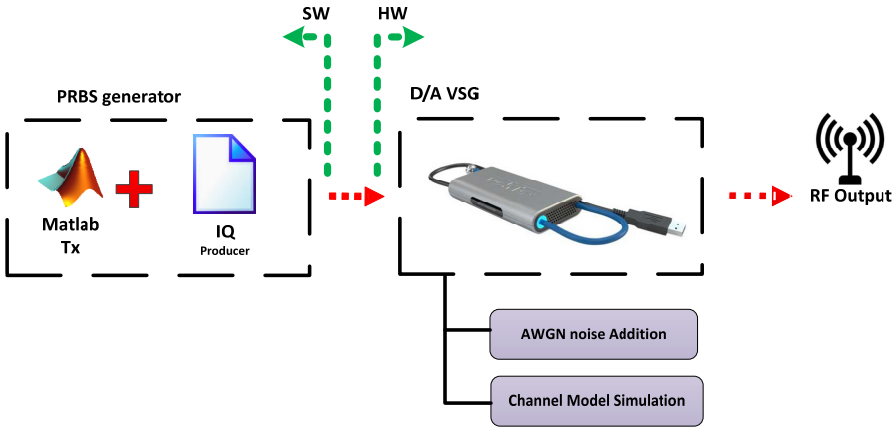

Figure 6.29. Transmitter structure for the LDM live demo.

The receiver set-up is also very similar to the equipment presented in Section 2. Nevertheless, in this case, instead of the Anritsu VSA, the ETTUS Research N20 USRP is used. This card is connected to the SDR LDM receiver through 1GBps ethernet connection (see

Figure 6.29). The generic purpose USRP digitalizer provides high-bandwidth, high-dynamic range processing capability. However, it cannot be said that the receiver is working real time, as it only captures one out of 12 frames due to the delay in the receiver part. However, this live demo is a really useful tool for quasi real time analysis of the LDM signal performance. As a matter of fact, for this live demo, the different configurations presented in the EVP part are included in the communication chain.

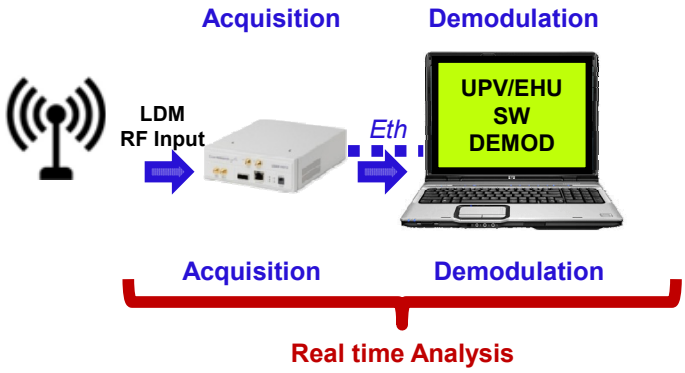

Figure 6.30. Block diagram of the LDM demo receiver structure.

In Figure 6.31 and Figure 6.32, the information provided by the SDR receiver developed by the UPV/EHU is shown. Figure 6.32 is a screen capture of the plotted results. In first place, the receiver shows the different constellations of the LDM signal: the theoretical UL constellation (red), the lower layer constellation (blue) and the multilayer signal constellation (black). In this case, the constellation is very clear due to high SNR conditions. In addition, some visual information related to the channel is also shown, in particular, the channel time impulse response and the overall RF spectrum.

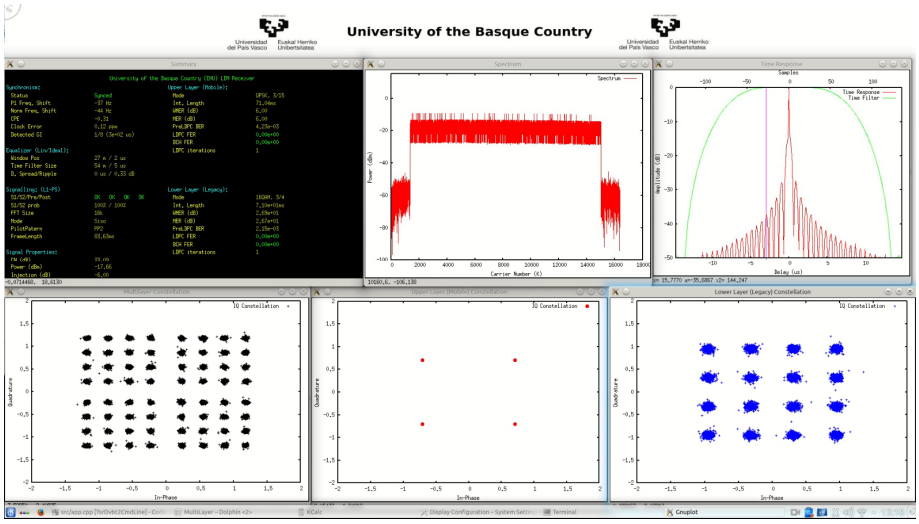

Figure 6.31. LDM SW information window.

Figure 6.32 is an amplified capture of the summary report window (black background) previously depicted. This window gathers all the information that can be extracted from an LDM signal. First of all, it offers the FER output for the upper and lower layers. Furthermore, it also presents the measured MER for each layer and the associated time interleaving length.

Regarding the carrier recovery, measured clock error and Common Phase Error, together with the main frequency shifts, are also indicated. Finally, it also shows the LDM signal parameters and displays if the signalling has been correctly decoded.

Figure 6.32. Summary report window of the SDR receiver.

Overall, this live DEMO is a very powerful tool that allows not only showing the LDM technical solution at work, but also evaluating and understanding its main implications. In particular, all the configuration modes presented in this Chapter have been implemented, and furthermore, apart from -4 dB and -5dB injection ranges, -3 dB and -6 dB have been also tested. Another important feature is that this live demo configuration can be easily updated, and therefore, is the perfect tool for testing the proposed changes in Phase 2 and 3 prior to go to the field. That way, the planning errors that may appear in the field can be previously solved in a controlled environment taking advantage of this Live test bench.

6. SUMMARY

This chapter has presented a complete Evaluation & Validation Platform for studying the feasibility and the performance of the newly proposed LDM multiplexing technique. The comprehensive analyse has ranged from the most theoretical mathematical formulation to the most practical field trials.

The first important contribution has been the validation of the theoretical models presented in Chapter 5. Nevertheless, a small extra degradation has been identified for the UL performance over very-scattered channels, probably due to a problem with the LLR calculation. This topic has been classified as a very interesting topic for the future work. Furthermore, it has been also proved that the large sized FFT are perfectly suitable for the mobile environments with maximum Doppler Frequencies up to 100 Hz, which is equivalent to 115km/h at a RF channel centered at 690 MHz.

Finally, it has been also demonstrated that the real implementation losses for LDM, when HW equipment is involved, are less than 2 dB for most stationary cases, which is within the impairment margin defined by most organizations. In the mobile channels, it strongly depends on the implemented configuration; the more robust the signal is the less it is affected. What is more, it has been shown that the LDM HW degradation is the same as SL case for both stationary and mobile channels. Therefore, it is expected that the 4dB or 5 dB gain obtained in Chapter 4 and 5 when compared with TDM/FDM, will be maintained for real implementations.

In short, LDM technology is a very promising alternative for simultaneously transmitting stationary and mobile services, whereas the mobile services are enhanced and the spectrum efficiency increased.

Number rules the universe.

-Phytagoras

CHAPTER 7: **CONTRIBUTIONS AND FURTHER WORK**

In this chapter, the main contributions of this work are gathered, the obtained results dissemination is presented, and finally, several research lines for future work are described.

1. CONTRIBUTIONS

The driving force for this work is the willing to contribute to the broadcasting standards of the future. In particular, this thesis is focused on solving two of the main historical issues of the digital television broadcasting, which in turn are two of the main objectives of this work: spectrum efficiency and mobile service delivery. As a matter of fact, the first part of the work has mainly dealt with the analysis of the current alternatives for offering mobile services, whereas the second part has been devoted to find new alternatives to improve the spectrum efficiency.

More precisely, the contributions of this work can be described according to the objectives defined in Chapter 1:

1.1 Study of mobile broadcasting reception

The second and third chapters of this work have included an assessment of technical requirements and research of possible solutions to provide better mobile services using the current broadcasting systems. In order to do that, firstly the physical bases of the time-varying channels have been presented, including a detailed mathematical development of the related Doppler Effect and inter-carrier interference noise. This theoretical work has been a fundamental part of the thesis as it has been where the foundations for all the solutions proposed later are laid.

As a first step, the doubly dispersive equalization techniques have been studied in Chapter 2. As a result, a new equalization algorithm has been proposed in Chapter 3, which improves the performance of the existing techniques in terms of the required minimum BER for QEF reception. In TABLE 7.1, the SNR receiving thresholds for the proposed hybrid equalizer and the best performing of the analyzed algorithms are compared for uncoded data streams.

TABLE 7.1. SNR thresholds for TU-6 channel with ideal and real channel estimation (required SNR to achieve BER=1x10^{-4}).

	TU-6($f_d \cdot T_U$=0.1)	
	Ideal	**Real**
MMSE-SIC	34 dB	35 dB
Proposed	29 dB	31 dB

1.2 Proposal of an alternative approach for improving the efficiency of mobile reception

In the final part of Chapter 2 and in Chapter 3, after analyzing the existing solutions for improving the ICI penalty, the major contribution has been to present a new approach for improving the receiver implementation efficiency over mobile scenarios. In particular, it has been demonstrated that even if the implementation of complex bi-dimensional equalization and channel estimation algorithms can offer significant gains for time-varying channels, the attached complexity does not worth it when channel codification is involved under very noisy channels. TABLE 7.2 shows the comparison between the proposed equalization algorithm and the one-dimension tap equalizer. It can be seen that for low code rates there is no gain, whereas the difference may increase up to 0.5 dB for less protected codes.

TABLE 7.2. SNR thresholds for TU-6 channel with LDPC coding included (required SNR to achieve BER=$1x10^{-4}$).

	TU-6($f_d \cdot T_U$=0.1)	
	CR=1/3	**CR=5/6**
1D	0.3 dB	10.5 dB
Proposed	0.3 dB	10.0 dB

In short, it has been demonstrated that, under low SNR conditions and when data is properly coded, there is no gain in using this kind of complex signal processing algorithms. Therefore, a new proposal to deal with mobile reception has been studied. As matter of fact, after a theoretical study of the ICI impact on the receiver performance over time-varying channels, it has been proved that a broadcasted signal can perfectly cope with the Doppler Effect if the FEC is robust enough. In other words, in order to be able to be received anywhere, the mobile signals should be so robust that the Doppler noise is masked under the existing Gaussian noise. Thus, the proposed new approach is based on employing one dimensional algorithms at the receiver and entrusting the ICI removing task to the FEC codes.

Figure 7.1 depicts a small representation of the theory behind the proposed alternative for dealing with LTV channels. ICI powers for 8k, 16k and 32k FFT sizes have been plotted, over three different use cases ranging from 90 km/h to 180 km/h. When the transmitted signal is protected with high code rates, the

working SNR is very low and the tolerable Gaussian noise is so high that the Doppler noise is masked, and thus, its influence is either small or negligible.

This conclusion leads to another contribution of this thesis. Based on the robustness of new FEC codes, it has been shown that large sized FFTs can be used for delivering mobile services, which might be directly applied to increase the spectral efficiency of broadcasting services.

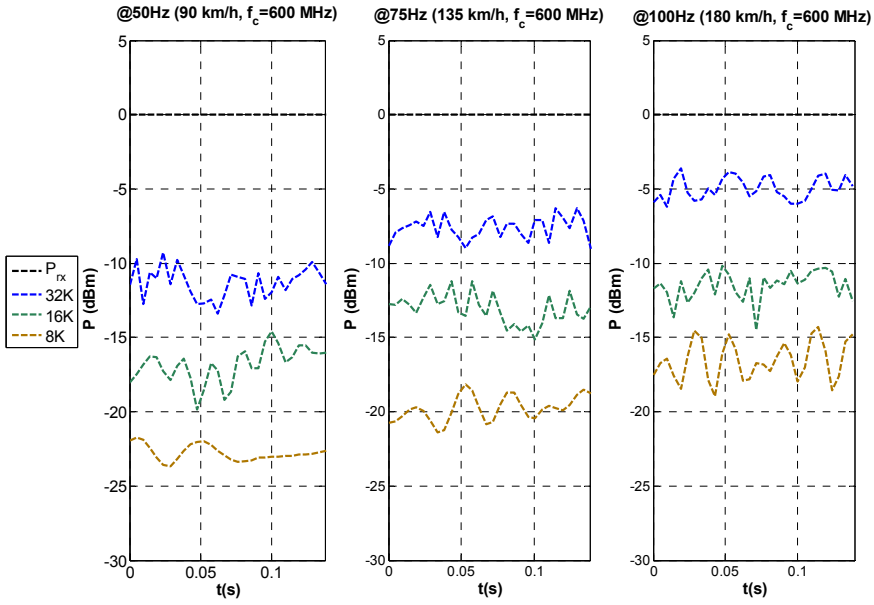

Figure 7.1. Doppler Noise and AWGN relation over very noisy channels.

1.3 **Proposal of a more spectrum-efficient and flexible solution for offering simultaneously stationary and fixed services**

The main contribution of this part of the work (Chapters 4, 5 and 6) has been to present a more spectrum-efficient technique for multiplexing stationary and mobile services. In particular, a comprehensive study and validation of the Layered Division Multiplexing (LDM) technique has been presented: a new proposal for delivering robust mobile and stationary fixed services over the same RF channel.

In short, this spectrum overlay technology is used to simultaneously transmit multiple program streams with different robustness for several services in one RF channel. It has been proved that a multi-layer system makes a more efficient and

flexible use of the spectrum, as each layer fully uses the entire RF channel bandwidth. The upper layer will normally be targeted for robust low SNR mobile services and robust stationary service with large coverage, whereas the lower layer would be best suited for high SNR, high data rate services.

Theoretical calculations have demonstrated that a combination of LDM and DVB-T2 can outperform a TDM scheme (DVB-T2+NGH). In a TDM scenario, it seems reasonable that a maximum of 50% of the resources (time) would be allocated to the mobile carrier, whereas in the LDM approach there is no restriction for the mobile/fixed power allocation ratio. The gain can be understood as a reduction of the required power for an error-free reception or as a capacity increase using the same transmission power. In particular 4 dB to 6 dB gain can be obtained for the mobile service when compared with TDM/FDM, whereas the stationary service threshold is maintained. Thus, the main advantages of the Layer Division Multiplexing are spectrum efficiency and flexibility. All layers transmit information simultaneously using 100% of the time and 100% of the RF bandwidth. It has better time and spectrum diversity to achieve higher aggregated data rate and better flexibility on robustness and data throughput on different transmission layers. TABLE 7.3 provides a comparison of several configuration modes for TDM and LDM systems, based on the results obtained in Chapter 6. In short, it can be seen how LDM shows the best trade-off for multiplexing different services. In fact, in a TDM system the mobile service is strongly penalized when the system offers high capacity stationary services.

TABLE 7.3. LDM vs TDM SNR comparison for different bit rates.

LDM		**NGH 50% Time**		**NGH 33.3% Time**		**NGH 25% Time**	
Data Rate	**SNR**	**Data Rate**	**SNR**	**Data Rate**	**SNR**	**Data Rate**	**SNR**
1.87 Mbps QPSK 3/15	-2.1	1.89 Mbps QPSK 2/5	-0.2	2.08 Mbps QPSK 2/3	3.3	1.75 Mbps QPSK 11/15	4.3
Lower layer with -4 dB injection		**DVB-T2 50% Time**		**DVB-T2 66.7%Time**		**DVB-T2 75% Time**	
14.21 Mbps 16QAM 3/4	15.5	14.21 Mbps 256QAM 3/4	20.0	14.43 Mbps 64QAM 3/4	15.1	14.18 Mbps 256QAM 1/2	13.2
18.24 Mbps 64QAM 2/3	18.9	-	N.A.	19.24 Mbps 256QAM 3/4	20.0	18.94 Mbps 256QAM 2/3	17.7
25.25 Mbps 256QAM 2/3	23.2	-	N.A.	-	N.A	20.52 Mbps 256QAM 5/6	22.0

Apart from the theoretical analysis of the best solution for the simultaneous delivery of stationary and mobile services, another contribution of this work has been the more practical approach presented in Chapter 6. The validation process has included three different practical set ups that work as an assembly line: first, a

simulation platform, second, a HW based laboratory set up, and finally, a whole transmission and reception infrastructure for carrying out field trials. This way, the whole performance of the newly proposed technique has been tested in this work, from the very theoretical point of view to the more practical field trials. The results have shown that the presented LDM multiplexing technique is a proper solution, which outperforms the previously existing TDM and FDM techniques. Moreover, it has also been demonstrated that the performance loss due to hardware implementation is comparable to the current TDM based receivers. In conclusion, the feasibility of the proposed frequency domain technique has been fully validated. Apart from the theoretical studies, another important contribution is that for this work the first LDM transmitter and receiver have been developed.

Finally, it should be noted that, apart from the technical contributions described above, another remarkable achievement of this work has been to participate in one of the proposals for the ATSC physical layer, which in fact is in its way to become part of the future ATSC 3.0 standard. In addition, this work has also contributed to the DVB TM-T Study Mission Group (SMR), where it is being considered as a very promising technology for future broadcasting developments.

2. DISSEMINATION

2.1 International Journals

Title: "Large Sized FFTs over Time Varying Channels"
Authors: Montalban, J.; Velez, M.; Angulo, I; Angueira, P.; Wu, Y.
Publication: IEE Electronics Letters, vol.50, no.15, pp.1102-1103.
Date: July 2014
Contributions: This paper proves that is feasible to use large size FFTs for time-varying channels. Furthermore, there is also presented a theoretical estimation for quantifying the loss due to the ICI.

Title: "Cloud Transmission: System Performance and Application Scenarios"
Authors: Montalban, J.; Zhang, L.; Gil, U.; Wu, Y.; Angulo, I.; Salehian, K.; Park, S. I. Rong, B.; Li, W.; Kim, H.M.; Angueira, P.; Velez, M.
Publication: IEEE Transactions on Broadcasting, vol. 60, no. 2, pp. 170-184.
Date: March 2014
Contributions: This paper presents the first theoretical analysis and performance results for the Cloud-Txn concept and the LDM multiplexing technique that grew from it.

Title: "Empirical Doppler Characterization of Signals Scattered by Wind Turbines in the UHF Band under Near Field Condition"
Authors: Angulo, I.; Montalban, J.; Cañizo, J.; Wu, Y.; de la Vega; D.; Guerra, D.; Angueira, P.
Publication: International Journal of Antennas and Propagation
Date: March 2013
Contributions: This paper characterizes empirical Doppler spectra obtained from real samples of signals scattered by wind turbines with rotating blades under near field condition. The theoretical descriptions given in the first three chapters of this work were an important contribution to this research work.

Title: "A measurement-Based Multipath Channel Model for Signal Propagation in Presence of Wind Farms in the UHF Band"
Authors: Angulo, I.; Montalban, J.; Cañizo, J.; Wu, Y.; de la Vega; D.; Guerra, D.; Angueira, P.

Publication: IEEE Transactions on Communications, vol. 61, no. 11, pp. 4788-4798.

Date: January 2013

Contributions: This paper presents a complete Tapped Delay Line (TDL) channel model to characterize multipath propagation in presence of a wind farm, including novel scattering modeling and Doppler spectra characterization. The theoretical descriptions given in the first three chapters of this work were an important contribution to this research work.

2.2 International Conferences

Title: "On Approaching to Generic Channel Equalization techniques for OFDM based Systems in Time Variant Channels"

Authors: Montalban, J.; Velez, M.M.; Prieto, G.; Eizmendi, I.; Berjon-Eriz, G.; Ordiales, J.L.

Conference: IEEE International Symposium on Broadband Multimedia Systems and Broadcasting (BMSB)

Date: June 2011

Place: Germany

Contributions: In this paper, the main objective was to prove that the most known equalization algorithms for OFDM signals in time variant channels with mobile reception scenarios were part of a generic theoretical model.

Title: "Platform for advanced DVB-T2 system performance measurement"

Authors: Prieto, G; Ansorregui, D.; Regueiro, C.; Montalban, J.; Eizmendi, I.; Velez, M.

Conference: IEEE International Symposium on Broadband Multimedia Systems and Broadcasting (BMSB)

Date: June 2013

Place: UK

Contributions: This paper presents a platform for carrying out advanced DVB-T2 system performance measurements in a flexible way. The platform is based on a software receiver with a boosted performance achieved by using both cluster computing and GPU processing. The simulations performed in this thesis helped the validation of the receiver.

Other Comments: Best Paper Award.

Title: "Cloud Transmission Frequency Domain Cancellation"
Authors: Montalban, J.; Bo Rong; Yiyan Wu; Liang Zhang; Angueira, P.; Velez, M.
Conference: IEEE International Symposium on Broadband Multimedia Systems and Broadcasting (BMSB)
Date: June 2013
Place: UK
Contributions: The contribution of this paper was to explain and justify the spectrum overlay technology and corresponding main frequency domain cancellation techniques.

Title: "Cloud Transmission: System Simulation and Performance Analysis"
Authors: Montalban, J.; Bo Rong; Sung Ik Park; Yiyan Wu; Jeongchang Kim; Heung Mook Kim; Liang Zhang; Nadeau, C.; Lafleche, S.; Angueira, P.; Velez, M.
Conference: IEEE International Symposium on Broadband Multimedia Systems and Broadcasting (BMSB)
Date: June 2013
Place: UK
Contributions: The main contribution of this work has been to demonstrate that the proposed Cloud-Txn system and meets the future needs of the broadcasting industry.

Title: "Channel capacity distribution of Layer-Division-Multiplexing system for next generation digital broadcasting transmission"
Authors: Zhang, L.; Wu, Y. ; Heung Mook, K. ;Park, SI; Angueira, P.; Montalban, J; Velez, M.
Conference: IEEE International Symposium on Broadband Multimedia Systems and Broadcasting (BMSB)
Date: June 2014
Place: China
Contributions: This paper presents a fundamental analysis on the channel capacity allocation among the different layers of a LDM-based transmission system. The theoretical study presented on this work was used partially in this paper.

Other Comments: Best Paper Award.

Title: "Error Propagation in the Cancellation Stage for a Multi-Layer Signal Reception"

Authors: Montalban, J.; Angulo, I. ; Velez, M. ; Angueira, P. ; Regueiro, C. ; Yiyan Wu ; Liang Zhang ; Wei Li.

Conference: IEEE International Symposium on Broadband Multimedia Systems and Broadcasting (BMSB)

Date: June 2014

Place: China

Contributions: The paper analyzes the possible error propagation due to the cancellation stage and the corresponding impact on the layers performance.

2.3 International Consortiums for Regulation and Standardization

Title: "A Joint Proposal by Communications Research Centre (CRC), Canada, and Electronics and Telecommunications Research Institute (ETRI), Korea, to the ATSC 3.0 PHY Layer CfP"

Organism: Advanced Television Systems Committee, ATSC

Date: September 2013

Contributions: In the last part of this proposal there have been included several HW laboratory tests and field measurements results carried by the University of the Basque Country. This practical validation of the LDM proposal has been a fundamental step for the understanding of this new promising concept.

Title: "DVB Technical Module MIMO Study Mission Report"

Organism: Digital Video Broadcasting, DVB.

Date May 2014

Contributions: This technical report of the DVB community looks for new techniques, which have the potential to be included in the next generation broadcasting standards. The University of the Basque country has included in the study the LDM proposal. What is more, during the TM 98 meeting a comprehensive tutorial about LDM has been presented in the Technical Module.

---

3. FUTURE WORK

Taking into account the contributions and results presented in this work, the following step should be directed to complete the remaining open questions and breaking ground research lines that have already appeared:

- The theoretical Doppler analysis should be extended to other channel models such as PI, PO or the MR. The inclusion of additional channel models will lead to a more complete picture of the influence of time-varying channels on OFDM receiver.
- Analyze in depth the concept behind direct decoding of the lower layer demodulation mentioned in Chapter 4. It must be studied as a chance for deploying low complexity LDM receivers, where the cancellation stage is not required anymore.
- Extend the LDM/TDM/FDM theoretical capacity comparison to other channels such as RAYLEIGH. It is expected that the difference in rich multi-scattered environments will be higher.
- Develop the 2D FEC product code bit time interleaver and study the possibilities for its inclusion in the LDM system.
- Increase the multiplexing capabilities of the LDM multiplexing technique adding multiple PLPs to the legacy layer. In this case, the implications in the time interleaver module should be carefully studied.
- Gain a Deep insight into the distortion detected in the UL signal, probably due to a mismatch in the LLR calculation when LDM is used.
- Carry out a more complete field trials and a posteriori comprehensive analysis of the LDM configurations presented in this thesis.
- Build a hardware prototype of the already existing LDM receiver.

If I have seen further it is by standing on the shoulders of giants.

-Isaac Newton

REFERENCES AND GLOSSARY

REFERENCES

[1] "The world in 2011: ICT facts and figures," tech. rep., International Telecommunication Union (ITU), October 2011.

[2] Rancy, F.; Zilles, E.; Guitot, J.-J., "Transition to digital TV and digital dividend," Telecommunication in Modern Satellite Cable and Broadcasting Services (TELSIKS), 2011 10th International Conference on, vol.1, no., pp.13-20, 5-8 Oct. 2011.

[3] Final acts of the World Radiocommunication Conference 2007 (WRC-07), ITU, 2007.

[4] Final acts of the World Radiocommunication Conference 2012 (WRC-12), ITU, 2012.

[5] Digital Video Broadcasting, Next Generation System to Handheld, Physical Layer Specification (DVB-NGH), DVB, Nov. 2012

[6] ATSC Technology Group 3.0, "Call for Proposals for ATSC 3.0 Physical Layer", March 26, 2013.

[7] "A Global Approach to the future of Terrestrial Television Broadcasting," Future of Broadcast Television Summit, Nov. 10-11, 2011, Shanghai, China.

[8] J.H. Udelson, The Great Television Race: A History of the American Television Industry. University of Alabama Press, 1982.

[9] "Report and order of Federal Communications Commission," Washington, DC, FCC Doc. 53-1663, Dec. 17, 1953.

[10] M.S. Alencar, Digital TV Systems. Cambridge University Press, 2009.

[11] Yiyan Wu; Hirakawa, S.; Reimers, U.H.; Whitaker, J., "Overview of Digital Television Development Worldwide," Proceedings of the IEEE , vol.94, no.1, pp. 8-21, Jan. 2006

[12] Y. Ninomiya, "The Japanese scene," IEEE Spectr., vol. 32, no. 4, pp. 54–57, Apr. 1995.

[13] T. Fujio, "High definition television," NHK Tech. Monograph 32, Jun. 1982.

[14] B. Fox, "The digital dawn in Europe [HDTV]," IEEE Spectr., vol.32, no. 4, pp. 50–53, Apr. 1995.

[15] R. J. G. Ellis, The PALplus Story. Manchester, U.K.: Architects' Publishing Partnership Ltd., 1997.

[16] M. A. Isnardi, T. Smith, and B. J. Roeder, "Decoding issues in the ACTV system," IEEE Trans. Consum. Electron., vol. 34, no. 1, pp. 111–120, Feb. 1988.

[17] "ETSI EN 300 744 V1.5.1", Digital Video Broadcasting (DVB): Framing, channel coding and modulation for digital terrestrial television, 2004.

[18] Advanced Television System Committee, A/53: ATSC Digital Television Standard, 2011.

[19] Association of Radio Industries and Business (ARIB), Japan, "Terrestrial Integrated Services Digital Broadcasting (ISDB-T) - Specification of channel coding, framing structure and modulation," September 1998.

[20] "The world in 2013, facts and figures", International Telecommunication Union.

[21] Yiyan Wu; Pliszka, E.; Caron, B.; Bouchard, P.; Chouinard, G., "Comparison of terrestrial DTV transmission systems: the ATSC 8-VSB, the DVB-T COFDM, and the ISDB-T BST-OFDM," Broadcasting, IEEE Transactions on , vol.46, no.2, pp.101-113, Jun 2000.

[22] "Mobile Video User Forecast by Region", Gatner, February 2012.

[23] China Standard for Radio Film and Television Industry, "Framing Structure, Channel Coding and Modulation for Digital Television Terrestrial Broadcasting System," 2006.

[24] J. Song, Z. Yang, L. Yang, K. Gong, C. Pan, J. Wang and Y. Wu, "Technical Review on Chinese Digital Terrestrial Television Broadcasting Standard and Measurements on Some Working Modes," IEEE Trans. Broadcast., vol. 53, pp. 1–7, March 2007.

[25] European Telecommunications Standards Institute EN 302 304 V1.1.1, Digital Video Broadcasting (DVB); Transmission system for handheld terminals (DVB-H), 2004.

[26] G. Faria, J.A. Henriksson, E. Stare and P. Talmola, "DVB-H: Digital Broadcast Services to Handheld Devices," Proc. IEEE, vol. 94, pp. 194– 209, January 2006.

[27] Advanced Television Systems Committee, "ATSC-Mobile DTV Standard, Part 2 - RF/Transmission System Characteristics," October 2009.

[28] El-Moghazi, M.; Whalley, J.; Irvine, J., "Allocating spectrum: Towards a commons future," Dynamic Spectrum Access Networks (DYSPAN), 2012 IEEE International Symposium on , vol., no., pp.1-9, 16-19 Oct. 2012

[29] Beutler, Roland. The digital dividend of terrestrial broadcasting. Springer, 2012.

[30] International Telecommunications Union, Final Acts of the European VHF/UHF Broadcasting Conference, Stockholm, Sweden, 1961.

[31] International Telecommunications Union, Final Acts of the Regional Administrative Radio Conference for the Planning of VHF/UHF Television Broadcasting in the African Broadcasting Area and Neighbouring Countries, Geneva, Switzerland, 1989.

[32] J.A Ibanez, Thorsten. Lhomar, T. Dalibor, and L. Zanin. Mobile TV over ·G networks-Service and enablers evolution. 1, 2008.

[33] Berg, K.; Uusitalo, M.A.; Wijting, C., "Spectrum access models and auction mechanisms," Dynamic Spectrum Access Networks (DYSPAN), 2012 IEEE International Symposium on , vol., no., pp.97-104, 16-19 Oct. 2012.

[34] ETSI TS 102 831 V1.2.1 (08/12) Implementation Guidelines for a Second Generation Digital Terrestrial Television Broadcasting System (DVB-T2), European Telecommunications Standards Institute, Geneva. 2012

[35] Digital Video Broadcasting (DVB) TM-H NGH, Call for Technologies (CfT), v 1.0 19, November 2009.

[36] Digital Video Broadcasting (DVB) CM-NGH, Commercial Requirements for DVB-NGH, v 1.01, June 2009.

[37] Gozalvez, D.; Gomez-Barquero, D.; Vargas, D.; Cardona, N., "Combined Time, Frequency and Space Diversity in DVB-NGH," IEEE Transactions on Broadcasting, vol.59, no.4, pp. 674-684, Dec. 2013.

[38] 3GPP TS 36.300 V9.7.0, Technical Specification Group Services and System Aspects; Evolved Universal Terrestrial Radio Access (E-UTRA) and Evolved Universal Terrestrial Radio Access Network (E-UTRAN); Overall Description; Dec. 2008.

[39] Walker, G.K.; Jun Wang; Lo, C.; Xiaoxia Zhang; Gang Bao, "Relationship Between LTE Broadcast/eMBMS and Next Generation Broadcast Television," Broadcasting, IEEE Transactions on , vol.60, no.2, pp.185-192, June 2014.

[40] Crussiere, M.; Douillard, C.; Gallard, C.; Le Bot, M.; Ros, B.; Bouttier, A.; Untersee, A., "A Unified Broadcast Layer for Horizon 2020 Delivery of Multimedia Services," Broadcasting, IEEE Transactions on , vol.60, no.2, pp.193-207, June 2014.

[41] Bill Meintel, "Broadcast Spectrum Issues in North America," Future of Broadcast Television Summit, Nov. 10-11, 2011, Shanghai, China.

[42] ATSC News Release, "Advanced Television Systems Committee Invites Proposals for Next-Generation TV Broadcasting Technologies", March 26, 2013.

[43] "A Global Approach to the future of Terrestrial Television Broadcasting," Future of Broadcast Television Summit, Nov. 10-11, 2011, Shanghai, China.

[44] F.P. Fontan and P.M. Espieira, Modelling the Wireless Propagation Channel: A simulation approach with Matlab. Wiley Publishing, 2008.

[45] Turnbull, G., "Maxwell's equations [Scanning Our Past]," Proceedings of the IEEE , vol.101, no.7, pp.1801-1805, July 2013.

[46] Lindell, I.V., "Huygens' principle in electromagnetics," Science, Measurement and Technology, IEE Proceedings - , vol.143, no.2, pp.103-105, Mar 1996.

[47] Stüber, G. L.; Principles of mobile communication. Springer, 2011.

[48] J.D. Parsons and J. Wiley. The mobile radio propagation channel, volume 67. Wiley Online Library, 1992.

[49] M. Patzold, U. Killat, Y. Shi, and F. Laue. A deterministic method for the derivation of a discrete WSSUS multipath fading channel model. European Transactions on Telecommunications, vol.7,pp. 165-175, 1996.

[50] Oppenheim, Alan V., Ronald W. Schafer, and John R. Buck. Discrete-time signal processing, vol. 2. Englewood Cliffs: Prentice-hall, 1989.

[51] Vaidyanathan, P.P., "Generalizations of the sampling theorem: Seven decades after Nyquist," Circuits and Systems I: Fundamental Theory and Applications, IEEE Transactions on , vol.48, no.9, pp.1094-1109, Sep 2001.

[52] A.V. Oppenheim, A.S. Willsky, and S.H. Nawab. Signals and systems. Prentice-Hall signal processing series. Prentice Hall, 1997.

[53] P, Bello. Characterization of randomly time-variant linear channels. IEEE transactions on communications systems, 1963.

[54] Chang R.W., "Orthogonal frequency multiplex data transmission system," US. Patent 3,488,445, Filed November 1 1966, Patented January 6, 1970.

[55] Chang R.W., "Synthesis of band-limited orthogonal signals for multichannel data transmission," Bell Systems Technical Journal, vol. 45, pp. 1775-1796, December 1966.

[56] ETSI, "102 733 (V1.3.1). Digital video broadcasting (DVB); Implementation guidelines for a second generation digital terrestrial television broadcasting system (DVB-T2)," European Telecommunication Standards Institute, August 2012.

[57] ETSI, "300 401 (v1.4.1). Radio broadcasting systems; Digital audio broadcasting (DAB) to mobile, portable and fixed receivers," European Telecommunication Standards Institute, 2006.

[58] "ARIB STD-B31 Ver.1.5", Transmission system for digital terrestrial television broadcasting, 2003.

[59] "3GPP TR 36.211 (V8.6.0). Digital video broadcasting (DVB); Evolved Universal Terrestrial Radio Access (E-UTRA).

[60] "IEEE standard for local and metropolitan area networks part 16: Air interface for fixed and Mobile Broadband Wireless Access Systems amendment 2: Physical and

medium access control layers for combined fixed and mobile operation in licensed bands and corrigendum 1," March 2006.

[61] W. Jakes, "Microwave Mobile Channels," New York: Wiley, vol. 2, pp. 159–176, 1974.

[62] T. Pollet, M. Van Bladel, and M. Moeneclaey, "BER sensitivity of OFDM systems to carrier frequency offset and Wiener phase noise," Communications, IEEE Transactions on, vol. 43, no. 234, pp. 191 –193, Feb 1995.

[63] K. Sathananthan and C. Tellambura, "Probability of error calculation of OFDM systems with frequency offset," Communications, IEEE Transactions on, vol. 49, no. 11, pp. 1884 –1888, Nov 2001.

[64] G. Durisi, V. Morgenshtern, and H. Bolcskei, "On the sensitivity of noncoherent capacity to the channel model," in Information Theory, 2009. ISIT 2009. IEEE International Symposium on, July 2009, pp. 2174 –2178.

[65] M. Russell and G. Stuber, "Interchannel interference analysis of OFDM in a mobile environment," in Vehicular Technology Conference, 1995 IEEE 45th, vol. 2, Jul 1995, pp. 820 –824 vol.2.

[66] P. Robertson and S. Kaiser, "The effects of Doppler spreads in OFDM (A) mobile radio systems," in Vehicular Technology Conference, 1999. VTC 1999 - Fall. IEEE VTS 50th, vol. 1, 1999, pp. 329 –333 vol.1.

[67] Y.-S. Choi, P. Voltz, and F. Cassara, "On channel estimation and detection for multicarrier signals in fast and selective rayleigh fading channels," Communications, IEEE Transactions on, vol. 49, no. 8, pp. 1375 –1387, Aug 2001.

[68] W. G. Jeon, K. H. Chang, and Y. S. Cho, "An equalization technique for OFDM and MC-CDMA in a time-varying multipath fading channels," in Acoustics, Speech, and Signal Processing, IEEE International Conference on, vol. 3, 1997, pp. 2529–2532.

[69] S. Chen, G. Dai, and T. Yen, "Zero-forcing equalization for OFDM systems over doubly-selective fading channels using frequency domain redundancy," Consumer Electronics, IEEE Transactions on, vol. 50, no. 4, pp. 1004 – 1008, Nov. 2004.

[70] X. Cai and G. Giannakis, "Bounding performance and suppressing intercarrier interference in wireless mobile OFDM," Communications, IEEE Transactions on, vol. 51, no. 12, pp. 2047 – 2056, DEq. 2003.

[71] P. Schniter, "Low-complexity equalization of OFDM in doubly selective channels," Signal Processing, IEEE Transactions on, vol. 52, no. 4, pp. 1002 – 1011, April 2004.

[72] Hou, Wen-Sheng, and Bor-Sen Chen. 2005. ICI cancellation for OFDM communication systems in time-varying multipath fading channels. Wireless Communications, IEEE Transactions on, vol. 4, pp 2100-2110.

[73] C. Paige and M. Saunders, "LSQR: An algorithm for sparse linear equations and sparse least squares," ACM Transactions on Mathematical Software (TOMS), vol. 8, no. 1, pp. 43–71, 1982.

[74] T. Hrycak, S. Das, G. Matz, and H. Feichtinger, "Low complexity equalization for doubly selective channels modeled by a basis explansion, Signal Processing, Transaction on, pp. 5706-5719, November 2010.

[75] P.-J. Bouvet, M. Helard, and V. Le Nir, "Low complexity iterative receiver for linear precoded OFDM," in Wireless And Mobile Computing, Networking And Communications, IEEE International Conference on, vol. 1, Aug. 2005, pp. 50–54.

[76] J. Barry, E. Lee, and D. Messerschmitt, Digital communication. Springer, 2004.

[77] T. Cui and C. Tellambura, "Joint data detection and channel estimation for OFDM systems," Communications, IEEE Transactions on, vol. 54, no. 4, pp. 670 – 679, April 2006.

[78] S. Zhou and G. Giannakis, "Finite-alphabet based channel estimation for OFDM and related multicarrier systems," Communications, IEEE Transactions on, vol. 49, no. 8, pp. 1402 –1414, Aug 2001.

[79] M. Clark, L. Greenstein, W. Kennedy, and M. Shafi, "Matched filter performance bounds for diversity combining receivers in digital mobile radio," Vehicular Technology, IEEE Transactions on, vol. 41, no. 4, pp. 356 –362, Nov 1992.

[80] F. Ling, "Matched filter-bound for time-discrete multipath rayleigh fading channels," Communications, IEEE Transactions on, vol. 43, no. 234, pp. 710 –713, Feb 1995.

[81] A. Molisch, M. Toeltsch, and S. Vermani, "Iterative methods for cancellation of intercarrier interference in OFDM systems", Vehicular Technology, IEEE Transactions on, vol. 56, no. 4, pp. 2158 –2167, July 2007.

[82] L. Scharf and C. Demeure, Statistical signal processing: detection, estimation, and time series analysis. Addison-Wesley Reading, MA, 1991, vol. 148.

[83] A. Duel-Hallen, "Decorrelating decision-feedback multiuser detector for synchronous code-division multiple-access channel," Communications, IEEE Transactions on, vol. 41, no. 2, pp. 285 –290, Feb 1993.

[84] P. Wolniansky, G. Foschini, G. Golden, and R. Valenzuela, "V-BLAST: an architecture for realizing very high data rates over the rich-scattering wireless channel," in Signals, Systems, and Electronics, URSI International Symposium on, Oct 1998, pp. 295–300.

[85] K. Fang, L. Rugini, and G. Leus, "Low-complexity block turbo equalization for OFDM systems in time-varying channels," Signal Processing, IEEE Transactions on, vol. 56, no. 11, pp. 5555–5566, 2008.

[86] H. Hijazi and L. Ros, "Joint data QR-detection and kalman estimation for OFDM time-varying Rayleigh channel complex gains," Communications, IEEE Transactions on, vol. 58, no. 1, pp. 170 –178, January 2010.

[87] H. Hijazi, L. Ros, G. Jourdain et al., "OFDM channel parameters estimation used for ICI reduction in time-varying multipath channels," European Wireless Conference, 2007.

[88] C. Paige and M. Saunders, "Solution of sparse indefinite systems of linear equations," Journal on Numerical Analysis, pp. 617–629, 1975.

[89] G. Golub and C. Van Loan, Matrix computations. The Johns Hopkins Univ Press, 1996, vol. 3.

[90] Y. Saad and M. Schultz, "GMRES: A generalized minimal residual algorithm for solving nonsymmetric linear systems," SIAM Journal on scientific and statistical computing, vol. 7, no. 3, pp. 856–869, 1986.

[91] W.-S. Hou and B.-S. Chen, "ICI cancellation for OFDM communication systems in time-varying multipath fading channels," Wireless Communications, IEEE Transactions on, vol. 4, no. 5, pp. 2100 – 2110, Sept. 2005.

[92] H.-C. Wu, X. Huang, Y. Wu, and X. Wang, "Theoretical studies and efficient algorithm of semi-blind ici equalization for ofdm," Wireless Communications, IEEE Transactions on, vol. 7, no. 10, pp. 3791–3798, 2008.

[93] L. Rugini, P. Baneli, and G. Leus, "Low-complexity banded equalizers for OFDM systems in Doppler spread channels," EURASIP Journal on Applied Signal Processing, vol. 2006, pp. 1–13, 2006.

[94] L. Rugini, P. Banelli, and G. Leus, "Simple equalization of time-varying channels for OFDM," Communications Letters, IEEE, vol. 9, no. 7, pp. 619–621, 2005.

[95] H. Sampath, S. Talwar, J. Tellado, V. Erceg, and A. Paulraj, "A fourth-generation mimo-ofdm broadband wireless system: design, performance, and field trial results," Communications Magazine, IEEE, vol. 40, no. 9, pp. 143–149, Sep.

[96] T. Hrycak, S. Das, G. Matz, and H. Feichtinger, "Low complexity equalization for doubly selective channels modeled by a basis explansion, Signal Processing, Transaction on,pp5706-5719, November 2010.

[97] Y. Mostofi and D. Cox, "ICI mitigation for pilot-aided OFDM mobile systems," Wireless Communications, IEEE Transactions on, vol. 4, no. 2, pp. 765 – 774, March 2005.

[98] M. Failli, "Cost 207 digital land mobile radio communications," Commission of the European Communities, 1989.

[99] J.-J. van de Beek, O. Edfors, M. Sandell, S. K. Wilson, and P. O. Borjesson, "On channel estimation in OFDM systems," Proceedings of VTC'95, pp. 715–719, July 1995.

[100] L. Zhang, Z. H. Hong and L. Thibault, "Improved DFT-Based Channel Estimation for OFDM Systems with Null Subcarriers," IEEE VTC Fall 2009, May 20-23, Sept. 2009.

[101] S. Coleri, M. Ergen, A. Puri, and A. Bahai, "Channel Estimation Techniques Based on Pilot Arrangement in OFDM Systems," IEEE Trans. on Commun., vol. 48, No. 3, pp. 223-229, Sept. 2002.

[102] Montalban, J.; Velez, M.; Angulo, I.; Angueira, P.; Wu, Y., "Large size FFTs over time-varying channels," Electronics Letters , vol.50, no.15, pp.1102,1103, July 17 2014 doi: 10.1049/el.2014.1301

[103] Y.Wu, B.Rong, K.Salehian and G.Gagnon, "Cloud Transmission: A New Spectrum-Reuse Friendly Digital Terrestrial Broadcasting Transmission System," IEEE Trans. on Broadcasting, vol. 58, no. 3, pp. 329-337, Sept. 2012.

[104] Bo Rong, Sung Ik Park, Yiyan Wu, Heung Mook Kim, Jeongchang Kim, Gilles Gagnon, and Xianbin Wang, "Signal Cancellation Techniques for RF Watermark Detection in ATSC Mobile DTV System:, IEEE Trans. Vehicular Technology, vol.60, no. 8, pp. 4070-4076, Oct. 2011.

[105] Sung Ik Park, Hyoungsoo Lim, Heung Mook Kim, Yiyan Wu, and Wangrok Oh, "Augmented Data Transmission for the ATSC Terrestrial DTV System", IEEE Trans. on Broadcasting, vol. 58, no. 2, June 2012.

[106] Cloud-Txn: A Joint Proposal by Communications Research Centre (CRC), Canada, and Electronics and Telecommunications Research Institute (ETRI), Korea, to the ATSC 3.0 PHY Layer CfP", September 2013.

[107] Montalban, J.; Bo Rong; Sung Ik Park; Yiyan Wu; Jeongchang Kim; Heung Mook Kim; Liang Zhang; Nadeau, C.; Lafleche, S.; Angueira, P.; Velez, M., "Cloud Transmission: System simulation and performance analysis," Broadband Multimedia Systems and Broadcasting (BMSB), 2013 IEEE International Symposium on , vol., no., pp.1-5, 5-7 June 2013.

[108] Montalban, J.; Bo Rong; Yiyan Wu; Liang Zhang; Angueira, P.; Velez, M., "Cloud Transmission frequency domain cancellation," Broadband Multimedia Systems and Broadcasting (BMSB), 2013 IEEE International Symposium on, vol., no., pp.1-4, 5-7 June 2013.

[109] Cheng Feng; Hongyu Cui; Meng Ma; Bingli Jiao, "On Statistical Properties of Co-channel Interference in OFDM Systems," Communications Letters, IEEE, vol.17, no.12, pp. 2328-2331, December 2013.

[110] DVB Fact Sheet (2000, March). DVB-T Hierarchical Modulation.

[111] Sung Ik Park; Heung Mook Kim; Yiyan Wu; Jeongchang Kim, "A Newly Designed Quarter-Rate QC-LDPC Code for the Cloud Transmission System," IEEE Trans. on Broadcasting , vol.59, no.1, pp.155-159, March 2013.

[112]B. Liu, Y. Li, B. Rong; L. Gui, Y. Wu, "LDPC-RS Product Codes for Digital Terrestrial Broadcasting Transmission System," IEEE Transactions on Broadcasting, vol.60, no.1, Mar. 2014.

[113] Y Li, B. Liu, B. Rong, Y. Wu, G. Gagnon, L. Lin, W. Zhang, "Rate-Compatible LDPC-R-S Product Codes Based on Raptor-like LDPC Codes,", Proceedings of the International Symposium on Broadband Multimedia Systems and Broadcasting 2013 (BMSB2013), London, UK, June 2013.

[114] M. Cha , K. Gummadi and P. Rodriguez "Channel selection problem in live IPTV systems", Proc. ACM SIGCOMM Poster, 2008.

[115] J. Lee , G. Lee , S. Seok and B. Chung Advanced scheme to reduce IPTV channel zapping time, pp.235 -243 2007.

[116] Montalban, J.; Liang Zhang; Gil, U.; Yiyan Wu; Angulo, I.; Salehian, K.; Sung-Ik Park; Bo Rong; Wei Li; Heung Mook Kim; Angueira, P.; Velez, M., "Cloud Transmission: System Performance and Application Scenarios," Broadcasting, IEEE Transactions on , vol.60, no.2, pp.170-184, June 2014.

[117] Montalban, J.; Angulo, I.; Velez, M.; Angueira, P.; Regueiro, C.; Yiyan Wu; Liang Zhang; Wei Li, "Error propagation in the cancellation stage for a multi-layer signal reception," Broadband Multimedia Systems and Broadcasting (BMSB), 2014 IEEE International Symposium on , vol., no., pp.1-5, 25-27 June 2014.

[118] Prieto, G.; Ansorregui, D.; Regueiro, C.; Montalban, J.; Eizmendi, I; Velez, M., "Platform for advanced DVB-T2 system performance measurement," Broadband Multimedia Systems and Broadcasting (BMSB), 2013 IEEE International Symposium on , vol., no., pp.1-7, 5-7 June 2013.

[119] Oliver Haffenden, "The Common Simulation Platform", BBC Research White Paper 196, May, 2011.

[120] D. Gómez-Barquero, Next Generation Mobile Broadcasting, CRC Press.

GLOSSARY

In this section there alphabetically ordered the acronyms and abbreviations that appear through this document.

AM	Amplitude Modulation
ARIB	Association of Radio Industries and Business
ATSC	North American Advanced Television Committee
BICM	Bit-Interleaved Coded Modulation
BBC	British Broadcasting Corporation
BER	Bit Error Rate
BST-OFDM	Band-Segmented Transmission OFDM
CENELEC	European Committee for Electrotechnical Standardization
C/I	Carrier to Interference Ratio
C/N	Carrier to Noise Ratio
CRC	Communications Research Centre
DAB	Digital Audio Broadcasting
DBA	Digital Broadcast Analyzer
DVB	Digital Video Broadcasting
DTT	Digital Terrestrial Television
NGH	Next Generation Handheld
DTMB	Digital Terrestrial Broadcast
EAS	Emergency Alert System
EBU	European Broadcasting Union
EC	European Commission
E-MBMS	Enhanced multimedia broadcast/Multicast Service

ETRI	Electronics and Telecommunications Research Institute
ETSI	European Telecommunications Standards Institute
FCC	Federal Communications Commission
FDD	Frequency Division Duplexing
FDM	Frequency Division Multiplexing
FEC	Forward Error Correction
FEF	Future Extension Frames
FFT	Fast Fourier Transform
FM	Frequency Modulation
FOBTV	Future of Broadcasting Television Initiative
HDTV	High Definition Television
ICI	Inter-carrier Interference
IFFT	Inverse Fast Fourier Transform
ITU	International Telecommunication Union
ISDB	Integrated Services Digital Broadcasting
ISI	Inter Symbol Interference
JCIC	Joint Committee on Intersociety Coordination
LDM	Layered Division Multiplexing
LDPC	Low Density Parity Check
LL	Lower Layer
LTE	Long Term Evolution
LOS	Line Of Sight
MEDIAFLO	Media Forward Link Only

MF	Matched Filter
MFB	Matched Filter Bound
MIMO	Multiple-Input Multiple-Output
MMSE	Minimum Mean Square Error
MPE-FEC	Multiprotocol Encapsulation-Forward Error Correction
MSE	Minimum Square Error
NTSC	National Television System Committee
NLOS	Non-Line of Sight
OFDM	Orthogonal Frequency Division Multiplexing
PIC	Parallel Interference Cancellation
PAPR	Peak-to-Average Power Ratio
PRBS	Pseudo-Random Binary Sequence
QEF	Quasi-Error-Free
RF	Radiofrequency
SARFT	State Administration of Radio Film and Television
S-DMB	Satellite Digital Multimedia Broadcasting
SDTV	Standard Definition Television
SECAM	Sequential Couleur A Memoire (SECAM)
SIC	Sequential Interference Cancellation
SIS	Successive Interference Cancellation
SFN	Single Frequency Networks
SL	Single Layer
SNR	Signal to Noise Ratio

SVC	Scalable Video Coding
SVD	Singular Value Decomposition
TDD	Time Division Duplexing
T-DMB	Terrestrial Digital Multimedia Broadcasting
TDM	Time Division Multiplexing
TFS	Time Frequency Slicing
TIMI	Terrestrial Interactive Multiservice Infrastructure
UHDTV	Ultra High Definition Television
UHF	Ultra High Frequency
UL	Upper Layer
UPV/EHU	Universidad del País Vasco / Euskal Herriko Unibertsitatea
VHF	Very High Frequency
WIMAX	Worldwide Interoperability for Microwave Access
WSSUS	Wide-Sense Uncorrelated Scattering
ZF	Zero Forcing